University of Alberta
Department of Civil Engineering

Studies of Reinforced Concrete Shear Wall - Frame Structures

by

R.P. Nikhed

J.G. MacGregor

P.F. Adams

June, 1970

STUDIES OF REINFORCED CONCRETE

SHEAR WALL-FRAME STRUCTURES

by

R.P. NIKHED

J.G. MACGREGOR

P.F. ADAMS

June, 1970

Department of Civil Engineering

The University of Alberta

Edmonton, Canada

ABSTRACT

The primary objective of this report was the development of an approximate method of analysis to predict the behaviour of multi-story shear wall-frame structures with reasonable accuracy and study the behaviour by a test of a reinforced concrete shear wall-frame structure.

The analysis was performed on an equivalent lumped model under incremental lateral load and fixed vertical load and traces the second order elastic-inelastic response of the structure. Conditions of equilibrium are formulated on the deformed structure to include the secondary, P-Δ, effects in columns and shear walls. The analysis does not consider the axial shortening of the columns and shear wall but the width of wall has been taken into consideration. Time effects, temperature changes and shear deformations in the members and joints are neglected.

The analysis uses an iterative procedure. The computer program developed for the analysis uses moment area and slope deflection equations modified to consider the presence of plastic hinges in the members. A method has been developed to derive the equivalent lumped structure. Using this analysis, good correlation was obtained with other analyses. A design example has been presented.

Rationalized methods were developed to predict the moment-

thrust-curvature relationships for the cross-sections of the members. The computer program developed for the purpose considers rectangular reinforced concrete cross-sections and can consider tensile stress in the concrete and unsymmetrically placed reinforcement.

A four story, one bay shear wall-frame structure was tested under incremental lateral load and fixed vertical load applied at the top of column and wall. The behaviour shown by this test was compared to the behaviour predicted by the present analysis and a good correlation was obtained.

TABLE OF CONTENTS

LIST OF SYMBOLS

A	=	Area of cross-section
a	=	Gauge length of measuring station
A_{st}	=	Area of reinforcing steel
b	=	Width of cross-section
c,s	=	Stability functions
D	=	Depth of wall section
DL	=	Dead load
d'	=	Cover of cross-section
E	=	Modulus of Elasticity
E_c	=	Modulus of Elasticity of concrete
E_s	=	Modulus of Elasticity of reinforcing steel
F	=	Force at floor level after force fitting
f_c	=	Compressive stress in concrete
f'_c	=	Compressive strength of concrete
f''_c	=	Flexural strength of concrete
f_r	=	Modulus of rupture of concrete
f_s	=	Stress in reinforcing steel
f_t	=	Tensile stress in concrete
f'_t	=	Tensile stress of concrete
f_y	=	Yield strength of reinforcing steel
G	=	Modulus of rigidity
H	=	Lateral load at floor level
h	=	Story height
I	=	Moment of inertia of cross-section

I_c	=	Moment of inertia of concrete
I_s	=	Moment of inertia of reinforcing steel
L	=	Span length of a member
LL	=	Live load
M	=	Moment at a section
M_p	=	Plastic moment capacity of a cross-section
M_u	=	Ultimate moment capacity of a cross-section
P_o	=	Ultimate load capacity of a cross-section under pure axial load
P_u	=	Ultimate load capacity of a cross-section subjected to bending
P_t	=	Percentage of reinforcing steel
r	=	Radius of gyration of cross-section
S	=	Stiffness ratio, EI/L, of a member
T	=	Force in the rod of wall base connection
t	=	Depth of cross-section
V	=	Shear force
WL	=	Wind load
w_b	=	Uniformly distributed load to cause end hinges in a restrained beam
Δ	=	Sway deflection at floor level
δ	=	Vertical deflection of the edge of shear wall
θ	=	Slope at a section
ρ	=	Story sway
μ	=	Poisson's Ratio
γ	=	Ratio of moment capacities in the positive region to that of negative region in a restrained beam
η	=	Ratio of moment capacities at the windward to that of leeward end of a restrained beam

α	=	Reduction factor applied to the ultimate moment capacity of beam
β	=	Ratio of wind moment to ultimate moment capacity of a restrained beam
λ	=	Load factor or load parameter
ϕ	=	Curvature at a section
ε	=	Strain in a cross-section
ε_4	=	Strain in the extreme compressive fibre of a cross-section
ε_1	=	Strain in extreme tensile fibre of a cross-section
ε_0	=	Compressive strain in concrete corresponding to maximum concrete stress
ε_{ult}	=	Ultimate tensile strain in concrete
ε_s	=	Strain in reinforcing steel

PART I

INTRODUCTION

CHAPTER I

INTRODUCTION

The social and economic development of urban areas requires the
construction of high rise commercial and residential buildings. Recent
years have seen the construction of many tall buildings and their numbers are
increasing rapidly. Such construction has proved the necessity for more
                                                              for
and more knowledge of the behaviour of such buildings and analyses capable
                                                            ʌ
of accessing, with sufficient accuracy and rapidity, the overall strength of
the buildings.

The planning and design of tall buildings requires the provision
of sufficient resistance against lateral loads in all directions. This
stiffness can be achieved in many ways depending upon the height and plan
of the building. The most usual planning concept uses shear walls to
provide the required rigidity. In the twentieth century large number of
tall reinforced concrete buildings have been built with shear walls so
located that they act as columns in addition to resisting the lateral forces.
In most cases, in addition to carrying vertical and lateral loads, shear
walls are used for the purpose of enclosing service areas. As a result,
shear walls can take a variety of shapes. The object of this thesis is to
present an approximate method of analysis for shear wall-frame structures
and justify this analysis by laboratory test and discussion.

The modern trend of reinforced concrete design has shown increas-

ing use of ultimate load theory. This design method tends to be more economical and logical than working stress design because it predicts the dependable load carrying capacity of the structure and the design can be so arranged that the appropriate load factor can be achieved. Most of the presently available analyses for shear wall frame structures, reviewed in CHAPTER II, are limited to the elastic regime and tend to give rise to different load factors for different members in a structure. Consequently, the information from such an analysis is not sufficient to design by a limit design procedure and it does not constitute the true behaviour of the structure.

The theory of "plastic hinges" is now widely accepted to establish the behaviour of steel members at failure. However, this type of failure is still being investigated for multi-story structures. The trial and error method of choosing the plastic hinge configuration in the mechanism method of analysis has the serious disadvantage that there is no guarantee that the worst possible hinge configuration has been chosen. The recent development of electronic computers has made it possible for engineers to perform more satisfactory analyses of multi-story steel structures.

Because of the complex nature of behaviour of reinforced concrete members, the development of the comparable theories for reinforced concrete structures has not been so marked. Since reinforced concrete columns lack ductility, an ultimate load theory for concrete structures, in which collapse is forced to occur due to beam hinging by creating a strong column and weak beam design[H2] could be used. This method has the disadvantage of the trial and error method of choosing the worst mechanism and leads to the overdesigning of the columns. The most satisfactory and probably eventual

analysis method for concrete structure seems to be the technique of analysing a mathematical model on a computer through each stage in its loading history. This method has the advantage that the load history dependence of the stress-strain curve can be included in the program.

In tall buildings, the axial loads in columns are significant and produce additional overturning moments commonly referred to as P-Δ moments; where P is the axial load and Δ is the displacement due to sidesway. The effect of these "secondary" moments is to reduce the capacity of the structure to resist lateral loads. These moments must be considered in the analysis of tall buildings[D3]. In an unbraced structure the P-Δ effects are significant and increase as the inelastic action progresses causing a rapid softening of the structure. If the members are sufficiently slender, it is conceivable that the failure load could be initiated by elastic instability before any portion of the structure reached the inelastic behaviour range. On the other hand in a laterally braced structure the P-Δ effects are reduced due to lateral stiffness of the structure and hence less danger of elastic instability failure exists. The response of a structure is significantly influenced by the shear wall, which provides a sort of bracing system. Although the problem has been studied[C5], there is no specific way to differentiate between braced and unbraced structures. It is mentioned elsewhere[A2] that "what constitutes adequate bracing in any given case must be left to the judgement of the engineer, depending on the arrangement of the structure in question".

For shear wall-frame structures, it has been common practice to design the frame for the vertical load and shear wall to resist the lateral loads only[B15]. For a building of relatively small height this assumption is adequate but considerable error results when it is applied to high

buildings. Therefore this assumption seems to be an over-simplification.
The behaviour of a building depends on the way it is built and not in the
way it is arbitrarily assumed to behave. When the frame portion of the
building is fairly rigid by itself, the interaction between the shear wall
and frame can result in considerably more rigid and efficient design. The
redistribution of the lateral forces resulting from the inelastic action
would influence the interaction behaviour in a shear wall frame system.
Therefore, a realistic approach to assess the load sharing between shear
wall and frame is an obvious necessity for a rational and economical design.

An attempt has been made in this thesis to present an approximate
computer analysis to trace the second order elastic-inelastic behaviour of
shear wall frame structures. A brief review of the previous work on such
structures is given in CHAPTER II. CHAPTER III presents the proposed
method of analysis. The assumptions made in CHAPTER III are critically
examined in CHAPTERS IV, V and VI. The cross-sectional response is dis-
cussed in CHAPTER IV. CHAPTER V describes the response of the members
and joints. CHAPTER VI is devoted to the discussion of the simplified
structure assumed in the analysis. CHAPTER VII describes the fabrication
and testing of a four story, one bay reinforced concrete shear wall frame
structure. The test and the processing of test data are discussed in
CHAPTER VIII and the actual and predicted behaviour are compared in CHAPTER
IX. CHAPTER X summarises and concludes the dissertation.

CHAPTER II

REVIEW OF THE PREVIOUS WORK

2.1 Introduction

For the investigation of the problem outlined in CHAPTER I, it is necessary to employ a method of analysis to trace the response of shear wall-frame structure as loading progresses to failure.

A brief review of the extent of the present information on the elastic and inelastic action of multi-story structures is included in this CHAPTER. The review considers five different aspects which influence the study of shear wall frame structures. The areas of this survey of literature are as follows:

1. Cross-sectional behaviour in the form of moment-curvature relationship and material properties.

2. Analysis of frames.

3. Analysis of shear walls.

4. Analysis of shear walls combined with frames.

5. Tests on concrete structures.

2.2 Moment Curvature Relationship

An extensive study on plain and reinforced concrete columns was carried out in the period 1929 to 1933 under the sponsorship of the American Concrete Institute[R1]. The most important conclusion of this study was that the full concrete cylinder strength cannot be taken as the failing strength of a reinforced concrete column, and a factor, 0.85, was established to be multiplied to the cylinder strength of concrete. This value of 0.85 was confirmed by the studies made by Hognestad[H1]. For analysing his test results, Hognestad proposed a new stress-strain relationship for concrete in flexure. There is a discontinuity in the slope of the curve at its maximum value and the concrete is assumed to fail at an ultimate strain of 0.0038.

The stress-strain relationship for concrete is the subject of much debate, since the mechanism of failure of concrete is not completely understood. Based on various literature,[N1,D1,K3,B12,W3] MacGregor proposed a stress-strain curve for concrete[M5] which has been used in this thesis. This stress-strain curve is described in CHAPTER IV.

For cross-sections which consist of linearly elastic material it is possible and convenient to write a single expression relating moment, thrust and curvature. Unfortunately, the response of reinforced concrete section is extremely complex and it is difficult to write an M-P-ϕ expression as a simple function. Different authors have tried different approaches. Most methods use a trial and error procedure, involving considerable computations, and define the relationships among moment-thrust-curvature by a number of discrete points. Such presentation have been facilitated considerably by the use of electronic computer. Two methods

of such analysis, suggested by Ernst, Hromadik and Riveland[E1] in 1953, are as follows:

1. The values of axial load, P, and moment, M, can be obtained for a given value of outer fibre compressive strain, ε_4, and using various values of ε_1. The moment-curvature and axial load-curvature curves for values of ε_4 can be plotted. From a series of such curves for different values of ε_4 a moment-curvature curve at constant axial load can be obtained.

2. For a given axial load, P, and a given outer fibre compressive strain, ε_4, it is possible to find the value of ε_1, by trial. The process can be repeated for various values of ε_4 to get a direct moment-curvature curve at constant axial load, P.

Broms and Viest[B2] used the Hognestad stress-strain curve and derived four equations relating the axial load and the moments to the outer fibre strains, for four different possible strain configurations.

Chang[C2] rederived these equations and used them to derive the moment-curvature relationship using the first approach. Breen[B11] considerably improved this procedure.

Pfrang[P1] established contours of equal curvature to define the combination of axial loads and moments for a given curvature. By interpolating a sufficient number of contours the moment-thrust-curvature relationship can be established.

All of the above analyses used the Hogenstad stress-strain curve

and neglected the tensile stress of concrete. Fowler[F2] has suggested an analysis using the second approach for getting direct moment-curvature relationship for a given axial load. Different stress-strain curves were used. The ultimate strain limit was not taken as the criteria for failure.

An analysis similar to that presented by Fowler[F2] using the stress-strain curve proposed in reference[M5] including the effect of tensile stress of concrete is presented in CHAPTER IV, to define the behaviour of reinforced concrete cross-sections.

2.3 Analysis of Frames

Several theories and methods have been developed for the analysis of single and multi-story frames. The structural action of a multi-story frame can be classified as follows:

1. The frame can resist gravity load without lateral deflection of the floors until loads are increased to the load corresponding to an elastic sway buckling failure.

2. The frame can resist gravity load without lateral deflection at floor level and does not fail in sway mode. The frame fails by plastic hinging.

3. The frame can resist gravity load with lateral deflection of floor level. Failure occurs by inelastic buckling.

4. The frame can resist both gravity and lateral load with lateral deflection of floor level and the frame fails by instability. This is characterized by a gradually increasing

lateral deflection, first under a growing load and later
after reaching a maximum load, under a diminishing load.

The various methods for evaluating the elastic buckling load
have been summarized by Bleich[B1]. The elastic and inelastic solution
of buckling load of symmetrical three story structures subjected to
uniformly distributed gravity loads have been described by Lu[L2].
He has also suggested that the solution described for a three story frame
may be applied to taller frames by first dividing them into several
three-story tiers. The case, where the failure results from a trans-
lational instability of the structure is the most practical problem. In
most cases, much of the frame is strained into the inelastic range before
the buckling loads are reached.

Merchant[M1] has proposed a Rankine type formula,
$\frac{1}{\lambda_F} = \frac{1}{\lambda_P} + \frac{1}{\lambda_C}$, for the evaluation of inelastic buckling capacity of
the structure, λ_F, where λ_P is a function of rigid-plastic collapse
load and λ_C is the function of elastic critical load. Horne[H3] has
justified this formula and it was experimentally verified by Majid[M7].

Wood[W2] illustrated the loss in structure stiffness in the
presence of plastic hinges by inserting real hinges in the structure and
computed "deteriorated elastic critical load". His illustrations indicated
the tendency for structures to become unstable prior to the formation of
enough hinges to render the structure into a mechanism. However, it is
not possible to predict the deteriorated state of the structure without
advance knowledge of the actual history of the order of hinge formations.
Even then, only an upper and lower bound to the collapse load can be

obtained.

Recently, computer oriented elastic-plastic analyses of unbraced
plane frames have been developed by assuming point plastic hinges and
elastic-perfectly plastic section behaviour.

Jennings and Majid[J1] developed an iterative procedure to per-
form an elastic-plastic analysis of unbraced frames loaded by static,
proportional concentrated loads. The solution is derived using a matrix
technique having joint displacement as unknowns. This analysis yields
the complete load-deflection characteristic and the order of plastic
hinge formation. Davies[D2] extended this analysis for cyclic loading
and considered the effects of hinge reversals by a locked hinge with a
rotational discontinuity.

Parikh[P2] formulated a second order elastic-inelastic analysis
employing slope deflection equations. An iteration procedure was used
for solving the simultaneous equations. Korn[K5] has also developed a similar
solution except that he uses matrix techniques to solve the simultaneous
equations.

Heyman[H2] has proposed a design method for multi-story frames
in which beams were designed by plastic methods and columns were designed
to be elastic up to the design ultimate load. An approximate method to
calculate the deflection has also been proposed.

Daniels and Lu[D3] proposed a subassemblage method to analyze
unbraced frames subjected to vertical and lateral loads. Isolated parts
of a multi-story frame were analyzed as independent units with the point

of contraflexure in the columns being assumed to be at mid-height. Sub-sequently, this model is reduced to a number of subassemblages, each consisting of a column restrained by the adjoining beams. Both inelastic action and the second order P-Δ effects are included in this analysis.

Kloucek[K1] suggested a simplified solution for elastic analysis of the sidesway of a multi-story closed system. The true multi-story system is replaced by a substitute cantilever with the same loading. The substitute member stiffness factors of the cantilever were obtained by addtion of all the column stiffness factors on the same floor of the original frame. The beams were represented by "knots" at each floor with the stiffness factors of the "knots" determined by adding an imaginary member having a rotational stiffness equal to sum of all the beam stiff-ness factors on one floor multiplied by a factor "A". The factor "A" is a fairly insensitive quantity. Many examples were solved to show the rapidity and validity of the method. Lightfoot[L1] has illustrated this method and has solved two examples.

2.4 Analysis of Coupled Shear Walls

This section is devoted to some of the literature available for the analysis of groups of shear walls coupled by beams.

The analysis of coupled shear walls is due in large part to Rosman and Beck [R3,R4,B9]. Rosman established the solution in the form of a trigonometric series using the principle of least work. In subse-quent work he used a direct mathematical solution[R3]. He derived solutions for a wall with two symmetric bands of openings, with various conditions of support at the lower end (piers on rigid basement, on separate

foundations and on various forms of column supports). Two loading cases,
a uniform wind load, and a point load at the top of the building were
considered. Beck[B9], who used a similar approach as Rosman, presented
an approximate method of analysis where a continuous system replaces the
discontinuous system. He assumed that all connecting beams had
the same distance from each other and, except the end beam, had
the same stiffness. The end beam had one half the cross-section and
one half the moment of inertia of a normal connecting beam. He treated
the single case of two uniform coupled shear walls on a rigid foundation,
subjected to a uniformly distributed lateral load. Useful graphs to
enable bending moment, axial force and deflection have been presented.

Frischman, Prabhu and Toppler[F1] have used two different
methods, both based on the principle of analysis for a rigidly jointed
framework, to deal with the coupled shear walls. Equivalent column
method has been used, by which a multi-bay structure can be reduced to
a single column by the lumping together of all column stiffnesses, with
a single beam restraint at each story level, given by the addition of
the beam stiffnesses, to analyze the coupled shear walls. The problem
was reduced to a single second order differential equation, by using a
continuous distribution of restraints and loads, to evaluate the bending
moments in the continuous system. A conventional method using the flexi-
bility approach was also used. A similar approach was used by Coull
and Choudhury[C4] who have presented curves for the moments and maximum
deflection.

2.5 Analysis of Shear Walls Combined with Frames

Several investigators have considered the problem of load

distribution in the combined frames and walls system. Because of the high in plane stiffness of floor slabs, most investigators have been concerned with the plane frame wall system.

Rosenblueth and Holz[R2] present an approximate analysis of the interaction between single shear wall and a rigidly jointed frame structure. The shear carried by the frame in any one story was assumed to be proportional to the average slope in that story whereas the moments and shears in beams supported by the wall were proportional to the flexural slope of the wall. Newmark's method of successive approximation was suggested as a solution. Column shortening and foundation deformations were neglected.

Cardan[C1] reduced the problem to the solution of second order linear differential equations, giving the slope of the shear wall. The properties of frames and walls were assumed to be constant throughout the height. Axial deformations were neglected and the wind loads were assumed to be distributed throughout the height of the structure.

Bandel[B10] suggested the analysis of shear trusses, to replace an equivalent shear wall, combined with frames. Power series solution was suggested which requires the solution of a set of simultaneous equations. Column shortening was considered but axial deformations of the beams were neglected and a fixed end foundation condition was assumed.

A computer program, using the stiffness method of analysis, taking flexure, shear and axial deformation into account, was developed by Clough, King and Wilson[C3]. The axial deformation of beams was neglected.

It was assumed that the building was laid out in a regular rectangular grid pattern, with each floor level constrained to translate but not rotate under the action of lateral forces. It was further assumed that the shear walls were of uniform width throughout the entire height, although variations in stiffness of shear walls were allowed.

Khan and Sbarounis[K2] presented a method of successive approximation on a substitute structure derived for the purpose of analysis. The derivation of the substitute structure resembled that used by Kloucek[K1] or Lightfoot[L1]. Forced convergence techniques have been used to arrive at an elastic solution. In this way, convergence is tied directly to the physical reality that the deflections of the entire structure must lie between zero and the free deflection of the shear wall. This method will converge for any combination of structural stiffnesses although at different rates. A number of influence curves were presented for use in preliminary design. The analysis proposed in this thesis is on somewhat similar lines.

Gould[G1] replaced the frame by a system of rotational and translational springs. The finite difference technique was used to solve the fourth order governing beam equations giving the wall deflection at each floor level.

A computer analysis, which traces second order elastic-plastic behaviour of planar reinforced concrete structures as loading progresses to failure, was presented by Clark, MacGregor and Adams[C5,C6]. The analysis considers axial shortening of the columns and shear walls and includes the effect of finite width of shear wall. Time effect and shear

deformations on the members and joints are neglected.

Winokur and Gluck[W7] presented a method of analysis for asymmetric multi-story structures. They have shown that the rotational constraints of the stiffening elements in their planes at the floor diaphragms are important factors which are to be taken into account in analysis.

A number of other papers[A4,B14,G2,J2,K4,P3,S2,T1,T2,W5,W6] are also available which illustrate the problem and solutions have been suggested with various assumptions.

2.6 Tests of Shear Walls and Shear Wall-Frame Structures

Though much has been said about the analysis of multi-story structures, experimental studies should not be forgotten. Although many experimental studies have been carried out on multi-story frame structures, relatively few experimental studies of shear wall-frame structures have been carried out.

The first major tests were carried out in the United States in full scale by atomic explosions at Eniwetok. Abbreviated reports were presented by Whitney, Anderson and Cohen[W1]. Approximate methods based on simple strength of materials theories were proposed to predict the stiffness and ultimate capacity of simple shear wall structures subjected to lateral loads.

A large number of tests were made by Benjamin and Williams [B3,B4,B5,B6], on single story brick and reinforced concrete shear walls

with and without openings and on one or two story parallel reinforced concrete shear wall assemblies connected by diaphragms.

A model test on a reinforced mortar eight story shear wall-frame was described in reference [A4]. The stories were each one foot high. Photoelastique methods were also used in this investigation.

A model scaled at 1:64 was tested by Barnard and Schwaighofer [B14] to establish the width of "slab strip", which acts as the connecting media between shear wall coupled by slab floors, and to determine the validity of an analysis presented. The walls for the model were cut from 1/4 inch thick epoxy sheets and the floor slabs were slotted to fit around the walls and then glued to the walls using an epoxy glue. The model was tested in horizontal position with the base being rigidly fixed.

Twenty three story models constructed from 1/4 inch thick per-spex sheets were tested by Jenkins and Harrison [J2] to compare their analysis under bending and torsion.

2.7 Conclusions

Extensive literature is available on different aspects of the problems encountered in dealing with multi-story structures. Some of these papers are reviewed briefly in the previous sections. The review indicates that many questions regarding the behaviour of shear wall frame structures are yet unanswered. Most of the studies were limited to elastic cases only. In many cases the analytical procedures are cumber-some requiring extensive computation work and not suitable for design

office use.

Very few actual laboratory tests have been reported especially on reinforced concrete shear wall-frame structures. Many tests have been performed to describe the behaviour of the members.

In view of the above limitations it was felt necessary to derive an approximate rapid, elastic-plastic analysis of shear wall frame structures, and to check this analysis by tests on large scale reinforced concrete models. This is undertaken in this thesis.

PART II

APPROXIMATE ANALYSIS OF REINFORCED CONCRETE
SHEAR WALL-FRAME STRUCTURES

CHAPTER III

APPROXIMATE ANALYSIS

3.1 Introduction

A computer analysis of shear wall-frame structures under incremental lateral loads and constant vertical load is described in this CHAPTER. The analysis traces the second order elastic-plastic behaviour of the structure as the loading approaches the ultimate value. To simplify the problem the analysis deals with the reduced structure shown in FIGURE 3.1. The formulation of the analysis and the assumptions made are outlined in this CHAPTER. A design example is calculated using this analysis in APPENDIX A. The validity of the assumptions will be discussed more fully in CHAPTERS IV, V and VI. The analysis will be compared to the results of a test of a four story frame in CHAPTER IX.

3.2 Assumptions in the Analysis

The assumptions made in deriving this analysis fall into several major categories. The first group includes those dealing with the behaviour of the structural members, joints and plastic hinges in the structure. These assumptions are discussed in detail in CHAPTERS IV and V.

1. (a) It is assumed that the moment rotation relation-
        ship for the individual frame members can be
        idealised as elastic-plastic for the beams and
        columns and elastic-strain hardening for the
        shear walls, as shown in FIGURES 3.2(a) and (b).

    (b) All members in the idealised structure are assumed
        to be prismatic. That is, the stiffness and ulti-
        mate moment capacity may vary from member to
        member but not along the length of a given member.
        It is possible to develop moments of opposite sign
        at the two ends of the member. The
        ultimate moment capacity, M_p, and stiffness, EI,
        of the members are derived in CHAPTER IV.

    (c) The stiffness factors C and S commonly used in the
        slope-deflection equations have been assumed to
        remain sufficiently close to 4 and 2 that these
        values can be used. In deriving the M_p value for
        the cross-section, however, the axial load is taken
        into account.

    (d) Shear deformations are neglected.

    (e) The joints are rigid prior to hinging of the members
        and do not undergo shearing distortions.

    (f) The plastic hinges in the columns and beams are
        assumed to be point hinges at the ends of the members.

(g) Plastic hinges in the walls are assumed to form in a segment of preset small finite length.

(h) The hinges are assumed to have an infinite rotation capacity.

The second and most important group of assumptions deals with the derivation of the simplified model used in the analysis. This group of assumptions is derived and discussed in detail in CHAPTER VI.

2. It is assumed that the load-deflection behaviour of multi-story shear wall-frame structures can be represented by the simplified or "lumped" structure shown in FIGURE 3.1. This assumption implies that:

(a) Each floor is assumed to act as a diaphragm of infinite rigidity and it is assumed that the structure does not rotate about a vertical axis. Thus, all points on a given floor level are assumed to undergo the same lateral deflection. This assumption allows the entire building to be considered as a plane frame.

(b) The shear walls in any one story can be represented by a single wall with a moment curvature relationship defined by superimposing the moment curvature relationships of each of the individual walls in that story. The resulting moment-curvature relationship is approximated by a bi-linear curve. The

slope of the second branch of this curve may be
small but not zero and the ratio of the slope
of the second branch to that of the elastic portion
of the curve must be the same in all stories. The
neutral axis of the wall is assumed to coincide
with the centroid of the uncracked wall.

(c) The columns in any one story are assumed to be
represented by a single column as shown in FIGURE
3.1. The lumped column is assumed to have a stiff-
ness and a plastic moment capacity equal to the sum
of the corresponding values for all the columns
being lumped together in a given story.

(d) The beams linking the shear wall to the rest of the
structure (link-beams) in each story are assumed
to be represented by a single link beam as shown in
FIGURE 3.1. The lumped link beam has a length equal
to the average length of all the link beams in the
story except that the lumped link beams must have
the same length in all stories. The stiffness,
EI/L, of the lumped link beams shall be taken as the
sum of the link beams in the story in question. The
plastic moment capacity of the lumped beam shall be
taken as $\alpha \Sigma M_p$ for all the corresponding beams. The
term α, a reduction factor, is discussed in section
6.2.2.2.

(e) The remaining beams connecting adjacent columns in
each floor are assumed to be represented by a single

beam as shown in FIGURE 3.1. The two ends of this
beam are assumed to undergo the same rotations. That
is, the point of contraflexure in the beam is assumed
to be at mid-span.

(f) The lumped beams are assumed to have a length, L_B,
equal to the average length of all the corresponding
beams under consideration. The moment of inertia,
I_{LB}, and the plastic moment capacities of the lumped
beams, M_{PLB}, are given by equations:

$$I_{LB} = 2L_{LB} \cdot \Sigma(I_B/L_B) \qquad \ldots \ldots (3.1)$$

$$M_{PLB} = \Sigma\alpha(M_{PB1} + M_{PB2}) \qquad \ldots \ldots (3.2)$$

These equations are derived in sections 6.2.1 and
6.2.2.2. The term α is discussed in section 6.2.2.2.

(g) The foundation conditions are represented by elastic
rotational springs at the bases of the column and
the wall of the lumped model. The spring constants
are obtained by adding the known or assumed foundation
spring constants of all the columns or walls in the
real structure.

The third group of assumptions deals with the loads to be applied
to the lumped structure. These assumptions are discussed in CHAPTER VI.

3. (a) It is assumed that the total vertical load in a story

can be applied as a concentrated load. Thus, there
are no dead and live load moments on the beams in
the lumped structure. The vertical loads remain
constant throughout the analysis.

(b) The lateral loads are assumed to be concentrated at
the floor levels. The lateral loads are incremented
during the analysis.

(c) The loads are assumed to be applied statically and
act in the plane of the structure.

The fourth group of assumptions concern special aspects of
behaviour of entire structure. These are as follows:

4. (a) It is assumed that there is no out-of-plane behaviour
of the members such as lateral-torsional-buckling
etc. and it is assumed that none of the members fail
due to buckling prior to the attainment of the ulti-
mate load.

(b) Temperature changes and differential axial settlement
or shortening are neglected.

3.3 Method of Analysis

To determine the deflected shape of a structure subjected to a
static load, the conditions of equilibrium and compatibility must be
satisfied. The usual methods for such an analysis are the displacement

(or stiffness) method or the force (or flexibility) method.

In the displacement method the joint displacements are treated
as unknowns and equilibrium conditions of external and internal forces
are used to solve for these unknowns. In the force method, the redundant
forces are treated as unknowns and consistent deformation conditions are
then used to solve for these unknowns.

The present analysis uses an iterative technique in which both
the above procedures have been used to arrive at a solution. For this
purpose the analytical model has been divided into the frame system and
the wall system shown in FIGURE 3.1. The procedure used requires the
following steps:

A. Apply all the lateral load to the free wall system. The
   deformations are then computed(FIGURE 3.3).

B. Force the frame system through the deflections computed
   in step A at each floor level and compute the shear
   induced in the frame due to this force-fitting (FIGURE
   3.4).

C. Compute the shears and moments in the wall system in each
   story due to the applied loads and the force fitting
   process   (FIGURE 3.5).

D. Calculate the deflections, Δ_{wi}, and rotations, θ_{wi}, of
   the wall system due to the shears and moments computed
   in step C. A "forced-convergence correction" was applied
   to obtain the initial trial deformations of the $(n+1)^{th}$

cycle. The correction used in this analysis is described
in reference (K2).

E. Steps A through D are repeated in order until the desired
accuracy has been achieved.

This basic procedure was originally described by Khan and
Sbarounis[K2] for structures in the elastic range. It is extended in
this report to trace the second-order elastic and inelastic behaviour
of the structure.

A computer program was written in Fortran IV language for
IBM system OS/360 to carry this out. The flow diagram, program
nomenclature and the listing of the program are presented in APPENDIX
B.

The program takes into account the inelastic action of the
structure due to the formation of plastic hinges and the secondary
moments caused by the P-Δ effect. To take this effect into consider-
ation the equilibrium equations are formulated on the deformed structure.

The steps in the program are outlined below:

1. The program starts by reading in all the data necessary
to describe the problem. This includes the number of
structures to be considered, the dimensions and properties
of the structural members in the lumped frame shown in
FIGURE 3.1, the loading and load increments, and the
convergence limit.

2. The stiffness, EI/L, of all the beams and columns in the
    lumped frame are computed and the vertical load acting
    on the frame is also computed. This load remains constant
    while the lateral load on the structure is incremented to
    determine the load-deflection characteristics. Each story
    of the shear wall is divided into a desired number of
    segments and systemized for the calculations.

3. The entire lateral load is applied to the shear wall and
    the moment at the centre of each segment is calculated
    by considering the wall as a free cantilever. The rotations
    and deflections are calculated at every segment using moment-
    area principles. The vertical displacement at the junction
    of the shear wall and the frame is computed as the product
    of the rotation of the wall and one-half the wall width.
    FIGURE 3.3 shows the deflected shape of the shear wall
    under the entire lateral load, where $\theta_{Wi}^{(1)}$, $\Delta_{Wi}^{(1)}$ and
    $\delta_{Wi}^{(1)}$ are the rotation, lateral displacement and vertical
    displacement of the wall. The initial subscript W repres-
    ents the shear wall, while i represents the floor under
    consideration and the superscript (1) represents the
    initial iteration cycle. The story height is H_{si}. In
    the latter stage of the analysis a reduced value of the
    wall stiffness is used for any wall segment where a hinge
    has been detected.

4. The frame system is forced into the deflected shape of the
    wall as defined by the deformations computed above. This

step is shown in FIGURE 3.6.

Next the frame joint rotations are computed. In FIGURE 3.6 B_i is the beam-to-column joint, W_i is the joint at the connection of the wall and the right side beam and F_i is the left end of the left side beam. Under lateral loads beam B_iF_i will have a point of contraflexure approximately at midspan. This is enforced in the structural model by assuming that the joints B_i and F_i have equal rotations and that the left end support, F_i, is free to translate.

At each joint the slope-deflection equations are written and by using the moment equilibrium equations, an expression is developed which relates the joint rotation to the deformations of the adjacent joints and the member properties. The detailed derivation of this equation is given in APPENDIX B. A set of equations is generated by applying the moment equilibrium equation to all the beam-to-column joints in turn. The joint rotations are then computed using the Gauss-Seidel Iteration Method. The moments at potential hinge locations in the members of the substitute frame can now be computed. Next the vertical and horizontal shears at the junctions of the wall and frame system are computed.

5. At each floor level, the moment to be applied to the wall system for the next cycle of iteration, M_{Wi}, is the algebraic sum of the moment, M_{WBi}, at the end W_i of the right beam and the moment produced by the beam shear multiplied by half the wall width. FIGURE 3.5 shows typical

forces at floor level i. In the initial iteration, the moment, M_{Wi}, is assumed to be zero. This is corrected in subsequent cycles.

6. The net out-of-balance forces are applied to the wall and the resulting deflections, $\Delta_{Wi}^{(2)}$, rotations $\theta_{Wi}^{(2)}$ and vertical displacements $\delta_{Wi}^{(2)}$ are computed as described in Step (3).

7. In order to speed convergence, the frame is not forced into the deformation mode defined by $\Delta_{Wi}^{(2)}$, etc. Instead the frame is forced into the position defined by:

$$\theta'_{Wi}^{(2)} = \frac{\theta_{Wi}^{(1)} \cdot \theta_{Wi}^{(1)}}{\theta_{Wi}^{(1)} - \theta_{Wi}^{(2)}} \qquad \ldots\ldots(3.3)$$

$$\Delta'_{Wi}^{(2)} = \frac{\Delta_{Wi}^{(1)} \cdot \Delta_{Wi}^{(1)}}{\Delta_{Wi}^{(1)} - \Delta_{Wi}^{(2)}} \qquad \ldots\ldots(3.4)$$

and $\delta'_{Wi}^{(2)} = \theta'_{Wi}^{(2)} \cdot D_{Wi}/2$ $\qquad \ldots\ldots(3.5)$

where D_{Wi} is the width of the shear wall at the i th floor. The analysis now returns to Step (4) and the steps (4) to (7) are repeated. For any cycle (after the initial cycle), the forcing Equations (3.3), (3.4) and (3.5) are replaced by:

$$\theta'_{Wi}^{(n)} = \frac{\theta_{Wi}^{(1)} \cdot \theta_{Wi}^{(n-1)}}{\theta_{Wi}^{(n-1)} - \theta_{Wi}^{(n)}} \qquad \ldots\ldots(3.6)$$

$$\Delta'_{Wi}{}^{(n)} = \frac{\Delta_{Wi}{}^{(1)} \cdot \Delta_{Wi}{}^{(n-1)}}{\Delta_{Wi}{}^{(n-1)} - \Delta_{Wi}{}^{(n)}} \qquad \dots\dots(3.7)$$

and $\delta'_{Wi}{}^{(n)} = \theta'_{Wi}{}^{(n)} \cdot D_{Wi}/2 \qquad \dots\dots(3.8)$

where n denotes the cycle in progress.

For any cycle (except the initial cycle) convergence tests for rotations and deflections are performed at the end of Step (5) to determine whether further iteration is required.

The system has converged if the quantities

$$\frac{\theta'_{Wi}{}^{(n)} - \theta'_{Wi}{}^{(n-1)}}{\theta'_{Wi}{}^{(n)}} \qquad \text{and} \qquad \frac{\Delta'_{Wi}{}^{(n)} - \Delta'_{Wi}{}^{(n-1)}}{\Delta'_{Wi}} \qquad \text{are less}$$

than a specified limit.

8. If the system has not converged as defined above, then force F_i and moment M_{WBi} (FIGURE 3.5) at each floor are applied on the shear wall and the Steps from (6) to (8) are repeated.

9. On the other hand, if the system has converged, the P-Δ effect is considered next. The total axial load at each floor level of the structure has been read into the program. The increased story shears due to the P-Δ effect are simulated by increasing the applied lateral loads. The additional force H'_{1i} is calculated on the basis of the deformations obtained from the analysis under the lateral

loads H_i. The derivation is given in section 3.4. Next the lateral loads $(H_i + H'_{1i})$ are applied on the shear wall system and Steps (3) to (8) are repeated. The deformations of the structure obtained from this analysis are compared with the deformations obtained from the analysis under lateral loads H_i only.

10. If the deformations obtained from the two analyses do not agree (within a specified limit) new additional forces H'_{2i} are computed as above using the deformations of the structure taken from Step (9). Steps (3) and (10) are then repeated until the desirable agreement in deformations at each floor level are achieved.

11. If the deformations agree, the shear resisted by the frame is then deducted from the total lateral load to determine the shear to be resisted by the wall.

12. The program then proceeds for detection of hinges by comparison of computed moments at critical sections to that of their plastic moment capacity. If no hinges have formed the lateral loads are increased by a preset factor times the original starting load and step (3) through (11) are repeated. One incrementing factor is used in the elastic range and a second smaller incrementing factor is used after hinging has occurred. If, on the other hand, hinges are detected for the first time in the history of the analysis the locations and moment values are printed out and the loads are decreased to the

previous values increased by the load increment to be used for the inelastic range. When hinges are detected in the first loading the previous load is assumed to be zero. Following this, steps (3) through (12) are repeated.

From now on the loads are incremented by the inelastic factor and steps (3) through (12) are repeated to get the load-deflection characteristics.

The analysis ends if: 1. the desired number of points on the load-deflection curve has been obtained; 2. the lateral deflections have become larger than a preset value; 3. convergence within given limit is not achieved in a given cycle.

The manner in which the inelastic action has been included, implies that the stiffness deterioration lags the actual stiffness deterioration by one load increment. To minimize this effect, it is desirable to use smaller increments in the inelastic range.

3.4 Inclusion of the P-Δ Effect

The P-Δ effect plays a dominant role in the behaviour of flexible structures. The vertical load ,P, on the structure, acting through a side-sway displacement, Δ, produces an additional overturning moment commonly known as the P-Δ moment. Consider a single story structure, which has been displaced by an amount Δ and is subjected to vertical loads, P,

as shown in FIGURE 3.7. To balance the P-Δ moment an additional shear of $P\Delta/H_s$ is required in the columns of the frame.

In this analysis, the P-Δ effect has been taken into account by analyzing the structure under an equivalent lateral force. In FIGURE 3.8(a), H_i is the applied lateral load at the i th floor. Due to this applied lateral force system, a lateral deflection Δ_{1i} will be produced.

The story moment between the i th and (i-1)th floor due to the P-Δ effect is obtained by taking moments about the i th floor of all the axial loads above this level. Similarly, by taking moments at each level, the other story moments are obtained. The extra shear due to the P-Δ effect, V'_i, is given by:

$$V'_i = \frac{P_i(\Delta_{1i} - \Delta_{1(i-1)})}{H_{si}} \qquad \ldots(3.9)$$

where H_{si} is the story height and P_i is the total vertical load on the structure above the i th floor.

The additional lateral load, H'_{1i}, simulating the P-Δ effect can then be determined and is given by:

$$H'_{1i} = V'_1 - V'_{i+1} = P_i(\Delta_{1i} - \Delta_{1(i-1)})/H_{si}$$

$$- \frac{P_{i+1}(\Delta_{1(i+1)} - \Delta_{1i})}{H_{s(i+1)}} \qquad \ldots(3.10)$$

The structure is now reanalyzed under the lateral force system, $H_i + H'_{1i}$ (without considering vertical loads). In FIGURE 3.8(b), Δ_{2i} is

the lateral deflection corresponding to the new lateral force system.
The deflections Δ_{2i} etc. are then compared with the deflections, Δ_{1i}
etc. If these deflections do not agree (within a specified convergence
limit) the additional horizontal force, H'_{2i}, due to the P-Δ effect
for the next cycle is given by :

$$H'_{2i} = \frac{P_i(\Delta_{2i} - \Delta_{2(i-1)})}{H_{si}} - \frac{P_{i+1}(\Delta_{2(i+1)} - \Delta_{2i})}{H_{s(i+1)}} \qquad \dots\dots(3.11)$$

The structure is again analyzed under the lateral force
system $H_i + H'_{2i}$. The process is continued until the changes in
lateral deflections are within the convergence limit.

The vertical load at each floor level has been read into the
program. In the present method of simulating the P-Δ effect a constant
vertical load has been used throughout the analysis. In the actual
structure the girder shears will introduce tension in one column and
compression in the other. This will not change the total vertical
load or the gross P-Δ effect.

3.5 Functions of the Main Program and Subroutines

To perform the computer analysis, several subroutines were
employed in conjunction with the main program. A brief description
of these subroutines are presented here.

In the 'MAIN' program, the number of problems to be solved
is read in. The Subroutine "SR" is called. This subroutine reads in
the data required for the analysis of the first structure. It computes
the co-ordinates of each floor from the base and the stiffness of all

the members. All the input quantities are printed out. Control is then returned to the 'MAIN' program.

The maximum number of load increments to be used in the analysis is specified. The initial load system (i.e. first increment) is applied to the shear wall system.

Subroutine 'BAKA' is called. 'BAKA' computes the distribution of lateral load between the frame and the shear wall systems. The moments and deformations at each segment of the wall are computed. The convergence formula is then applied (except in the first cycle) to the deflections and rotations. The deformations as computed by the convergence formula are enforced on the frame system. The joint rotations of the frame system are computed in Subroutine 'FRAME' by the Gauss-Seidel Iteration Method. In 'BAKA', the moments at all locations are compared with the plastic moment capacities (except during the first load increments). If a hinge is detected, the moment is set equal to the plastic moment capacity for all subsequent load increments. The deformations are compared with those of the previous cycle of iteration. If the deformations are within preset limit of one another, control returns to the 'MAIN' program. If the deformations are not within the preset limit, the process is repeated within 'BAKA'. In this manner the forces and deformations (elastic) for a given loading condition are completely known.

Equivalent horizontal forces simulating the P-Δ effect are computed. These are added to the initial horizontal load and the total forces are then applied to the structure. The structure is analyzed by

recalling Subroutine 'BAKA'. The deflections obtained from the two analyses (i.e. with and without axial load) are compared; if they are within preset limit, the results of the last analysis are printed out by Subroutine 'ROFA' and 'SR3'..

On the other hand, if the deflections are not within preset limit, new equivalent horizontal loads, are computed on the basis of the latest set of deflections. The process is repeated until the deflections have converged.

Inelastic action of the shear wall is considered in the 'MAIN' program. At each segment of the shear wall, the computed moment is compared with the plastic moment capacity. If the moment exceeds the plastic moment capacity of the story, the moment of inertia of the plastified wall segment is reduced according to the M-ϕ diagram. This reduced stiffness is used in subsequent steps in the analysis.

In Subroutine 'SR1', the formation of plastic hinges in the members of the frame system is detected.   If a hinge is detected, the location of the plastic hinge is printed out with the magnitude of the moment. Control then returns to 'MAIN' program.

If the structure is still elastic, the horizontal load is incremented and the structure is reanalyzed. On the other hand, if a hinge has formed at some location in the structure, the horizontal load is decremented so that the structure is still elastic. The structure is then reanalyzed with this reduced load. Subsequent increments in

load are reduced in magnitude to trace the inelastic range as closely
as possible. The program stops for the reasons specified earlier.
It then returns to beginning to analyze the next structure.
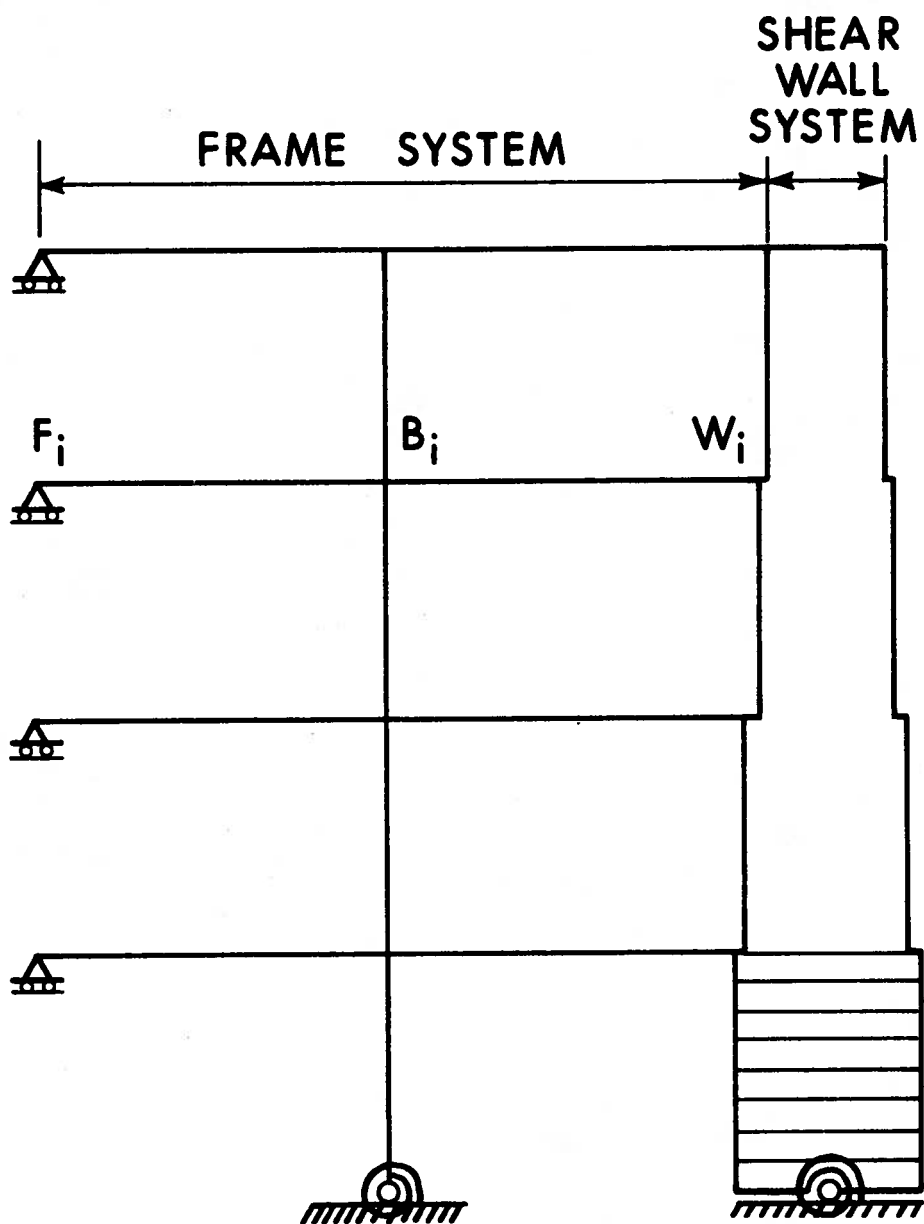
FIGURE 3.1 ANALYTICAL MODEL FOR ANALYSIS
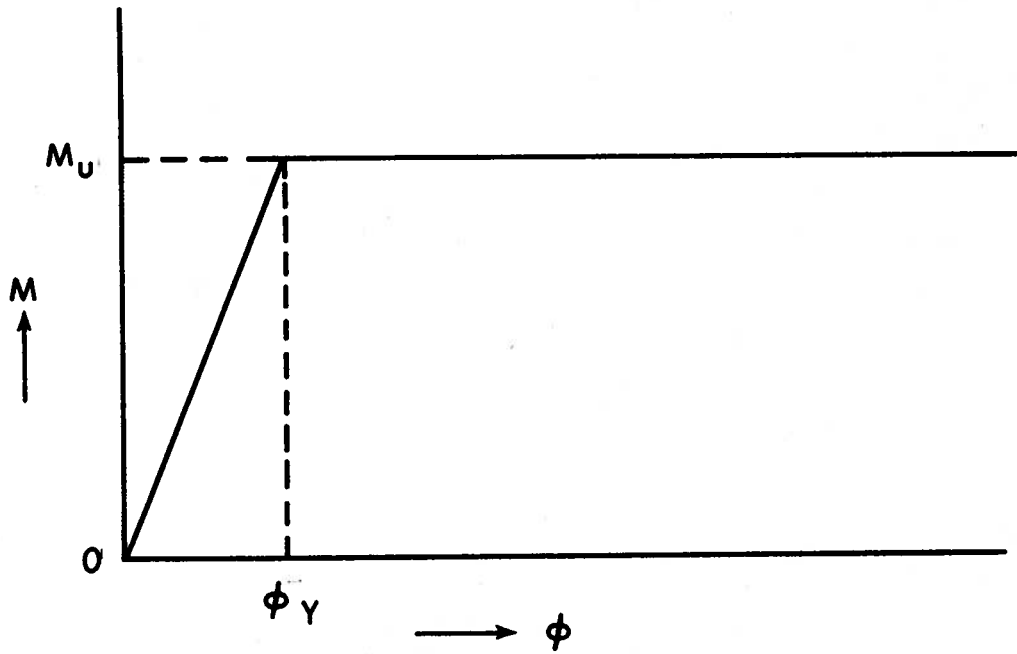
(a) FOR BEAMS AND COLUMNS
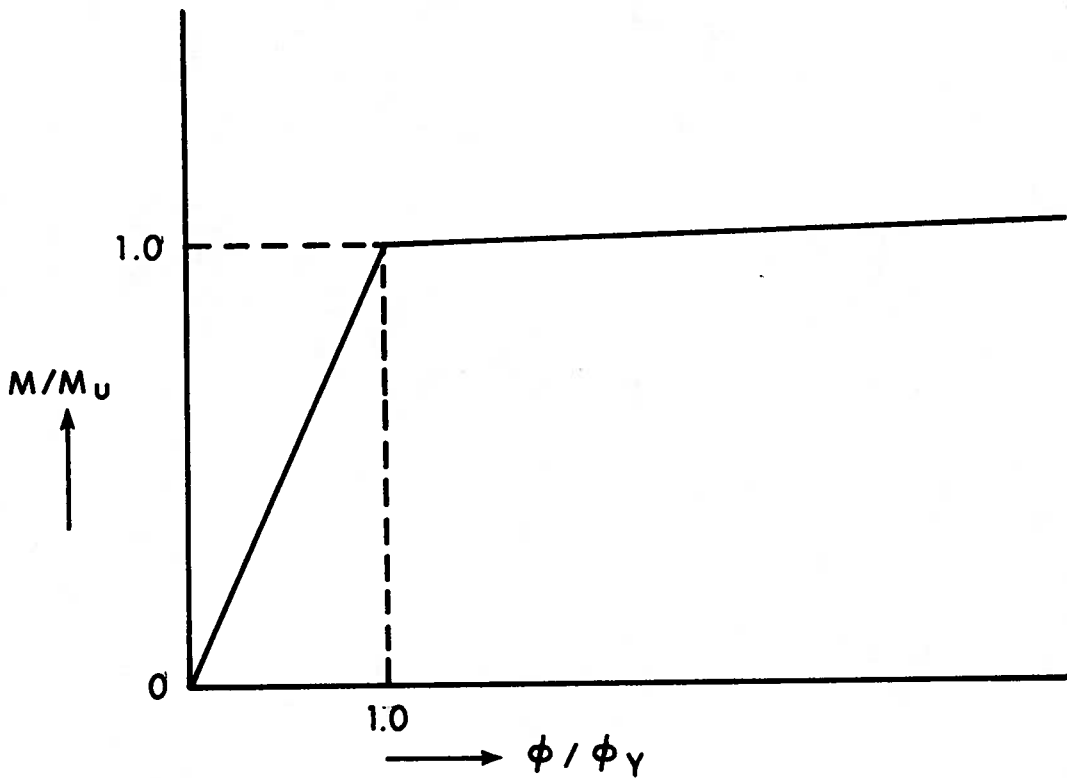
(b) FOR WALLS

FIGURE 3.2 MOMENT CURVATURE RELATIONSHIP

41
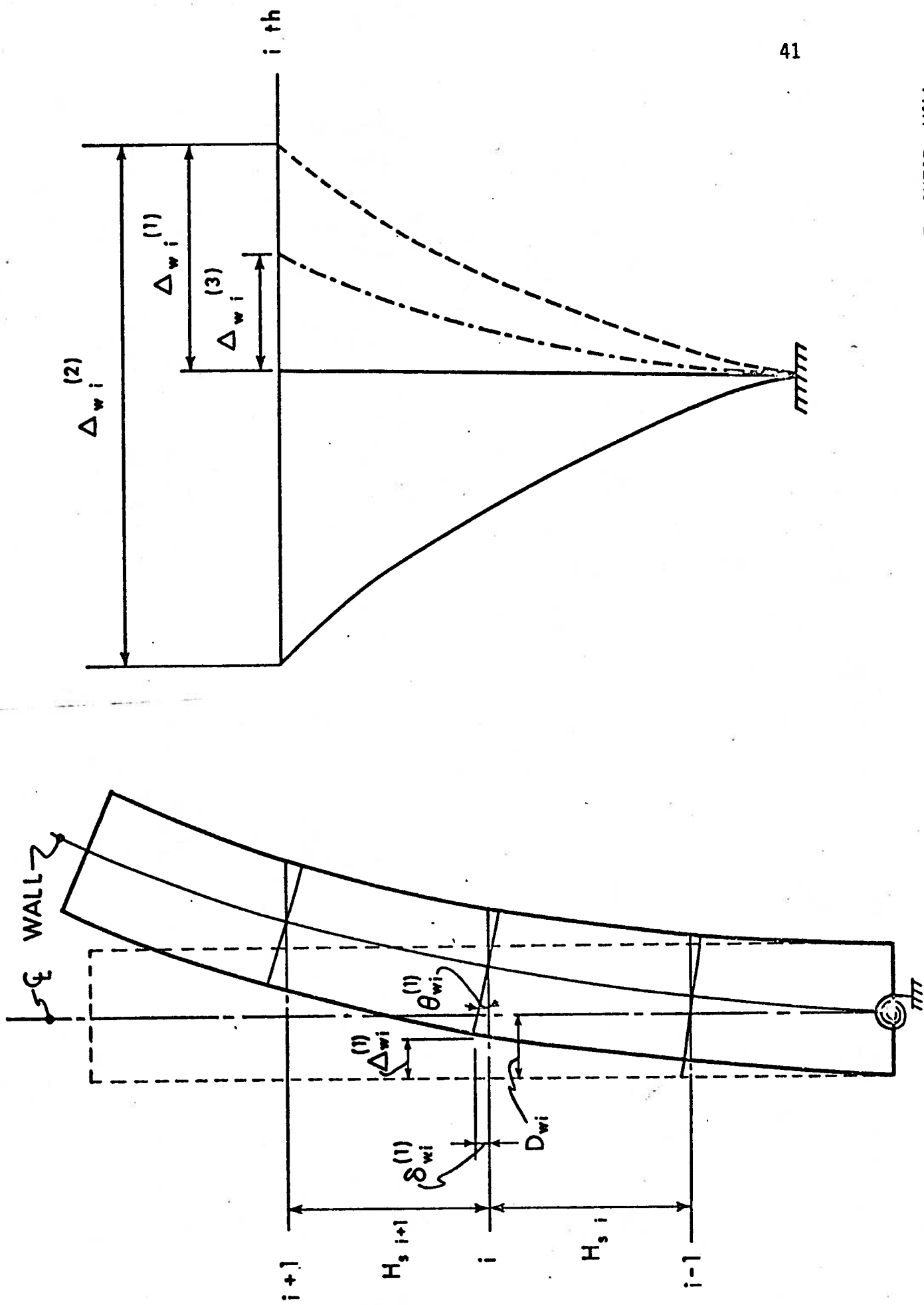
FIGURE 3.4 DEFLECTED SHAPE OF THE SHEAR WALL
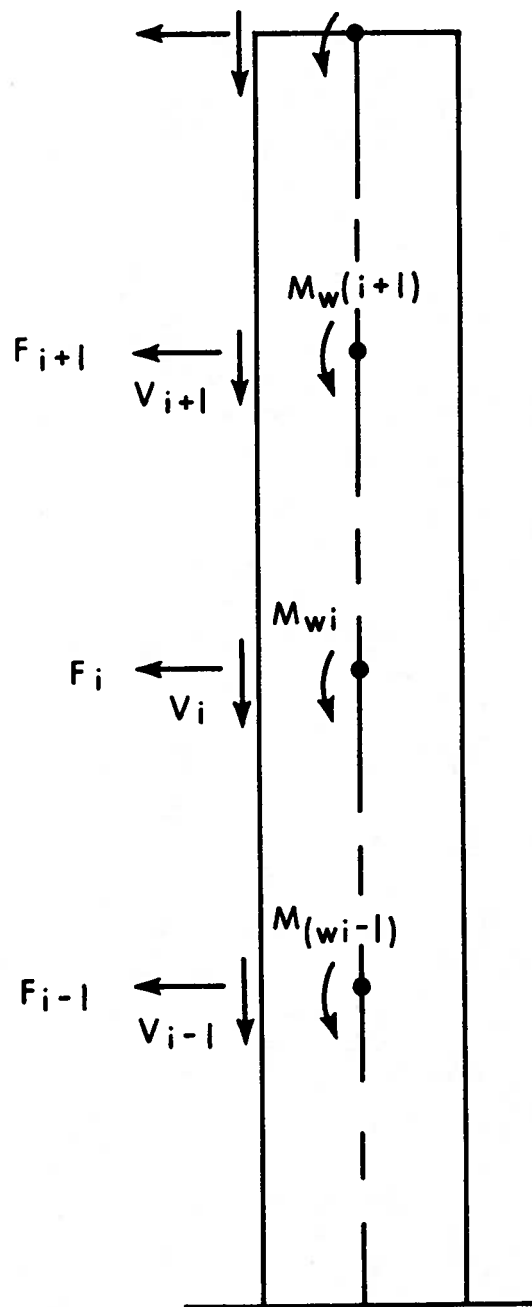
FIGURE 3.5 STRESSES IN WALL SYSTEM DUE TO FORCE FITTING
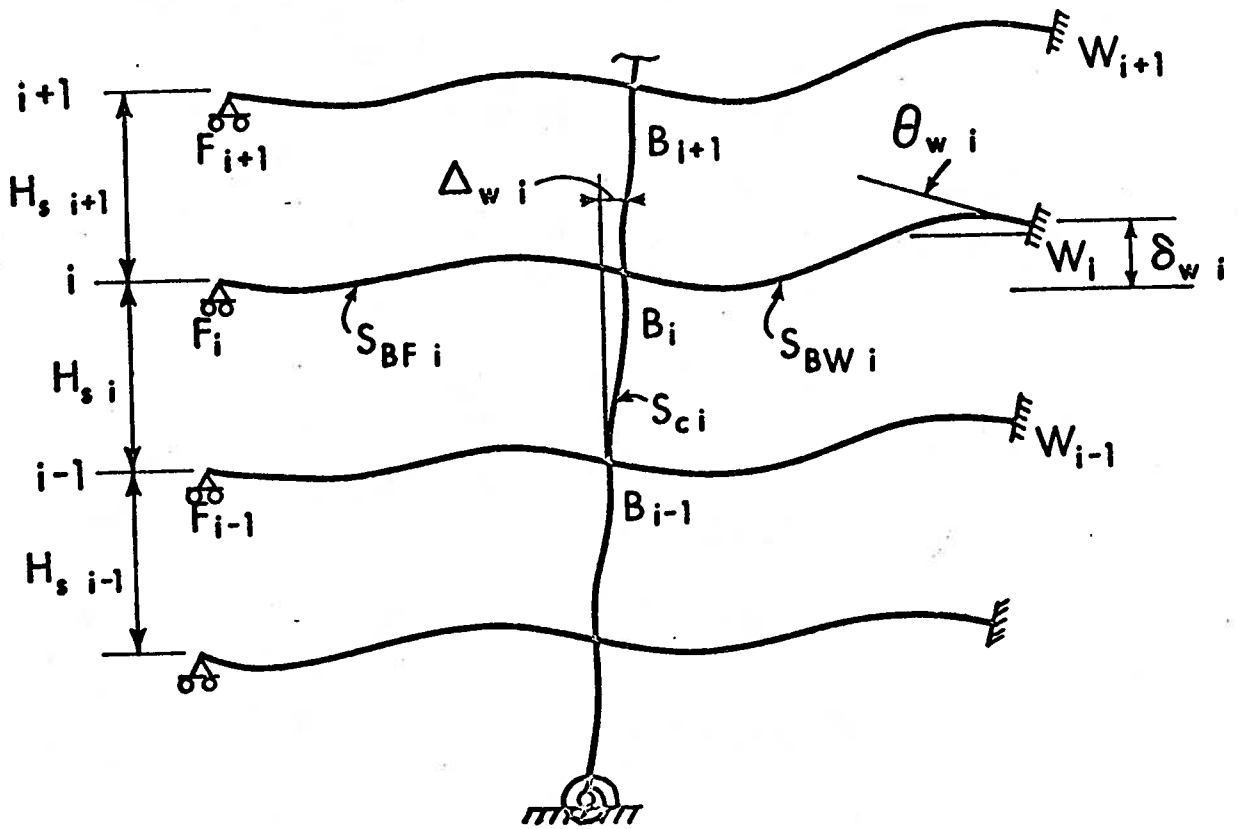
FIGURE 3.6 DEFELECTED FRAME

FIGURE 3.8 P - Δ EFFECT - MULTI - STORY STRUCTURE

44
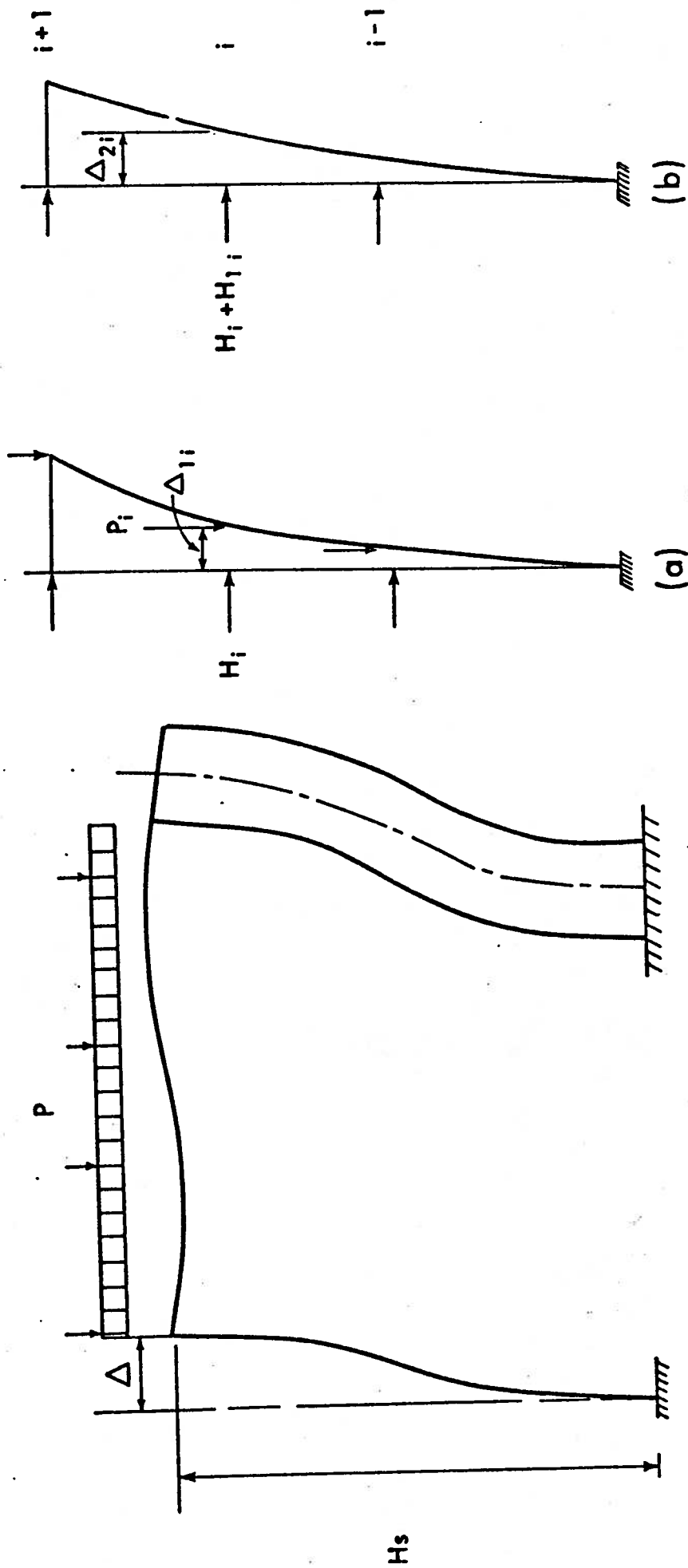
FIGURE 3.7 P - Δ EFFECT - SINGLE STORY FRAME

CHAPTER IV

RESPONSE OF CROSS-SECTIONS

4.1 Introduction

The theoretical analysis presented in CHAPTER III assumes
that the behaviour of cross-sections of the members can be represented
by bi-linear moment-curvature relationships. A method of tracing the
theoretical load-moment-curvature (P-M-ϕ) response of reinforced
concrete cross-sections is presented in this CHAPTER. This analysis
predicts the ultimate capacity of the cross-section and the response
of the cross-section at loads less than the ultimate load. It differs
from previous analysis by considering the tensile stresses in the
concrete. The theoretical load-moment-curvature diagrams were used
in the computation of moments and thrust from the curvatures measured
in the frame test. Approximate load-moment-curvature diagrams based
on the theoretical diagrams are also presented in this CHAPTER. These
are intended for use in design.

Throughout this CHAPTER the abbreviation P-M-ϕ will be
used to refer to the term "load-moment-curvature".

4.2 Analysis of Load-Moment-Curvature Response of Reinforced Concrete Cross-Sections

For the purpose of this report, moment-curvature relationships

will be computed for the case of constant axial load and changing moment and curvature. For a known value of axial load and curvature, it is possible to find the value of moment by trial and error. This can be repeated for different values of curvature to get the entire moment-curvature relationship for the given axial load. The procedure can be repeated for as many different values of axial loads as necessary to get a set of moment-curvature characteristics for the section. If desired, interaction diagrams can be prepared from these curves.

The following assumptions were made in deriving the $P-M-\phi$ relationships for reinforced concrete section:

1. The section is rectangular.

2. The stress-strain curves for concrete and reinforcing steel are those presented in section 4.2.1 and 4.2.2, respectively.

3. The maximum stress developed in concrete is 0.85 times the standard 28 day compressive strength. This has been verified by extensive tests[H1].

4. At all loads, plane section perpendicular to the axis of the member remain plane.

5. Creep and shrinkage deformations are neglected. If desired, creep deformations can be approximated by increasing the short-time strains. This approximation is discussed in references (M2) and (M6).

4.2.1 Concrete Stress-Strain Curve

For the purpose of defining the stress-strain

response of concrete, the stress-strain curves[M5] defined by equations (4.1) and (4.2) are assumed to define the behaviour in compression and tension, respectively, in members loaded in flexure or combined axial load and bending. The relationships are illustrated in FIGURE 4.1 for concrete having a compressive strength of 4000 psi.

$$\frac{f_c}{f_c''} = 2(\frac{\epsilon}{\epsilon_o}) - 1.03 (\frac{\epsilon}{\epsilon_o})^{1.67} \qquad ....(4.1)$$

$$\frac{f_t}{f_t'} = 2(\frac{\epsilon}{\epsilon_{ult}}) - (\frac{\epsilon}{\epsilon_{ult}})^3 \qquad ....(4.2)$$

where
$$\epsilon_o = \frac{2f_c''}{E_c}$$

$$f_t' = 7\sqrt{f_c'}$$

$$\epsilon_{ult} = \frac{2f_t'}{E_c}$$

f_c'' is compressive strength of concrete loaded in flexure and is assumed to be 85 percent of the concrete strength in direct compression[H1].

The stress-strain curves were derived to satisfy the following requirements:

1. The stress-strain curve should be continuous in tension and compression[B12]. In applying the stress-strain curve in this analysis the ACI code value of the modulus of elasticity was used although any other convenient value could be used.

2. Concrete loaded in combined bending and compression is
    assumed to fail at a limiting strain of 0.0035[K3,C7].
    Under these loadings, concrete will generally fail at
    strains greater than this value. If it does this
    assumption will always result in computed ultimate
    moments which are equal to or less than the greatest
    moment, the section can carry. This can be seen from
    an examination of P-M-ϕ diagrams such as those shown
    in FIGURE 4.3.

3. There should be reasonable agreement between measured
    and computed compression stress-strain curves for strains
    less than 0.0035.

4. There should be reasonable agreement between the measured
    and computed tension stress-strain curves [W3].

5. The maximum tensile strength in a split tension test is
    assumed to be $f_t' = 7 \sqrt{f_c'}$ [N1].

6. The modulus of rupture, computed as $f_r = 6M/bt^2$ is
    about 40 percent greater than the tensile strength of
    concrete. That is, the modulus of rupture should be
    about $10 \sqrt{f_c'}$ [N1].

4.2.2 Reinforcing Steel Stress-Strain Curve

        The assumed steel stress-strain for reinforcing
steel is shown in FIGURE 4.2. It is assumed that the yield point
and modulus of elasticity are identical in tension and compression.

The effect of strain hardening was neglected. In view of the large deformations attendant to the development of the stresses in the strain hardening range, this assumption is fairly reasonable.

4.2.3 <u>Computer Analysis for Load-Moment-Curvature Relationship</u>

As the axial loads and moments are varied the cross-section can have three different strain configurations:

1. The full section is under compression.

2. One face of the section is under compression and the other is under tension but uncracked.

3. One face of the section is under compression and the other is under tension and cracked.

The relationships between axial load, fibre strains, moment and curvature for each of these cases are derived in APPENDIX C.

A computer program was written to generate the moment-curvature relationship for a given axial load. The program was written for IBM, OS/360 system in Fortran IV language. The flow diagram, the nomenclature used in the program and a listing of the program are given in APPENDIX C. The principal steps in the program are described below:

1. The number of cross-sections to be analyzed and the material properties, cross-sectional dimensions and axial load, P, on each section are read. If the ten-

sile stresses in the concrete are to be neglected, the ultimate tensile strain is specified as zero. The area of steel in each layer and the distance from the tension face to the respective centroids is also read. The pertinent data are then written out.

2. The ultimate capacity of the section under pure axial load is then calculated in the form $P/btf_c"$. This is the upper limit of axial load on the section. If this axial load is less than the axial load under consideration, computations are terminated.

3. A value of curvature times depth, ϕt, is assumed.

4. A trial value of extreme compressive face strain, ε_4, is assumed and the extreme tensile face strain corresponding to the curvature assumed in step (3) is then computed.

5. The subroutine "PM" is then used to find the corresponding strains in each layer of steel and the strain domain for the calculation of axial load and moments. This subroutine then calculates the load, $P/btf_c"$, and the moment, $M/bt^2f_c"$, for the assumed strain distribution.

6. The calculated value of the load, $P/btf_c"$, is then compared with the value of $P/btf_c"$ for which the P-M-ϕ curve is being computed. If the difference is one percent or less, it is assumed that a solution has been

found which satisfies P, M, ϕt, and ε_4. The computed moment and curvature represent one point on the load-moment-curvature diagram for the cross-section. For values of P/btf_c'' less than 0.05, an acceptable solution is assumed to exist when P/btf_c'' differs from the given value by 0.001 or less. If the convergence is not satisfactory the extreme compressive fibre strain is increased by 0.000001 and steps (4) through (6) are repeated in order until the loads converge.

7. Following convergence in Step (6) the value of curvature is then increased to find another point on the P-M-ϕ diagrams and steps (4) through (7) are repeated in order. This is continued until the maximum compression strains reach 0.0040 at which time the program moves on to consider another section. The limiting strain of 0.0040 was taken so that a point near the strain of 0.0035 could be found in the data.

This program was also modified to generate P-M-ϕ diagrams for a given cross-section subjected to a series of values of P/btf_c'' ranging in increments of 0.1 from 0.0 to the ultimate axial load capacity of the cross-section. The maximum moment from each of these curves is stored and used to construct an interaction diagram for the column cross-section.

4.3 Effect of Various Parameters on Load-Moment-Curvature Relationships

Prior to discussing the approximate P-M-ϕ relationships assumed in the analysis the main parameters affecting this relationship will be studied. For this study a symmetrically reinforced, rectangular cross-section, 2 percent longitudinal reinforcement in each of the two faces, 4,000 psi concrete strength and 50,000 psi steel strength with a cover ratio of 0.1 was chosen. The basic section is illustrated in FIGURE 4.3.

4.3.1 Effect of Axial Load

P-M-ϕ diagrams for the basic section with axial loads ratios, P/btf_c'' , equal to 0, 0.2, 0.4, 1.0, 1.2 and 1.4 are plotted in FIGURE 4.3 to show the effect of axial load on the moment curvature relationship. The latter two curves correspond approximately to eccentricity ratios, e/t, of 0.1 and 0.05 respectively while P/btf_c'' equal to 0.4 is approximately the balanced load. The ultimate axial load capacity, P_u/btf_c'' , of the basic section was 1.55. The solid lines in FIGURE 4.3 correspond to compression failures, the broken lines to a balanced failure and the dashed lines to tension failures. The interaction diagram for this column is plotted in FIGURE 4.4 with a solid line. The horizontal lines in this figure correspond to the moment-curvature diagrams in FIGURE 4.3. It can be seen that the stiffness and ultimate moment capacities depend on the axial load on the cross-section. For columns failing in tension the P-M-ϕ diagrams are essentially elastic-plastic. This is not true for columns failing in compression. It can also be seen that the rotation capacity of the cross-section decreases as the load is increased. For high values of axial load

the rotation capacity is very small.

4.3.2 Effect of Cross-Sectional Properties

The basic cross-section was reanalyzed assuming the yield strength of the reinforcement was 40,000 psi. The moment-curvature diagrams for P/btf_c'' equal to 0.3 and 0.8 has been plotted in FIGURE 4.5 for comparison. As can be seen the yield strength of reinforcement does not have any effect on the moment-curvature relationship prior to the yielding of reinforcement. After the reinforcement yields the change in moment capacity is approximately constant and varies roughly in proportion to the yield strength of reinforcing steel. It should be noted that for compression failures the initial non-linearity in the moment-curvature diagram frequently results from the yielding of the compression reinforcement.

To study the effect of concrete strength the chosen section was reanalyzed for 3000 psi concrete strength. Moment-curvature diagrams for the two concrete strength have been compared in FIGURE 4.6 for values of P/bt equal to 1020 and 2040 psi. It can be seen that the reduction in moment capacity due to decrease in concrete strength is more for high value of curvatures and axial loads. By reducing the concrete strength the value of $q = p_t f_y/f_c'$ is increased so that the axial stress of 1020 psi is much closer to the balanced load in the case of 3000 psi concrete than it is for 4000 psi concrete. As a result a reduction in rotation capacity was exhibited as can be seen in

FIGURE 4.6. The intial slope of the curves is reduced a little

as the concrete strength decreases. This corresponds approxi-

mately to a reduction in the portion of the EI term which depends

on the modulus of elasticity of concrete. The rotation capacity,

stiffness and moment capacity are reduced with a reduction in

material strength.

To study the effect of the reinforcement ratio the

chosen section was analyzed for 4 percent and 1 percent total

longitudinal reinforcement. The comparison of the two analyses

is shown in FIGURE 4.7. It is noted that the ultimate capacity

of the section is greatly effected by reinforcement ratio. The

change in the slope of initial part of the curve shown in

FIGURE 4.7 is partly due to the reduction in percentage of

reinforcement. The effect of cracking of concrete will be

discussed later. It can also be seen that rotation capacity

for the beam section ($P/btf_c'' = 0.0$) is larger for smaller percen-

tage of reinforcement.

To study the effect of the cover ratio the chosen

section was analyzed for ratios of d'/t equal to 0.15 and 0.10

for fifteen different axial loads. The values of Mu correspond-

ing to each cover ratio can be compared in FIGURE 4.4 in the

form of interaction diagram. It can be seen that the cover

ratio has a significant effect on the moment capacity of the

cross-section for low axial loads. Under pure moment the ultimate

moments vary essentially in the ratio of the distances between

the layers of reinforcement. The effect of cover on moment

capacity diminishes as the axial load increases. The cover ratio
does not have any effect on the ultimate capacity under pure
axial load

P-M-ϕ diagrams for the values of P/btf_c'' equal to 0.3 and
0.8 and cover ratio of 0.1 and 0.15 are compared in FIGURE 4.8.
It is observed that the increase in cover ratio reduces the stiff-
ness of the section especially at low axial loads. This is due in
part to the reduction in the moment of inertia of the steel about
the centroid of the column.

4.3.3 Effect of Tensile Stress in the Concrete

Moment-curvature diagrams computed with and without
tensile stresses in the concrete are compared in FIGURE 4.7(a)
and (b) for two sections having one and four percent longitudinal
reinforcement for axial loads, P/btf_c'', equal to zero and 0.5 .
The tensile stress in the concrete affects the initial part of
the curve prior to cracking but has no significant effect on the
ultimate capacity of the sections considered. The kink in the
M-ϕ curve of FIGURE 4.7(b) for P/btf_c'' equal to 0.5 is observed
due to the transition of axial load from inside to outside of the
kern of the section.

The effect of the tensile stress diminishes as the
axial load and/or the steel percentage increases. The behaviour
portrayed in FIGURE 4.7(a) for the pure bending case ($P/btf_c'' = 0$)
is quite typical of the behaviour expected from a typical under-

reinforced beam section. In the case of extremely under-reinforced cross-sections, the cracking moment may exceed the ultimate moment of the cracked section resulting in an unstable P-M-ϕ relationship.

4.4 Load-Moment-Curvature Relationship for Use in Approximate Analysis of Reinforced Concrete Shear Wall-Frame Structures.

In the analysis presented in CHAPTER III it is assumed that the load-deflection curve of the structure can be computed by using an idealized elastic-plastic moment-curvature (M-ϕ) relationship for the beams and columns and an elastic-strain hardening moment-curvature diagram for the shear walls as shown in FIGURE 3.2(a) and (b) respectively.

4.4.1 Derivation of Approximate Load-Moment-Curvature Relationships for Use in the Analysis

The assumed P-M-ϕ diagram for a cross-section may be defined by establishing four parameters:

1. The initial slope or EI value.
2. The moment, Mp, at which the curve bends.
3. The slope of the second branch of the curve.
4. The limiting rotation capacity of the section.

If the theoretical P-M-ϕ curves are available, each of these terms can be established by fitting the approximate curve to the theoretical diagram. This procedure was used in deriving the P-M-ϕ curves used in the analysis of the test frame. In the more general design case, however, each of these values must be estimated at least approximately.

1. <u>Value of EI</u> - The stiffness or effective EI of a structural cross-section at any given curvature will be given by the ratio M/ϕ. Using $P-M-\phi$ curves similar to those developed earlier in this CHAPTER, it is possible to define secant or tangent EI values. As shown in FIGURE 4.7, the actual EI varies significantly from this at any stage prior to yielding. This variation may be due to the reinforcement ratio, p_t, the stage of cracking, the axial load level, or a number of other variables discussed in SECTION 4.3.2. Traditionally, structural analysis of concrete structures is based on the EI of the uncracked concrete section. It can be concluded from FIGURES 4.3, 4.5 to 4.8 that in the normal frame, where beams are cracked and have one percent tension reinforcement while the generally uncracked columns have a total of about two to four percent longitudinal reinforcement, the EI of the uncracked concrete section is not sufficiently accurate. This problem has also been discussed by Okamura et al.[O1].

For the design of slender columns the ACI column committee[M9] has proposed the following value of EI:

$$EI = \frac{E_c I_c}{5} + E_s I_s \qquad \qquad ....(4.3)$$

where E_c and E_s are the modulus of elasticity of concrete and steel respectively. I_c and I_s are the moments of inertia of the concrete and the steel, respectively, about centroidal axis. As shown in reference (M9), however, the equation (4.3) tends to underestimate the effect of the concrete term and overestimate

the steel term. A somewhat better approximation would be:

$$EI = \frac{E_c I_c}{2.5} + 0.85\ E_s I_s \qquad \ldots.(4.4)$$

This value is plotted with fine radial lines on FIGURES 4.3, 4.5 to 4.8. The examination of these lines reveals that the equation (4.4) gives the same trends as the main variables discussed in section 4.3.

For the preliminary calculations, the EI values of the members of the structure could be approximated, using the equation (4.4), assuming rectangular beams with one percent reinforcement in each face and assuming the columns have two percent reinforcement in each face. Shear walls may be assumed to have one percent reinforcement.

2. <u>Value of M_p</u> - The ultimate moment capacity of the cross-section varies significantly as shown in FIGURES 4.3 to 4.8. This variation may be due to axial load level, reinforcement ratio, p_t, or a number of other variables discussed in section 4.3. The ultimate moment capacities, M_p, for a given reinforced concrete section can be obtained by drawing interaction diagram of the form shown in FIGURE 4.4. However, it is not always possible to draw such diagrams easily. For simplicity in preliminary calculations, the M_p values of the members of structure could be taken as equal to the ultimate moment of the section for the loading considered as computed by ACI code. This is somewhat a conservative estimate.

3. <u>Slope of Second Branch of the Curve</u> -   For beams and
columns the slope of the second branch of the P-M-φ curve is
assumed equal to zero. This approaches the truth for loads less
than the balanced load as shown by the dashed lines in FIGURE 4.3.
For columns failing in compression, plotted in solid lines in
FIGURE 4.3, it is necessary to arbitrarily approximate the theoreti-
cal curve with two straight lines. For the shear wall this slope
is assumed to be positive, non-zero and small. This will generally
be a reasonably good assumption for practical shear walls near
the base of a building.

4. <u>Rotation Capacity</u> -   For simplicity an infinite
rotation capacity will be assumed for the section. This is
reasonably true for sections failing in tension in view of the
large rotational capacities of such sections as can be seen in
FIGURES 4.3, 4.5 to 4.8. It is not good assumption for columns
failing in compression. For this reason hinges should not be
allowed to occur in columns unless special binding is provided
in the region of the hinge. This is discussed more fully in
reference (C6).

4.4.2 <u>Discussion of Assumed Load-Moment-Curvature Relationship</u>

The load-moment-curvature relationship was assumed to
be elastic perfectly plastic for the columns and beams and an
elastic-strain hardening relationship was assumed for the wall.
The slope of the strain-hardening range will generally be assumed
to be small.

Several moment-curvature diagrams showing the effect of various parameters have been presented in SECTION 4.3. In general it is concluded that a normal beam section closely approximates the assumed elastic-perfectly plastic moment-curvature diagram with a long range of rotation capacity. Therefore the idealization made here is quite reasonable since the error involved is very small. Furthermore the rotational capacity of a normal beam is very large and will not limit the strength of the structure.[C6].

For axially loaded sections failing in tension, that is, for section in which the reinforcement yields before the concrete crushes, the moment-curvature diagram was found to approach the idealised diagram. Therefore this assumption seems to be quite reasonable for the axial loads below the balanced load of the section.

For column sections it was found that the moment-curvature diagrams tend to move away from the elastic-perfectly plastic relationship as the axial load is increased. The sections failing in compression exhibited curved moment-curvature diagrams rather than bi-linear diagrams. In addition, these sections had a very limited rotational capacity. For the columns, the sections could be so chosen that a weak beam and strong column design is achieved for the building.
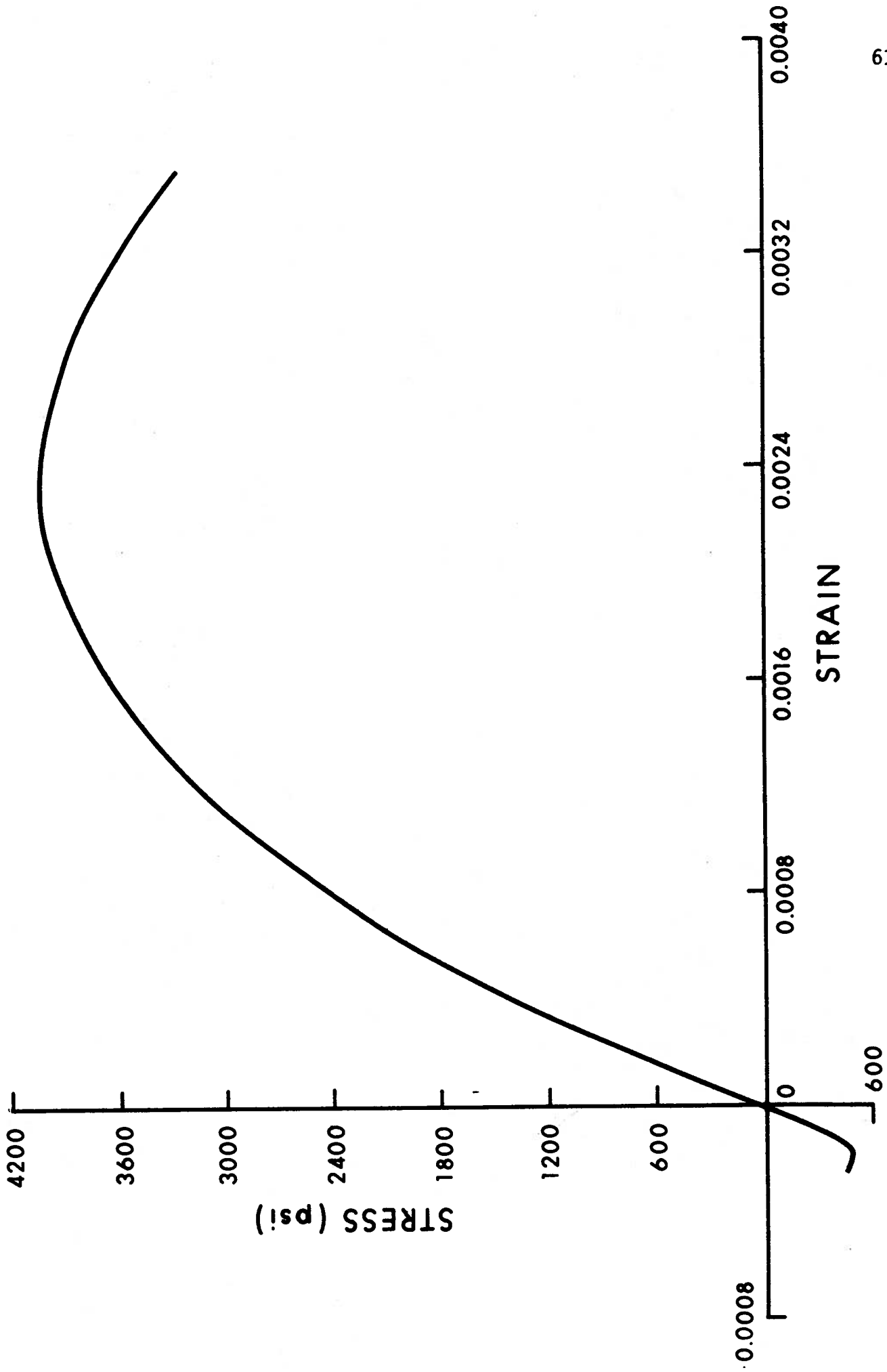
FIGURE 4.1 STRESS - STRAIN CURVE FOR 4000 PSI CONCRETE

61
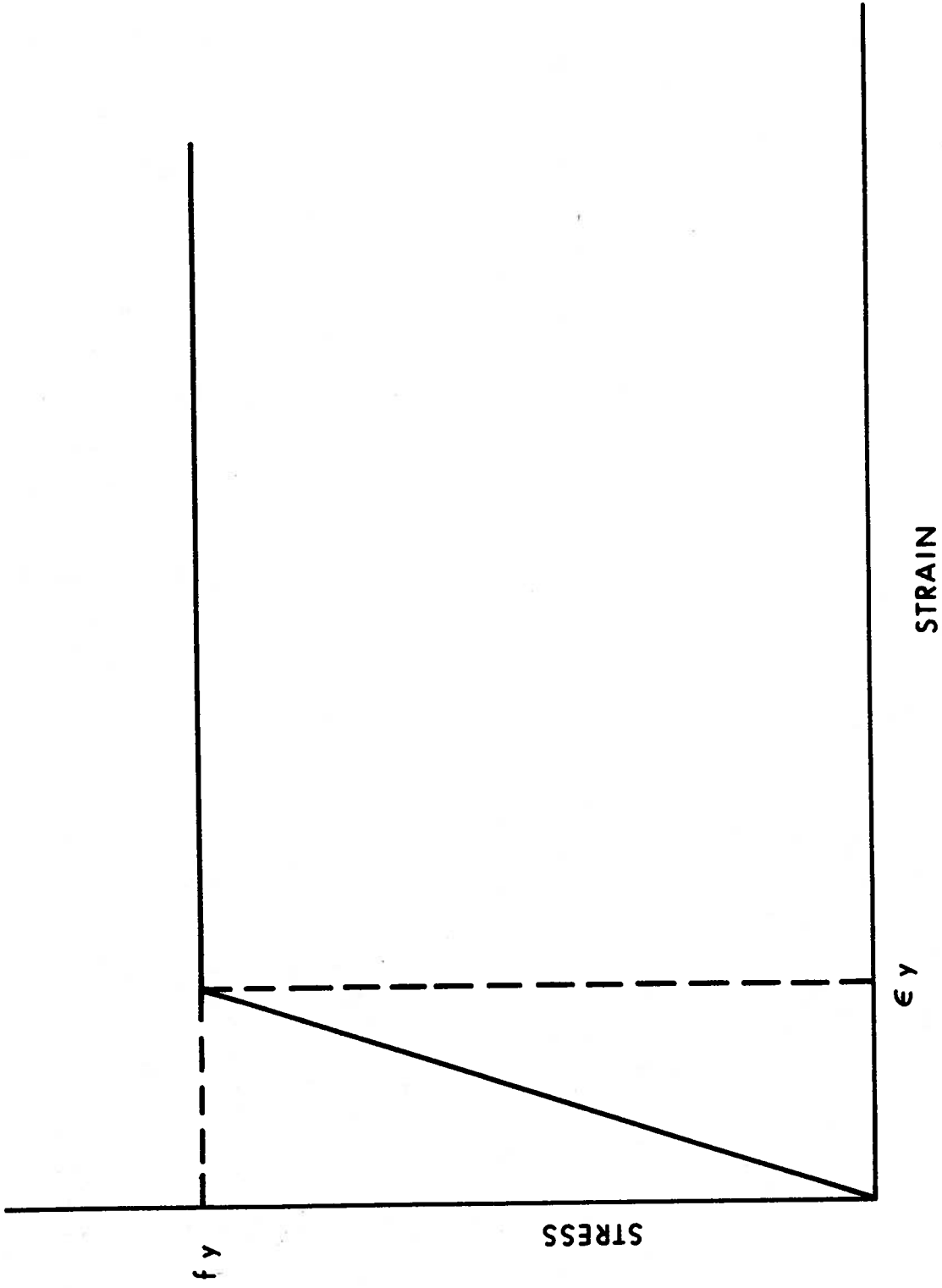
STRAIN

FIGURE 4.2 ASSUMED STRESS - STRAIN CURVE FOR REINFORCING STEEL
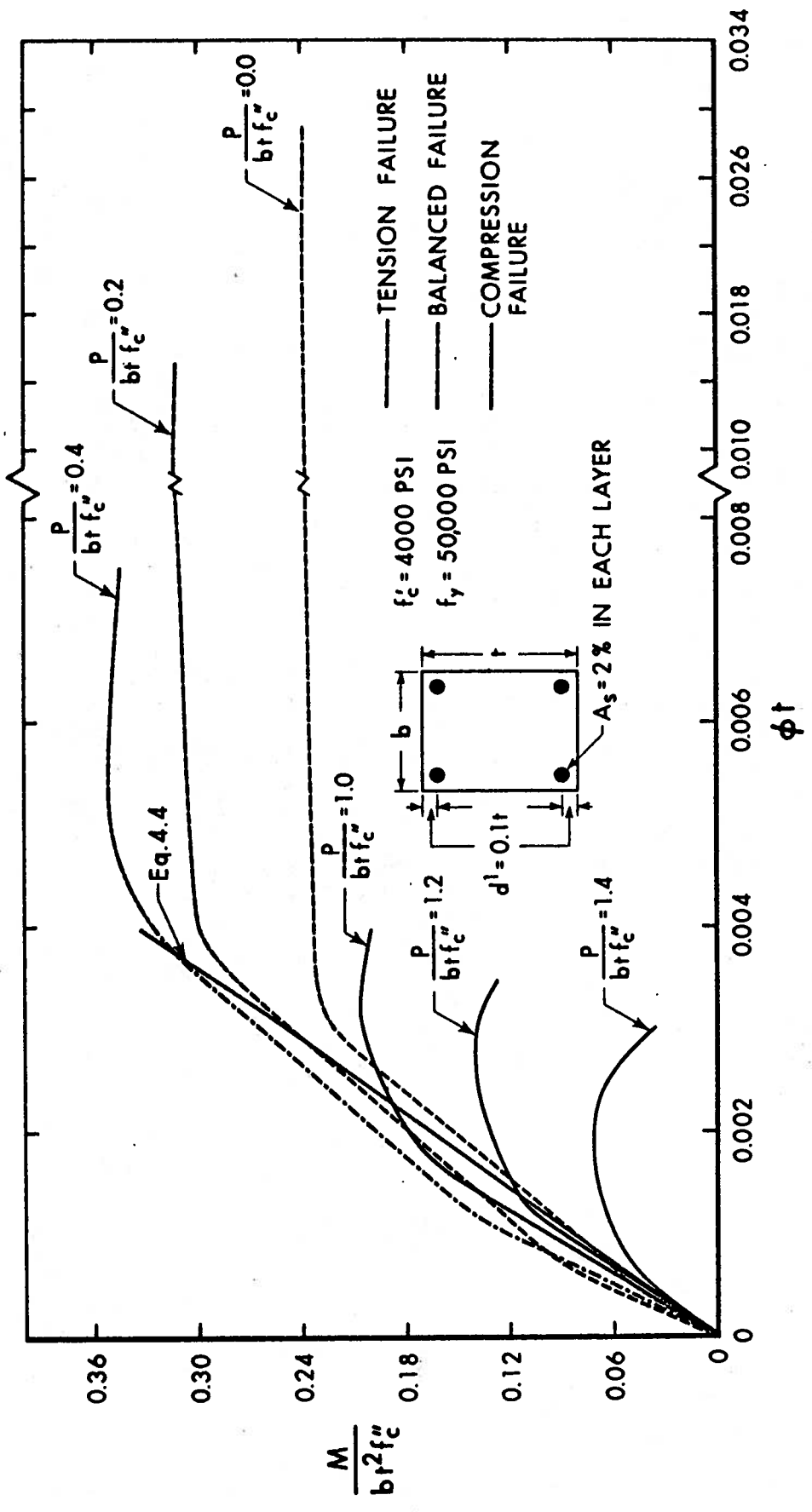
FIGURE 4.3 EFFECT OF AXIAL LOAD ON MOMENT CURVATURE

DIAGRAM FOR TIED COLUMN
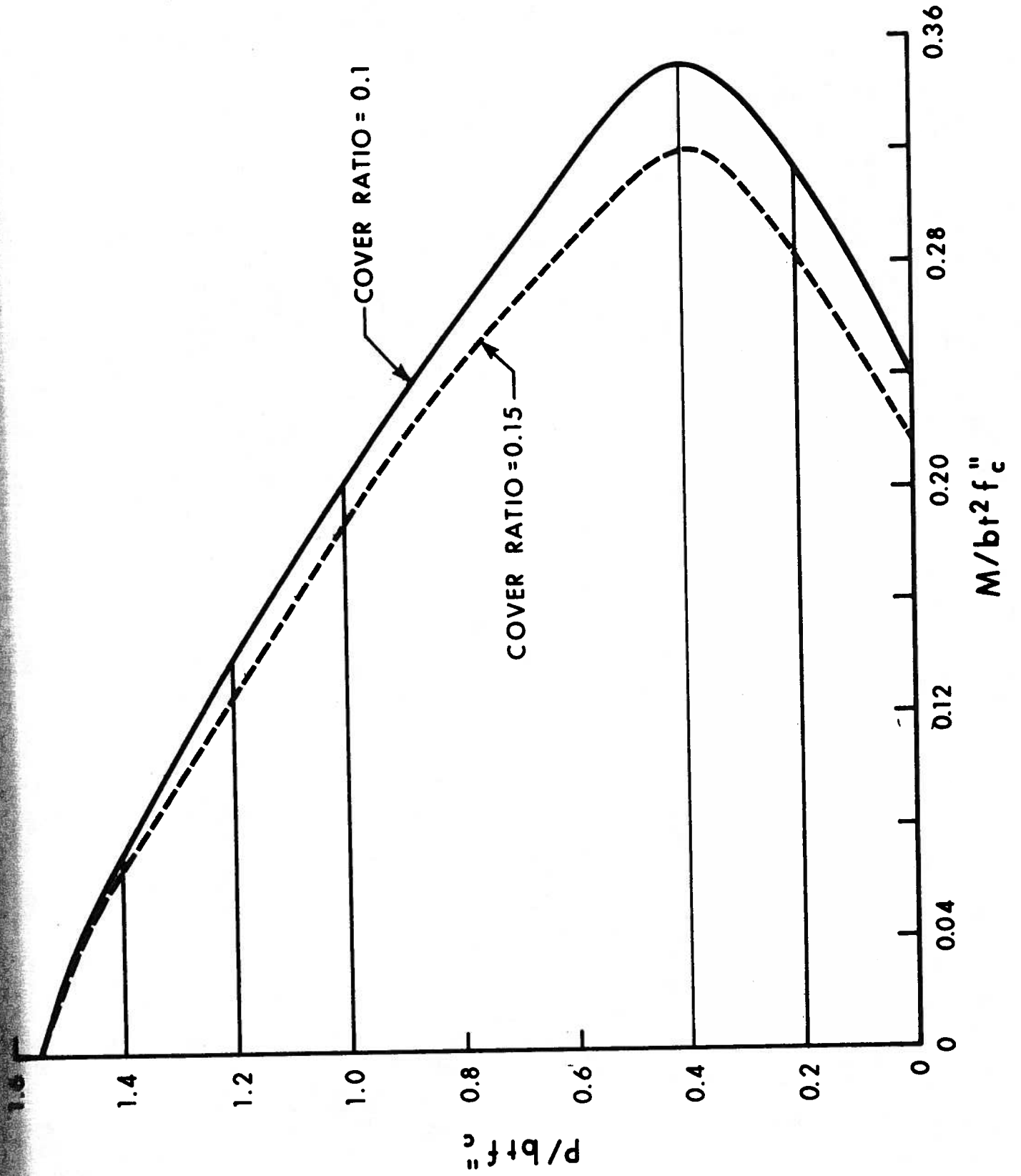
FIGURE 4.4 INTERACTION DIAGRAM FOR TIED COLUMN
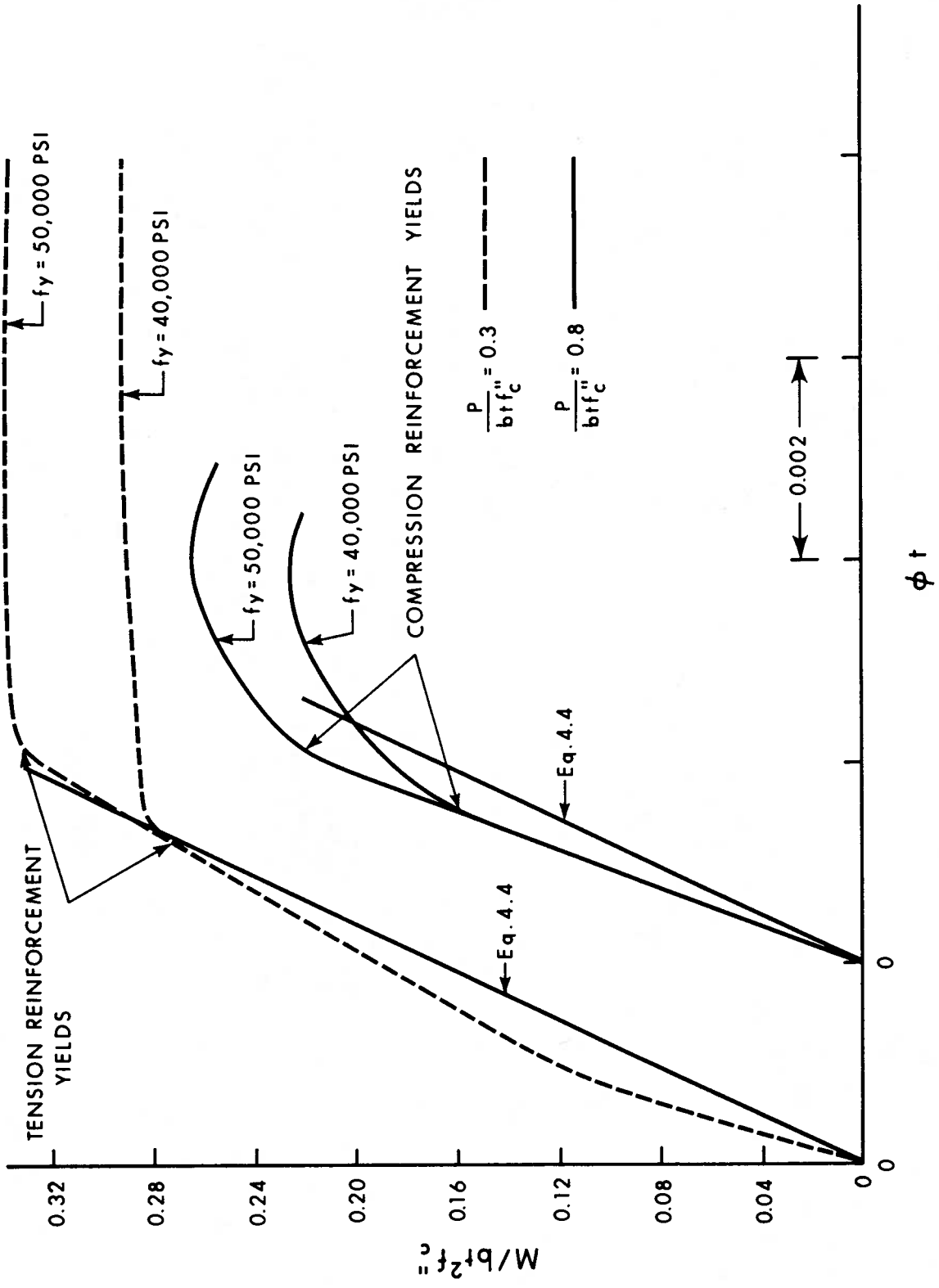
FIGURE 4.5 EFFECT OF YIELD STRENGTH OF STEEL ON MOMENT CURVATURE DIAGRAM
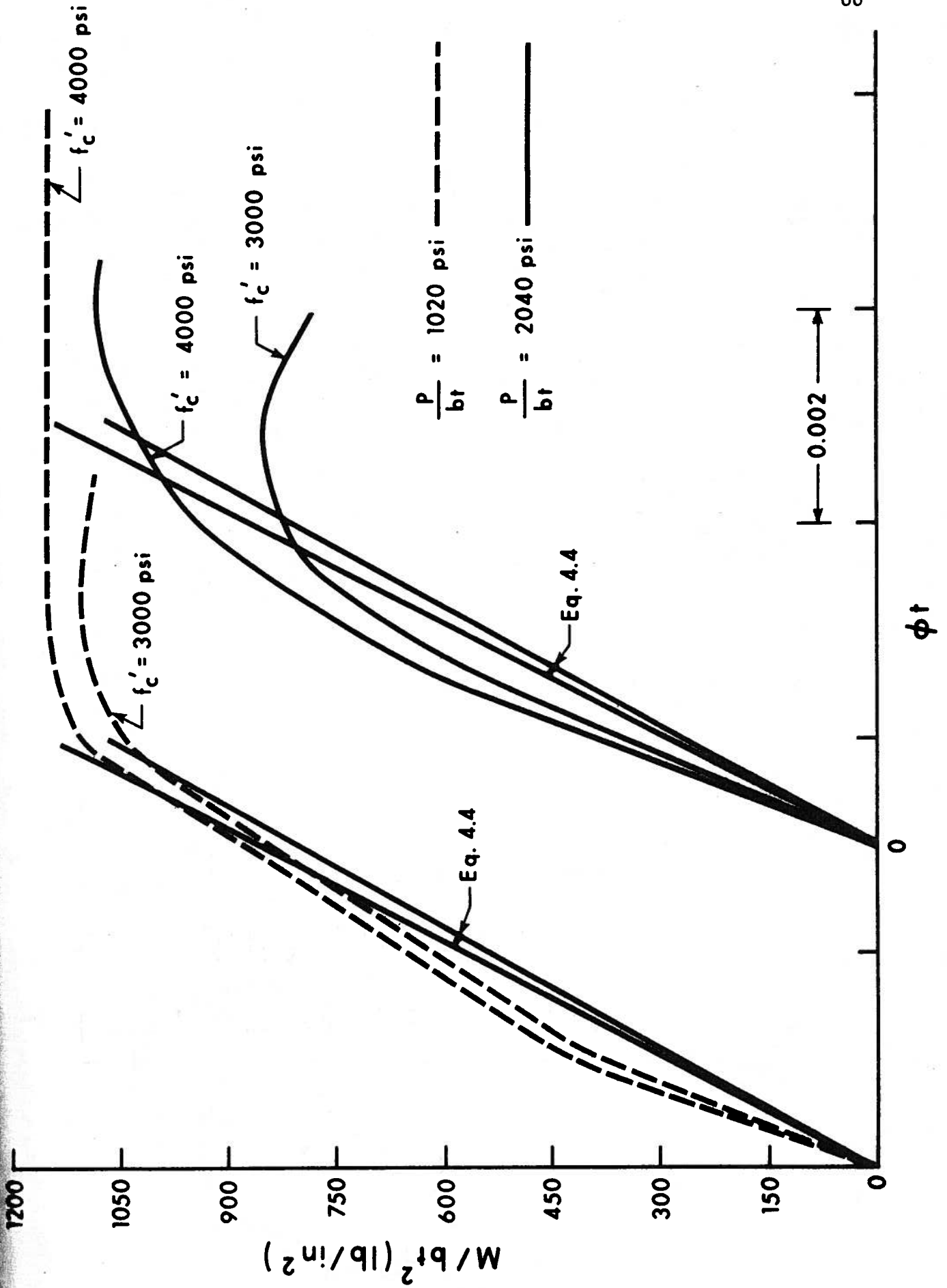
FIGURE 4.6 EFFECT OF CONCRETE STRENGTH ON MOMENT CURVATURE DIAGRAM
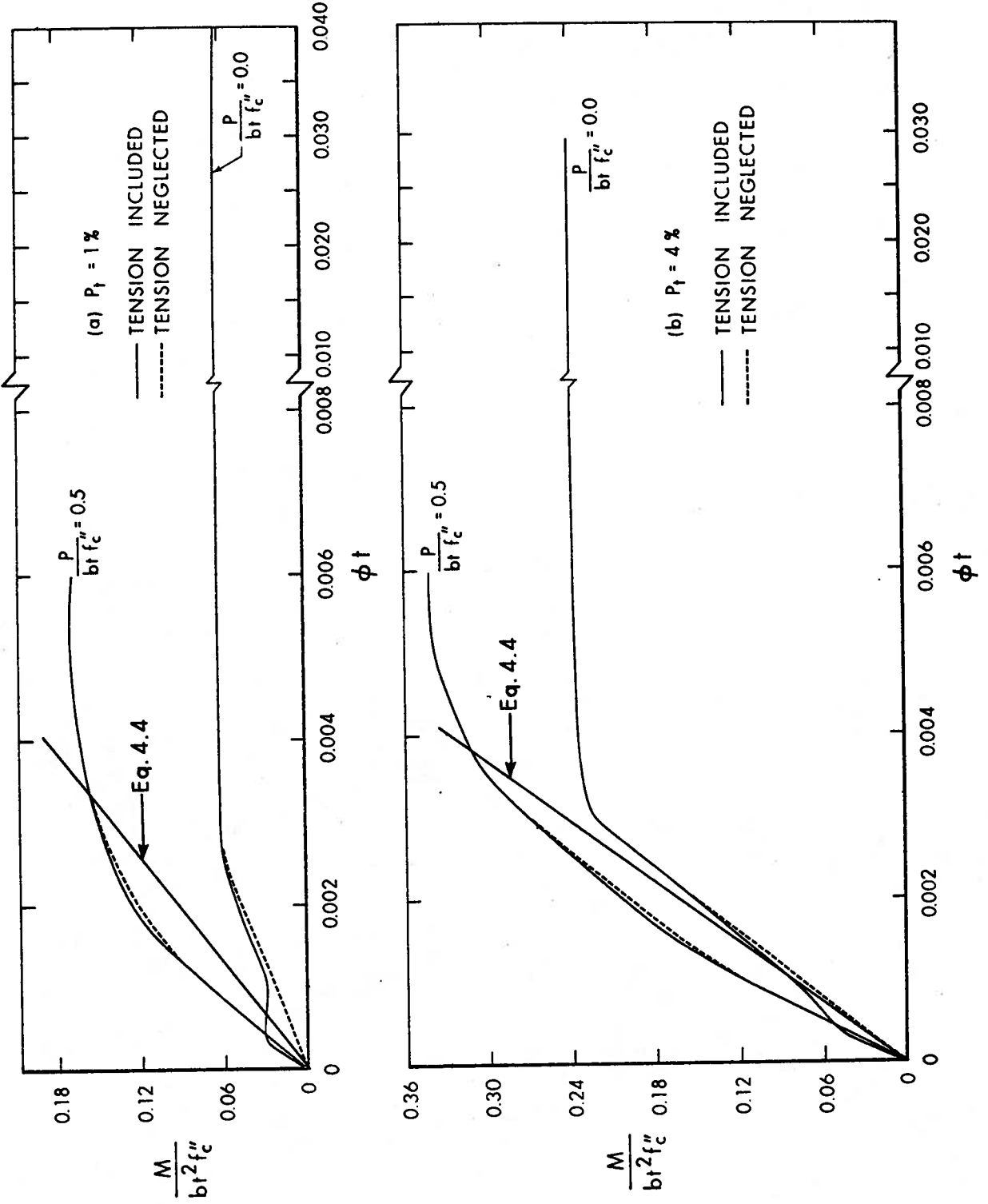
FIGURE 4.7 EFFECT OF REINFORCEMENT RATIO AND TENSILE STRESS

IN CONCRETE ON MOMENT CURVATURE DIAGRAM
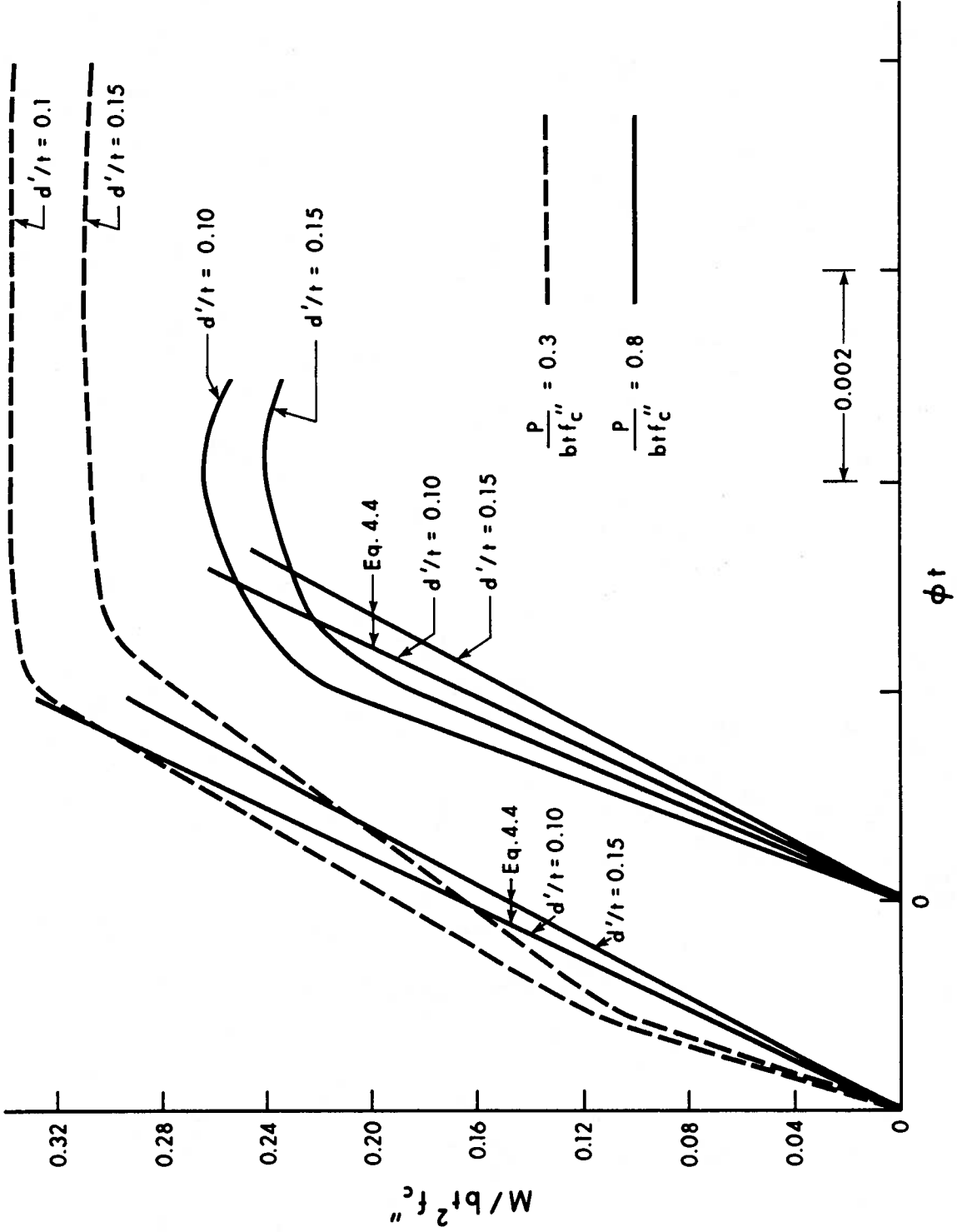
FIGURE 4.8 EFFECT OF COVER ON MOMENT CURVATURE DIAGRAM FOR TIED COLUMN

CHAPTER V

RESPONSE OF MEMBERS AND JOINTS

The shear wall frame analysis presented in CHAPTER III makes a number of assumptions which deal with the behaviour of the individual members in the structure. These assumptions are listed and discussed in this CHAPTER.

5.1 Effect of Axial Load on Member Stiffness

The stiffness factors C and S commonly used in slope deflection equations have been assumed to remain sufficiently close to 4 and 2 that these values may be used. In deriving the M_p value for the cross-section however, the axial load should be taken into account.

The slope deflection equations for a generalized member, subjected to end forces, P, only, can be written as:

$$M_A = \frac{EI}{L} \{ C\theta_A + S\theta_B - (C+S)\rho \} \qquad ....(5.1)$$

where M_A is the moment at the end A of the member AB. θ_A and θ_B are the slopes at the end A and B, respectively, ρ is the sway angle of the member AB and L is the length of the member AB. The C and S are given by equations (5.2) and (5.3).

$$C = KL \left(\frac{\sin KL - KL\cos KL}{2 - 2\cos KL - KL\sin KL} \right) \qquad ....(5.2)$$

$$S = KL \left(\frac{KL}{2-2\cos KL} - \frac{\sin KL}{KL\sin KL} \right) \qquad \dots(5.3)$$

where $K = \sqrt{\frac{P}{EI}}$

For zero axial load the terms C and S have the values of 4 and 2 and equation (5.1) reduces to:

$$M_A = \frac{EI}{L} (4\theta_A + 2\theta_B - 6\rho) \qquad \dots(5.4)$$

When the members are subjected to axial loads the moments induced by the deflections affect the distribution of moments. For an elastic member the values of the terms C and S vary as a function of the parameter $L\sqrt{P/EI}$.

For the beams the assumption that C and S remain constant is essentially true since the axial load in the beam generally remains very close to zero. In the case of shear walls the ratio $L\sqrt{P/EI}$ is small since the stiffness is high and the change in the values of C and S are not of significant importance. However, this assumption may be of concern in the case of columns.

For a rectangular reinforced concrete column the value of P_u is given by:

$$P_u = K f'_c bt$$

where K is a constant which varies between 1.0 to 1.8 for pure axial load. For eccentrically loaded columns K will be lower. For this

discussion assume that K equal to 1.0 and EI is approximately equal to 1000 f'_c btr^2 where r is the radius of gyration. Thus:

$$\frac{P}{EI} = \frac{1.0\ f'_c\ b\ t}{1000\ f'_c\ b\ t\ r^2} = \frac{0.001}{r^2} \qquad \dots (5.5)$$

Therefore $L \sqrt{P/EI} = 0.0316 \frac{L}{r}$ $\qquad \dots (5.6)$

Assuming that r equal to approximately 0.3 t for the rectangular section of depth, t, the equation (5.6) reduces to:

$$L \sqrt{P/EI} = 0.105 \frac{L}{t} \qquad \dots (5.7)$$

The value of $L \sqrt{P/EI}$ given by equation (5.7) increases as the value L/t increases. In a multistory building L/t seldom exceeds 20.[M9] The value of $L \sqrt{P/EI}$ will be equal to 2.10 and the corresponding values of C and S are 3.3745 and 2.1699. Therefore for the case of equal rotations at the two ends of the member and zero sway angle the assumption will be unconservative by the ratio 6/(2.1699 + 3.3745) = 1.08.

More than 90 percent of the columns in buildings will have L/t less than 8 [M9]. The value of $L \sqrt{P/EI}$ given by equation (5.7) will be equal to 0.84 and corresponding values of C and S are 3.9050 and 2.0240. Thus for most building columns this assumption will be unconservative by less than one percent. Therefore this assumption will be quite reasonable for all practical purposes.

5.2 Effect of Shear Deformation

The shear deformation may be of concern in the case of members

developing large shear such as shear walls. The relative magnitude of the flexural and shearing deformations can be estimated in the following analysis.

For a shear wall of height, h, acted upon by a shear force, V, the deflections due to bending and shear will be given by equations (5.8) and (5.9):

$$\Delta_M = \frac{Vh^3}{3EI} \qquad \qquad ....(5.8)$$

$$\Delta_V = \frac{1.2Vh}{AG} \qquad \qquad ....(5.9)$$

where A is the cross-sectional area and I is the moment of inertia of the section. The term 3 in equation (5.8) assumes that the wall acts as a cantilever and the term 1.2 in equation (5.9) is based on a rectangular section. E and G are the modulus of elasticity and modulus of rigidity respectively.

Substituting $G = E/2(1+\mu)$ and $I = Ar^2$ where r is the radius of gyration and can be taken as 0.3t for rectangular section and where μ is Poisson's Ratio which can be assumed to be equal to zero for reinforced concrete, the ratio of the deflections given by equation (5.8) and (5.9) is:

$$\Delta_M/\Delta_V = 1.54 \ (h/t)^2 \qquad \qquad ....(5.10)$$

For a variation of h/t from 1 to 2 for a one story wall the ratio of flexural to shear deflections given by equation (5.10) will vary from 1.54 to 6.17. In this case the shear deflections are significant. In a multi-story building, however, since the wall generally

acts as a cantilever for several stories the ratio h/t will generally

exceed 5. In this case Δ_M/Δ_V will exceed 38. In this case the shear

deflection is very small in comparison to flexural deflection and can

be ignored.

In the case of columns the factor 3 in equation (5.8) should

be taken as 12. The coefficient 1.54 in equation (5.10) reduces to

0.385. For h/t equal to 8 and 20, respectively, the ratios of flexural

to shear deflection are 24.7 and 154.

Thus the shear deformations will generally be small in

comparison to bending deformations in columns and will tend to be small

for walls. It is reasonable therefore to neglect the shear deflections

in approximate analysis. The comparison of test results also shows

that the shear deflections of columns and walls are not of considerable

importance.

In the examples of 10 and 20 story buildings presented in

reference (G2), the shear deformation was found to be greatest in

the bottom part of the shear wall. These examples are also analyzed by

approximate analysis and have been compared in CHAPTER VI.

5.3 Behaviour of Plastic Hinges

In CHAPTER III the following three assumptions were made to

define the properties of plastic hinges in the members:

(a) Plastic point hinges form at the centre of the beam-

column joint and at the face of the wall in the case of

beam to wall joints.

(b) In case of shear wall the hinges form in pre-specified small finite width.

(c) Plastic hinges have infinite rotation capacity.

In the frame test described in PART III of this report the plastic hinges in the beams occurred at about 0.25d from the face of the columns and the face of the wall as shown in FIGURE 5.1 which shows the third floor beam in the test specimen. As a result the moments at the centreline of the column were about 8 percent higher than the computed plastic moment. The assumed hinge location leads to a conservative estimate of the hinging load. The degree of conservatism is not serious for normal frame structures, but can be in the case of the exterior wall of a "tube-in tube" type of building where the clear span of the beam is generally less than 80 percent of the beam span measured centre-to-centre of the columns. In this case it would seem reasonable to increase the plastic moment capacity of the beams to be used in the analysis by the ratio of the centre-to-centre span divided by the clear span.

The assumption that the hinges can undergo any needed rotation is reasonable for the beams which can generally develop very large curvature, at hinges, as shown in FIGURE 4.3 and 4.7. The assumption may be far from the truth in the case of columns failing in compression, however, since the rotation capacity of such members is small as shown in FIGURE 4.3. Walls fall in between beams and columns but generally will fail in tension and thus generally will be able to develop large curvatures and rotations. Thus the analysis will

lead to a reasonable prediction of frame behaviour provided column

hinges do not form. This will occur if a strong column and weak

beam design is used.

5.4 Behaviour of Joints

In CHAPTER III it was assumed that the joints were rigid prior

to hinging of the members at the joints and did not undergo any shear-

ing deformations. The shears induced in the joint by the compression

and tension forces at the end of the beams frequently lead to diagonal

cracks within the joint as shown in FIGURE 5.1(a). The forces causing

such a crack are shown in FIGURE 5.2. For such cracks to occur the

joint must undergo a shearing distortion which leads to the reduction

in the joint stiffness. As a result of assuming stiff joint, the

analysis will lead to an unconservative estimate of the ultimate loads

and deflections. If ties are provided in the joint to transmit the

shears after inclined cracking in the joint, the shearing distortion

of such joints will not be significant. Ties were provided in the beam

to column joints in the test frame. Hanson and Conner[H4] have dis-

cussed the strength of such joints. To take account of the flexibility

of the beam to wall joint, an equivalent length method, in which beam

length is extended in the shear wall beyond the face by 1/2 of the

beam depth, has been suggested in reference (M10). As will be seen

later, in the analysis of test frame in CHAPTER IX, extending the beam

length of the test frame by 1/2 the beam depth resulted in less than two

percent reduction in the beam moments and little difference in the

overall behaviour is found. Therefore it can be concluded that the

assumption of rigid joint is reasonable for an approximate analysis.
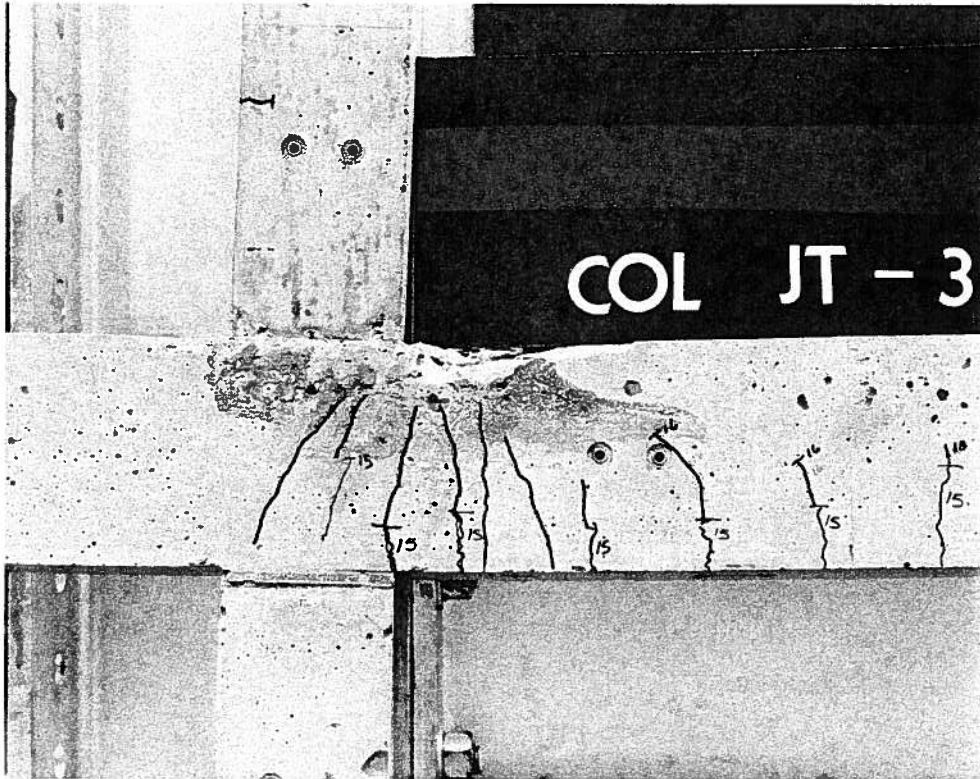
(a) COLUMN TO BEAM JOINT
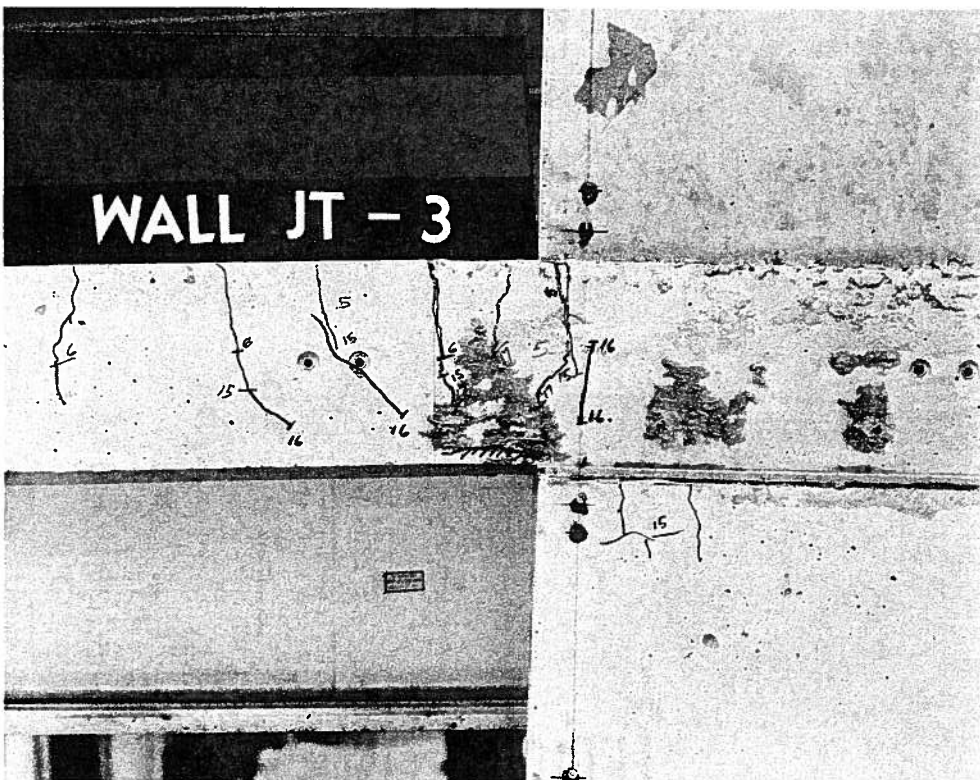
(b) WALL TO BEAM JOINT

FIGURE 5.1 THIRD FLOOR BEAM ENDS IN TEST SPECIMEN
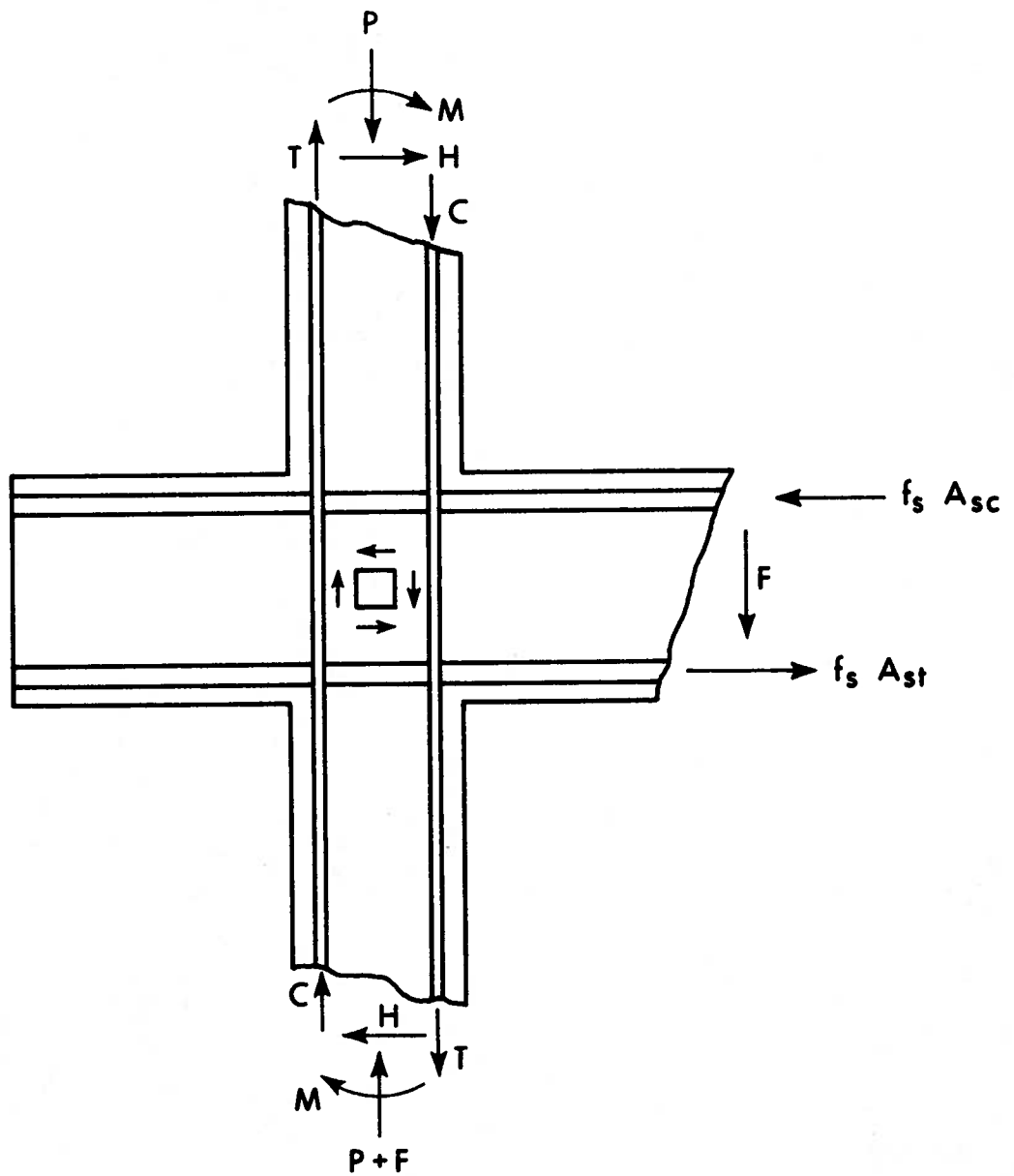
FIGURE 5.2 FORCES ON BEAM - COLUMN JOINT

CHAPTER VI

DEVELOPMENT OF THE LUMPED EQUIVALENT

STRUCTURE

6.1 Introduction

In this CHAPTER, an attempt has been made to determine the
arrangement of a lumped or equivalent structure, so that the analysis
developed in CHAPTER III can be used to predict the ultimate load
of the real structure with reasonable accuracy.

CHAPTER III contains a preliminary discussion of the simpli-
fied or equivalent structure. The lumped model used for the analysis
was similar to the elastic model used by Kloucek[K1], Goldberg[G2] and
Lightfoot[L1] for the analysis of plane frame. An extensive discussion
of the lumping procedure has been presented by Kloucek. Also a large
number of examples are presented to show the validity of the procedure
in the elastic range. Khan and Sbarounis[K2] used a similar approach
for elastic shear wall-frame structures.

In developing the lumped structure, the chosen examples will
be analyzed by the approximate method developed in CHAPTER III and the
response so obtained compared with that obtained from a more rigorous
analysis of the complete structure, using the method developed in
reference (C6). The load deflection curves for the building or frame
under consideration will be compared to show the accuracy obtained by

using the lumped model.

6.2 Development of the Lumping Procedure

In the discussion of the lumping procedure the frame members will be considered first. It has been assumed that the shear wall is forced to undergo the same sway deformation as the structural frame. FIGURE 6.1 shows the floor plan of a typical building with the vertical supporting structure consisting of walls and frames. The lateral force is assumed to be applied parallel to the plane of the frames.

A symmetrical rectangular portal frame subjected to a horizontal load is shown in FIGURE 6.2(a). Each column has a moment of inertia, I_C, and the beam moment of inertia is represented by I_B, M_{PC} and M_{PB} are the ultimate moment capacities of the column and beam respectively. The lumped model for this frame is shown in FIGURE 6.2(b). I_{LB} and I_{LC} are the moments of inertia of the lumped beam and column in the simplified structure. M_{PLC} and M_{PLB} are the moment capacities of the lumped column and beam respectively. Both the original and the lumped structures were analyzed by slope-deflection procedure for a horizontal load, H, applied at the top of the frame. For the two frames to have identical deformations the following relationships must be satisfied:

$$I_{LC} = 2 I_C \qquad \qquad ....(6.1)$$

$$I_{LB} = 2 I_B \qquad \qquad ....(6.2)$$

$$M_{PLC} = 2 M_{PC} \qquad \qquad ....(6.3)$$

$$M_{PLB} = 2 M_{PB} \qquad ....(6.4)$$

In the model shown in FIGURE 6.2(b) the length of the beam is $L_B/2$. Alternately, it is possible to have the length of the beam in the lumped model equal to that in the real frame provided both ends of the beam are rotated through the same angle. This later procedure has been followed in the analysis in CHAPTER III to avoid confusion in the input data.

6.2.1 Lumping of Multibay Frames under the Action of Lateral Load Only

For a multibay frame having equal bay lengths and subjected only to a lateral load, the following relationships similar to equations (6.1) to (6.4) must be satisfied for the lumped model shown in FIGURE 6.2(b)

$$I_{LC} = \Sigma I_C \qquad ....(6.5)$$

$$I_{LB} = 2 \Sigma I_B \qquad ....(6.6)$$

$$M_{PLC} = \Sigma M_{PC} \qquad ....(6.7)$$

$$M_{PLB} = 2 \Sigma M_{PB} \qquad ....(6.8)$$

where I_C and I_B represent the moments of inertias of columns and beams respectively, whereas M_{PC} and M_{PB} are the ultimate moment capacities of the columns and beams respectively. In the case of unequal bay lengths, the beam in the lumped structure can be assigned a length equal to the average length of all the beams

in the original structure. The moment of inertia of the lumped beam is given by:

$$I_{LB} = 2 L_{LB} \cdot \Sigma(I_B/L_B) \qquad ....(6.9)$$

where L_{LB} is the average length of the beam.

In the event of unequal plastic moment capacities at the two ends of the beam in a story, the plastic moment capacity of the lumped beam is given by:

$$M_{PLB} = \Sigma(M_{PB1} + M_{PB2}) \qquad ....(6.10)$$

where M_{PB1} and M_{PB2} are the plastic moment capacities of the left and right ends, respectively, of each beam in the story.

6.2.1.1 Check of Basic Lumping Procedure

To justify the above procedure, several one story structures, one bay to seven bays in width were analyzed. The results of the approximate analysis developed in CHAPTER III were compared with those of the more rigorous analysis developed in reference (C6). In each case the story height was 11 feet and the bay width was 18 feet. The beams were of reinforced concrete, 10 inches x 20 inches in cross-section with 2 percent steel; the columns were 10 inches x 10 inches with 4 percent reinforcement. Each frame was analyzed under the action of a horizontal load applied at the top of the frame. A typical comparison of the two

analyses is given in FIGURE 6.3 for a four bay, one story frame. The dashed line shows the results given by the rigorous analysis developed in reference (C6) and the solid line shows the results of the approximate analysis. The initial slopes of the load-deflection curves are almost identical. The difference in the two curves becomes noticeable as inelastic action of the structure becomes severe. The sequence of hinge formation as predicted by the two analyses is shown in FIGURE 6.3 and explains this difference. The rigorous analysis predicts that the first hinges will form at the bases of the three interior columns, whereas the second hinges, at the bases of the exterior column form later in the loading history. By lumping these columns, the approximate analysis predicts that all hinges form together, that is, at the base of the lumped column; causing the change in the hinging load. However, the difference is not significant. The ultimate load for this structure was 75.2 kips by the approximate analysis whereas the rigorous analysis predicts an ultimate load of 74.4 kips. Thus for this frame, the approximate analysis overestimated the ultimate load by about one percent. All other frames analyzed in this section, exhibited similar trends in load-deflection curves and the sequence of formation of hinges. TABLE 6.1 compares the ultimate loads predicted by the two analyses, for all the frames. In all cases the approximate analysis tended to overestimate the ultimate load from 1.0 to 2.2 percent.

6.2.1.2 Effect of Variations in Relative Stiffness of Beams

and Columns

To investigate the effect of varying the beam to column stiffness, the four bay, one story structure, described in section 6.2.1.1 was selected as a model. Seven different sets of columns, varying in cross-section from 10 inches x 10 inches to 34 inches x 34 inches with four percent reinforcement, were considered. All frames were analyzed under the action of a horizontal load applied at the top of the frame, by both methods; that is, the approximate analysis developed in CHAPTER III and the rigorous analysis developed in reference (C6). No vertical loads were considered. A typical example is shown in FIGURE 6.4. In this case the columns were 20 inches square. The dashed line gives the results of the analysis developed in reference (C6), whereas the solid line is that of the approximate analysis. Both analyses predicted similar load-deflection curves and hinging patterns. The initial slope of the load-deflection curves given by the two analyses are almost identical as can be seen in FIGURE 6.4. The ultimate load predicted by the rigorous analysis was 557.5 kips whereas approximate analysis predicted an ultimate load of 568.0 kips. Thus the approximate analysis over-estimated the ultimate load of this frame by 2 percent. All other frames analyzed in this paragraph yielded similar comparisons. FIGURE 6.3 also shows a frame in this series. The hinging sequence differed for the two frames. TABLE 6.2 compares the ultimate

loads for all the frames. The ratio of column to beam
stiffness varied from 0.24 to 42.06. By varying this
quantity it was possible to have different hinging sequence
for different frames in the rigorous analysis. In all cases
the approximate analysis tended to overestimate the ultimate
load by 0.5 to 4.5 percent. The errors tended to increase
as the column stiffnesses increased.

6.2.1.3 Effect of Unequal Beam Spans

In the previous sections only those frame having
equal bay legnths have been considered. However, many
structures have unequal bay lengths and subsequently beams
of different length in the same story. In the approximate
analysis, however, all the beams in a floor have to be
lumped together causing the hinges to form simultaneously
in all the beams of a given floor. To compensate for this
effect the use of average bay length has been suggested
above. The moment of inertia of the lumped beam will be
given by equation (6.9) whereas the ultimate moment
capacities will be given by equation (6.8), or (6.10) if
no transverse loads are present on the beams.

To study the effect of span variation, two of
the four bay, one story, frames discussed above were con-
sidered. The first frame had 10 inch square columns and the
second 20 inch square columns. The beam length was 11 feet
in one, two or three of the four bays whereas all other bay

lengths were 18 feet. Various possible combinations were considered, resulting in 11 different frames for each column size. All 22 frames were analyzed under the action of a horizontal load, applied at the top of the frame, by both the approximate and the rigorous methods. No vertical loads were applied to the structure. In all cases, both analysés predicted similar load-deflection curves and hinging patterns for the structures. The initial slope of the load deflection curves for the frames were found to be almost idential by both methods. Two typical load-deflection curves are presented in FIGURES 6.5 and 6.6. In both FIGURES 6.5 and 6.6 the dashed lines represent the results of the rigorous analysis whereas the solid lines represent the results obtained by the approximate analysis. FIGURE 6.5 is representative of the first set of frames, which had 10 inches square columns. These frames failed in a sway mechanism. The ultimate load predicted by the rigorous analysis for the frame shown in FIGURE 6.5 was found to be 74.5 kips whereas the approximate analysis predicted an ultimate load of 75.2 kips. Thus the approximate analysis overestimated the ultimate load by approximately one percent. FIGURE 6.6 shows the results of a similar frame, chosen from the second set, which had 20 inches square columns. These frames failed in a combined mechanism. The ultimate load for the frame shown in FIGURE 6.6 was found to be 522 kips by the approximate analysis whereas the rigorous analysis predicted an ultimate load of 525 kips. In this case the approximate analysis underestimated the load by 0.6 percent. The ultimate loads for frame

considered in this section are given in TABLE 6.3. In all cases the error was found to be within ± 1.4 percent.

6.2.2 Lumping of Multibay Frames Subjected to Combined Loads

In section 6.2.1 the lumping procedure for frames subjected to lateral load, has been derived. However, the structure will carry vertical load in addition to lateral load. The vertical load in a structure could be applied as concentrated loads on the tops of columns or as the uniformly distributed loads on the beams. It was assumed in CHAPTER III, that the effect of the total vertical load in a story could be simulated by placing concentrated loads on the column tops.

6.2.2.1 Effect of Column Top Loads

To study the effect of column top loads, the four bay, one story frame having 20 inch square columns, shown in FIGURE 6.4, was again analyzed. The ultimate axial load capacity, P_o, for this column is 2110 kips. Column top loads, P, varying from 25 kips to 2000 kips, producing 8 different loading conditions, were considered. The frames were analyzed by both the rigorous method and by the approximate method. The frames were lumped by the procedure developed in section 6.2.1 for the purpose of the approximate analyses. All frames were analyzed under the action of incremental horizontal load applied at the top of the frame, while the vertical load remained constant. Typical load-deflection curves from the two analyses are shown in FIGURE 6.7. In this case

the load on the top of each column was 500 kips, giving
P/P_o = 0.237. The dashed line in FIGURE 6.7 represents
the results obtained from the rigorous analysis whereas
the solid line represents the results of the approximate
analysis. The initial slopes of the load deflection
curves obtained by the two analyses are almost identical.
Similar hinging patterns were also predicted. The ultimate
lateral load predicted by the rigorous analysis was 633 kips,
whereas the approximate analysis predicted an ultimate
load of 642 kips. Thus the approximate analysis overestimated
the ultimate load by about 1.5 percent. All other frames
exhibited similar load-deflection curves and similar hinging
patterns were obtained by the two analyses. TABLE 6.4
compares the ultimate loads for all frames. The error was
about 2 percent for P/P_o less than 0.25, increasing
exponentially to 11 percent for P/P_o = 0.95. These errors
are probably due to the fact that the effect of axial
load on the coefficient C and S commonly used in slope-
deflections equations are ignored by the approximate
analysis. This problem has also been discussed in section
5.1.

6.2.2.2 Effect of Uniformly Distributed Loads on Beams

To study the effect of applying a uniformly dis-
tributed load to the beams, the four bay, one story structure
was analyzed under the influence of incremental lateral load
and a constant uniformly distributed vertical load on the

beams. The lumped models, derived using the principles dev-
eloped in section 6.2.1, were analyzed by approximate method
whereas the corresponding actual frames were analyzed by the
rigorous analysis. The results show that the approximate
analysis tended to grossly overestimate the ultimate load
depending upon the magnitude of uniformly distributed load.
Accordingly, it is necessary to reduce the ultimate moment
capacity of the beams in the approximate analysis. The
following analysis was performed to find the reduction factor
which can be applied to the ultimate moment capacities
of the beam. In such cases the equation (6.8) and (6.10)
can be redefined as:

$$M_{PLB} = 2 \Sigma\alpha \cdot M_{PB} \qquad \dots(6.11)$$

$$\text{or} \quad M_{PLB} = \Sigma\alpha (M_{PB1} + M_{PB2}) \qquad \dots(6.12)$$

where α is the reduction factor.

A sway mechanism will require two beam hinges plus
hinges at the bases of the columns. If no load is applied
between the ends of a restrained beam in a laterally loaded
frame, and if the point of contraflexure is at mid-span of
the beam, the moment diagram for the beam will be as shown
in FIGURE 6.8(a) and the beam plastic hinges will occur
simultaneously as shown in FIGURE 6.8(b). When gravity
loads are applied between the ends of the beam, the
negative moments due to the vertical load add to the wind

moments at the leeward end of the beam, as shown in FIGURE 6.8(c) reducing the lateral load required to cause hinging at that point; and subtract from the wind moments at the other end tending to develop a hinge configuration as shown in FIGURE 6.8(d).

Consider a restrained beam of span, L, and ultimate moment capacity M_p, in both positive and negative moment regions, subjected to a constant uniformly distributed load, w per unit length, and a wind moment distribution characterized by the end moments, M_W. As the wind moment, M_W, is increased, the first hinge forms at the leeward end of the beam; on further increase in the wind moment, a second hinge will form either at the windward end or in between the ends of the beam. The results obtained from such an analysis are plotted in FIGURE 6.9 for various ratios γ of midspan moment capacity to end moment capacity. The term γ will be explained in the next paragraph. The ratio $\beta = M_W/M_p$ is plotted on the vertical axis whereas the values of wL^2/M_p are plotted on the horizontal axis. For a known value of wL^2/M_p the ultimate moment capacity of the beam should be multiplied by the corresponding value of β obtained from FIGURE 6.9 to get the correct mechanism load. If the value of β is taken corresponding to the first hinge configuration, the result obtained by the approximate analysis of the frame will be too conservative since the second hinge is forced to form at the first hinging load. If the higer value of β, given by the

second curve is used, the result will be unconservative since the first hinging load is increased. Therefore, it is suggested that the quantity α, in equation (6.10) should lie close to the mean of the two values of β obtained from FIGURE 6.9. The mean value of β is plotted in FIGURE 6.10.

In reinforced concrete structure, however, the positive moment capacity is normally less than the negative moment capacity. The extreme case would correspond to the elastic gravity load moments which for a fixed ended beam lead to a mid-span plastic moment capacity equal to half the plastic moment capacity at the ends. Let the plastic moment capacity in the positive moment region is given by γM_p where M_p is the plastic moment capacity in the negative moment region. Normally the value of γ will vary from 0.5 to 1.0. The results of similar analysis described in previous paragraphs for various values of γ varying from 0.5 to 1.0 are shown in FIGURE 6.9. The mean value of β obtained from FIGURE 6.9 are plotted in FIGURE 6.10. From the FIGURE 6.10 it can be seen that the value of α can be approximated in straight line relationship with wL^2/M_p and a sufficiently accurate approximation to the values of α will be given by the equation:

$$\alpha = 1.0 - 0.015 \, (7-3\gamma) \, (wL^2/M_p) \qquad \ldots (6.13)$$

For the case of beams with equal positive and negative M_p's, that is, $\gamma = 1.0$, the equation (6.13) will result in:

$$\alpha = 1.0 - 0.06 \ (wL^2/M_p) \qquad \qquad ....(6.14)$$

and for the case of beams having half the value
of negative M_p's in the positive moment region the equation
(6.13) will result in:

$$\alpha = 1.0 - 0.0825 \ (wL^2/M_p) \qquad \qquad ....(6.15)$$

The other case of the reinforced concrete struc-
ture will be the case of a beam which will have different
moment capacities at the two ends. The leeward end of the
beam will have greater value of moment capacity than the
windward end. If η is the ratio of the windward end
moment capacity, M_p, to the leeward end moment capacity
the value of α given by equation (6.13) will be sufficiently
accurate as long as the hinge does not form at the wind-
ward end of the beam. For most of the structure this is
true and this condition is satisfied if:

$$\frac{1-\eta}{2} \leq \alpha \leq \eta \qquad \qquad ....(6.16)$$

If the value of α obtained by equation (6.13)
does not satisfy the equation (6.16), a conservative esti-
mate can be obtained by taking α equal to 0 or η depending
upon whether the value of α obtained from equation (6.13)
is less than $(1-\eta)/2$ or greater than η.

In the analysis of a large building structure it

would become tedious if α has to be computed for every beam in the structure. Accordingly, it is desirable to have one general value of α which could be used at least in the preliminary analyses of multi-story structures. Such a factor can be derived from FIGURE 6.10. In the design of reinforced concrete buildings by the 1970 ACI code proposed, it will be necessary to design the structure for ultimate loads of:

$$U = 1.4DL + 1.7LL \qquad \qquad \dots(6.17)$$

or $\quad U = 0.75 (1.4DL + 1.7LL + 1.7WL) \quad \dots(6.18)$

where $\quad U =$ required ultimate load capacity of section.

$$DL = \text{dead load}$$
$$LL = \text{live load}$$
and $\quad WL = \text{wind load}$

A well designed shear wall-frame structure will come very close to satisfying both equations (6.17) and (6.18) simultaneously. Normally the beams will be designed for the moment capacity, M_p, equal to $wL^2/10$ to satisfy the equation (6.17). At the ultimate state under lateral loads the beams will carry a gravity load of 0.75(1.4DL + 1.7LL) or 75 percent of the design gravity load. For this load the value of wL^2/M_p is 7.5 and the corresponding value of α, given by FIGURE 6.10, should vary from 0.62 for the case of equal positive and negative plastic moment capacities

to 0.44 for the case of beams having half the value of end moment capacity in the positive moment region.

The correction factor α will lead to a better prediction of the load at which the beam mechanisms form in the structure and hence a better prediction of the load at which significant softening of the structure begins. On the other hand, however, the work done in deforming the beam will be underestimated considerably with a resulting decrease in the stiffness predicted for a structure containing beam hinges. This is illustrated in FIGURE 6.11. The work done in deforming the columns in mechanism (a), shown in FIGURE 6.11, through an angle θ is:

$$M_p \left(\theta + \frac{a}{b}\theta\right) + \gamma \, M_p \left(\theta + \frac{a}{b}\theta\right) = \frac{wb \cdot b \cdot a}{2 \, b}\theta + wa \cdot \frac{a}{2}\theta + H_1 h\theta$$

or
$$M_p(1+\gamma)\frac{L}{b} = \frac{waL}{2} + H_1 h \qquad \dots (6.19)$$

Combining equation (6.19) and (6.13) and solving for H_1 will result in:

$$H_1 h = M_p \left\{ (1+\gamma)\frac{L}{b} - \frac{(1-\alpha)a/L}{0.03(7-3\gamma)} \right\} \qquad \dots (6.20)$$

The work done in deforming the columns in mechanism (b), shown in FIGURE 6.11, through an angle θ is:

$$2\alpha M_p \theta = H_2 h\theta$$

or
$$H_2 h = 2\,\alpha M_p \qquad \dots (6.21)$$

The ratio, H_2/H_1, will be given from equations (6.20) and (6.21) as:

$$\frac{H_2}{H_1} = \frac{2\alpha}{(1+\gamma)\frac{L}{b} - \frac{(1-\alpha)a/L}{0.03(7-3\gamma)}} \quad \ldots\ldots(6.22)$$

For the value of γ equal to one and suggested value of α equal to 0.62 the ratio H_2/H_1 given by equation (6.22) will be 0.785. In other words, approximate analysis will underestimate the ultimate horizontal load for the structure shown in FIGURE 6.11 by 21.5 percent. However, this error will be greatly reduced for the multi-story structure, since many of the beams will not contain hinges at the ultimate load. Thus it will be seen in example presented later in this CHAPTER, for large structures the load at the first major decrease in stiffness is predicted fairly well by the approximate analysis but the stiffness, after hinging, is underestimated by it.

To study the effect of a uniformly distributed load on the beam, the four bay, one story model analyzed earlier, was considered. The ultimate load capacity P_o, for each column was 2110 kips whereas each beam required a uniformly distributed load, W_b, of 11.44 kips per foot to form hinges at the ends under the vertical load only. Four different uniformly distributed loads varying from 0 to 76 percent of W_b were chosen. In each case, however, the total vertical load was 2500 kips corresponding to a ratio of P/P_o of approximately 0.24 for each column. All frames were analyzed

by both the rigorous and approximate methods. The values
of α used in the approximate analysis were taken from
FIGURE 6.10. Vertical loads remained constant while
the horizontal load applied at the top of the frame was
incremented in both the analyses. A typical example, in
which the uniformly distributed load was taken as 76
percent of W_b is shown in FIGURE 6.12. The initial slope
of the load-deflection curves obtained by the two analyses
are almost identical. The first hinge in the rigorous
analysis was detected earlier than in the approximate
analysis causing a discrepancy in the load-deflection curve
at this point. However, the approximate analysis predicts
a more rapid softening of the structure following the
formation of the first hinge producing approximately the
same ultimate load as that predicted by the rigorous analysis.
In this case the ultimate load predicted by the rigorous
analysis was 544 kips, whereas the approximate analysis
predicted an ultimate load of 522 kips. Thus the approxi-
mate analysis underestimated the load by 4 percent. TABLE
6.5 compares the ultimate loads obtained by both analyses
for all the frames. In all cases the approximate analysis
under-estimated the ultimate load by less than 4 percent
except for the first case where no uniformly distributed
load was present. In this case the approximate analysis
overestimates the ultimate load by about 1.5 percent.

The example frame considered above was reanalyzed

with the beam length of bays 1 and 3 set at 11 feet. The results are shown in FIGURE 6.13. A comparison of FIGURES 6.12 and 6.13 shows that for the frame having varying span lengths, the load-deflection relationship predicted by the approximate method agreed more closely with the results predicted by the rigorous analysis. The ultimate load predicted by the rigorous analysis was 584 kips whereas the approximate analysis predicted an ultimate load of 564 kips, underestimating the ultimate load by 3.4 percent.

6.2.3 Multi-story Structures

In an attempt to check the validity of the lumping procedure, derived in section 6.2.1 and 6.2.2, for multi-story frames linked to shear wall, several frames were analyzed by the program described in CHAPTER III and the results were compared with those obtained from the program developed in reference (C6). The member sizes of the basic four bay frame, used as an example in section 6.2.1.2, were used in frames of one, two, three and four stories. These frames were linked with a shear wall, 10 inches x 120 inches in cross-section, having one percent reinforcement. Hinged link beams were used to restrict the study to effects of the assumptions made in lumping of the frame itself. The frames were analyzed under the action of horizontal loads applied at each floor level. The roof level had one half the lateral load applied at each floor. No vertical loads acted on the structure. A typical three story structure is shown in FIGURE

6.14(a) and the lumped equivalent structure is shown in FIGURE 6.14(b). The four frames were analyzed by the rigorous method and by the approximate method and the results were compared. In all cases the initial slopes of the load-deflection curves were essentially equal. A typical load-deflection curve for the three story building is shown in FIGURE 6.15. The dashed line represent the results obtained from the rigorous analysis whereas the solid line is that of the approximate analysis. Both analyses predicted similar load-deflection responses and hinging patterns. Due to the slight differences in the predicted hinging pattern the two curves do not match exactly over the inelastic portions of the curves. The ultimate load for this frame was found to be 263 kips by the rigorous analysis and 260 kips by the approximate analysis. Thus the approximate analysis underestimated the ultimate load by 1 percent. The comparisons of the ultimate loads for all four frames are presented in TABLE 6.6.

A 20 story, two bay structure, shown in FIGURE 6.16 (a) was chosen as a second example and will be termed as frame "A". The structure consisted of a two bay rigid frame linked with a 10 inches x 60 inches wall by hinged link beams. The sizes of the frame members are taken from reference (C6). The equivalent lumped structure is shown in FIGURE 6.16(b). No gravity loads were considered except for the self weight and the value of α was taken as one. This structure was analyzed under the action of incremental loads applied at the floor levels. The load-deflection curves obtained from the

rigorous and approximate analyses are shown in FIGURE 6.17.
The dashed line shows the results obtained from the rigorous
analysis whereas the solid line is that of the approximate
analysis. The hinge configuration of this structure is shown
in FIGURE 6.18. The initial slopes of the load-deflection
curves are identical and the hinging patterns are also similar,
as can be seen in FIGURES 6.17 and 6.18. The load factor
predicted by the rigorous analysis is 2.7 whereas the approxi-
mate analysis predicted a load factor of 2.65. Thus the
approximate analysis underestimated the load by about 2 percent.

The above 20 story structure was also analyzed under
the action of incremental horizontal loads at each floor level
and constant vertical loads. This frame will be termed as
frame "B". Uniformly distributed loads of 4 kips per foot
were considered on all beams except the roof girders, which
were subjected to loads of 2.2 kips per foot. The value of α
was computed from FIGURE 6.10 for each beam. The load-deflection
curves obtained from both analyses are presented in FIGURE 6.19.
The dashed line was obtained by the rigorous analysis whereas
the solid line represents the approximate analysis. Due to the
differences in the hinging patterns predicted by the two
analyses, the curves differ slightly in the inelastic range.
hinging patterns obtained are shown in FIGURE 6.20. The approxi-
mate analysis predicts hinges at the ends of the beam whereas the
rigorous analysis predicts one hinge at the leeward end of the beam
and one between the two ends. The approximate analysis predicts
earlier failure of the structure.

This frame was also analyzed with various wall sizes. The load-deflection curves obtained by both analyses for a 10 inches x 80 inches wall, frame "C", and for a 10 inches x 96 inches wall, frame "D", are shown in FIGURES 6.21 and 6.22. In these cases similar comparisons between the two predicted load-deflection curves and hinging patterns were obtained. In the case of frame "D" the ratio of the wall stiffness to the sum of column stiffness varied from 4.87 in the bottom story to 300 in the top story. The choice of this ratio was limited in the sense that the analysis presented in reference (C6) does not converge for large differences of wall to column stiffness.

It can be concluded from the results of the frames A,B, C and D analyzed above, that the approximate analysis yields reasonable description of load-deflection curve for the multi-story structure when there is no vertical load present on the structure. The approximate analysis yield a slightly inaccurate but conservative description of load-deflection curve for the structure when the gravity loads are present on the structure. This is due to the way the approximate analysis takes into account the uniformly distributed load on the structure. As mentioned earlier the value of α is so chosen that the approximate analysis will always result in underestimation of the ultimate load. The designer may wish to use a different value of α to more closely predict some other part of the load-deflection curve such as the start of hinging. However, the discrepancy in the results obtained by approximate and rigorous

analysis are within tolerable limits as can be seen by the
results of frames A, B, C and D.

6.2.4 Lumping of Link Beams

In deriving the analysis it was assumed that the
beams linking the shear wall to the rest of the structure (link-
beams) in each story are assumed to be represented by a single
link beam as shown in FIGURE 3.1. The lumped link beam has a
length equal to the average length of all the link beams in
the story except that the lumped link beams must have the same
length in all stories. The stiffness, EI/L of the lumped link
beams shall be taken as sum of the stiffnesses of all the link
beam in the story in question. The plastic moment capacity of
the lumped beam shall be taken as $\alpha \Sigma M_p$ for all the corresponding
beams.

The assumptions concerning the use of the average
beam length and the derivation of the EI and M_p terms used in
the analysis have been discussed in sections 6.2.1, 6.2.1.3
and 6.2.2.2. These explanations will also apply to the link
beams. The general value of α derived in section 6.2.2.2 will
often be too low since the major portion of the moments in
the link beams often result from wind load rather than gravity
load.

6.2.5 Lumping of Shear Walls

In deriving the analysis it was assumed that the shear

walls in one story can be represented by a single wall with a moment-curvature relationship defined by superimposing the moment curvature relationships of each of the individual walls in that story. The resulting moment-curvature relationship is approximated by a bi-linear curve. The slope of the second branch of this curve may be small but not zero and the ratio of the slope of the second branch to that of the èlastic portion of the curve must be the same in all stories. The neutral axis of the wall is assumed to coincide with the centroid of the uncracked wall.

It is customary to assume that the wind shear resisted by the shear walls in a structure can be distributed between the various shear walls in each story in proportion to their individual stiffnesses. Khan[K4] has shown that this assumption will result in the correct moments and shears in the shear wall only if one of the following conditions is satisfied:

1. Each shear wall has constant section properties throughout the height of the building.

2. Where wall sections change, the relative stiffness of each wall remains unchanged throughout the height of the building.

In the examples presented by Khan[K4] and Tezcan[T1] the errors in the wall shears and moments estimated by distributing the total shear in the walls in any story in the ratio of the stiffnesses of the walls ranged from about -300 percent

to about +200 percent. The errors appeared to be smaller when the wall moments were distributed in this way rather than the wall shears.

Tezcan has shown, however, that the lateral deflection of a number of shear walls connected by hinged link beams is equal to the deflection of a single shear wall having a stiffness in each story equal to the sum of the individual wall stiffnesses in that story. Thus, the lateral deflections computed for a structure by lumping the wall stiffness as is done in this analysis will be essentially correct. To compute the shears and moments in the individual walls it is then necessary to force each individual wall through the computed deflections.

The effect of summing the EI/L values of the shear walls was studied using a ten story building containing three shear walls, inter-connected by linked beams at each floor level as shown in FIGURE 6.23(a). This structure was also discussed in reference (K4). A first order analysis of the actual structure was performed using a matrix method. In addition, the three walls were lumped together into the single cantilever as shown in FIGURE 6.23(b) which was also analyzed. In both cases analysis were limited to elastic range. The deflections at each floor level as predicted by the two analyses are compared in TABLE 6.7. The actual shears obtained by distributing the total shear in the ratio of the respective wall stiffnesses are presented in TABLE 6.8. An incorrect distribution of shears resulted from this procedure. Since the

lumped model yields almost correct deflections, the shears and moments can be computed from the deflected shape of the structure.

The final assumption considered in lumping the shear wall was that the neutral axis of the wall was at mid-depth of the wall. Although the exact location of the neutral axis depends on the shape of the wall, the distribution of the wall reinforcement and the axial load and moment in the wall, it will generally lie between the mid-depth and the compression face of the wall. This assumption affects the ultimate load in two ways: 1. The moments induced in the link beams differ on the two sides of the core as shown in FIGURE 6.24. This effect tends to cause hinging to start earlier than predicted on the windward side and later on the leeward side of the wall. Since the link beams on both sides of the wall are lumped together into one link beam, this assumption has relatively little effect on the overall behaviour predicted by the analysis. 2. If the two link beams are similar, more work will be done in raising the wall end of the windward beam than is dissipated by lowering the wall end of the leeward beam. This is not true if the neutral axis of the wall is at mid-depth. As a result the analysis will tend to underestimate the stability of the structure.

6.3 Analysis of Planar Structure

It is assumed in the analysis that each floor acts as a rigid diaphragm and that the structure does not twist about its longitudinal

axis.

Benjamin[B15] has shown that a frame analysis based on the assumption that the floor diaphragm are rigid, is satisfactory if the ratio of the diaphragm to frame rigidity is greater than 1.0.

The problem is also discussed by Goldberg[G2] who presents an exact first order analysis including shear and flexural deformations of the floor diaphragm and the walls. It is interesting to see the comparison of elastic deflections and wall shears at each floor level of ten and twenty story building taken from reference (G2). The comparison has been presented in section 6.4.

In an example presented in reference (W6), moving the shear wall from the middle of a 60 foot wide building to 7.5 and 15 feet from the middle led to reductions in deflection of the top of the wall by 4 and 15 percent, respectively. Generally, however, the non-symmetrical nature of the building tends to increase the maximum deflections of the most highly deflected frame.

6.4 Comparison with other Published Examples

The lumping procedure developed in this CHAPTER was checked in part by comparisons of the computed deflections with those of several published example structures. The example structures selected were reduced to their equivalent models and analyzed by the program developed in CHAPTER III.

Example one is a ten story, three bay steel frame first

presented in reference (P2). This structure had unequal bay lengths

and unequal stiffness in the four column lines. The actual struc-

ture and the lumped model are shown in FIGURE 6.25. The loading

and member sizes used for this frame are given in reference (P2).

All the beams had uniformly distributed load and the corresponding

values of α were computed from FIGURE 6.10. FIGURE 6.26 compares

the load deflection curve obtained by the approximate analysis

to that presented in reference (P2). The dashed line

shows the curve presented in Reference (P2) and the

solid line is that obtained by the approximate analysis. Good

agreement was found between the initial part of the two curves. The

discrepancies in the inelastic range of the curve are due to the

different hinging patterns predicted by the two analyses. Later

softening but earlier failure was predicted by the approximate

analysis.

Example two is a ten story building taken from reference

(G2). The structure is shown in FIGURE 6.27(a) whereas the lumped

model is shown in FIGURE 6.27(b). No axial load was considered.

Comparison of elastic deflections at each floor level and the wall

shears are presented in TABLE 6.9 and 6.10. When only bending de-

formations are taken into account, the error in the wall deflection

is within one percent in all floors whereas the error in the shear

force is two percent or less in all floors except for the first and

top, where the errors are about 7 and 35 percent respectively. The

comparison of the deflections obtained by approximate analysis with

the results of combined bending and shear deformation obtained in

reference (G2) are in greater error. The error in the bottom part of the building is more than the top part of the building. This is because of the fact that wall shear is greater in magnitude at the bottom part of the building. However, it should be remembered that small numbers have been compared. In terms of the shearing forces in the wall, however, the approximate analysis gave reasonable results.

Example three is a twenty-story building taken from reference (G2). The structure is shown in FIGURE 6.28(a) and the lumped model is shown in FIGURE 6.28(b). No axial load was present on the structure. The comparisons of elastic deflections and wall shears at each story level are presented in TABLE 6.11 and 6.12. The error in the wall deflection in all stories was within one percent in comparison to the bending deformation computed in reference (G2) and the error in wall shear was less than 5 percent except for the first floor and floors near the top of the structure. In comparison to the combined bending and shear deflections obtained in reference (G2), the approximate analysis resulted in greater error. This error was greater in the bottom part of the building since the bottom part of the building attracted greater wall shear in comparison to the top part of the building. Here also small numbers have been compared. The reasonable comparisons with Goldberg's bending deflection analysis suggests that for most normal buildings it is sufficiently accurate to consider the floor as a rigid diaphragm.

In example two the ratio of the wall to sum of the column stiffnesses varied from 514 at the bottom story to 5310 in the top

story. In example three the ratio of wall to sum of column stiff-
nesses varied from 219 at the bottom story to 788 in the top story.
The comparison was limited to elastic range only.

6.5 Discussion of Additional Assumptions

The final group of assumptions presented in CHAPTER III
dealt with specified aspects of member and frame behaviour, such
as there is no out of plane behaviour of the structure and there
is no axial deformation.

The out of plane behaviour is not a problem except for
thin walls. Many designers provide columns at the end of walls
to prevent this tendency.

Studies of concrete building designs have shown that
columns in multi-story shear wall frame structure will seldom
exceed $L/r = 35$. According to the long column sections proposed
for the 1970 ACI Code this length would have no effect on the
majority of the building columns. Therefore there will be no
buckling prior to mechanism failure.

In the braced structure H-50, studied in APPENDIX E of
reference (C6), the failure loads and deformations were influenced
very little by axial deformations. However, when differential
shortening of the columns and walls was severe, extensive hinging
occurred at loads as low as 90 percent of the service load. The
hinging caused an increase of 14 percent in the roof sway deflec-
tion at working loads for this particular example. It is important

therefore, for serviceability considerations to investigate
the possibility of relative axial deformations due to elastic
shortening corresponding to temperature changes, settlement and
other causes.

Axial deformations may also cause "cantilever"
deflections of the entire structure. Khan and Sbarounis[K2]
have proposed a modification to their method of analysis, by
which this can be accounted for, at least approximately. A
similar procedure could be used in the analysis proposed in
CHAPTER III.

6.6 Summary of Chapters IV, V and VI

The assumptions made in the analysis presented in CHAPTER
III have been discussed in CHAPTERS IV, V and VI.

The moment-curvature diagrams presented in CHAPTER IV
suggest that for concrete structures a strong column-weak beam
design is desirable in view of the limited rotational capacity
of column sections.

The study of the proposed lumping procedure and the
other assumptions indicates that the approximate analysis yields
a reasonable prediction of the load-deflection characteristics of
the building. The ultimate load predicted by this analysis was
close to the ultimate load predicted by various other analyses.
Good agreement was found between the deflections and hinging patterns

predicted by the rigorous and approximate analysis. The test results presented in CHAPTER IX of this report show that the analysis closely predicted the load deflection response and the development of hinges, although it overestimated the measured ultimate load by about six percent.

TABLE 6.1

COMPARISON OF ULTIMATE LOADS IN ONE STORY STRUCTURES,
ONE TO SEVEN BAYS IN WIDTH

No.	Number of Bays	Ultimate Load in Kips		Percent Error
		Analysis By Reference(C6)	Present Analysis	
1	ONE	29.75	30.40	+2.18
2	TWO	44.63	45.60	+2.18
3	THREE	59.50	60.40	+1.51
4	FOUR	74.44	75.20	+1.02
5	FIVE	89.31	90.80	+1.67
6	SIX	104.13	106.00	+1.80
7	SEVEN	119.00	120.40	+1.18

TABLE 6.2

COMPARISON OF ULTIMATE LOADS IN FOUR BAY,
ONE STORY STRUCTURES

No.	Column Size Inches	Ratio of column to Beam Stiffness $\dfrac{I_c/L_c}{I_B/L_B}$	Ultimate Load in Kips		Percent Error
			Analysis by Reference(C6)	Present Analysis	
1	10x10	0.24	74.44	75.20	+1.02
2	12x12	0.53	133.69	134.40	+0.53
3	16x16	1.83	325.00	332.00	+2.15
4	20x20	4.67	557.50	568.00	+1.97
5	24x24	9.99	807.50	824.00	+2.04
6	30x30	25.14	1380.00	1424.00	+3.19
7	34x34	42.06	1906.00	1992.00	+4.50

TABLE 6.3

COMPARISON OF ULTIMATE LOAD IN FOUR BAY, ONE STORY STRUCTURES

HAVING DIFFERENT BAY WIDTH

No.	Changed Width of Bay Number	Frames Having 10 Inch Square Columns			Frames Having 20 Inch Square Columns		
		Ultimate Loads in Kips		Percent	Ultimate Loads in Kips		Percent
		Analysis By Reference(C6)	Present Analysis	Error	Analysis By Reference(C6)	Present Analysis	Error
1	1	74.75	75.20	+0.60	525.00	522.00	-0.57
2	2	74.25	75.20	+1.28	525.00	522.00	-0.57
3	3	74.38	75.20	+1.11	525.00	522.00	-0.57
4	4	74.69	75.20	+0.69	525.00	522.00	-0.57
5	1 & 2	74.56	75.20	+0.85	525.00	522.00	-0.57
6	1 & 3	74.50	75.20	+0.94	525.00	522.00	-0.57
7	1 & 4	75.00	75.20	+0.27	525.00	522.00	-0.57
8	2 & 3	74.19	75.20	+1.36	524.06	522.00	-0.39
9	2 & 4	74.56	75.20	+0.85	525.00	522.00	-0.57
10	3 & 4	74.38	75.20	+1.11	525.00	522.00	-0.57
11	1, 2 & 3	74.50	75.20	+0.94	525.00	528.00	+0.57

TABLE 6.4

COMPARISON OF ULTIMATE LOADS IN
FOUR BAY, ONE STORY STRUCTURES
CARRYING LOADS AT THE TOP OF COLUMNS

No.	The Ratio P/P_o	Ultimate Load in Kips		Percent Error
		Analysis By Reference(C6)	Present Analysis	
1	0.01185	528.75	540.00	+2.13
2	0.02370	536.25	546.00	+1.82
3	0.04740	551.72	564.00	+2.23
4	0.09480	579.84	588.00	+1.41
5	0.23700	632.81	642.00	+1.45
6	0.47400	577.97	600.00	+3.81
7	0.71100	418.12	438.00	+4.75
8	0.9480	216.56	240.00	+10.82

TABLE 6.5

COMPARISON OF ULTIMATE LOADS IN
FOUR BAY, ONE STORY STRUCTURES
CARRYING UNIFORMLY DISTRIBUTED LOAD

No.	U.D. Load Load to Cause end hinges	Value of α	Ultimate Load in Kips		Percent Error
			Analysis By Reference(C6)	Present Analysis	
1	0.0	1.0	633.00	642.00	+1.45
2	0.3034	0.85	615.00	606.00	-1.46
3	0.4551	0.76	595.00	582.00	-2.23
4	0.7585	0.50	544.00	522.00	-4.00

TABLE 6.6

COMPARISON OF ULTIMATE LOADS IN
FOUR BAY AND ONE, TWO, THREE AND
FOUR STORY BUILDINGS

No. of Stories	Ultimate Load in Kips		Percent Error
	Analysis By Reference(C6)	Present Analysis	
1	687.50	690.00	+0.36
2	475.00	480.00	+1.05
3	263.00	260.00	-0.76
4	167.50	170.00	+1.49

TABLE 6.7

COMPARISON OF DEFLECTIONS IN A TWO BAY, TEN STORY SHEAR WALL STRUCTURE

Story	Moment of Inertia Ft^4				Horizontal Load Kips	Deflection Inches		Percent Error in Deflection
	Shear Wall 1	Shear Wall 2	Shear Wall 3	Total		Matrix Analysis of Structure	Lumped Cantilever Wall	
1	5	300	160	465	40	0.055	0.056	+1.8
2	5	300	160	465	40	0.206	0.209	+1.5
3	50	300	115	465	40	0.434	0.439	+1.2
4	50	50	365	465	40	0.736	0.728	-1.1
5	50	100	315	465	40	1.083	1.060	-2.1
6	100	100	265	465	40	1.459	1.422	-2.5
7	140	100	225	465	40	1.855	1.804	-2.7
8	130	200	135	465	40	2.263	2.197	-2.9
9	120	200	145	465	40	2.675	2.595	-3.0
10	100	200	165	465	20	3.089	2.995	-3.0

TABLE 6.8

COMPARISON OF ACTUAL SHEAR TO SHEAR DISTRIBUTED IN STIFFNESS RATIO

FOR TWO BAY, TEN STORY SHEAR WALL STRUCTURE

Story	Total Shear Kips	Shear Wall No. 1		Shear Wall No. 2		Shear Wall No. 3	
		Nominal Shear	Actual Shear	Nominal Shear	Actual Shear	Nominal Shear	Actual Shear
1	380	4.0	8.24	245.0	+300.05	131.0	69.90
2	340	3.65	-9.07	219.0	+ 39.71	117.35	303.61
3	300	32.0	-158.78	194.0	691.38	74.0	-238.06
4	260	28.0	128.16	28.0	206.61	204.0	-79.68
5	220	23.7	-21.20	47.4	- 85.51	148.9	332.55
6	180	39.0	-12.63	39.0	79.13	102.0	110.28
7	140	42.0	31.66	30.0	- 0.16	68.0	106.65
8	100	28.0	36.82	43.0	16.95	29.0	45.19
9	60	15.5	15.29	25.8	33.01	18.7	12.53
10	20	4.3	4.82	8.6	7.26	7.1	7.90

TABLE 6.9

COMPARISON OF DEFLECTIONS AND WALL SHEAR
IN TEN-STORY BUILDING (ONLY BENDING
DEFORMATIONS INCLUDED IN GOLDBERG'S ANALYSIS)

Story	Wall Deflections Inches			Wall Shear Kips		
	Goldberg's Analysis	Present Analysis	Percent Error	Goldberg's Analysis	Present Analysis	Percent Error
1	0.0055	0.00554	+0.73	251.158	270.115	+7.55
2	0.0202	0.02035	+0.74	231.869	236.955	+2.19
3	0.0370	0.03720	+0.54	202.257	201.170	-0.54
4	0.0571	0.05732	+0.39	172.082	171.735	-0.20
5	0.0796	0.07979	+0.24	142.234	141.950	-0.20
6	0.1038	0.10386	+0.06	113.445	113.255	-0.17
7	0.1289	0.12891	+0.01	85.338	85.245	-0.11
8	0.1546	0.15450	-0.06	58.033	57.175	-1.48
9	0.1805	0.18032	-0.10	32.644	32.185	-1.41
10	0.2066	0.20620	-0.19	9.654	6.280	-34.95

TABLE 6.10

COMPARISON OF DEFLECTIONS AND WALL SHEAR
IN TEN-STORY BUILDING (BENDING AND SHEAR DEFORMATIONS
INCLUDED IN GOLDBERG'S ANALYSIS)

Story	Wall Deflections, Inches			Wall Shear, Kips		
	Goldberg's Analysis	Present Analysis	Percent Error	Goldberg's Analysis	Present Analysis	Percent Error
1	0.0142	0.00554	-60.98	241.254	270.115	+11.96
2	0.0369	0.02035	-44.85	224.436	236.955	+ 5.57
3	0.0591	0.03720	-37.05	197.465	201.170	+ 1.88
4	0.0838	0.05732	-31.60	168.545	171.735	+ 1.89
5	0.1100	0.07979	-27.46	139.743	141.950	+ 1.58
6	0.1369	0.10386	-24.13	111.622	113.255	+ 1.46
7	0.1641	0.12891	-21.44	84.186	85.245	+ 1.26
8	0.1910	0.15450	-19.11	57.508	57.175	- 0.58
9	0.2175	0.18032	-17.09	32.658	32.185	- 1.40
10	0.2434	0.20620	-15.28	10.129	6.280	-38.00

TABLE 6.11

COMPARISON OF DEFLECTIONS AND WALL SHEAR
IN TWENTY-STORY BUILDING (ONLY BENDING
DEFORMATIONS INCLUDED IN GOLDBERG'S ANALYSIS)

Story	Wall Deflections, Inches			Wall Shear, Kips		
	Goldberg's Analysis	Present Analysis	Percent Error	Goldberg's Analysis	Present Analysis	Percent Error
1	0.0156	0.01572	+0.77	266.811	286.740	+ 7.47
2	0.0439	0.04394	+0.09	228.409	225.520	- 1.26
3	0.0778	0.07782	+0.03	193.345	190.735	- 1.35
4	0.1188	0.11874	-0.05	163.878	159.405	- 2.73
5	0.1656	0.16544	-0.10	142.166	141.730	- 0.31
6	0.2171	0.21684	-0.12	124.700	126.010	+ 1.05
7	0.2643	0.26390	-0.15	110.369	104.895	- 4.96
8	0.3137	0.31318	-0.16	104.405	103.470	- 0.90
9	0.3648	0.36418	-0.17	100.946	110.700	+ 9.66
10	0.4171	0.41638	-0.17	88.148	87.305	- 0.96
11	0.4702	0.46935	-0.18	75.937	79.590	+ 4.81
12	0.5237	0.52271	-0.19	61.201	61.905	+ 1.15
13	0.5773	0.57616	-0.20	47.490	49.840	+ 4.95
14	0.6309	0.62946	-0.23	33.473	32.480	- 2.97
15	0.6842	0.68244	-0.26	22.817	26.685	+16.95
16	0.7371	0.73499	-0.29	8.983	9.520	+ 5.98
17	0.7896	0.78705	-0.32	-3.665	-0.945	-74.22
18	0.8417	0.83863	-0.36	-17.549	-16.11	- 8.20
19	0.8935	0.88981	-0.41	-30.544	-27.525	- 9.88
20	0.9451	0.94074	-0.46	-37.257	-57.740	-54.98

TABLE 6.12

COMPARISON OF DEFLECTIONS AND WALL SHEAR IN
TWENTY-STORY BUILDING (BENDING AND SHEAR DEFORMATIONS
INCLUDED IN GOLDBERG'S ANALYSIS)

Story	Wall Deflections, Inches			Wall Shear, Kips		
	Goldberg's Analysis	Present Analysis	Percent Error	Goldberg's Analysis	Present Analysis	Percent Error
1	0.0280	0.01572	-43.85	248.448	284.740	+14.61
2	0.0635	0.04394	-30.80	215.392	225.520	+ 4.70
3	0.1026	0.07782	-24.15	184.025	190.735	+ 3.64
4	0.1477	0.11874	-19.60	157.310	159.405	+ 1.33
5	0.1980	0.16544	-16.44	137.365	141.730	+ 3.18
6	0.2524	0.21684	-14.09	121.269	126.010	+ 3.91
7	0.3016	0.26390	-12.50	108.240	104.895	- 3.09
8	0.3530	0.31318	-11.28	102.408	103.470	+ 1.04
9	0.4059	0.36418	-10.28	98.585	110.700	+12.29
10	0.4598	0.41368	- 9.44	86.810	87.305	+ 0.57
11	0.5142	0.46935	- 8.72	74.960	79.590	+ 6.18
12	0.5686	0.52271	- 8.07	60.905	61.905	+ 1.64
13	0.6229	0.57616	- 7.50	47.433	49.840	+ 5.07
14	0.6767	0.62946	- 6.98	33.933	32.480	- 4.28
15	0.7300	0.68244	- 6.51	23.099	26.685	+15.52
16	0.7896	0.73499	- 6.92	9.889	9.520	- 3.73
17	0.8345	0.78705	- 5.69	-2.504	- 0.945	-62.26
18	0.8857	0.83863	- 5.31	-15.798	-16.110	+ 1.97
19	0.9362	0.88981	- 4.95	-27.554	-27.525	- 0.10
20	0.9865	0.94074	- 4.64	-32.641	-57.740	+76.89
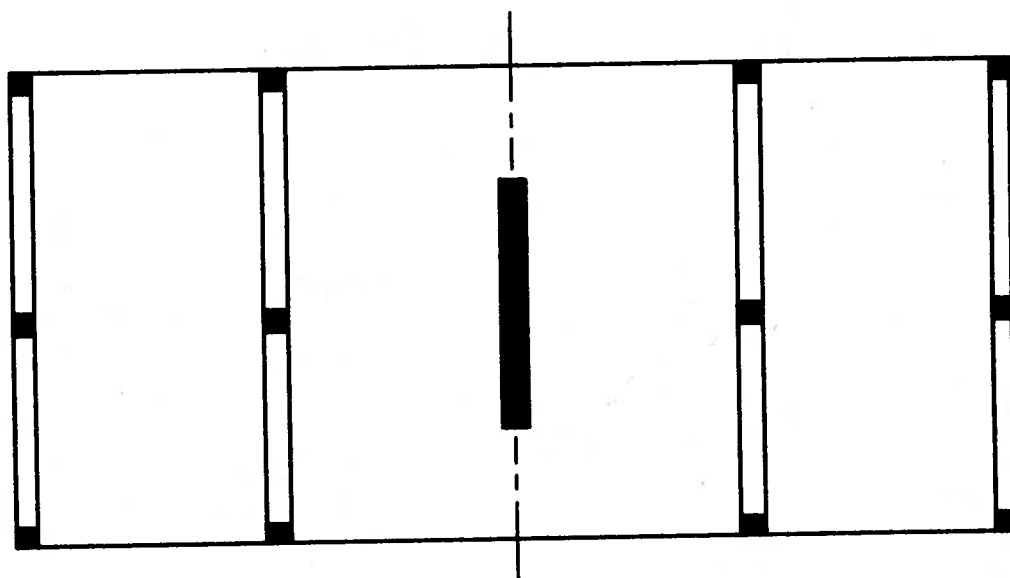
FIGURE 6.1 FLOOR PLAN OF A BUILDING
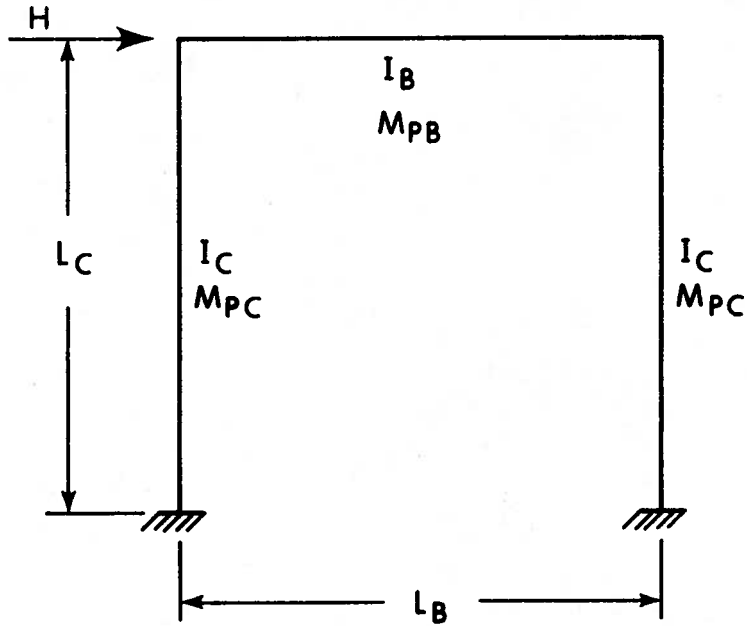
(a) PORTAL FRAME
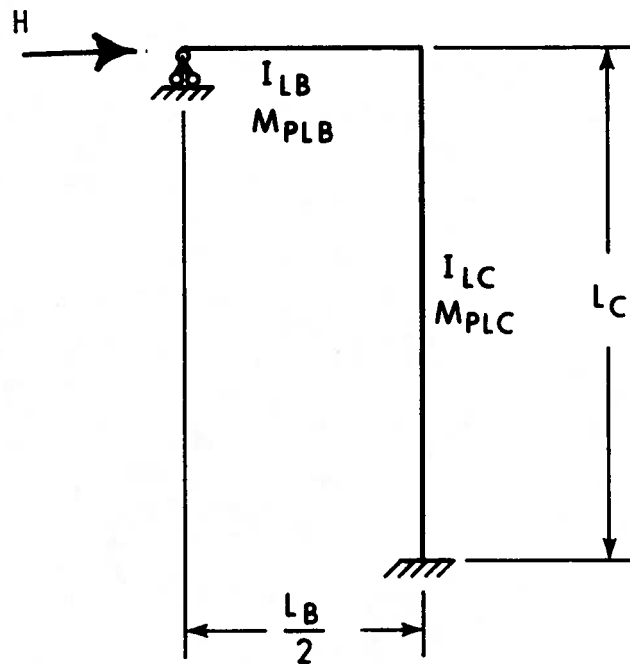
(b) LUMPED PORTAL FRAME

FIGURE 6.2 LUMPING OF A PORTAL FRAME

FIGURE 6.3 LOAD - DEFELECTION CURVE FOR FOUR BAY, ONE STORY FRAME

FIGURE 6.4 LOAD - DEFELECTION CURVE FOR FOUR BAY, ONE STORY FRAME

123
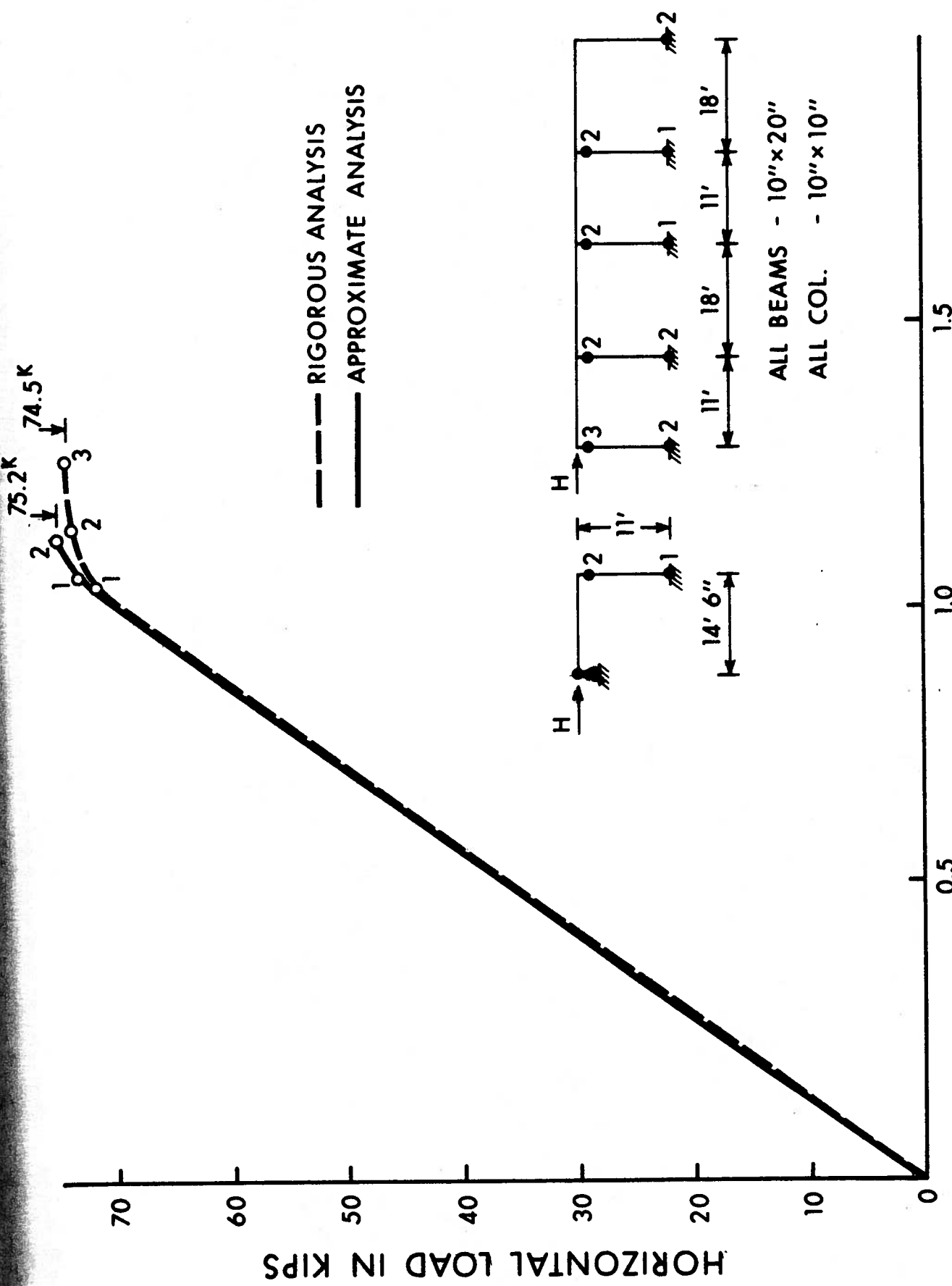
FIGURE 6.5 LOAD - DEFELECTION DIAGRAM FOR FOUR BAY, ONE STORY FRAME

125

FIGURE 6.6 LOAD - DEFELECTION CURVE FOR FOUR BAY, ONE STORY FRAME

FIGURE 6.7 LOAD - DEFLECTION CURVE FOR FOUR BAY, ONE STORY FRAME
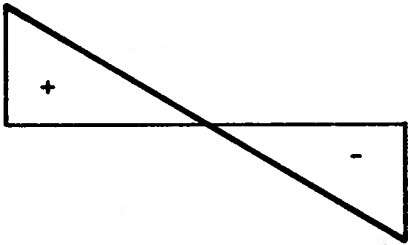
(a) WIND MOMENT IN A
RESTRAINED BEAM

(b) HINGE CONFIGURATION
CORRESPONDING TO (a)
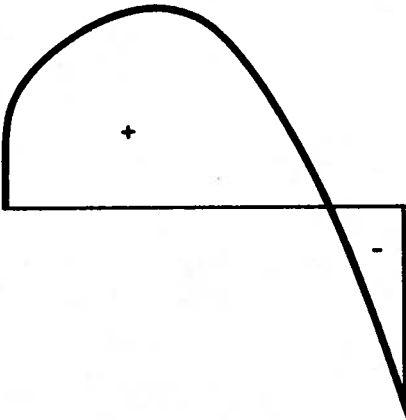
(c) COMBINED MOMENT IN
A RESTRAINED BEAM

(d) HINGE CONFIGURATION
CORRESPONDING TO (c)

FIGURE 6.8 MOMENTS AND HINGE CONFIGURATION IN A RESTRAINED BEAM
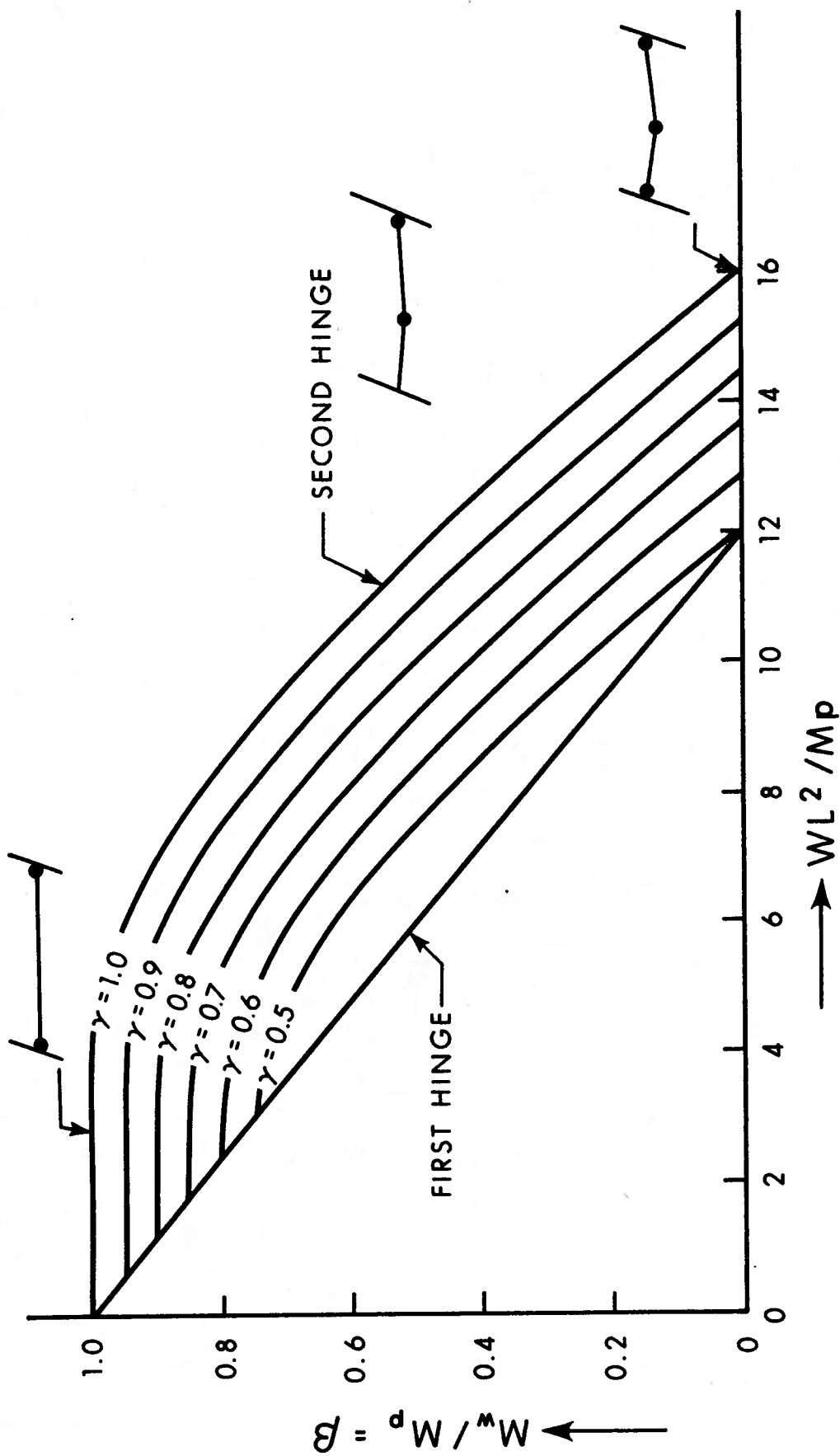
FIGURE 6.9 WIND MOMENT VS. UNIFORMLY DISTRIBUTED LOAD ON A RESTRAINED BEAM
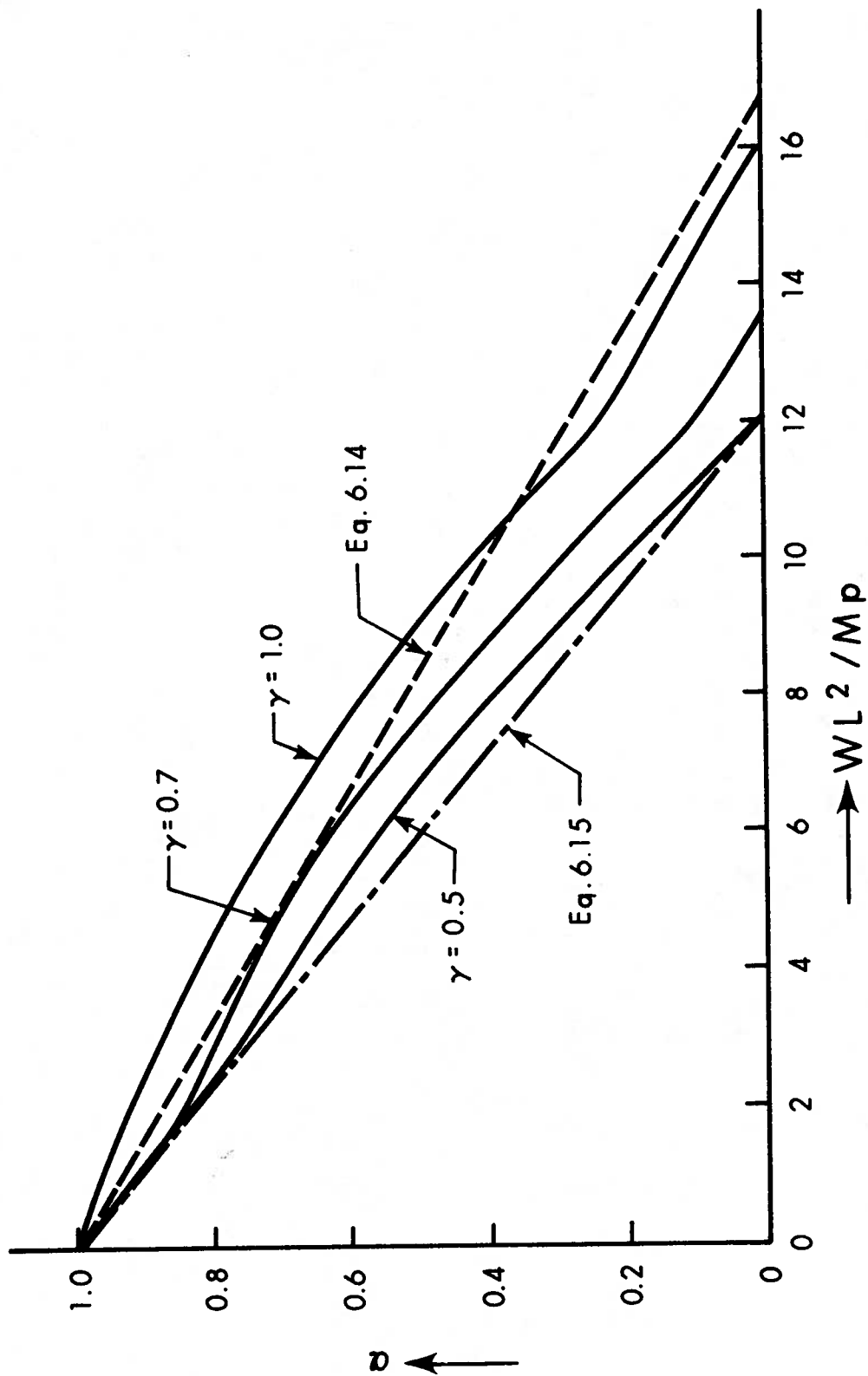
FIGURE 6.10 REDUCTION FACTOR FOR ULTIMATE MOMENT CAPACITY OF THE BEAM
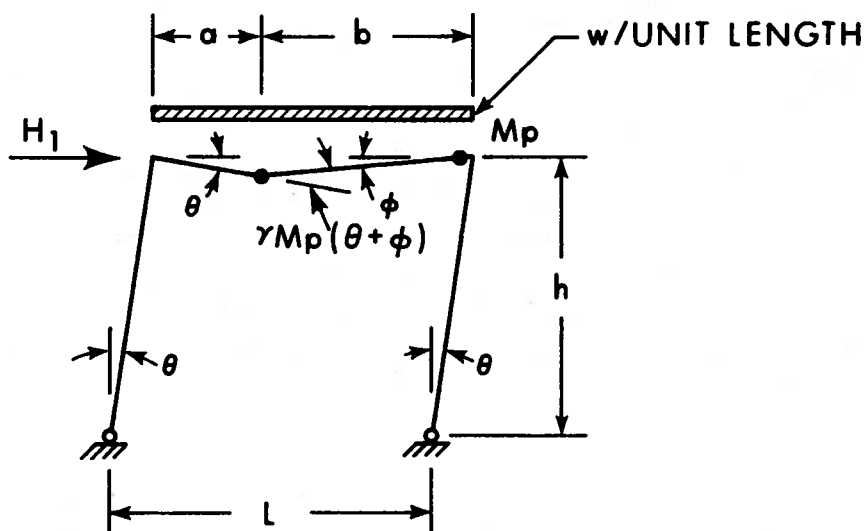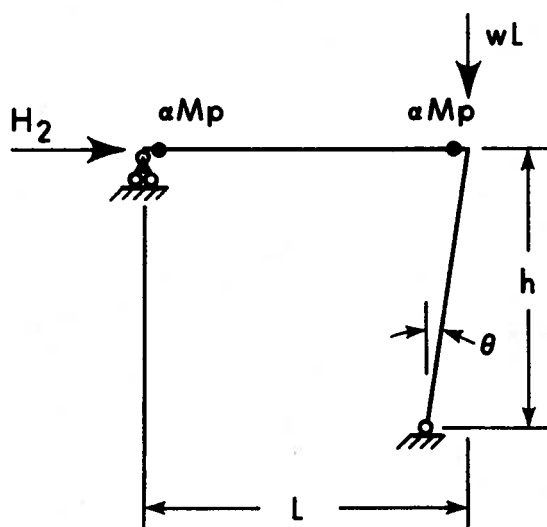
FIGURE 6.11 EFFECT OF FACTOR α ON THE CONSIDERATION OF
UNIFORMLY DISTRIBUTED LOADS

131

FIGURE 6.12 LOAD – DEFELECTION CURVE FOR FOUR BAY, ONE STORY FRAME

132
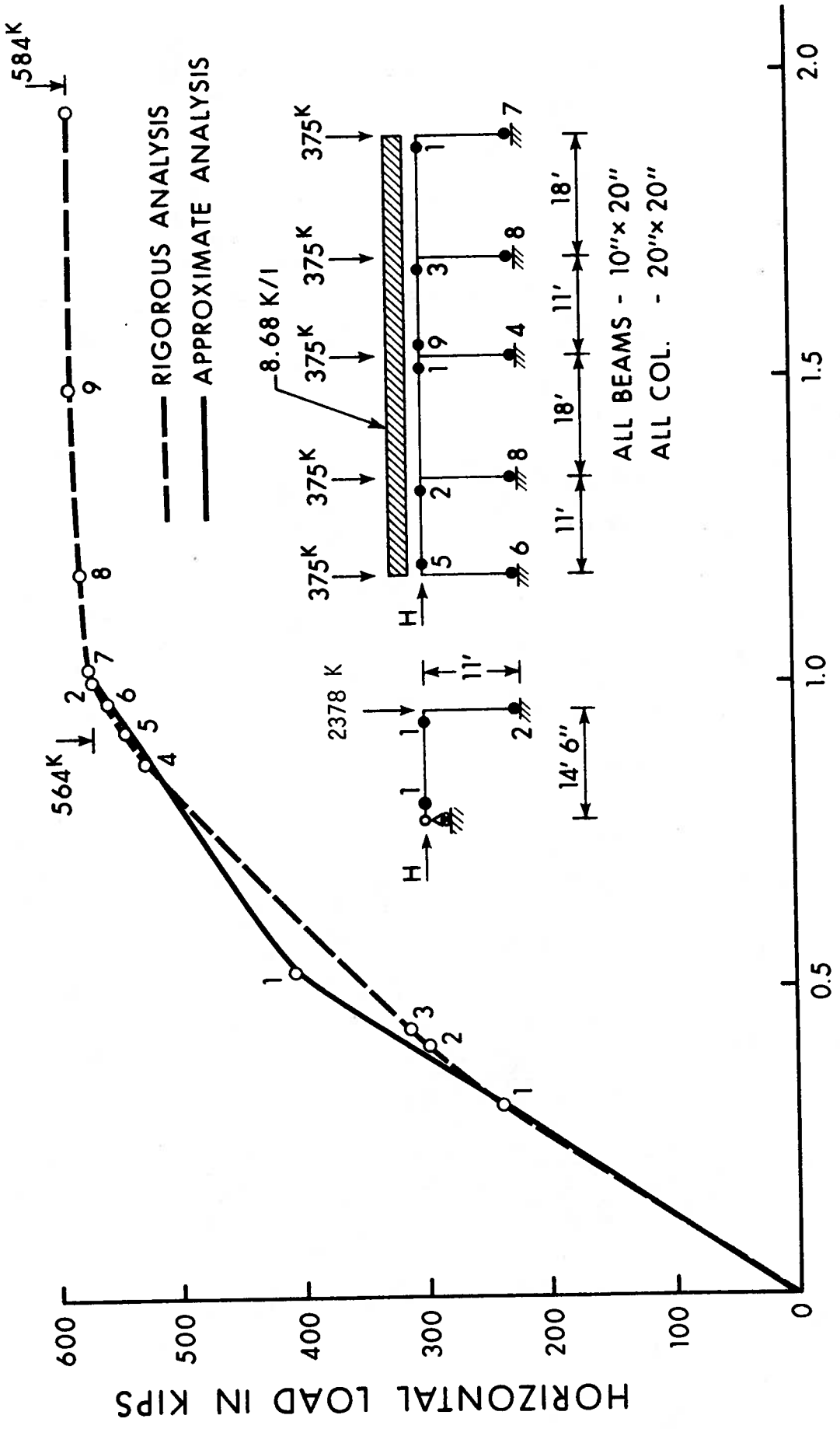
FIGURE 6.13 LOAD – DEFELECTION CURVE FOR FOUR BAY, ONE STORY FRAME
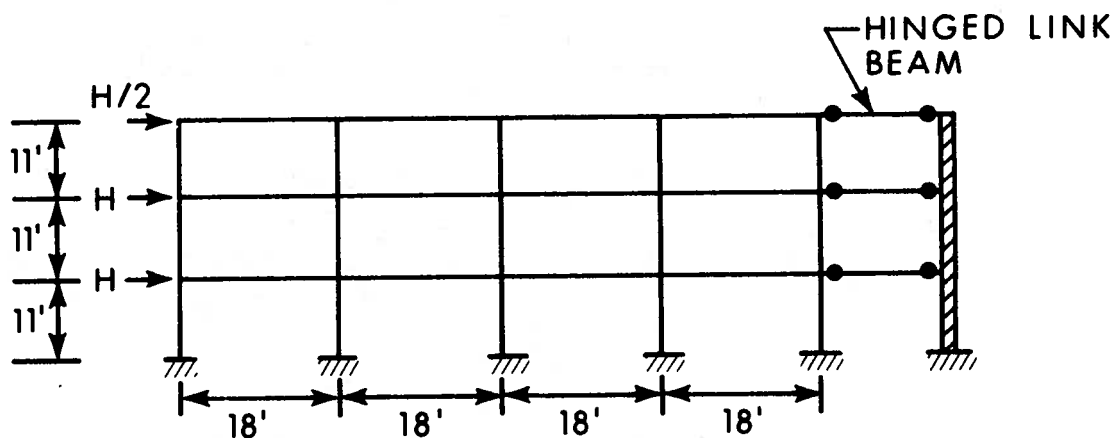
ALL COLUMNS — 20" × 20" WITH 4% STEEL

ALL BEAMS — 10" × 20" WITH 2% STEEL

ALL WALLS — 10" × 120" WITH 1% STEEL

(a) ACTUAL FRAME
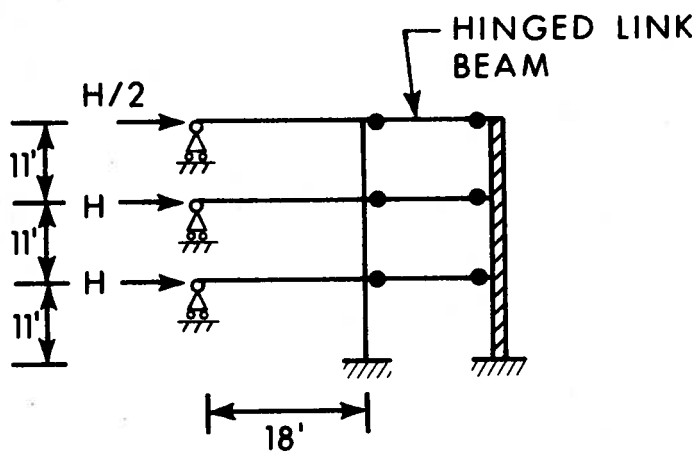
(b) LUMPED STRUCTURE

FIGURE 6.14 THREE STORY STRUCTURE
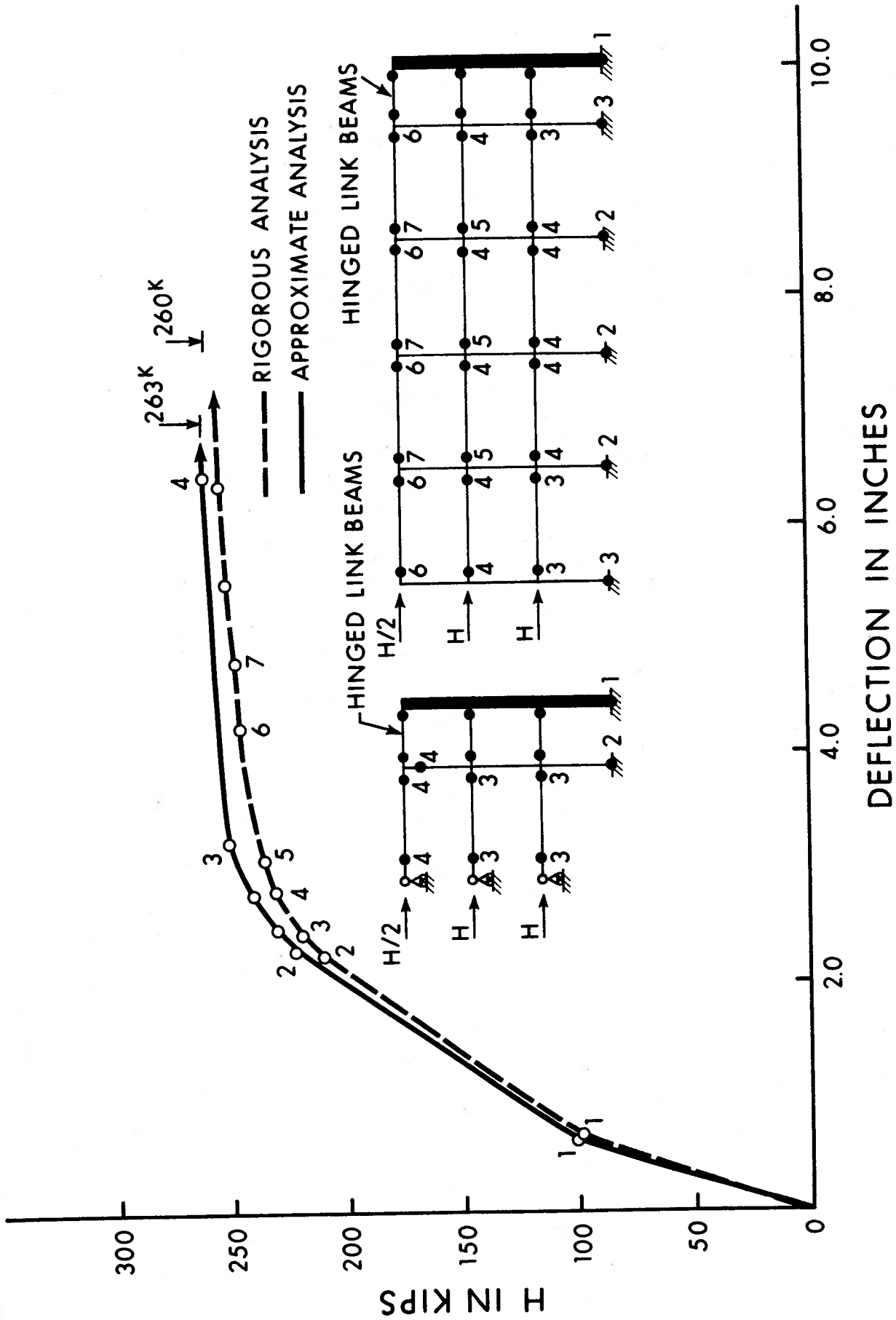
FIGURE 6.15 LOAD - DEFELECTION CURVE FOR FOUR BAY, THREE STORY BUILDING

134

135
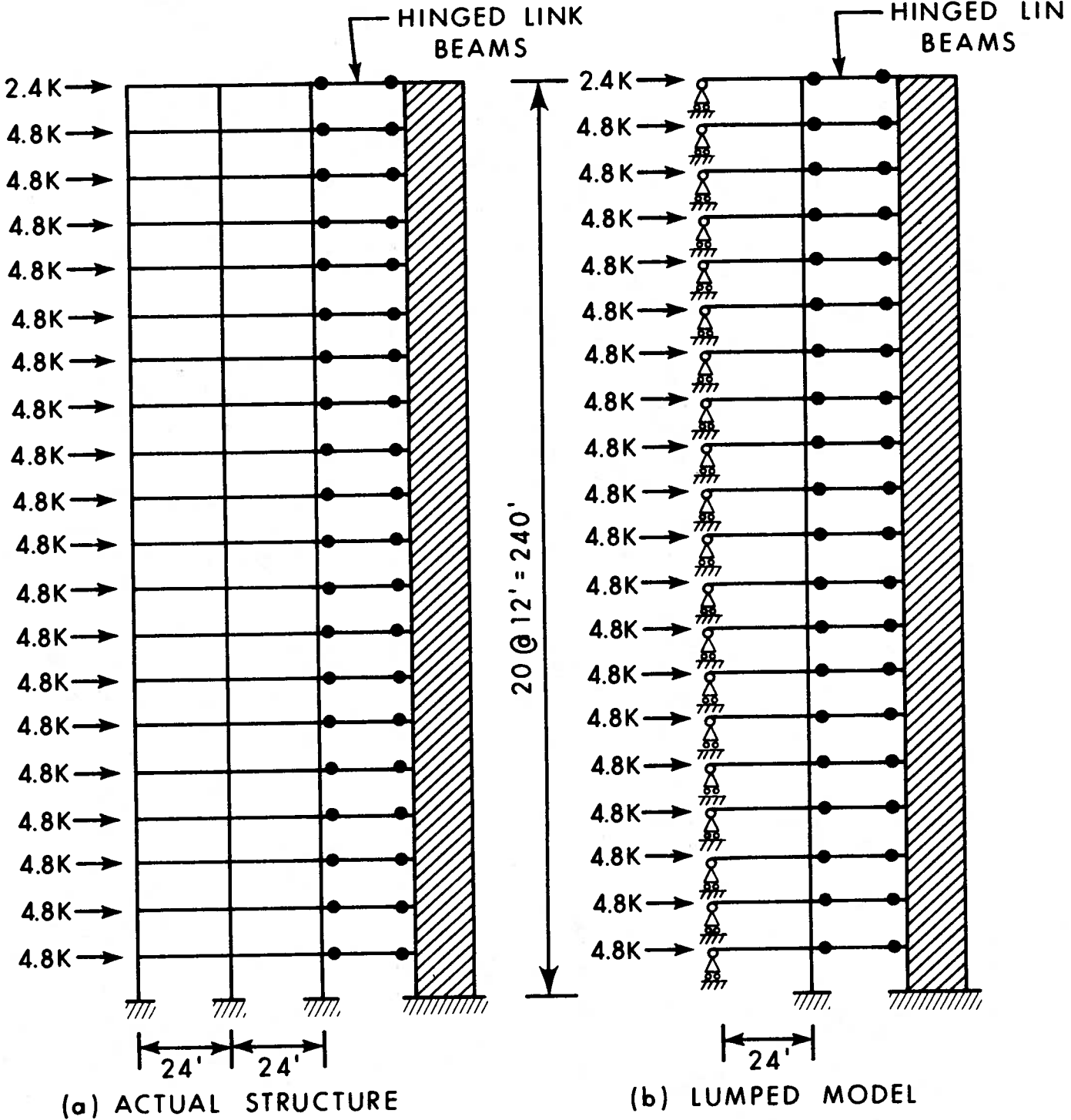
FIGURE 6.16 TWENTY STORY STRUCTURE
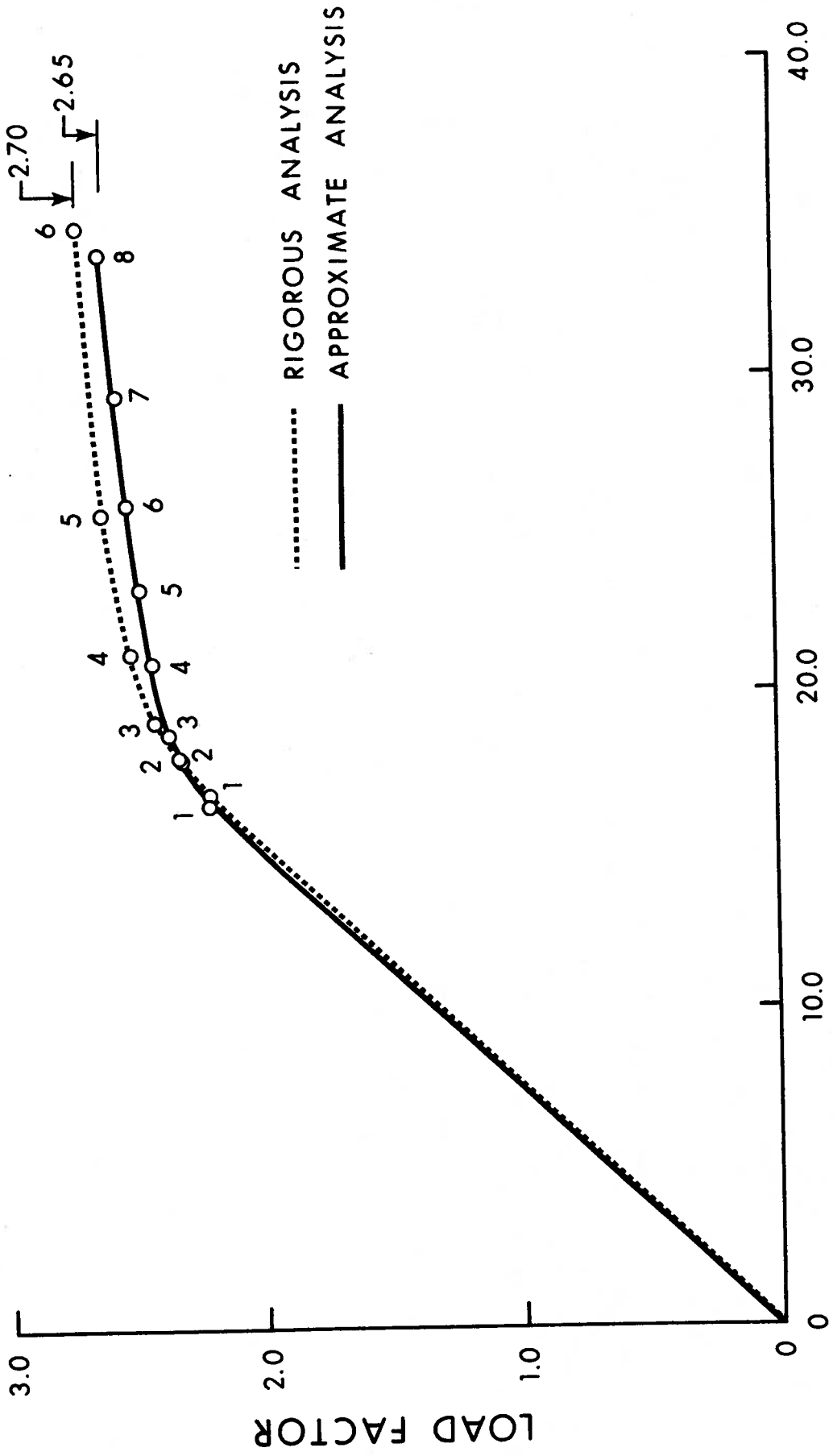
FIGURE 6.17 LOAD – DEFLECTION CURVE FOR TWENTY STORY BUILDING, FRAME 'A'

FIGURE 6.18 HINGE PATTERN IN TWENTY STORY BUILDING, FRAME 'A'
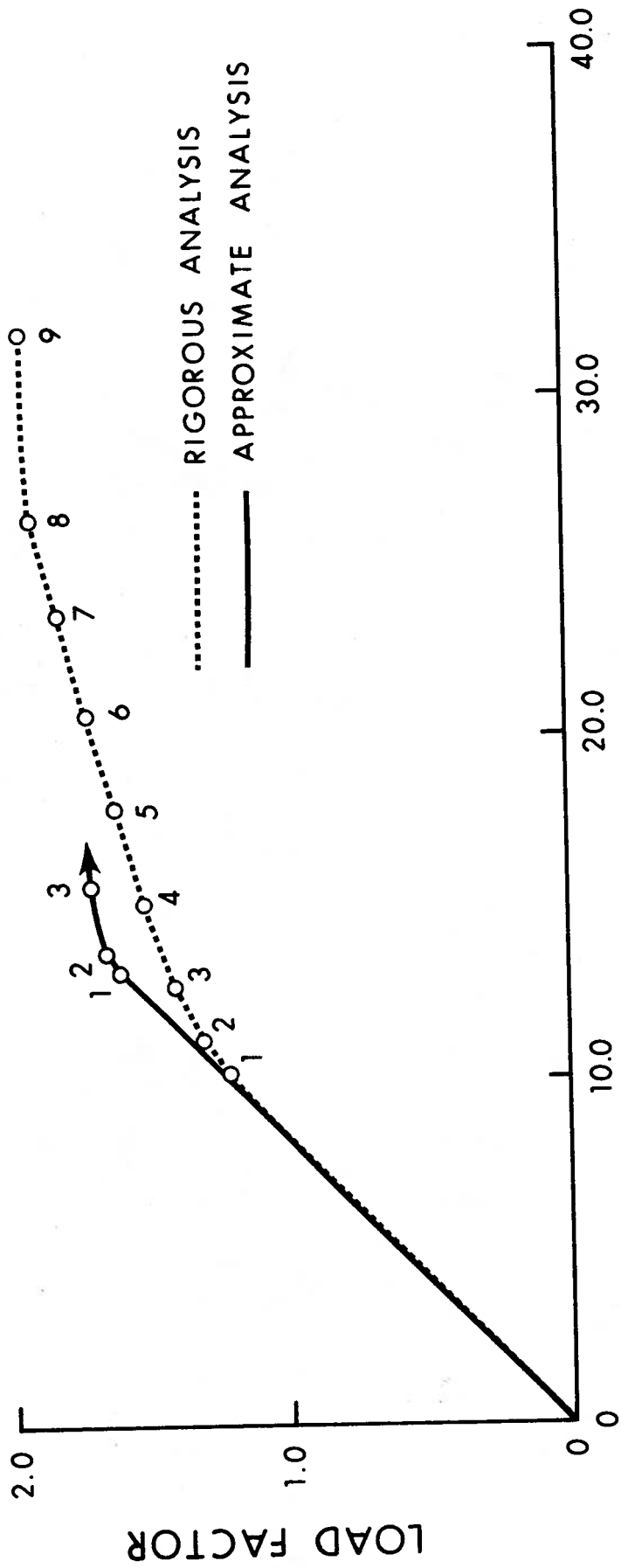
FIGURE 6.19 LOAD - DEFELECTION CURVE FOR TWENTY STORY BUILDING, FRAME 'B'

139

FIGURE 6.20 HINGE PATTERN IN TWENTY STORY BUILDING, FRAME 'B'
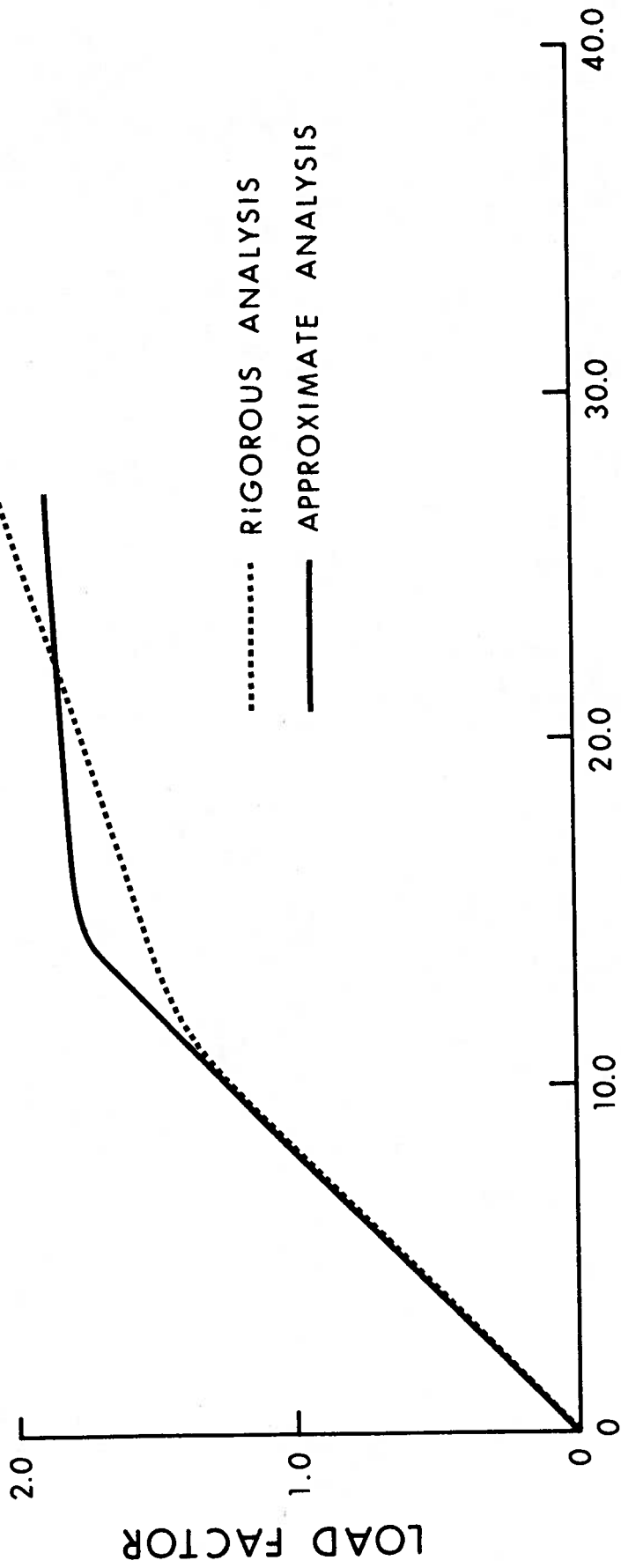
FIGURE 6.21 LOAD - DEFELECTION DIAGRAM FOR TWENTY STORY BUILDING, FRAME 'C'
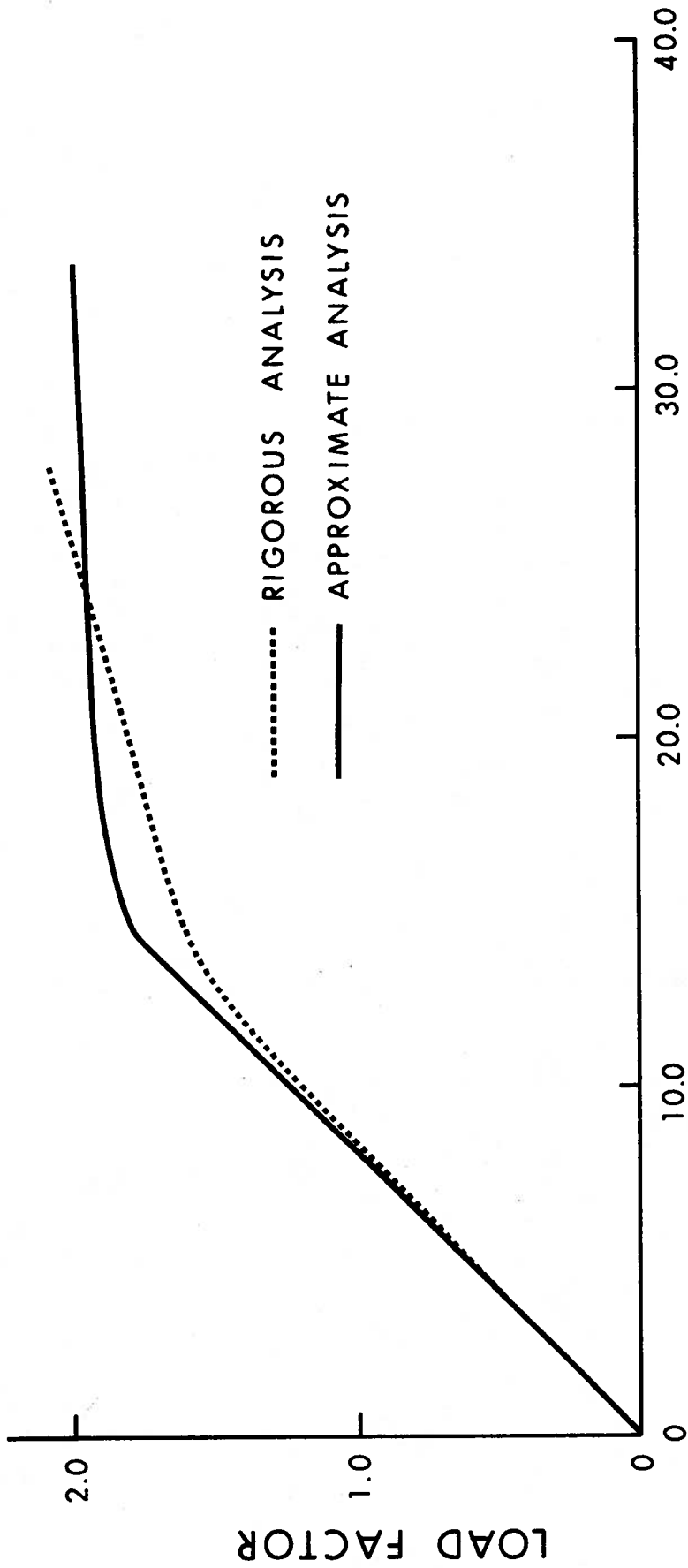
FIGURE 6.22 LOAD - DEFELECTION CURVE FOR TWENTY STORY BUILDING, FRAME 'D'

141
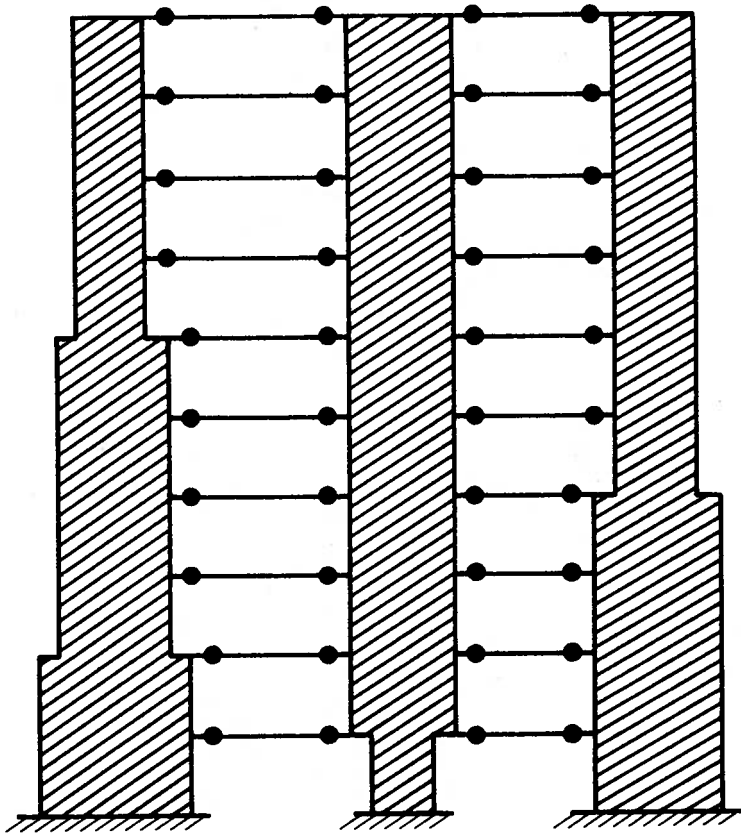
(a) ACTUAL COMBINATION OF WALLS
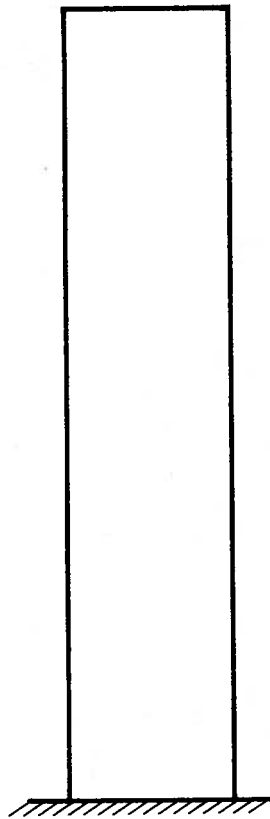
(b) LUMPED WALL

FIGURE 6.23 LUMPING OF WALLS
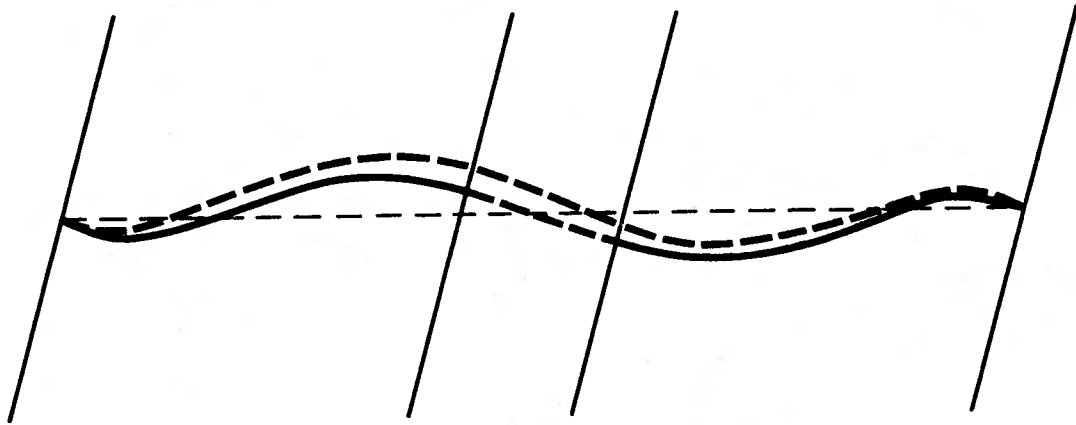
(a) DEFLECTED SHAPE OF THE STRUCTURE

– – – – ACTUAL
——— ASSUMED
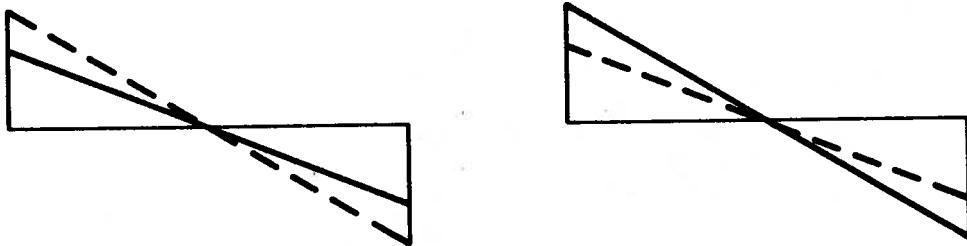
(b) MOMENT DIAGRAM

FIGURE 6.24 EFFECT OF MOVING NEUTRAL AXIS FROM CENTROID

144
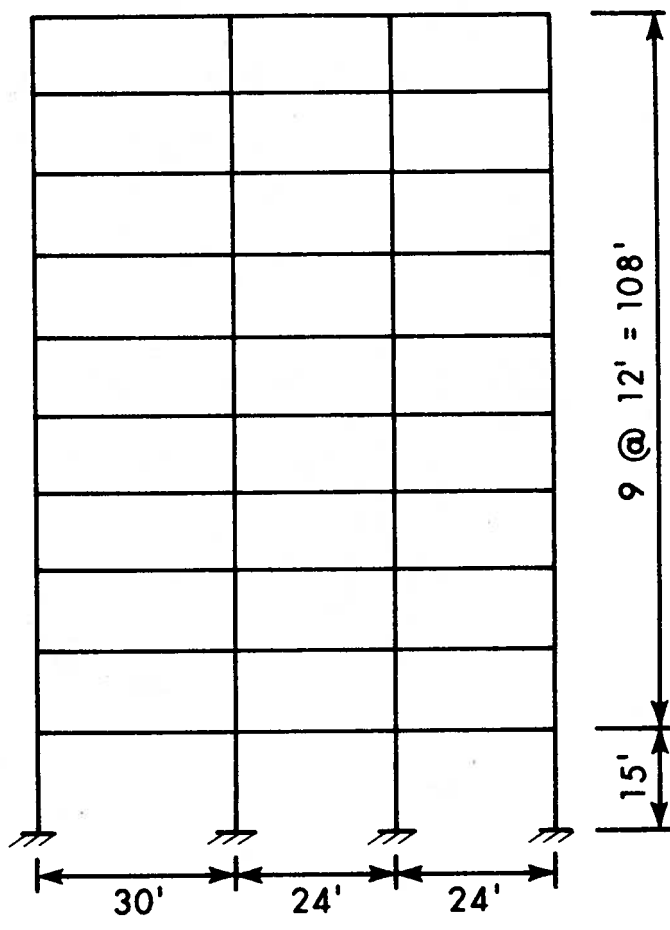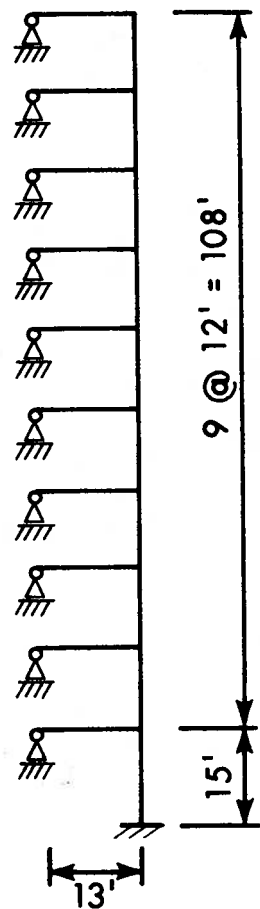
(a) ACTUAL FRAME

(b) LUMPED FRAME

FIGURE 6.25 TEN STORY STEEL FRAME
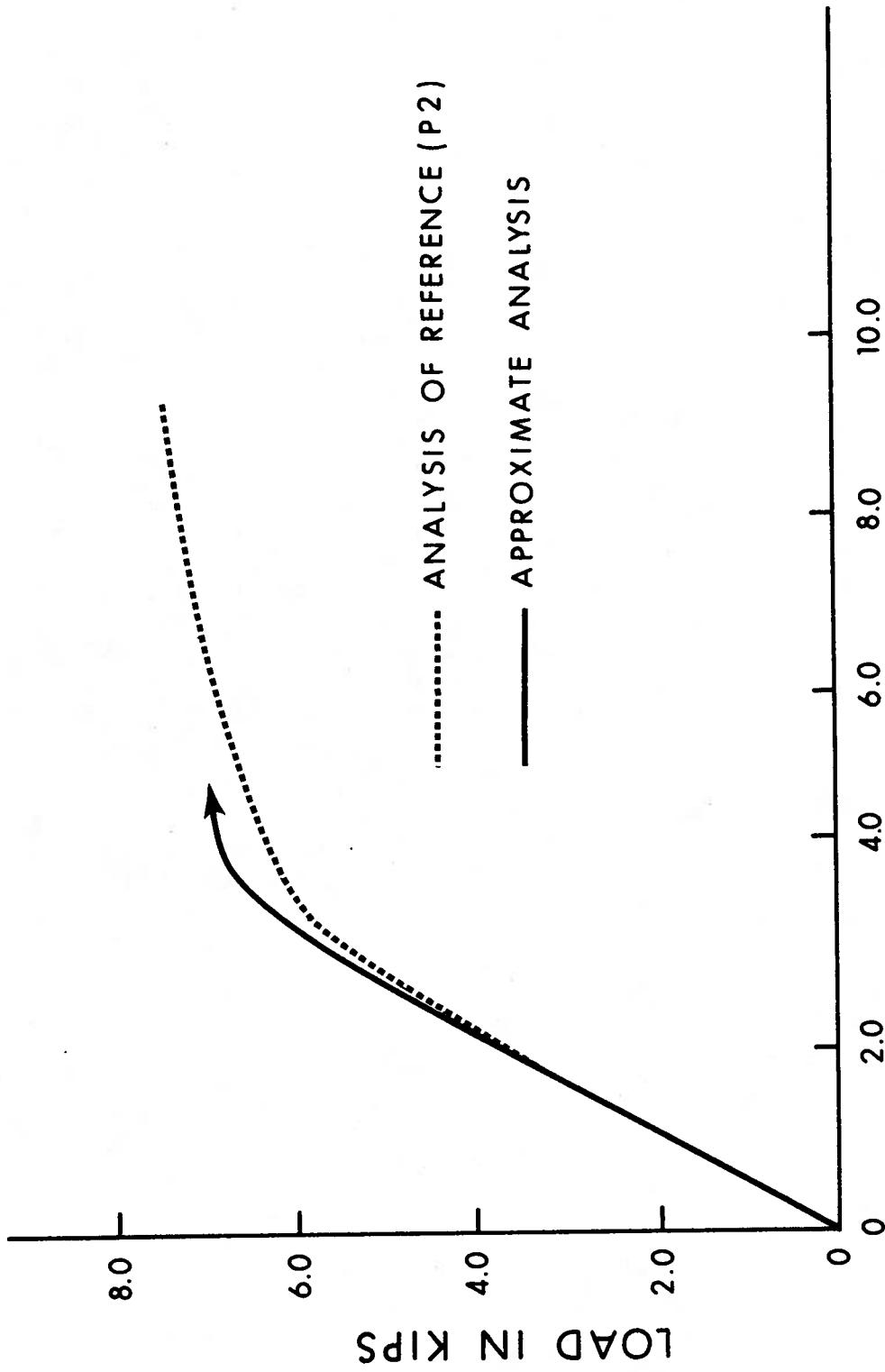
FIGURE 6.26 LOAD - DEFELECTION CURVE FOR TEN STORY STEEL FRAME

FIGURE 6.27 TEN STORY BUILDING WITH SHEAR WALL
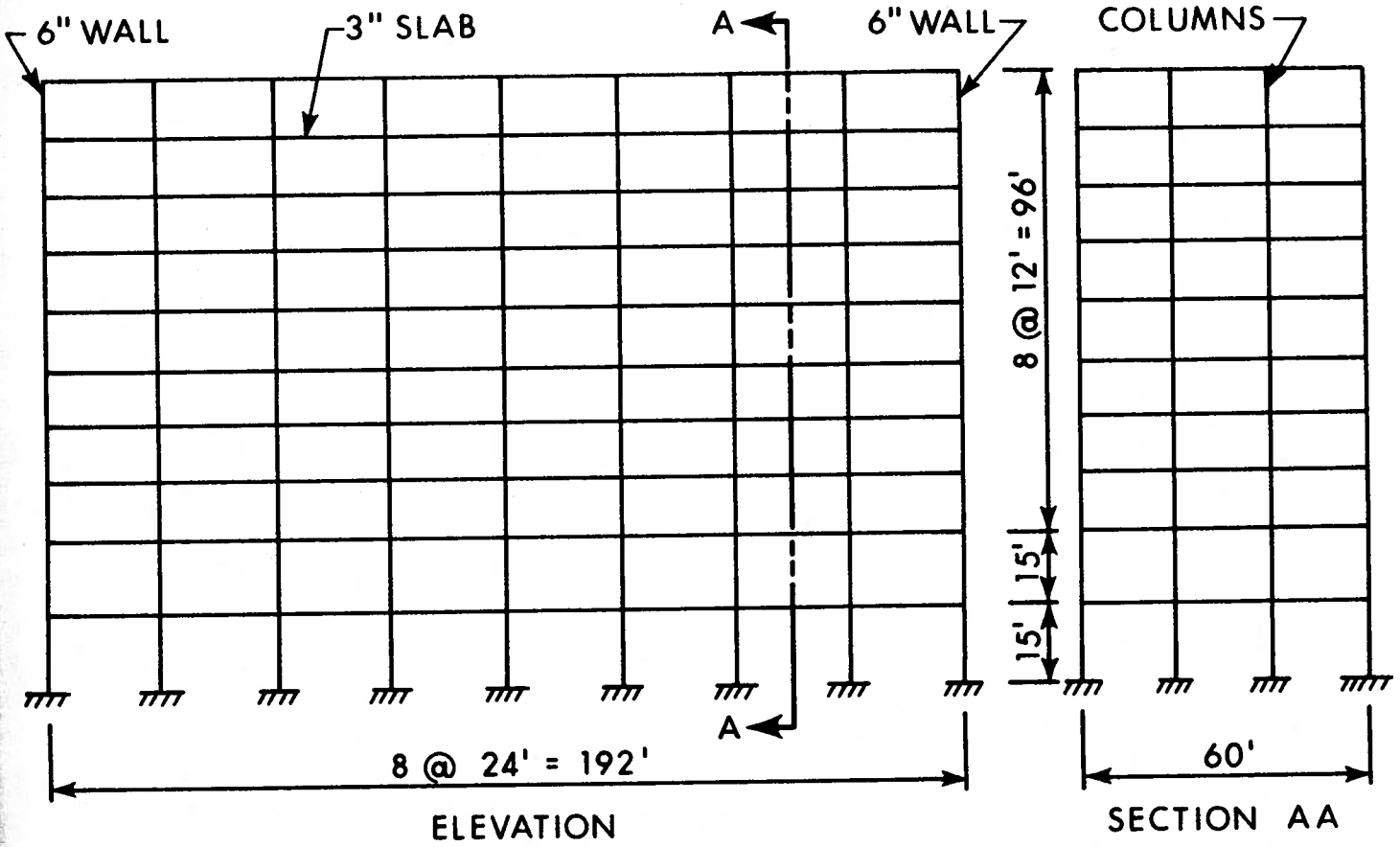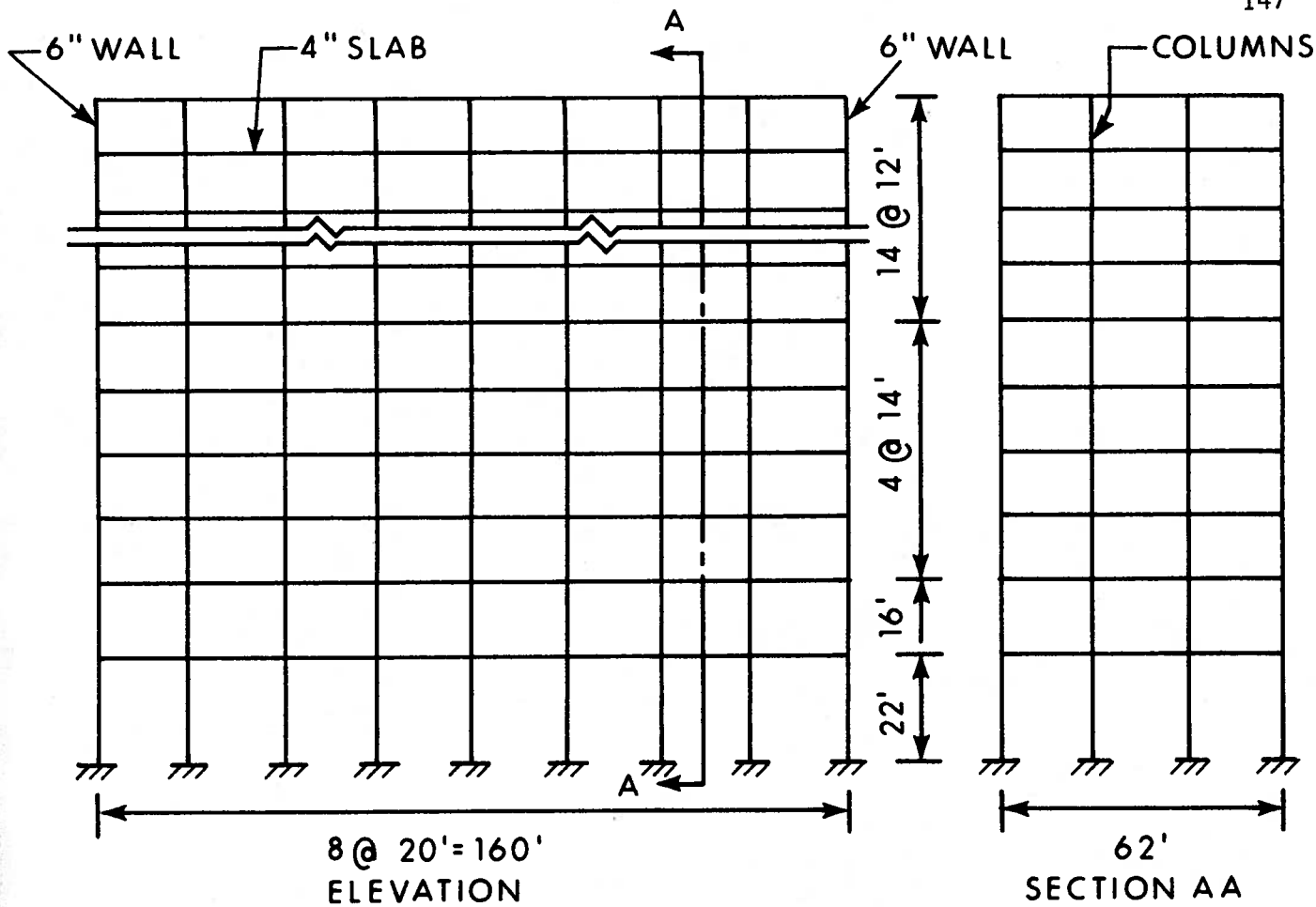
(a) ACTUAL STRUCTURE
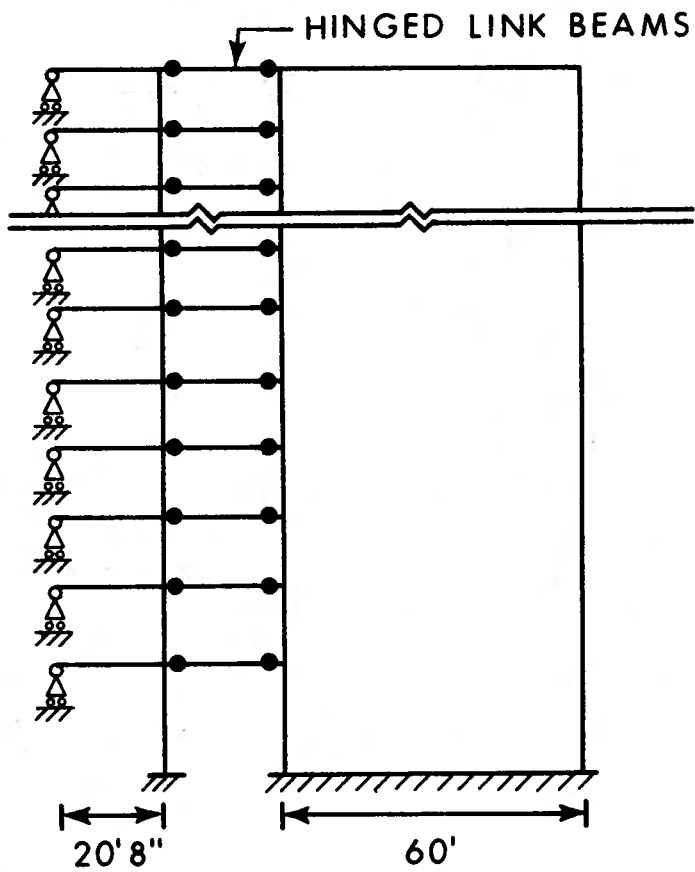
(b) LUMPED MODEL

FIGURE 6.28 TWENTY STORY BUILDING WITH SHEAR WALL

PART III

TEST OF A REINFORCED CONCRETE

SHEAR WALL-FRAME STRUCTURE

CHAPTER VII

TEST SPECIMEN

7.1 Introduction

        A 20 ft. high, one bay, four story reinforced concrete shear
wall-frame was tested to failure under a constant vertical load on the
columns and walls and lateral loads applied in increments, at the
floor levels. The test was carried out to trace the actual behaviour
of such a frame and to check on the accuracy of the analysis presented
in CHAPTER III.

        The test specimen was constructed and tested inside a steel
testing frame designed for this purpose. The frame provided the
reaction for the horizontal loading jacks and supports for observation
platforms and lateral bracing. Sectional elevations of the testing
frame, specimen and the loading apparatus are given in FIGURES 7.1
and 7.2. FIGURE 7.3 shows a photograph of the testing frame, specimen
and instrumentation during the test.

7.2 Layout of Specimen and Reinforcement

        The test specimen was a four story, one bay frame, having one
column and one shear wall interconnected with four beams as shown in
FIGURE 7.4. Each story was 5 foot high center to center of beams. The
columns, beams and walls had nominal cross-sections of 6 x 4½ in.,

149

6 x 6 in., and 6 x 24 in. respectively. The span of the beams was 84 inches from the center of the column to the inner face of wall. In addition all the beams had a projection of 7 inches from the outer face of the columns to ensure adequate anchorage for the beam rein- forcement. The various cross-section used for columns and beams and for walls are given in FIGURES 7.5(a) and (b) respectively. The measured dimensions of the members are listed in TABLE 7.1.

The reinforcement in the wall and column was welded to the respective base plates and extended vertically far enough to be anchored past the point where it was no longer required. The fourth story column had an additional No. 4 bar in the two faces. The beams were reinforced with four bars, two at the top and two at the bottom as shown in FIGURE 7.4. Details of the reinforcement in the column and wall joints are given in FIGURE 7.6. FIGURE 7.7 shows the clevis used for transferring the horizontal jack load to the wall joint.

The ties and stirrups in the columns and beams were made of No. 14 wires, wound in a spiral at 4½ inches on centers. Stirrups for the first two stories of the wall were made out of U-shaped No. 3 bars placed at 6 inches on centers. The legs of these stirrups were lapped on the width of the wall. In the third and fourth story walls, stirrups made of No. 9 wires were provided at 6 inches on centers. Two No. 3 bars were used as stirrups in the wall beam joints. The column beam joints had stirrups within the joint made of No. 9 wire at 2 inches on centers.

7.3 Construction of Specimen

The specimen was constructed one story at a time in the vertical position at the location where it was to be tested so that it was not cracked or stressed due to handling. The reinforcement cages for columns and walls were made in the horizontal position and lifted into place after they were welded to the respective base plates. The concrete was placed in stages. In a typical story the beam concrete was placed one day followed by the next higher column and wall the next day. The concrete was vibrated using a 5 foot long internal vibrator. TABLE 7.2 gives the date of casting and the age of the concrete in the various members on the day of testing. FIGURE 7.8 shows the specimen under construction.

7.3.1 Formwork

The formwork consisted of boxes made of 3/8 inch thick plastic coated ply-wood. These were braced at several points to prevent deflections due to the pressure of the concrete during casting. The column and wall forms could be opened at the two diagonally opposite corners to break them away from the sides of the member. The forms were designed so that the column and wall for one story supported the forms for the next higher beam which in turn supported the forms for the next higher story. The threaded inserts used to hold the rotation meters were bolted to the inside of the forms in the correct locations before casting. The forms were oiled before placing in position. Transits were used to align the formwork vertically. The forms were braced against the testing frame to keep them in vertical position during

casting.

7.3.2 Curing

The forms were loosened one day after casting to destroy the bond between forms and concrete. Once this had been done the formwork was put back in place and left until one week after the entire frame was completed to support the forms for higher stories and protect the concrete from drying. The tops of the beams were covered with wet burlap and polythene. After the forms were removed the frame was cured in the laboratory air at room temperature for 51 days before the test was carried out. The control cylinders made during the various casting stages were also cured in the same way.

7.4 Material Properties

7.4.1 Concrete

The concrete mix was designed to have an average strength of 3000 psi in 28 days. The slump used was 3 inches. The mix proportions were: cement 170 lbs., sand 530 lbs., coarse aggregates 370 lbs., water 100 lbs. The coarse aggregate was 3/8 inch maximum size. This mix was enough for one column and one wall plus six control cylinders. For the beams, half of this mix was enough to make one beam and six control cylinders. The cement used was high early strength portland cement and was fresh at the time of use. The concrete was mixed in a 9 cubic foot Eirich mixer.

153

Six standard control cylinders were made from each batch.
Three of these were tested in compression two days before the
test and one was tested in compression, three days after the
test. The strength reported in TABLE 7.2 is the average strength
of the four cylinders from each batch. The remaining two cylinders
were used for split tension tests whose average strengths are also
reported in TABLE 7.2.

7.4.2 Reinforcing Steel

Intermediate grade deformed reinforcing bar meeting ASTM
specification A-15 was purchased from a local supplier. All the
reinforcement of any one size came from the same heat. The heat
number, composition and standard mill test results of these bars
were supplied by the producer. Two specimens of each of the No. 3,
No. 4 and No. 5 bars were tested in tension. The loads and the
extension on a 2 inch gauge length were recorded by electrical drum
type recorder mounted on the testing machine. The properties of
the reinforcement are tabulated in TABLE 7.3. Typical stress-
strain curves for the bars tested are shown in FIGURE 7.9. The
yield strength of No. 6 bar was taken from the mill test. The
cross sectional areas of all the bars were taken from the mill
test. The value of modulus of elasticity, E, of these bars were
derived from the stress-strain curves shown in FIGURE 7.9.

7.5 Base Connection

The base connections used for the bases of the column and
wall are shown in FIGURES 7.10 and 7.11 respectively. The column

reinforcement extended through holes in the base plate to the bottom of the plate. The holes were enlarged at the bottom of the plate and the bars were welded in these holes. The base plate for the wall was a built up channel and the wall reinforcement was welded on the inside face of the flanges of the channel. In each case the welding was adequate to develop the strength of the bars.

Each base plate was connected to the floor of the laboratory by means of two 1½ inch diameter high strength steel threaded rods, 24 inches apart. The rods had a guaranteed yield strength of 128,000 psi and ultimate strength of 142,000 psi. The bolts extended through the test floor of the laboratory and were anchored by nuts bearing on the underside of the floor.

The construction of the wall and placing of curvature meters on the column limited the extension of these bolts above the floor. As a result the bolts used were too long and a sleeve, 5½ inches long, of 2 inch standard pipe was used as a spacer under the nuts. Although the bolts used were high strength steel and were adequate to take the loads anticipated at the base, the pipe sleeve in the wall base connection yielded at about half the anticipated failure load causing a premature failure of the frame. An identical piece of pipe, cut from the same pipe, was tested in compression in the laboratory to find the stress-strain characteristics of the pipe. From this information a moment curvature relationship was established for the base of the wall as discussed in section 8.10. This predicted moment curvature relationship was used in the

theoretical analysis and good agreement was obtained between the measured and computed behaviour.

7.6 Loading Apparatus

The loading devices were shown in FIGURES 7.1, 7.2 and 7.3. Separate hydraulic systems were used for the vertical and horizontal loads. For each system oil was pumped from a central supply by a pump operated by air pressure. The pumps automatically maintained a given oil pressure. Bleeder valves were used to maintain the desired load.

Horizontal loads were applied by tension jacks connected to the frame by the clevises shown in FIGURE 7.7. The jacks reacted against the testing frame. The three lower jacks were connected on the same hydraulic line so that equal loads could be applied by all three jacks. The fourth floor jack was connected to another hydraulic line. Hydraulic pressure gauges with a range of 0 to 10,000 psi were used to read the pressure between the pump manifold and jack and to facilitate the controlling of loads.

The apparatus used to apply vertical loads on the top of the columns and walls is shown in FIGURES 7.1 and 7.2. A loading beam, placed parallel to the beams in the frame, applied loads through rollers and plates to tops of the columns and walls. The rollers were positioned over the center of the wall and the column. A cross-beam, mounted on top of the center of the loading beam, was connected in turn to two tie rods of 3 x 1 inch cross-section. The lower ends of the tie rods were connected to two 100 ton hydraulic jacks acting in tension. These jacks

reacted, in turn, against gravity load simulator of the type developed at Lehigh University[Y1]. The gravity load simulator is a mechanism which can transmit vertical load but cannot resist horizontal load. Thus the line of action of the applied load remains vertical even if the structure sways. This was checked during the test using scales mounted on the simulator and loading beams read with a transit.

7.7 Lateral Braces

Five lateral braces were used to prevent the out of plane movement of the test specimen. Three were mounted on rods embedded in the projecting ends of the top three beams. Two more lateral braces were used to prevent out of plane movement of the loading beam at the top of the structure. The lateral braces were similar to those developed at Lehigh University[Y1]. The lateral braces consist of a mechanism which permits the specimen to deflect in its plane but does not allow lateral movement of the braced points. FIGURE 7.12 shows the details of one half of a lateral brace. The measurement of lateral movement on the fourth story wall indicated that no significant out of plane movements of the test specimen occurred during the test.

7.8 Instrumentation and Measurements

7.8.1 Introduction

The objective of this test was to observe the actual behaviour of the structure and try to relate it with the analysis described in CHAPTER III. To aid in this correlation, the following measurements were taken:

1. The applied vertical and horizontal loads were
    measured.

2. The concrete strains were measured at various
    positions along the length of the wall so that
    curvatures and moments could be computed.

3. Curvature were measured at a number of points
    along each of the columns and beams to enable
    the computation of moments.

4. The rotations were measured near the ends of the
    member.

5. Horizontal deflections were measured at each floor
    level as were the vertical deflections of the top
    of the column and wall. Lateral deflections were
    measured near the top of the wall.

The techniques adopted for the above measurements are
described briefly in the following sections.

7.8.2 Measurements of Loads

The horizontal and vertical loads were measured both by
oil pressure and by strains measured in previously calibrated bars.
The graduations on the oil pressure gauges, for horizontal jacks,
corresponded to approximately 350 lbs. of load per division. It
was possible to estimate the dial reading to the nearest third of
a division which corresponded to about 115 lbs. of load. Wherever
possible the loads were chosen to fall on a division mark. Between

the end of the jack ram and the device used to transmit the

loads to specimen was a 2 inch long section, one inch in

diameter on which strain gauges were mounted to measure the

jack load. Two longitudinal and two transverse strain gauges

were mounted on the circular piece to form the four arms of

wheat-stone bridge circuit. In this measurement the effect

of any bending or temperature change were compensated for [B7].

To measure the vertical load, one strain gauge was

mounted longitudinally on two faces of each tie rod. These

strain gauges were connected to form two opposite arms of

wheat-stone bridge circuit. The other two arms of the bridge

were provided by mounting two dummy strain gauges on similar

steel plates to provide temperature compensation.

The two jacks used to apply the vertical loads were

connected to a control panel with pressure gauges to measure

the pressure in each jack. The dial readings could be estimated

to the nearest third of a division which corresponded to about

650 lbs. in each jack. Loads were chosen to fall on a

division mark.

The strain gauges were all connected to a Dymec data

acquisition system which read the voltage difference between the

output terminals and printed this out on an automatic printer.

The jacks and pull rods were calibrated before the test to find

the correlation between the oil pressure, voltage difference

reading and the applied loads. The calibrations were found to be

linear.

7.8.3 Concrete Strain Measurements in the Walls

Strains were measured on the face of the wall using Whittemore and Demec gauges. The first two stories of the wall had Whittemore points at 10 inch intervals and the upper two stories had Demec points at 8 inch intervals. The gauge lines were used, located at half inch and 4 inches from the outer face of the wall and at 1¼ inches from the inner face of the wall, respectively. A diagram showing these points is given in FIGURE 7.13. The points were placed on opposite faces of the wall in alternate stories to facilitate taking the readings from the working platforms. Two groups of three measurement points on two adjacent cross-sections made up a curvature measuring station. In FIGURE 7.13 the curvature measuring stations are labelled by numbers in circles placed in the center of the curvature measuring station.

The Whittemore and Demec gauge readings could be reproduced to the nearest 10 and 12.5 micro-inches/inch of strains, respectively. This will result in a maximum error of 21.4 and 26.6 micro-inches/inch in the estimation of curvatures times depth, ϕt, for the wall sections, from Whittemore and Demec gauge readings, respectively. The concrete strain readings, in the first story, were found to be very erratic presumably due to the cramped working space between the gravity load simulator and the frame in this story.

7.8.4 Curvature Measurements in Columns and Beams

Curvatures were measured at two locations at each end of each column and one location at each end of each beam using curvature meters developed by Chang[C2]. The details of a typical curvature meter are shown in FIGURE 7.14. The meter consists of two steel reference frames which are attached to the members by four cap-screws screwed into the concrete surface and have 0.0001 inch dial gauges mounted at mid-depth of the specimen to read the relative deflections of the ends of the arms. The gauge length was 8-3/8 ± 3/8 inches and these gauges gave an average curvature over this length. In order to mount the meters at the joints, the curvature meter was modified for the attachment to the member. Similarly, the curvature meter used for top beam was modified to ensure against interference of the loading beam. The maximum error in the estimation of curvature times depth, ϕt, of the column and beam sections would be in order of 18.7 and 25 micro-inches/inch, respectively, if the dial gauge readings on the curvature meters are reproducable to nearest 0.0005 inch.

The locations of the measuring stations are shown in FIGURE 7.13. Two adjacent reference frames form a curvature measuring station. The numbers in circles, shown in FIGURE 7.13, indicate the measuring station numbers.

7.8.5 Rotation Measurements

The rotations of points on the columns and beams near each joint and at the center of the wall joints were measured

electrically. The location of the rotation meters are shown in
FIGURE 7.15. The measuring stations were labelled and are given
by the numbers in circle, shown in FIGURE 7.15.

The basic tool used to measure rotations is shown in
FIGURE 7.16. This rotation meter is essentially the same as
the rotation meter developed at Lehigh University [Y1]. Basically
the rotation meters consisted of a 0.03 inch thick spring steel
strip with a 9.56 lbs .weight clamped to the lower end. The
upper end of the strip was connected to two square bars which were
firmly screwed to a base plate. The base plate was fastened to
the specimen with 1/4 inch bolts screwed into inserts cast into
the members during construction of the specimen. The weight
tends to remain vertical as the structure rotates and bending
strains are induced in the spring steel strip which acts as a beam
under tension. By measuring the bending strain induced at the
end of the strip the rotation can be determined using the formulas
for a beam under tension.

Four active strain gauges were used to form the four
arms of a wheat-stone bridge to measure the strains as shown in
FIGURE 7.17. Gauges 1 and 4 were on one side of the strip and 2 and
3 on the other. This circuit compensated any temperature change and
the strain measured is four times the average strain induced in
the strip at the gauge point[B7]. All the rotation meters were
calibrated using a mechanical rotation meter, consisting of a level
bubble and micrometer. The calibration was found to be linear and
was approximately 525 micro inches/inch per degree of rotation.

7.8.6 Deflection Measurements

The horizontal deflections were measured using scales, divided in 50ths of an inch, mounted on the beams. The scales were read with a transit. The scales mounted on the top three beams were 12 inches long whereas the scale on first beam was 6 inches long. A scale was also mounted on the laboratory floor to check for movement of the transit.

To measure the vertical deflections, magnetic bars were attached to the plates below the rollers on which the loading beam sat. Vertical wires attached to these bars extended to dial gauges mounted on magnetic stands on the floor of the laboratory. The deflection measured in this way included a horizontal component due to the lateral deflection of the specimen. This was corrected for in computing the deflections although the maximum error did not exceed 0.05 inch.

A scale was mounted on one end of the fourth story wall and the lateral deflection was read with a second transit.

TABLE 7.1

MEASURED DIMENSIONS OF THE SHEAR WALL-FRAME SPECIMEN

Member	Length Inches	Cross-section		Steel Layer No. From Tension Face	Areas of Steel in.^{2}	Dist. of Steel Centroid From Tension Face Inch
		Width b Inch	Depth t Inch			
Col. 1	60.5	6.0	4.5	1	0.222	0.750
				2	0.222	3.750
Col. 2	60.0	6.0	4.5	1	0.222	0.750
				2	0.222	3.750
Col. 3	60.0	6.0	4.5	1	0.222	0.875
				2	0.222	3.625
Col. 4	60.0	6.0	4.5	1	0.415	0.750
				2	0.415	3.750
Beam 1 (Col. end)	84.0	6.0	6.0	1	0.386	0.750
				2	0.386	5.250
(Wall end)				1	0.386	1.125
				2	0.386	5.250
Beam 2 (Col. end)	84.0	6.0	6.0	1	0.610	0.937
				2	0.610	5.062
(Wall end)				1	0.610	1.437
				2	0.610	5.125
Beam 3 (Col. end)	84.0	6.0	6.0	1	0.610	0.937
				2	0.610	5.062
(Wall end)				1	0.610	1.625
				2	0.610	5.000

TABLE 7.1 (contd.)

Beam 4 (Col. end)	84.0	6.0	6.0	1	0.610	1.000
				2	0.610	5.000
(Wall end)				1	0.610	1.687
				2	0.610	5.062
Wall 1	60.5	6.0	24.0	1	0.860	1.250
				2	0.860	2.625
				3	0.610	4.125
				4	0.610	5.437
				5	0.610	18.563
				6	0.610	19.875
				7	0.860	21.375
				8	0.860	22.750
Wall 2	60.0	6.0	24.0	1	0.860	1.250
				2	0.860	2.625
				3	0.860	21.375
				4	0.860	22.750
Wall 3 and 4	60.0	6.0	24.0	1	0.860	1.250
				2	0.860	22.750

TABLE 7.2

AGE AND CONCRETE STRENGTH OF THE MEMBERS

Member	Date of Casting	Age on The Day of Test Days	Concrete Strength in Comp. Psi	Split Tensile Strength Psi
Col. 1	23. 9.68	80	3,303	513
Col. 2	1.10.68	72	3,195	417
Col. 3	8.10.68	65	3,348	509
Col. 4	11.10.68	62	3,497	488
Beam 1	30. 9.68	73	2,390	356
Beam 2	4.10.68	69	2,868	384
Beam 3	9.10.68	64	2,930	441
Beam 4	15.10.68	58	2,618	426
Wall 1	26. 9.68	77	3,360	529
Wall 2	1.10.68	72	3,195	417
Wall 3	8.10.68	65	3,348	509
Wall 4	11.10.68	62	3,497	488

TABLE 7.3

PROPERTIES OF REINFORCEMENT

Bar Size	Area* in^2	Yield Strength Psi	Ultimate Strength* Psi	Modulus of Elasticity Psi
No. 3	0.111	55,700	78,900	27.7×10^6
No. 4	0.193	53,000	80,800	27.4×10^6
No. 5	0.305	50,700	76,500	26.3×10^6
No. 6	0.430	54,900*	82,800	27.5×10^6

* Taken from Mill Test
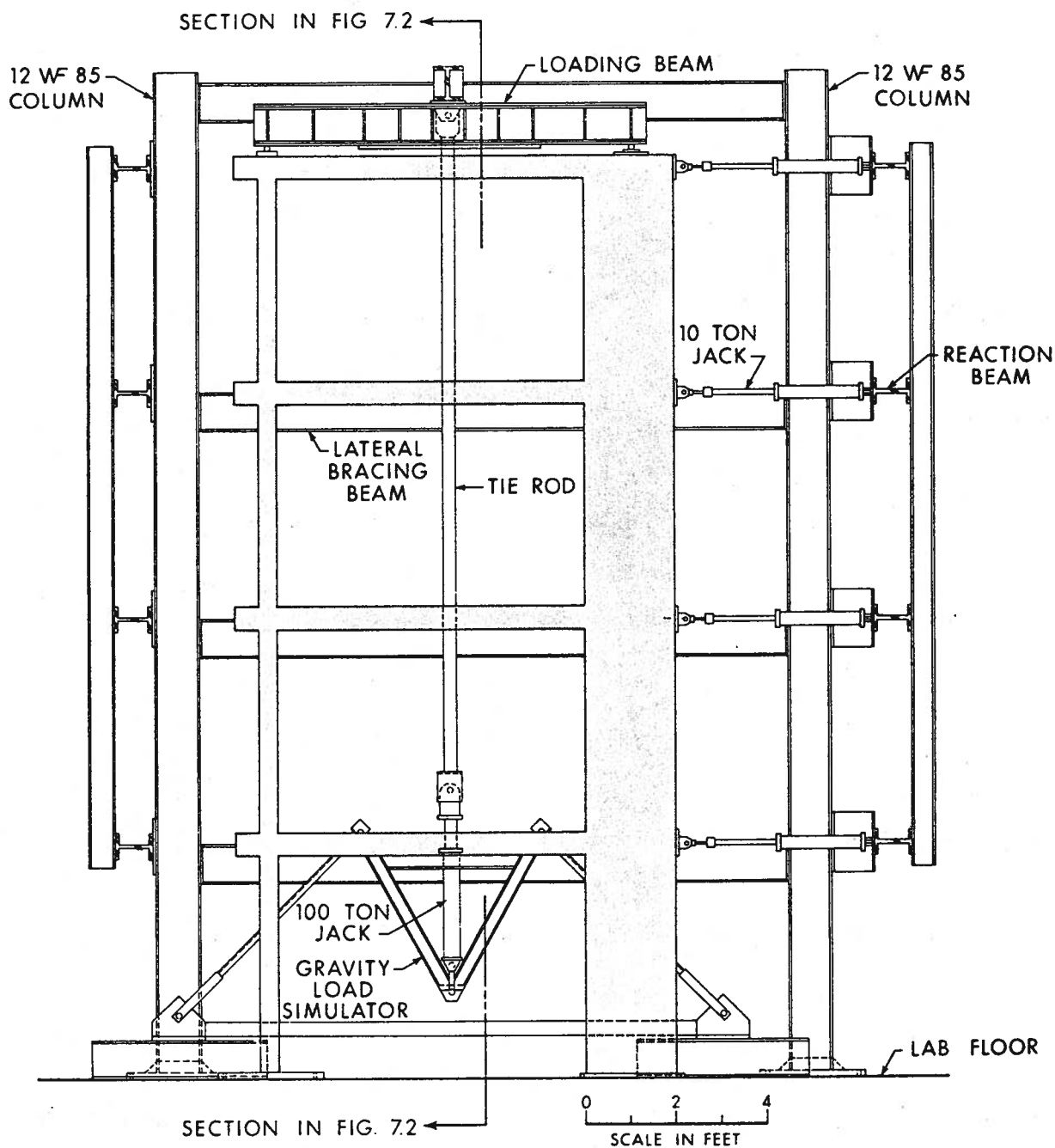
FIGURE 7.1 SECTIONAL ELEVATION OF TEST SPECIMEN INCLUDING

TESTING FRAME AND LOADING DEVICE

167
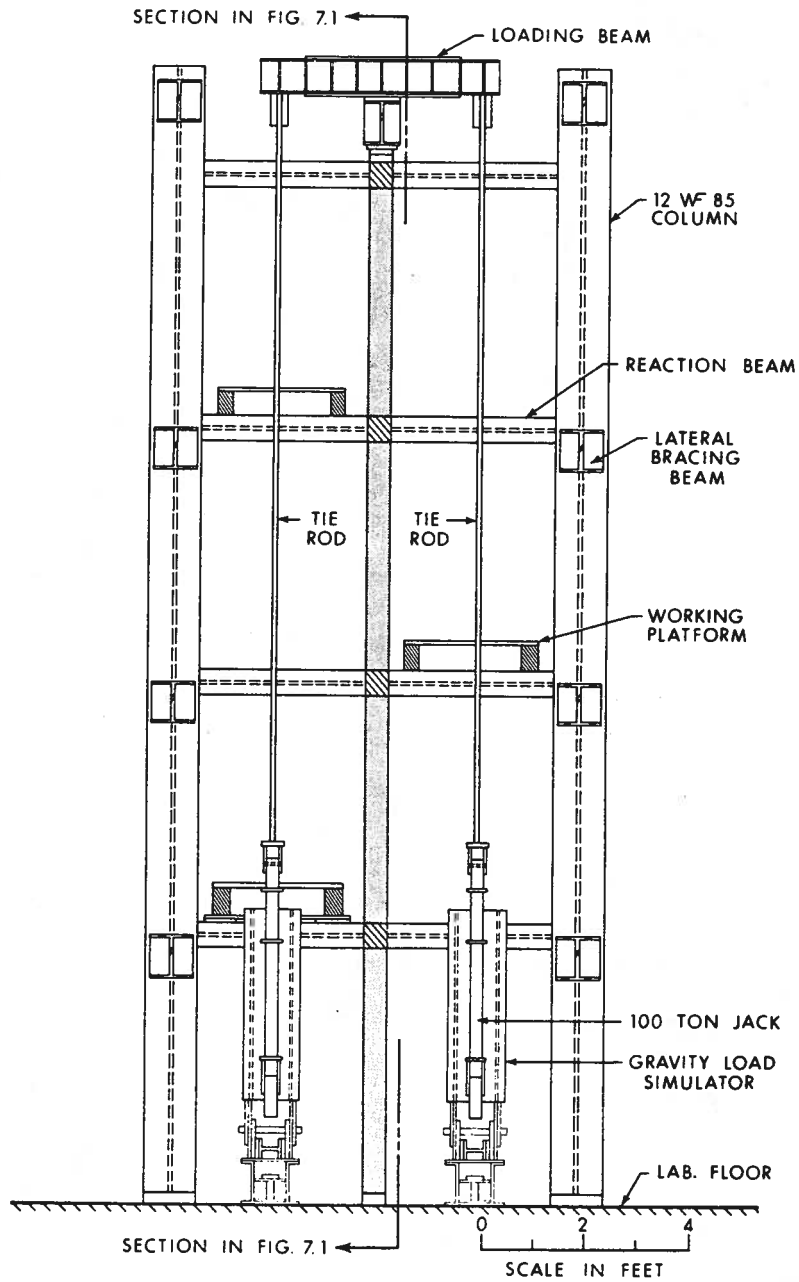
FIGURE 7.2 SECTIONAL SIDE ELEVATION SHOWING SPECIMEN, TESTING FRAME,
OBSERVATION PLATFORM AND VERTICAL LOADING DEVICE
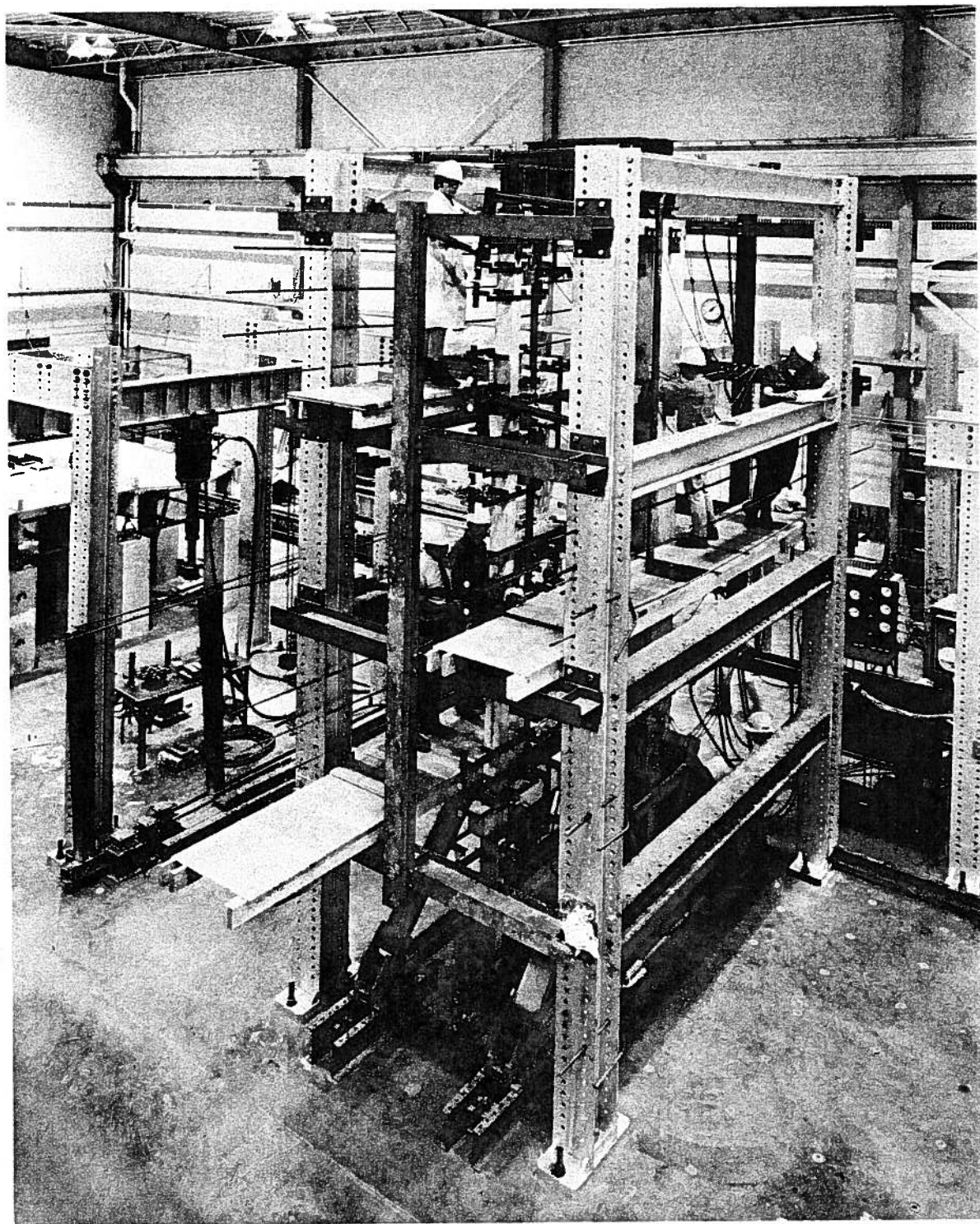
FIGURE   7.3   SPECIMEN   DURING   TEST

169
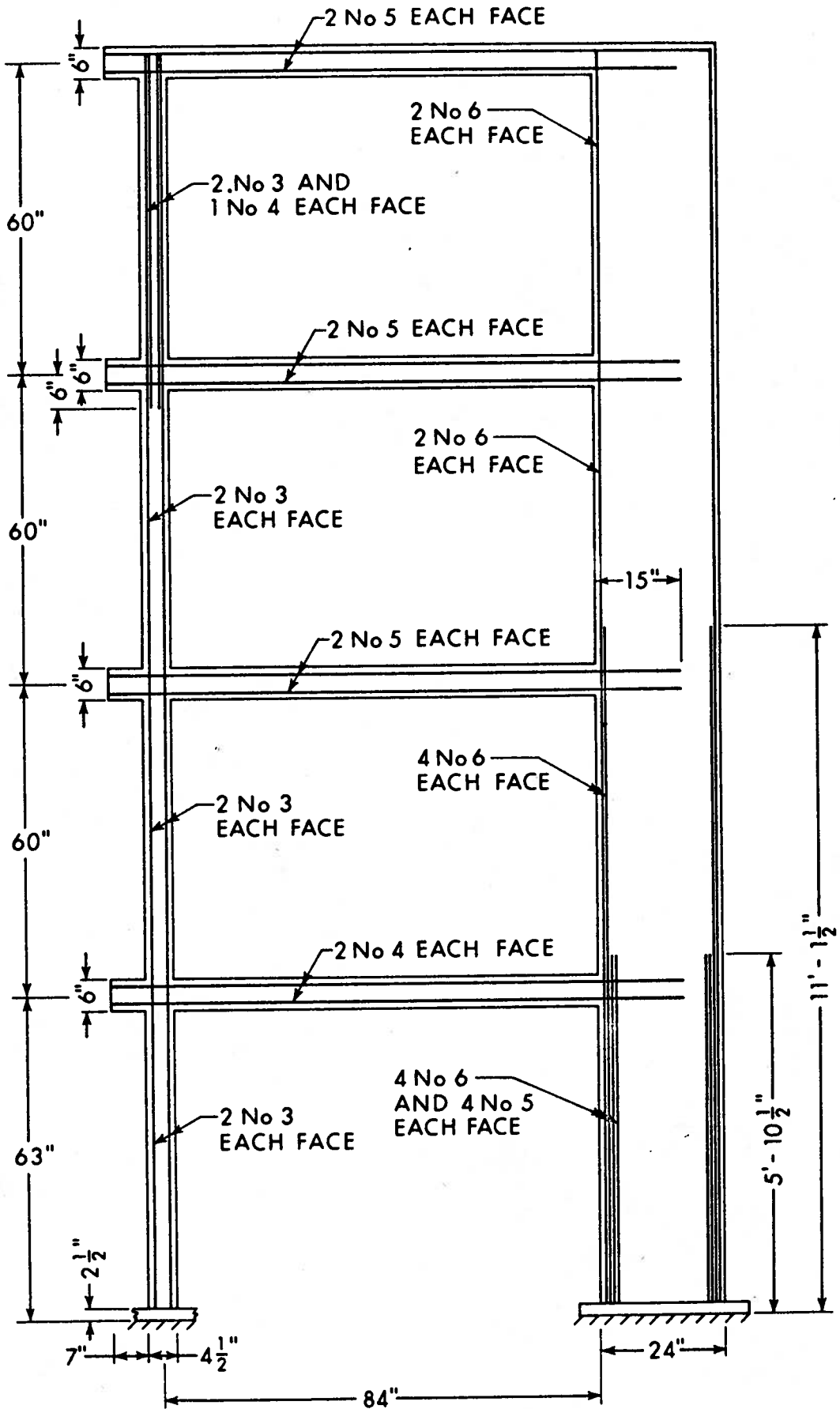
FIGURE 7.4   TEST SPECIMEN SHOWING MAIN REINFORCEMENT

SPIRALLY WOUND
N⁰ 14 WIRE TIES
AT $4\frac{1}{2}''$ O.C.
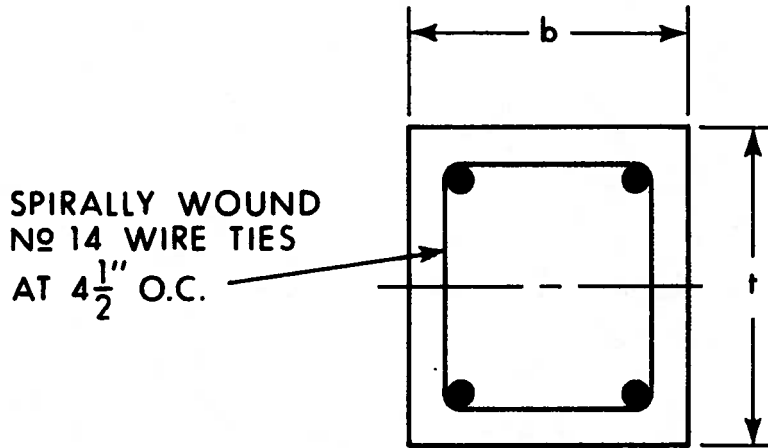
(a)   CROSS SECTION FOR BEAMS AND COLUMNS

2- ⌴ TIES AT 6" O.C.

-N⁰ 3 WIRE IN
  1st AND 2nd STORY

-N⁰ 9 WIRE IN
  3rd AND 4th STORY
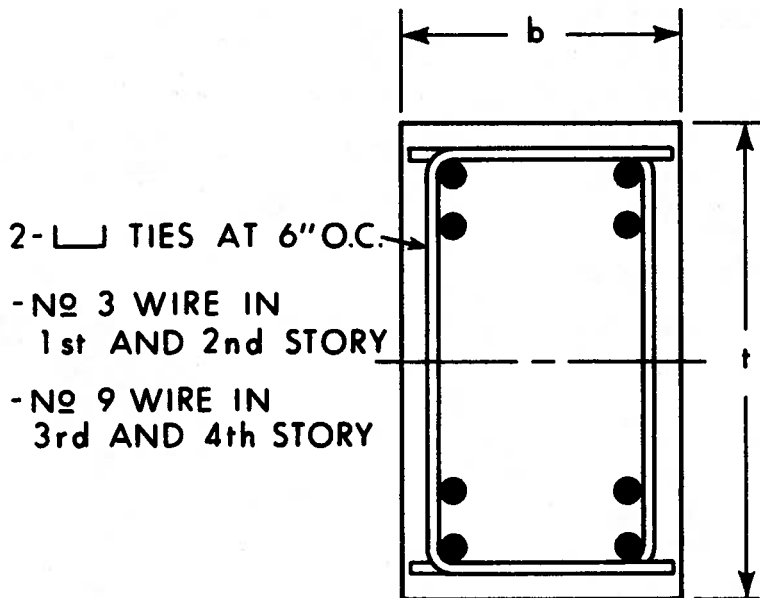
(b)   WALL CROSS - SECTION

FIGURE 7.5   CROSS-SECTIONS OF FRAME MEMBERS
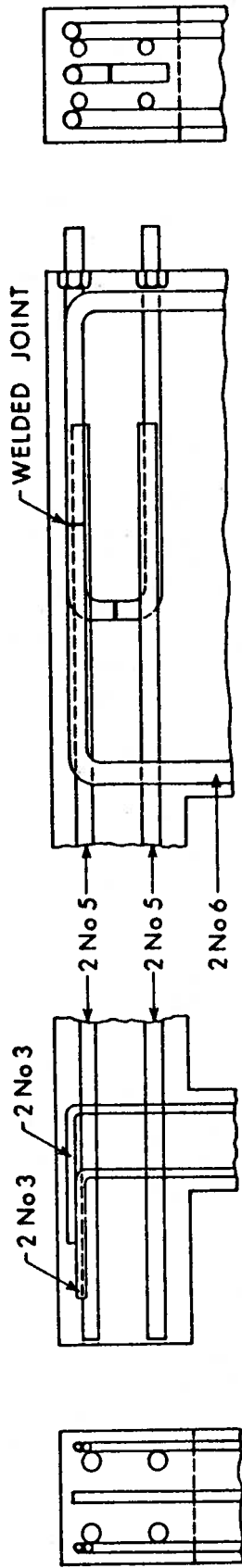
WELDED JOINT

TOP WALL - BEAM JOINT

TYPICAL WALL - BEAM JOINT

2 No 5
2 No 5
2 No 6

2 No 3
2 No 3
2 No 3

TOP BEAM - COLUMN JOINT

2 No 6
2 No 5

6"

24"

7"
4.5"

6"
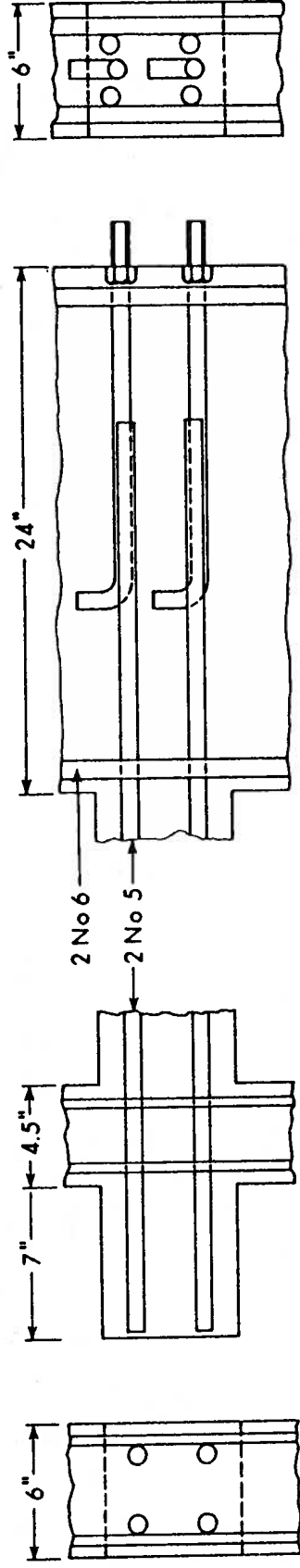
TYPICAL BEAM - COLUMN JOINT

FIGURE 7.6 JOINT DETAILS SHOWING MAIN REINFORCEMENT
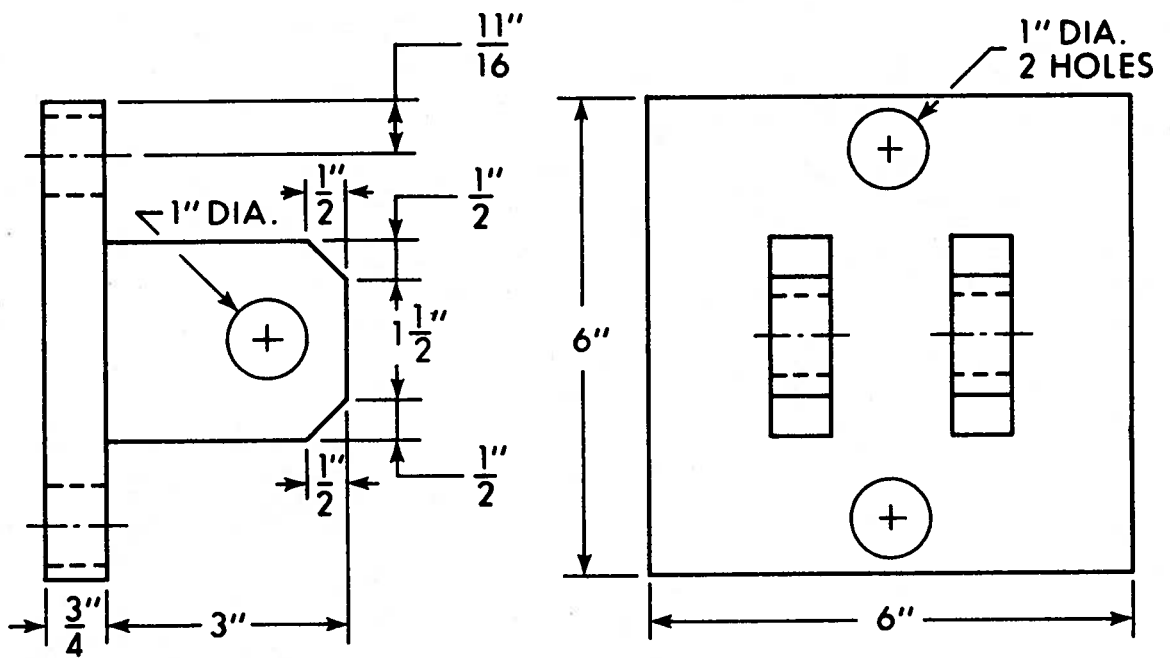
FIGURE 7.7 CLEVICE TO TRANSFER HORIZONTAL JACK LOAD
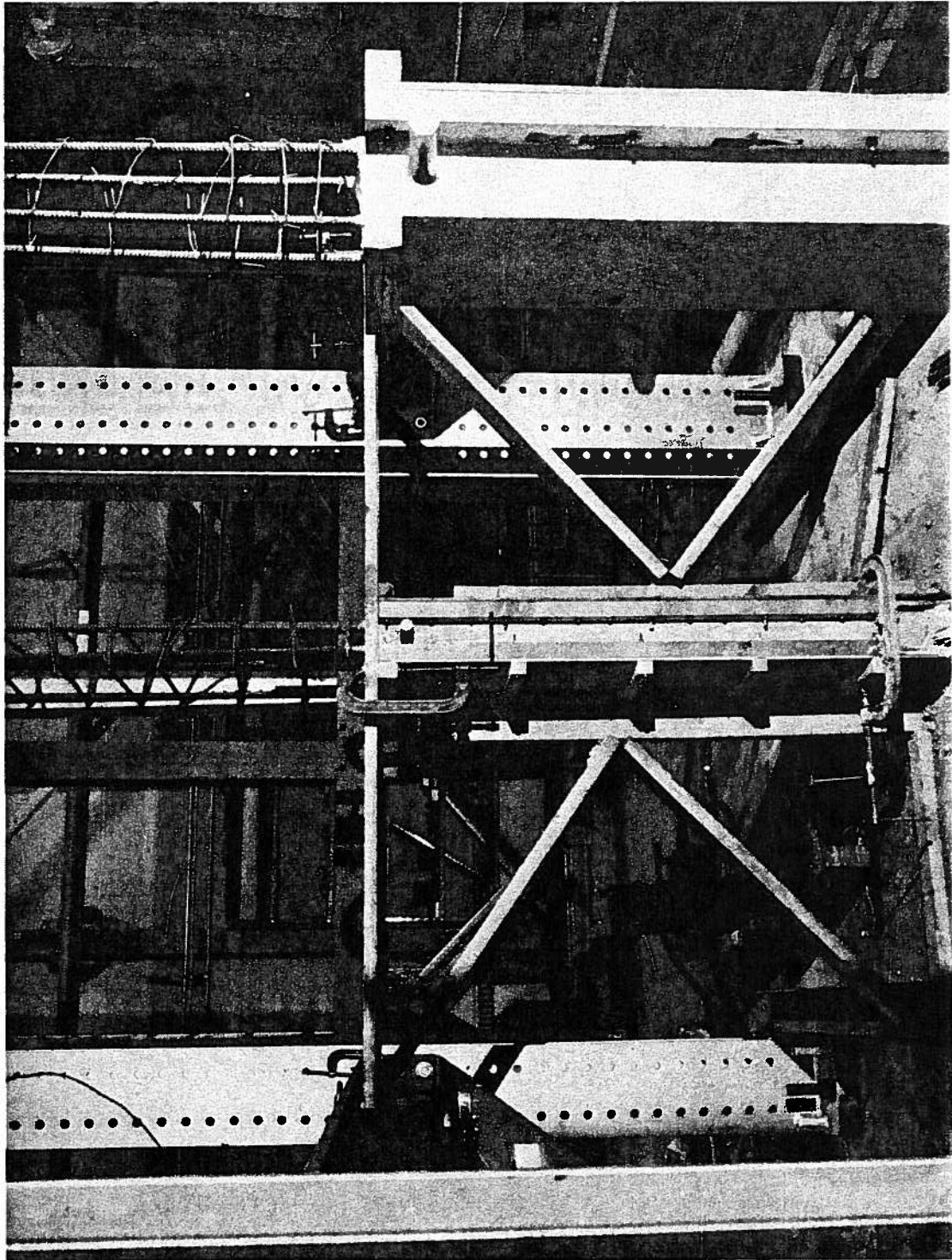
FIGURE 7.8 SPECIMEN UNDER CONSTRUCTION
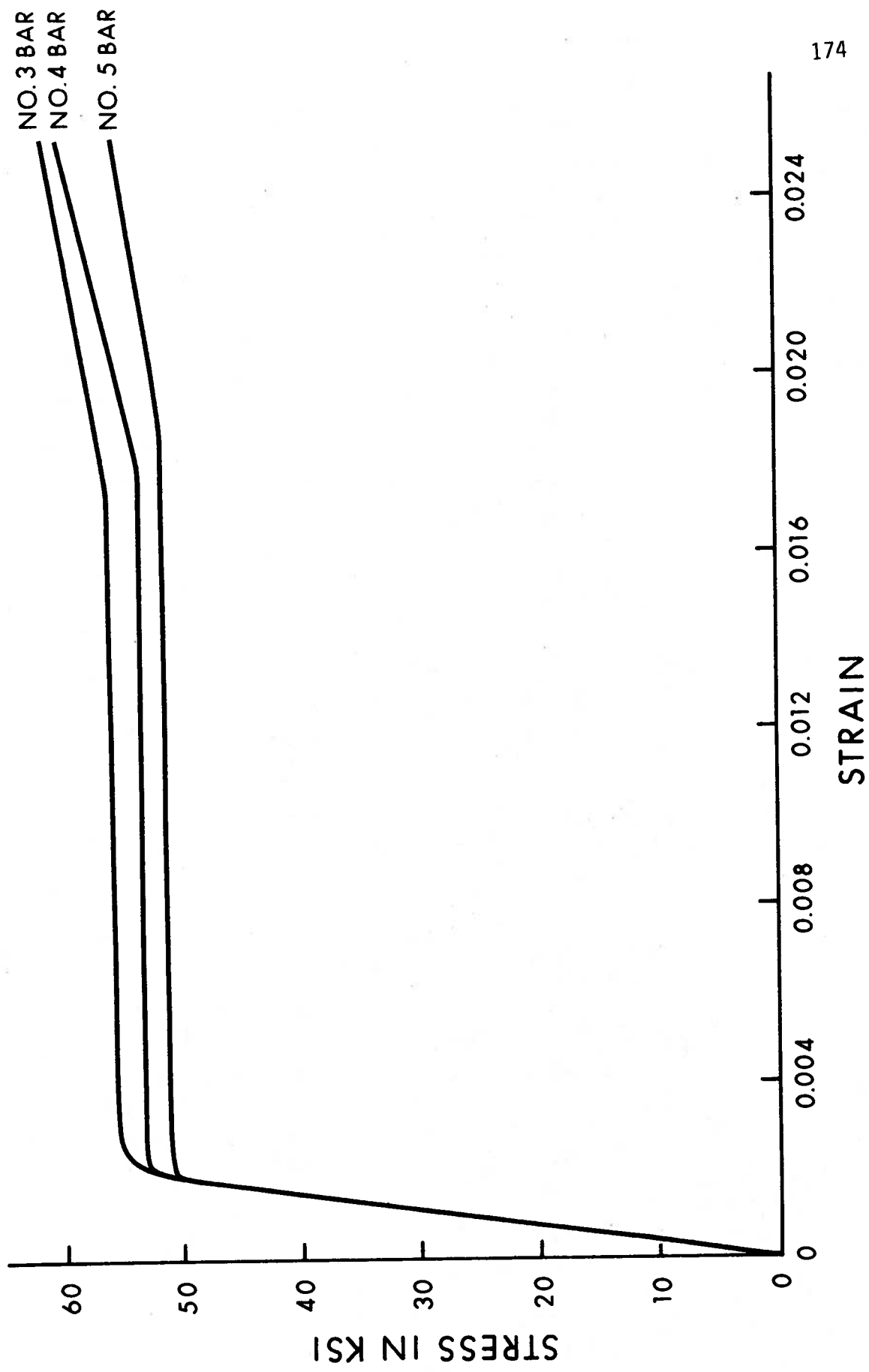
FIGURE 7.9 STRESS - STRAIN CURVE FOR REINFORCING STEEL

174

28"

6"

PLAN

24"

$4\frac{1}{2}$"

$2\frac{1}{2}$"

BASE PLATE
$2\frac{1}{2}$" × 6" × 28"

26"

LAB.
FLOOR

PLATE
1" × 8" × 8"

2" PIPE SPACER
$5\frac{1}{2}$" LONG

$1\frac{1}{2}$" BOLT
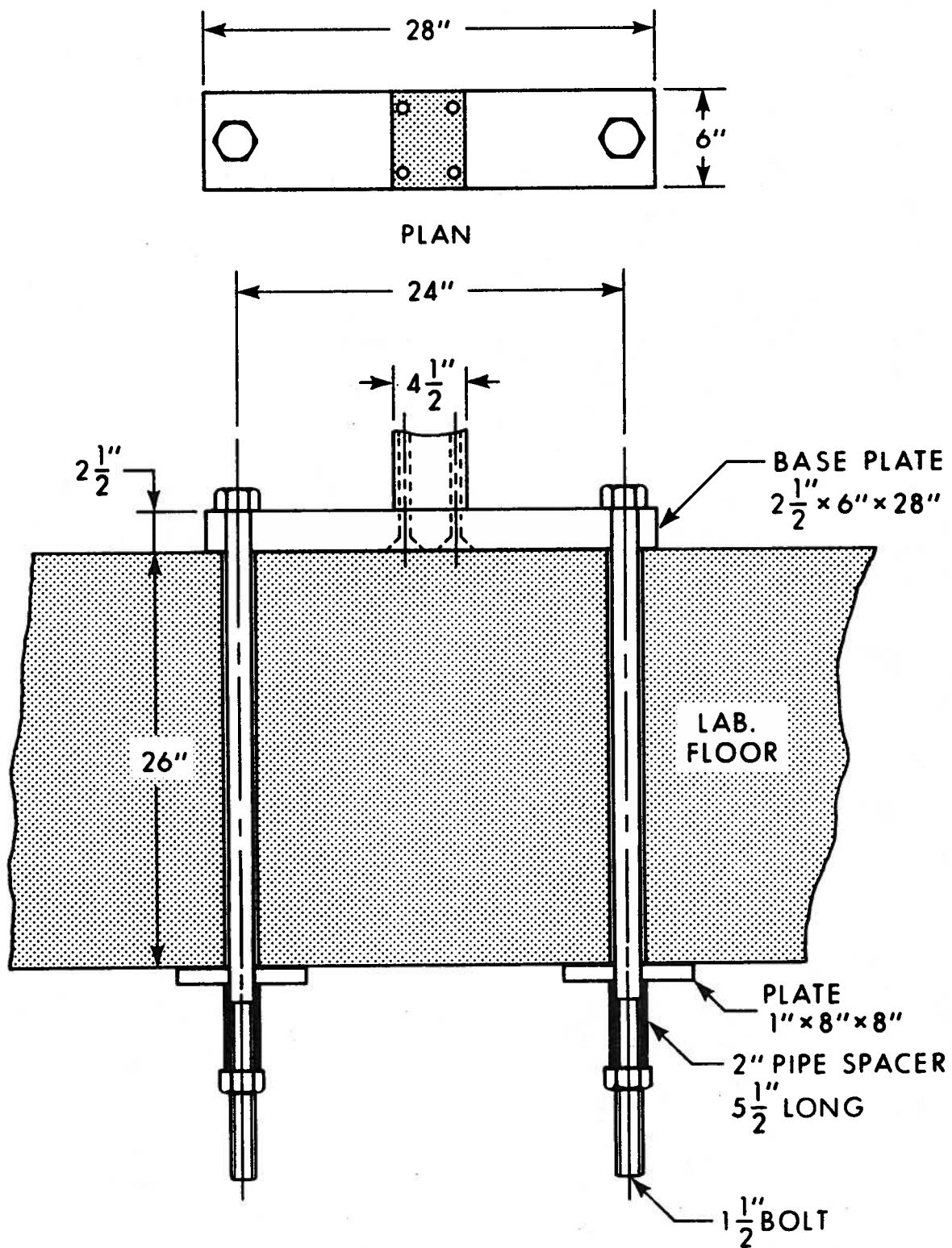
SECTIONAL ELEVATION

FIGURE 7.10 COLUMN BASE CONNECTION

28"

6"

PLAN

24"

$\frac{3}{4}$"×6"×28" PLATE

6"

$1\frac{1}{2}$"

$1\frac{1}{2}$"×6"×28" PLATE

PLATE END VIEW

26"

BUILT UP CHANNEL BASE PLATE

LAB. FLOOR

1"×8"×8" PLATE

2" PIPE SPACER $5\frac{1}{2}$" LONG

$1\frac{1}{2}$" BOLT
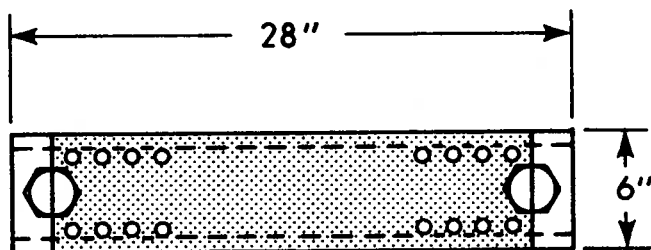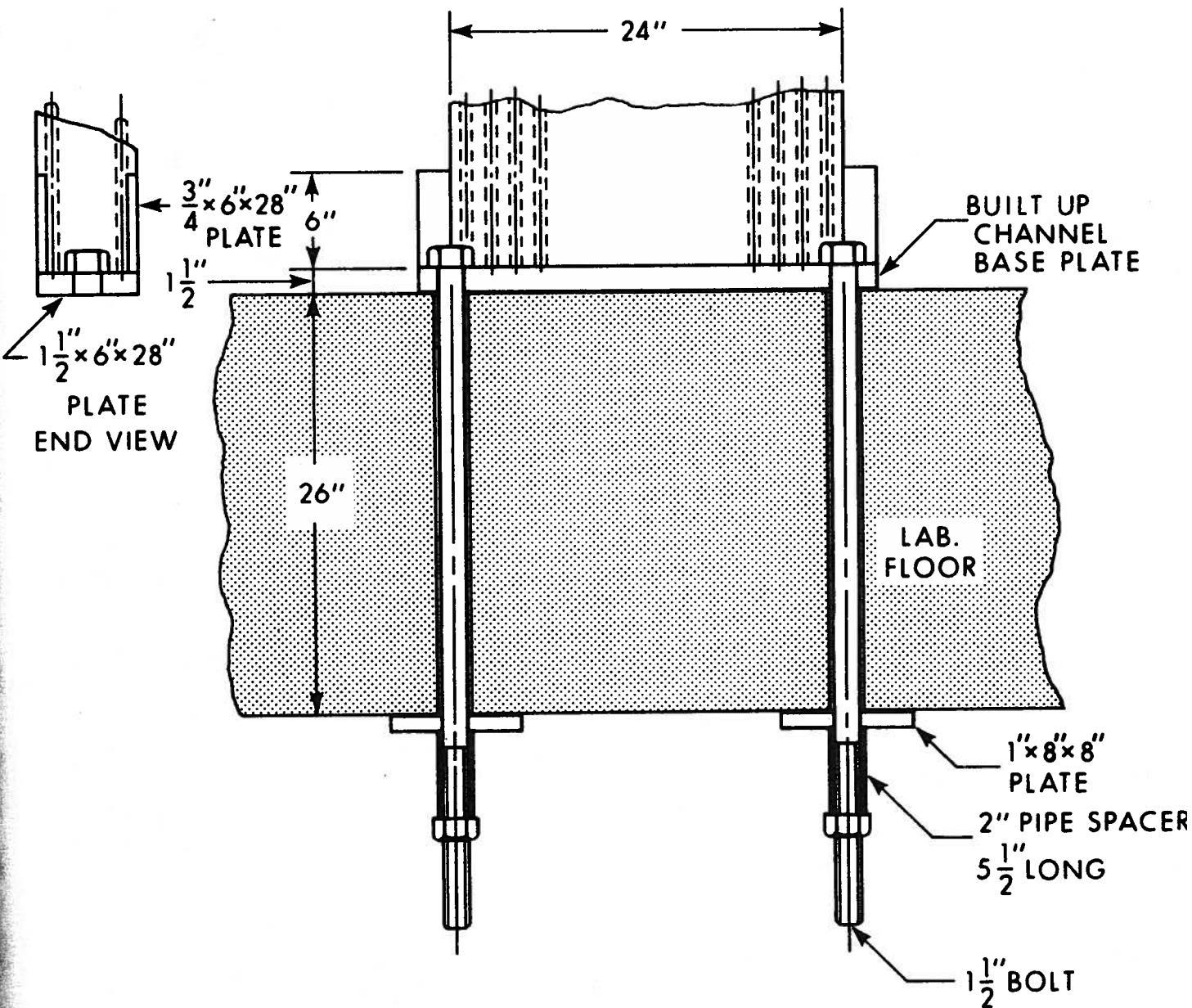
SECTIONAL ELEVATION

FIGURE 7.11 WALL BASE CONNECTION

$\frac{7}{8}$" DIA. HOLE

$\frac{5}{8}$" DIA. THREADED BAR

2"

$1\frac{1}{4}$"

$3\frac{1}{2}$"

$\frac{1}{4}$"

PLAN

$\frac{7}{16}$" DIA. HOLE

$\frac{3}{4}$" × $3\frac{3}{4}$" × $3\frac{1}{2}$" PLATE

$\frac{3}{4}$" × $3\frac{3}{4}$" × $3\frac{1}{2}$" PLATE

2" PIPE

2"

$\frac{3}{4}$"

$1\frac{1}{8}$"

$\frac{5}{8}$"

6"

3"

$\frac{1}{4}$"

$\frac{1}{2}$"

$\frac{1}{4}$"

3' - $\frac{3}{4}$"

$\frac{1}{2}$"

$\frac{1}{4}$"

$\frac{7}{8}$"

4"

$\frac{3}{4}$"

$\frac{3}{4}$"

$1\frac{1}{4}$" DIA. HOLE
(BRACING POINT)

ELEVATION

ANTISYMM.

ANTISYMM.
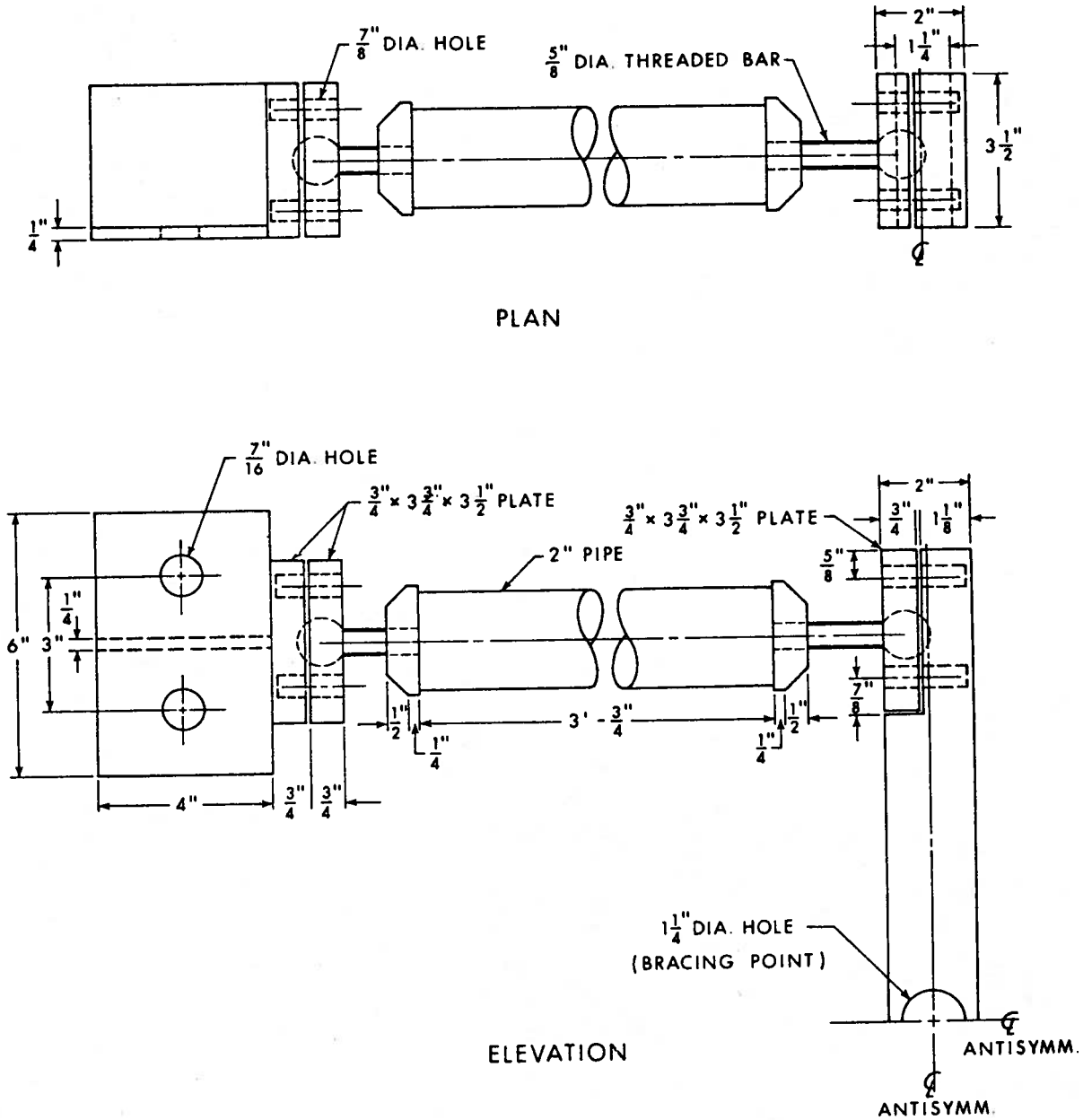
FIGURE 7.12 LATERAL BRACING SYSTEM

FIGURE 7.13 LOCATIONS OF CURVATURE MEASURING STATIONS
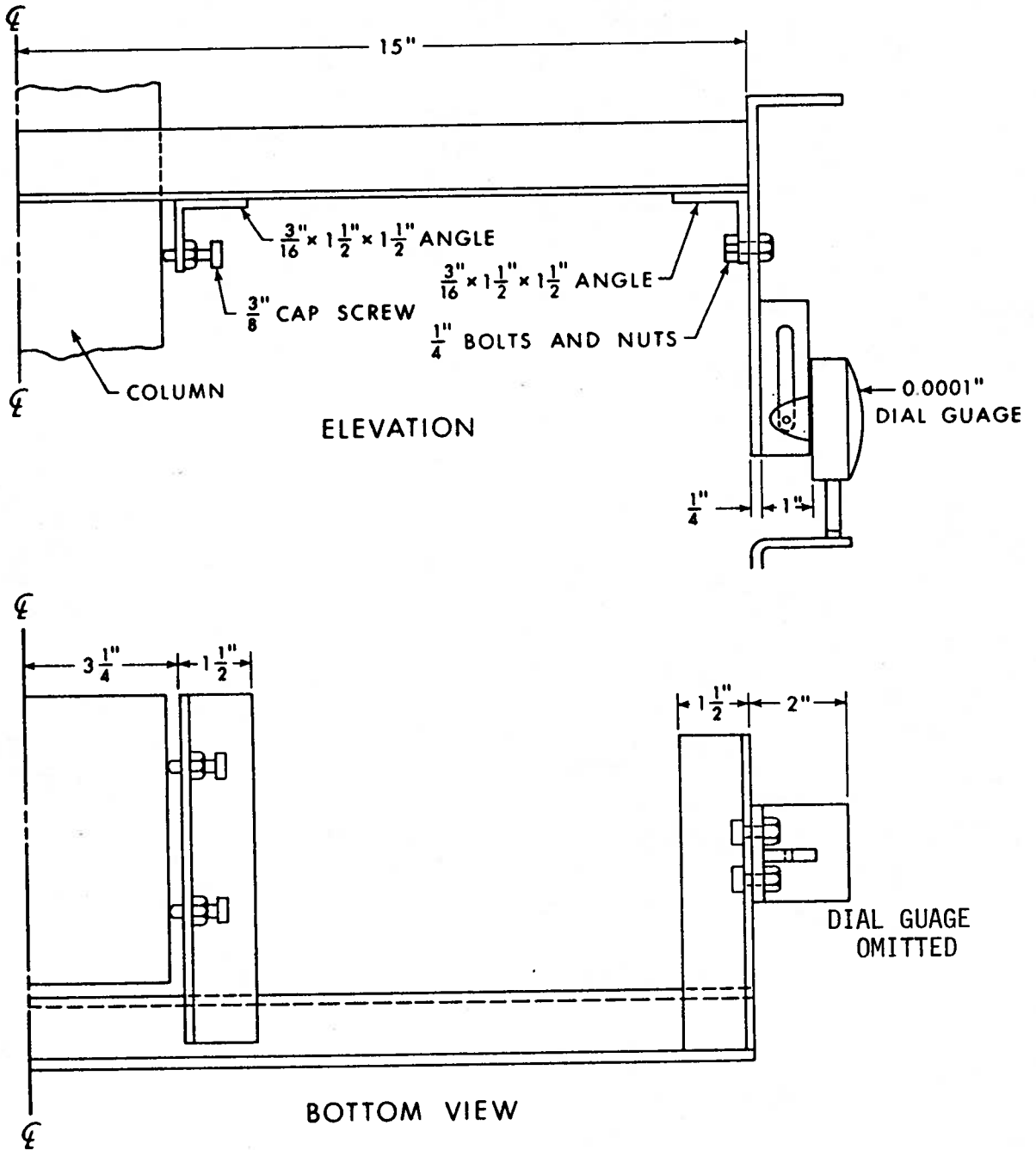
FIGURE 7.14 CURVATURE METER
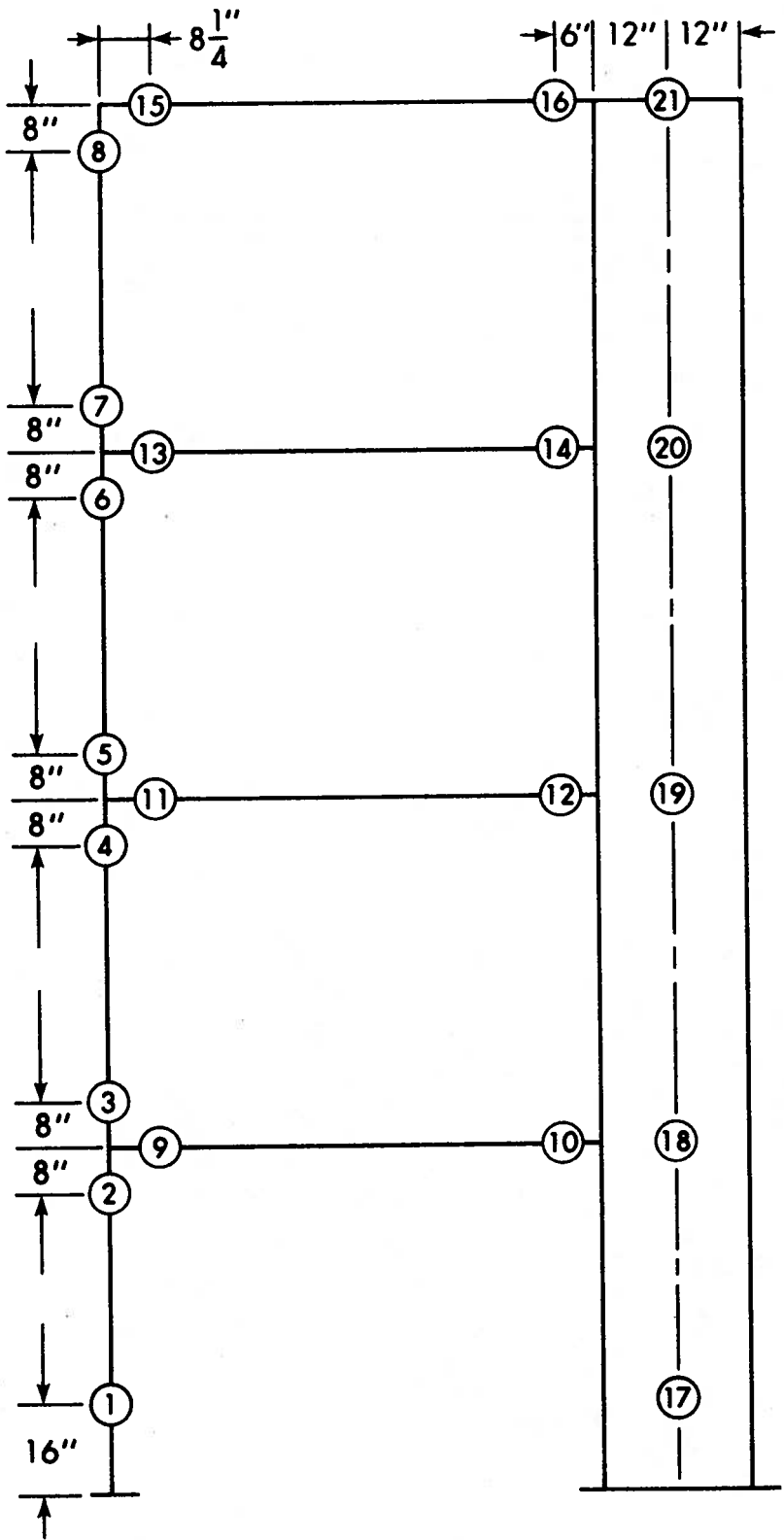
FIGURE 7.15 LOCATIONS OF ROTATION METERS
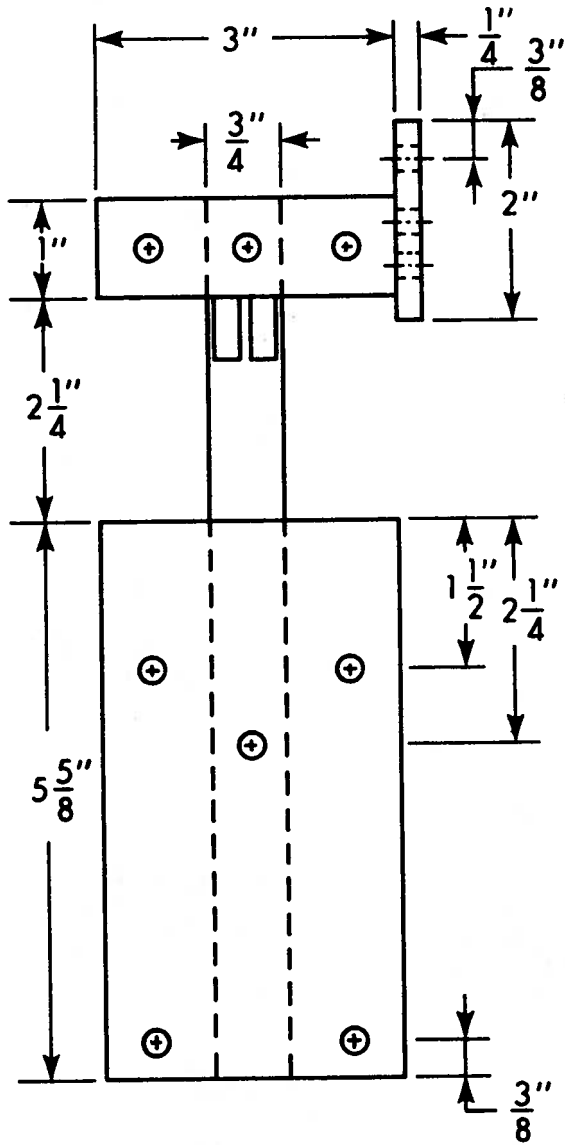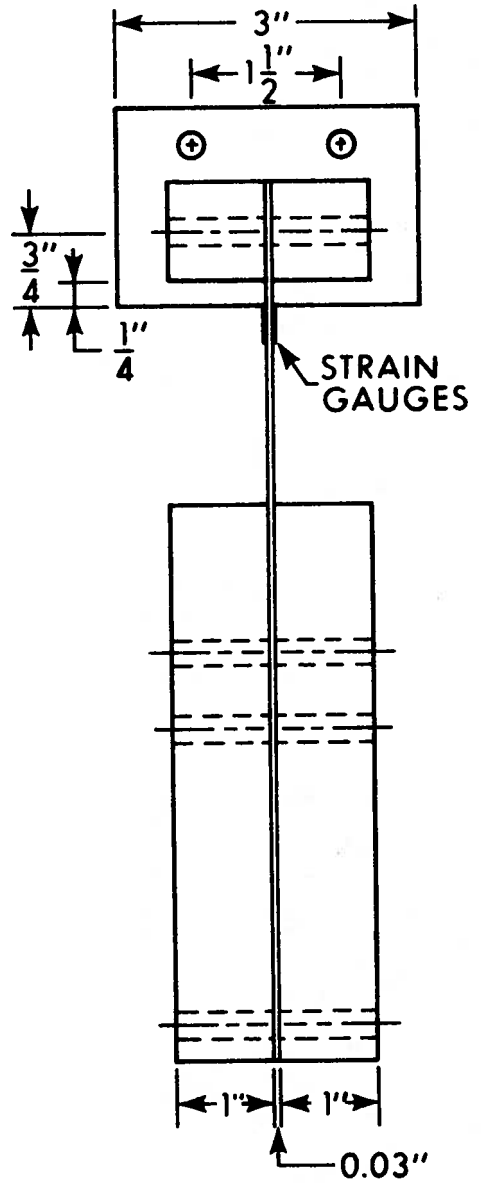
ELEVATION   L.H.S. VIEW

FIGURE 7.16 ROTATION METER
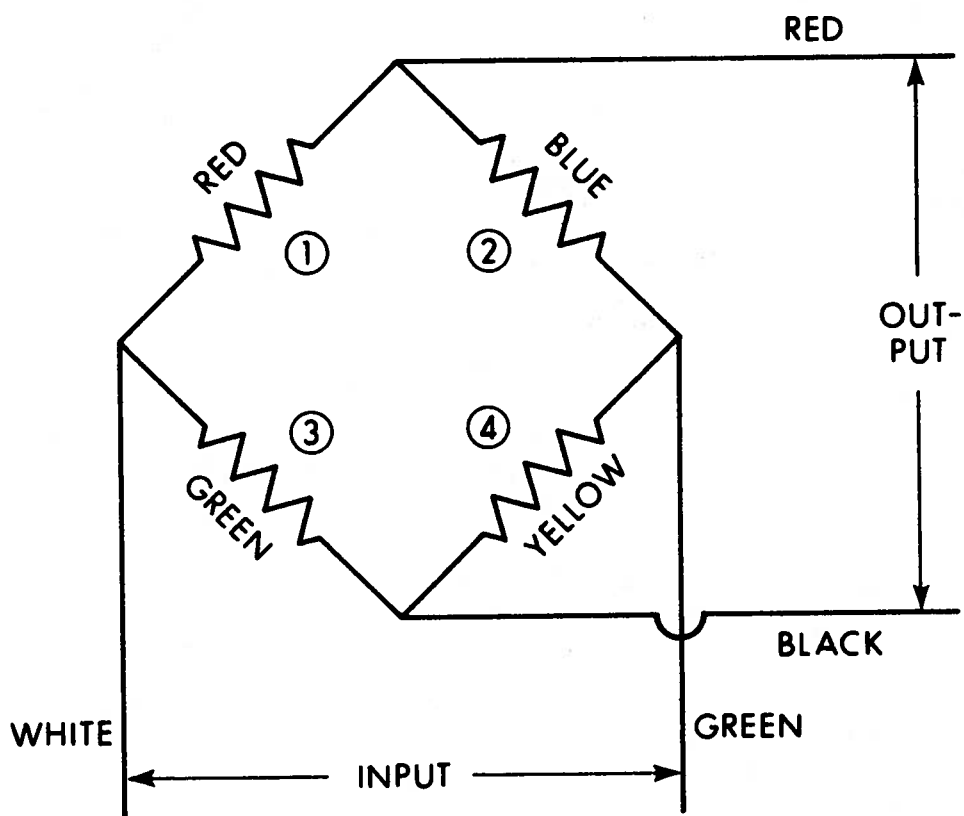
FIGURE 7.17 WHEAT - STONE BRIDGE CIRCUIT

CHAPTER VIII

TEST AND ANALYSIS OF TEST DATA

8.1 Introduction

The testing apparatus, procedure and instrumentation used in the test of the shear wall-frame specimen were described in CHAPTER VII. The dimensions, structural details and material properties of the speicmen are also described in that CHAPTER. The computations carried out in reducing the test data are presented here. The test results are compared with the theoretical analysis in CHAPTER IX.

8.2 Description of Load Application and Measurements

The shear wall-frame specimen was loaded on two subsequent days. After three load increments the Dymec electronic data recorder readings were found to be unreliable and the structure was unloaded and the test was postponed for a day while the Dymec was repaired. All the beams were cracked near the ends during this first test.

The test was started again on the second day and was continued to failure. TABLE 8.1 presents a brief history of the second test including time and application of loads. All the deflections, curvatures and other readings have been referenced to the beginning of the second test.

The testing and gauge reading was carried out by five groups

183

of two persons under the direction of one additional person. One group was fully responsible for applying and recording the loads, and printing the readings from the Dymec data logging apparatus. Each of the other four groups was responsible for reading and recording all dial gauges, Whittemore or Demec gauges and marking cracks on one story of the frame. The eleventh person was responsible for reading and recording the frame deflections and for the overall supervision of the test.

Following the test the frame was photographed and the actual cross-sectional dimensions recorded in TABLE 7.1 were measured.

8.3 Loads

The horizontal and vertical loads were computed using hydraulic pressure-load calibration charts, established before the test. The electrical resistance strain gauge readings were found to be completely undependable due to inconsistencies in the Dymec data logging system. In computing the vertical loads, the weight of the loading beam, cross-beam and tie rods, totalling 1360 lbs., was added to the vertical jack loads.

The measured loads from all six rams are presented in TABLE 8.2. At load number 7 the load could not be held constant. For this reason the loads were measured before taking the other measurements (load 7) and again, after all the other measurements had been finished (load 7A).

8.4 Cross-Section Response of the Members in the Test Frame

Theoretical load-moment-curvature relationships were computed for all the members of the test frame using the program described in CHAPTER IV, for the axial loads applied during the test. The load-moment-curvature characteristics for all sections were idealised to elastic-inelastic diagrams to comply with the assumptions made in CHAPTER III and the stiffnesses and ultimate moment capacities used in the theoretical analysis of the test frame were computed from these diagrams. On the other hand, the theoretical load-moment-curvature diagrams were used in computing moments from the curvatures measured during the test. The theoretical load-moment-curvature diagrams for all the columns, beams and walls are presented in FIGURES 8.1, 8.2 and 8.3 respectively along with the idealised P-M-ϕ diagrams used in the frame analysis.

8.5 Curvature

8.5.1 Curvatures in Columns and Beams

Curvatures were measured in the columns and beams using the device described in section 7.8.4. The average curvature and fibre strains can be computed from the formulae presented in APPENDIX D, using the dial gauge readings and parameters related to the measured dimensions of the curvature meters and the cross-sections. The initial dial gauge readings at load 1 were adjusted assuming that a linear variation of dial readings occurred under loads 1, 2 and 3 when only vertical loads were on the specimen. This was done to correct for slack, friction or initial movement of the dial gauges. TABLE D.1 in APPENDIX D lists the measured

curvature times the depth, ϕt, at all measurement stations,
for all loads. Positive curvature indicates compression in
inner face of the columns or the top face of the beams.

8.5.2 Curvatures in Walls

As mentioned in section 7.8.3 strains were measured,
in the wall, using Whittemore and Demec gauges. Three continuous
lines of these gauges were placed along the entire height of the
wall, giving the average strain over 10 or 8 inch gauge length
at three positions across the depth of section. Following the
assumption that the strain distribution is linear over the depth
of the wall, a least square line was fitted to the three readings
to describe the strain configuration. The derivation of this
line is described in APPENDIX D. At high load some of the Demec
points were lost on the tension face of the wall, so that readings
could be taken only at two positions. In these cases the strain
distributions were based on these two readings. The curvature
times depth, ϕt, from the fibre strains and geometry are listed
in TABLE D.1 in APPENDIX D for all the sections in the wall and
all the loads. Positive curvature indicates compression on the
outer face of the wall.

8.6 Moments

Moment-curvature relationships were presented in section 8.4
for all the frame members for all the applied axial loads. These
curves were used to find the average moment in the gauge length, at
each curvature measuring station. A linear interpolation was used to

estimate the moments falling between the computed points in these load-moment-curvature diagrams. The measured moments at the various stations are tabulated in TABLE D.2 in APPENDIX D, whereas the predicted moments are listed in TABLE 9.2 in CHAPTER IX. The error in the estimation of curvature times depth of section, ϕt, due to error in reading of dial gauges are given in CHAPTER VII. Using an error of 25 micro-inch/inch in the value of curvature times depth of section, ϕt, and FIGURES 8.1 and 8.2 the error in the estimation of moments are given by about 0.6 and 0.8 K-in. in the case of beams and columns, respectively in the intial part of the loading. Such error in the case of the wall, using FIGURE 8.3, is about 20 k-in. in bottom story to 12 K-in. in top story. These errors are reduced (see FIGURES 8.1, 8.2, 8.3) as the curvature of the section increases and the errors become very small when the hinges form.

The moment diagram for the entire structure is presented in CHAPTER IX for each load. The moment diagram for each member was fitted to the individual moment values by eye. The measured and predicted moments are compared in CHAPTER IX.

8.7 Computer Analysis of Data

The reduction of the test data, described in section 8.5 and 8.6, were performed by computer at the University of Alberta. A computer program was written, for this purpose in Fortran IV language for IBM OS/360 system. The flow diagram, nomenclature and the listing of the program are given in APPENDIX D. The various steps involved in the analysis are as follows:

1. The 'MAIN' program reads and writes all the data, such as cross-sectional dimensions and properties, member dimensions and properties, location and parameters of measuring stations and devices and all the dial gauges or strain readings taken during test.

2. The initial dial and strain readings were corrected as described in section 8.5

3. The 'MAIN' program then calls the subroutine 'FSAC' which computes the fibre strains and curvatures at all the stations. These strains and curvatures are then printed out.

(4. The 'MAIN' program then calls the subroutine 'BMKP', which in turn interpolates the moments at all the stations for the curvatures computed in step 3 using the appropriate load-moment-curvature curves presented in section 8.4. These moments are then printed out.

Another subroutine was also added to this program to compute the axial loads and moments on the section from the known fibre strains and curvatures computed in subroutine 'FSAC'. The axial loads and moments given by this subroutine were found to be unsatisfactory, since the dial gauge readings were accurate to 0.0001 inches while the axial loads and moments were found to be sensitive to gauge readings of one-hundredth of this amount. The moment computations based on curvatures are considerably more accurate as discussed in section 8.6, since the

curvature is the difference of fibre strains which tended to reduce the error.

8.8 Shears

The shear in the various members is equal to the algebraic sum of the moments at the ends of the member divided by the span of the member concerned. The shear for the various loads were computed from the measured moments. The P-Δ shears were calculated from measured deflections at all the floors and the measured vertical loads. The shear diagrams are plotted and compared to those from the analysis in CHAPTER IX.

8.9 Deflections

The deflection measurements at each floor level were reduced to get the actual deflections from the position of the frame at the start of the second test. The measured horizontal deflections at each floor level are tabulated in TABLE 8.3. The load deflection diagram for each floor is presented in CHAPTER IX and compared with the predicted deflections.

8.10 Response of the Base of Wall

As described in section 7.5 the base of the wall was anchored by two high strength bolts which reacted against pipe sleeves. One of these sleeves yielded during the test. A piece of the pipe of same length used in the wall connection was tested in compression. The measured load-shortening curve for the pipe is plotted in FIGURE 8.4. This curve was used to compute the wall base response to be used in theoretical analysis of the test frame. The connection is shown in

FIGURE 8.5(a). The total length of bolt which transferred the force from the wall base to the pipe, including the length of pipe and plate thickness was 32.5 inches before loading. The axial load applied to the wall was measured to be 50.2 kips. The wall width was 24 inches. If it is assumed that the center of the compression force, C, below the base plate coincides with one edge of the wall as shown in FIGURE 8.5(b), the relationship between the force in the pipe, T, and moment, M, in the base will be given by equations (8.1) and (8.2).

$$T \times 24 = M - 50.2 \times \frac{24}{2} \qquad \ldots (8.1)$$

$$\text{or} \qquad M = 24T + 602.4 \qquad \ldots (8.2)$$

The upward deflection, Δ_B, of corner B of the wall is equal to the sum of the lengthening of the anchor bolt and the shortening of the pipe sleeve. The bolt diameter was 1.5 inches and the modulus of elasticity, E, was taken as 29.6×10^6 psi. For each value of T a value of M from equation (8.2) and a value of Δ_B was computed. This was converted, in turn, into an equivalent curvature for use in the analysis by dividing by one tenth of the story height, since the analysis considered the wall divided into ten segments.

The resulting moment-curvature-relationship for the base of the wall is plotted in FIGURE 8.6. The vertical initial tangent in the diagram corresponds to the period when the pipe sleeve was not subjected to any compressive force.

For use in the shear wall frame analysis the moment-curvature relationship for the wall base was idealised as two straight lines as

shown in FIGURE 8.6. The first line was chosen to correspond to first line of the moment curvature diagram presented in FIGURE 8.3 for the first story wall cross-section. The second line is an approximation to the slope of the diagram plotted in FIGURE 8.6. This way the stiffness of the base was assumed to remain essentially the same as that exhibited by the wall in the elastic range. The moment-curvature diagram for the pipe began to drop for curvatures in excess of 0.080 and this has arbitrarily been taken as the limit of the wall rotation in the analysis.

8.11 Summary

The procedure used to reduce the data from the test of a four story shear wall-frame structure have been outlined in this CHAPTER. Computer programs used in the data reduction are presented in APPENDIX D. The reduced data are summarized in APPENDIX D and will be discussed and compared to the analysis in CHAPTER IX of this report.

TABLE 8.1

HISTORY OF TEST

Load No.	Time	Load in Kips		Top Story Defln. Inches	Remarks
		Total Vertical	Total Horizontal		
1	8.40	0	0	0	Start of Test
2	9.10	11.6	0	-0.02	
3	9.30	100.4	0	-0.07	
4	9.50	100.4	7.39	0.56	
5	10.10	100.4	14.49	1.48	Fairly extensive beam cracking
6	10.55	100.4	19.22	2.80	Base plate of wall lifted by 0.16 inch on west side. Crack at wall base extended to 2nd Whittemore line
7	11.30	100.4	21.96	7.08	Start of Readings
7A		100.4	19.73	7.13	End of Readings. Wall base plate lifted by 0.50 inch on west side. Crushing noted at wall end of 2nd, 3rd and top beams. Load difficult to maintain.
8	12.50	100.4	13.47	10.97	Wall base plate lifted by 1-1/8 inches at west end. Top beam column joint failed.
9	13.10	100.4	0	6.89	Horizontal loads released
10	14.05	0	0	7.05	All loads released.

TABLE 8.2

APPLIED LOADS DURING TEST

Load Number	Horizontal Lods in Kips				Vertical Loads in Kips	
	Floor 1	Floor 2	Floor 3	Floor 4	Tie Rod 1	Tie Road 2
1	0	0	0	0	0	0
2	0	0	0	0	5.8	5.8
3	0	0	0	0	50.2	50.2
4	2.10	2.10	2.10	1.09	50.2	50.2
5	4.13	4.13	4.13	2.10	50.2	50.2
6	5.48	5.48	5.48	2.78	50.2	50.2
7	6.26	6.26	6.43	3.01	50.2	50.2
7A	5.48	5.58	5.89	2.78	50.2	50.2
8	4.30	3.62	3.79	1.76	50.2	50.2
9	0	0	0	0	50.2	50.2
10	0	0	0	0	0	0

194

TABLE 8.3

MEASURED AND COMPUTED HORIZONTAL DEFLECTIONS

Deflections in Inches

Load No.	Floor 1		Floor 2		Floor 3		Floor 4	
	Measured	Computed	Measured	Computed	Measured	Computed	Measured	Computed
1	0	–	0	–	0	–	0	–
2	0	–	0	–	-0.01	–	-0.02	–
3	0 (-0.01)	–	-0.03 (-0.04)	–	-0.04	–	-0.07 (-0.08)	–
4	0.09 (0.10)	0.1063	0.24 (0.26)	0.2828	0.37 (0.41)	0.4855	0.52 (0.56)	0.6833
5	0.28 (0.29)	0.2080	0.67 (0.70)	0.5531	1.03 (1.08)	0.9492	1.41 (1.48)	1.3351
6	0.58 (0.59)	0.5023	1.33 (1.36)	1.1731	2.02 (2.07)	1.8873	2.74 (2.80)	2.5692
7	1.58	1.1169	3.46	2.5048	5.24	3.9965	7.08	5.4841
7A	1.61	–	3.50	–	5.29	–	7.13	–
8	2.61	–	5.51	–	8.14	–	10.97	–
9	1.55	–	3.35	–	5.08	–	6.89	–
10	1.71	–	3.55	–	5.28	–	7.05	–

* Deflections listed in parentheses are those measured immediately prior to applying the next load.
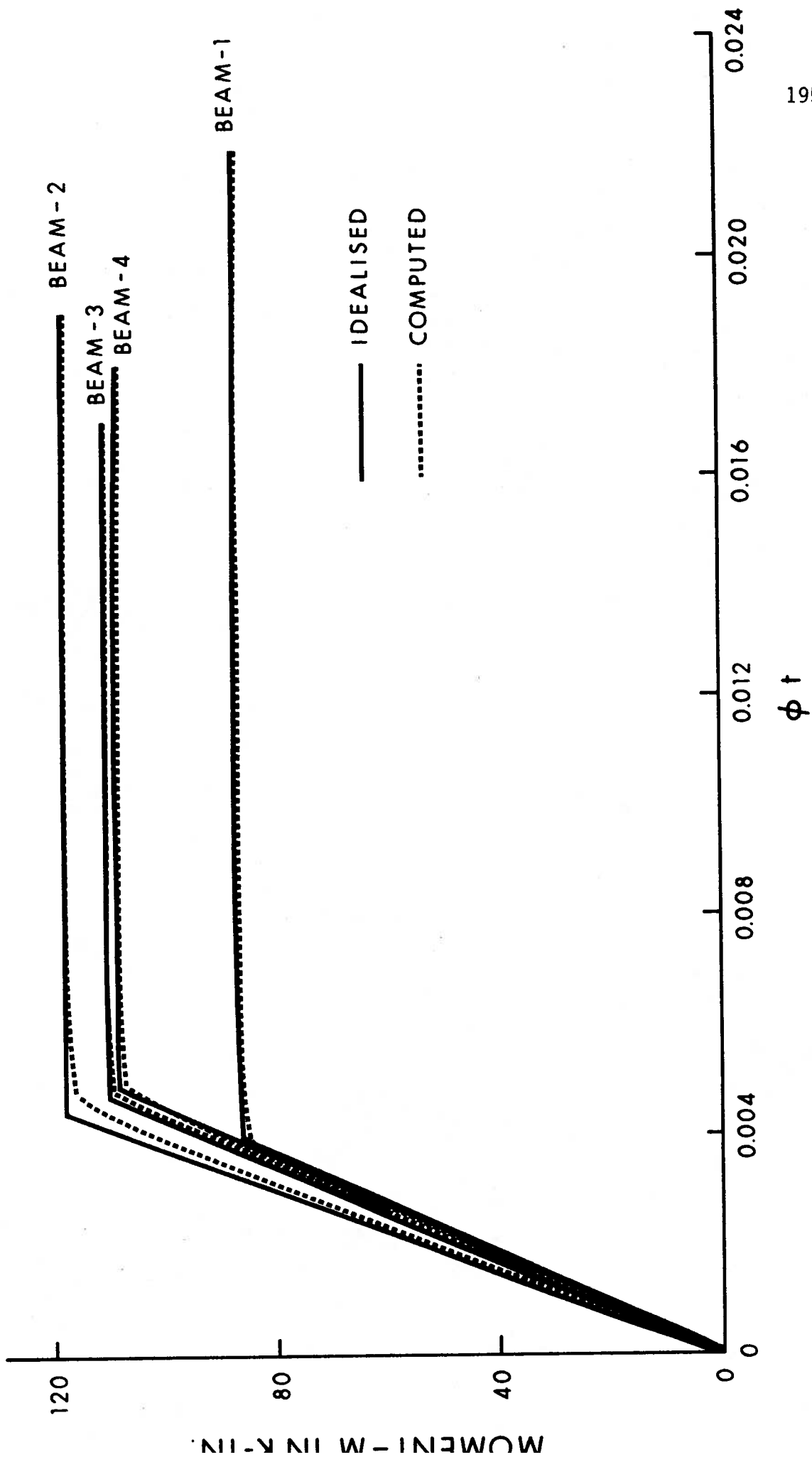
FIGURE 8.1 MOMENT - CURVATURE DIAGRAM FOR BEAM SECTIONS AT WALL END

195
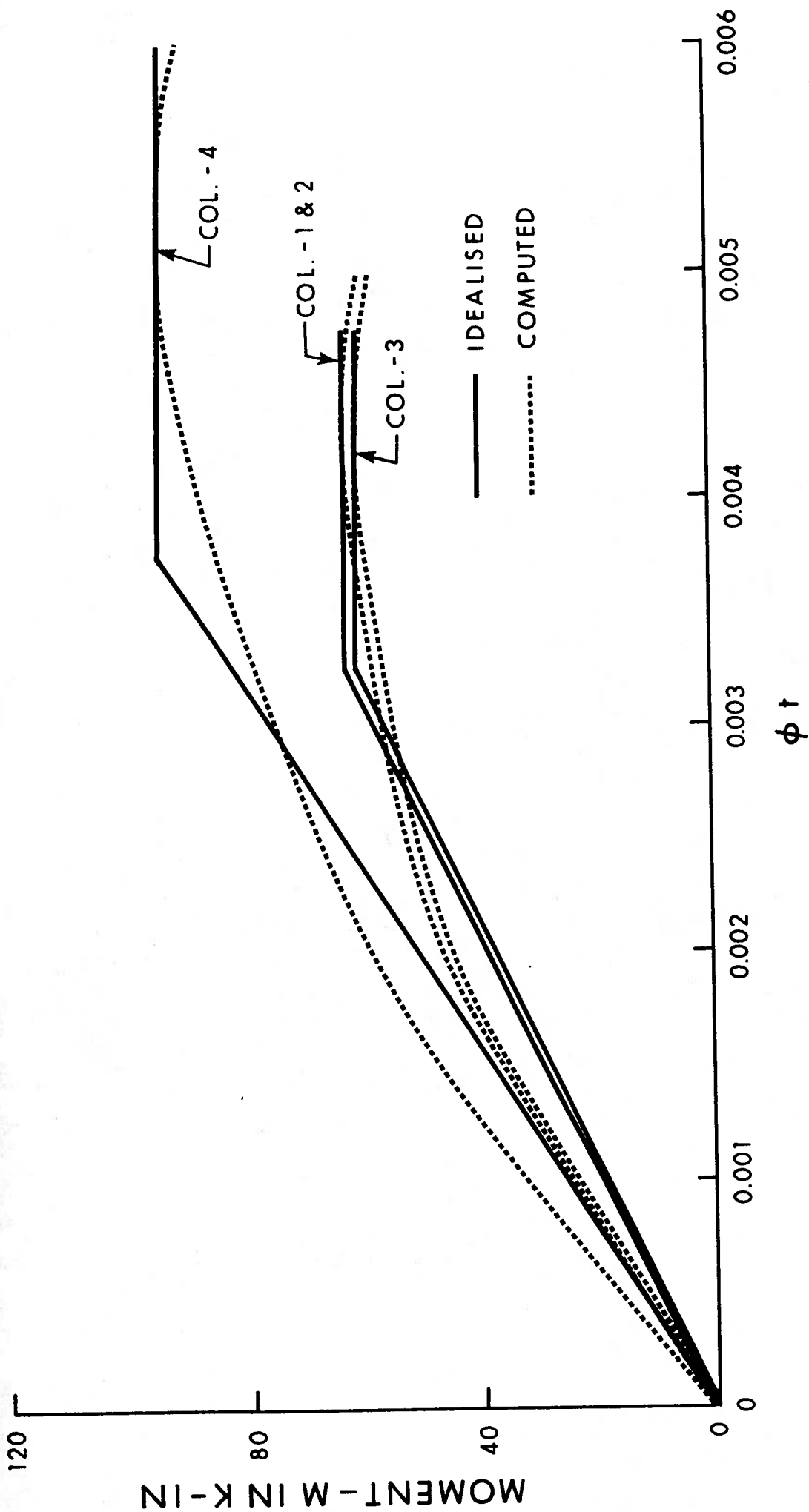
FIGURE 8.2 MOMENT - CURVATURE DIAGRAM FOR COLUMN SECTIONS

196
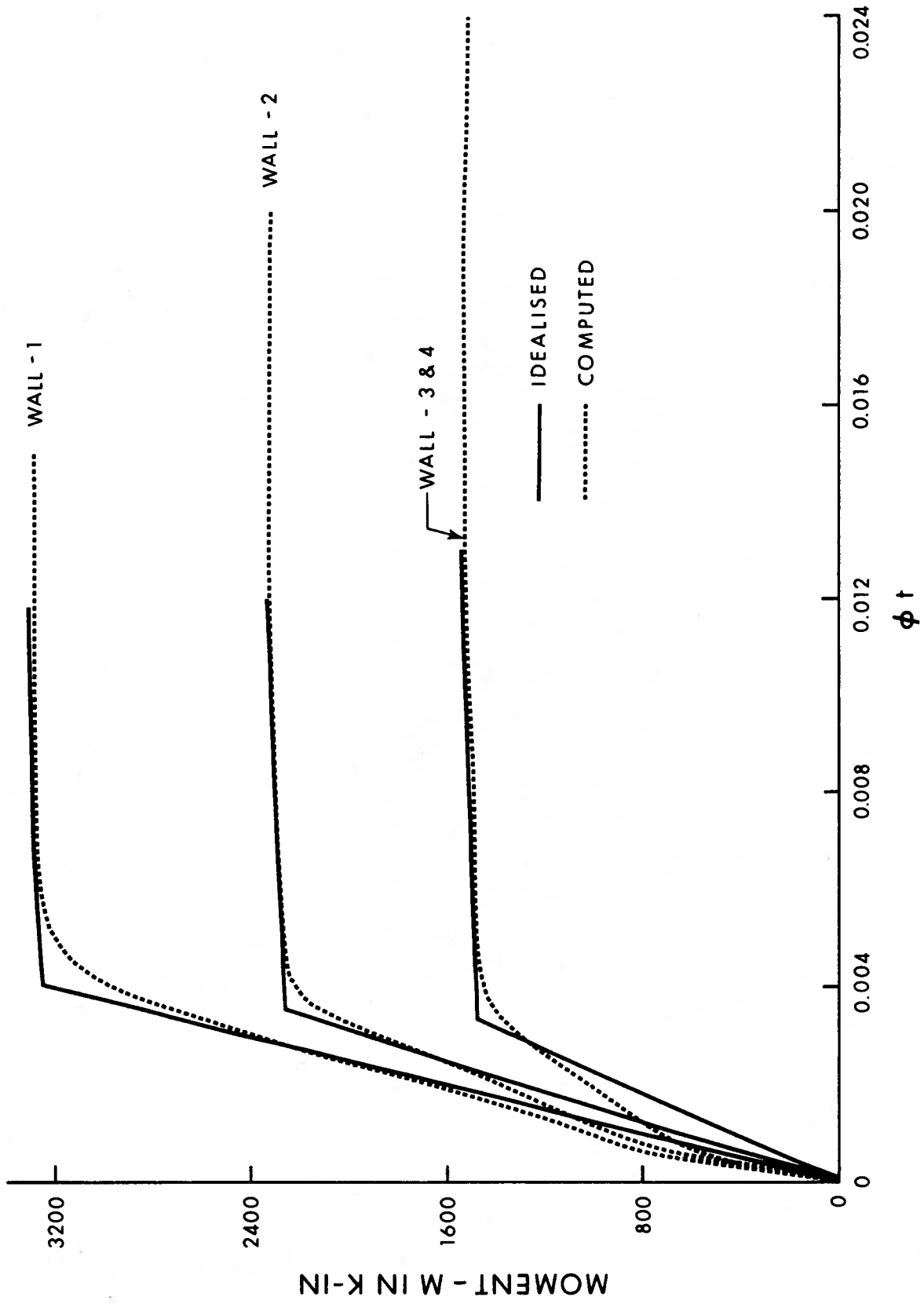
FIGURE 8.3 MOMENT - CURVATURE DIAGRAM FOR WALL SECTIONS
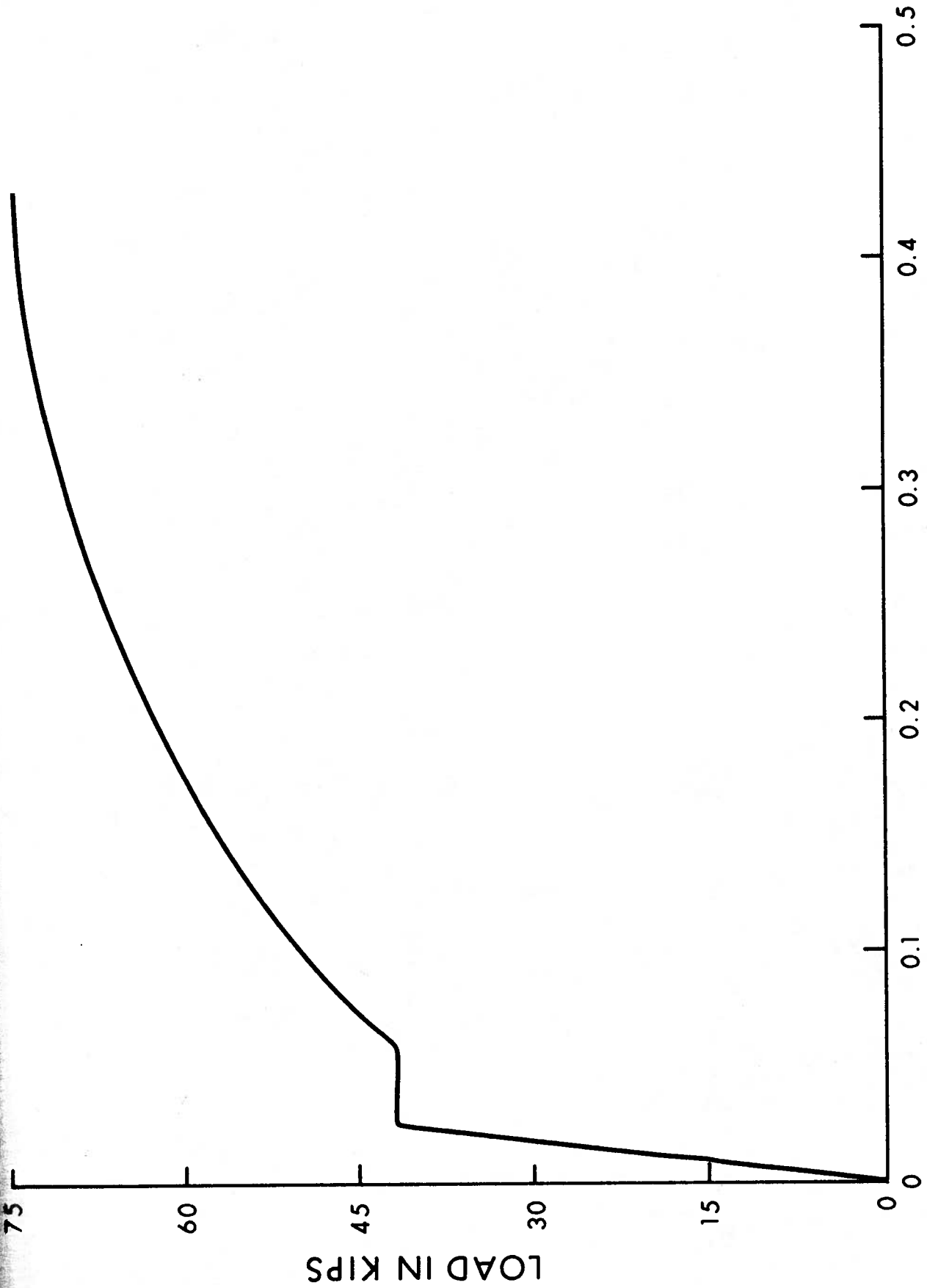
FIGURE 8.4 LOAD - SHORTENING CURVE FOR PIPE

198

24"

6"

BUILT UP
CHANNEL
BASE PLATE

B

A

$1\frac{1}{2}$"

26"

LAB. FLOOR

PLATE
1"×8"×8"

2" PIPE SPACER
$5\frac{1}{2}$" LONG

$1\frac{1}{2}$" BOLT

(a)   SECTIONAL ELEVATION

LENGTHNING
OF BOLT PLUS
SHORTENING
OF PIPE

Δ_B

B

A

T

C

(b)   SHOWING ROTATION OF WALL ABOUT A

FIGURE 8.5 WALL BASE MOVEMENT AND CONNECTION
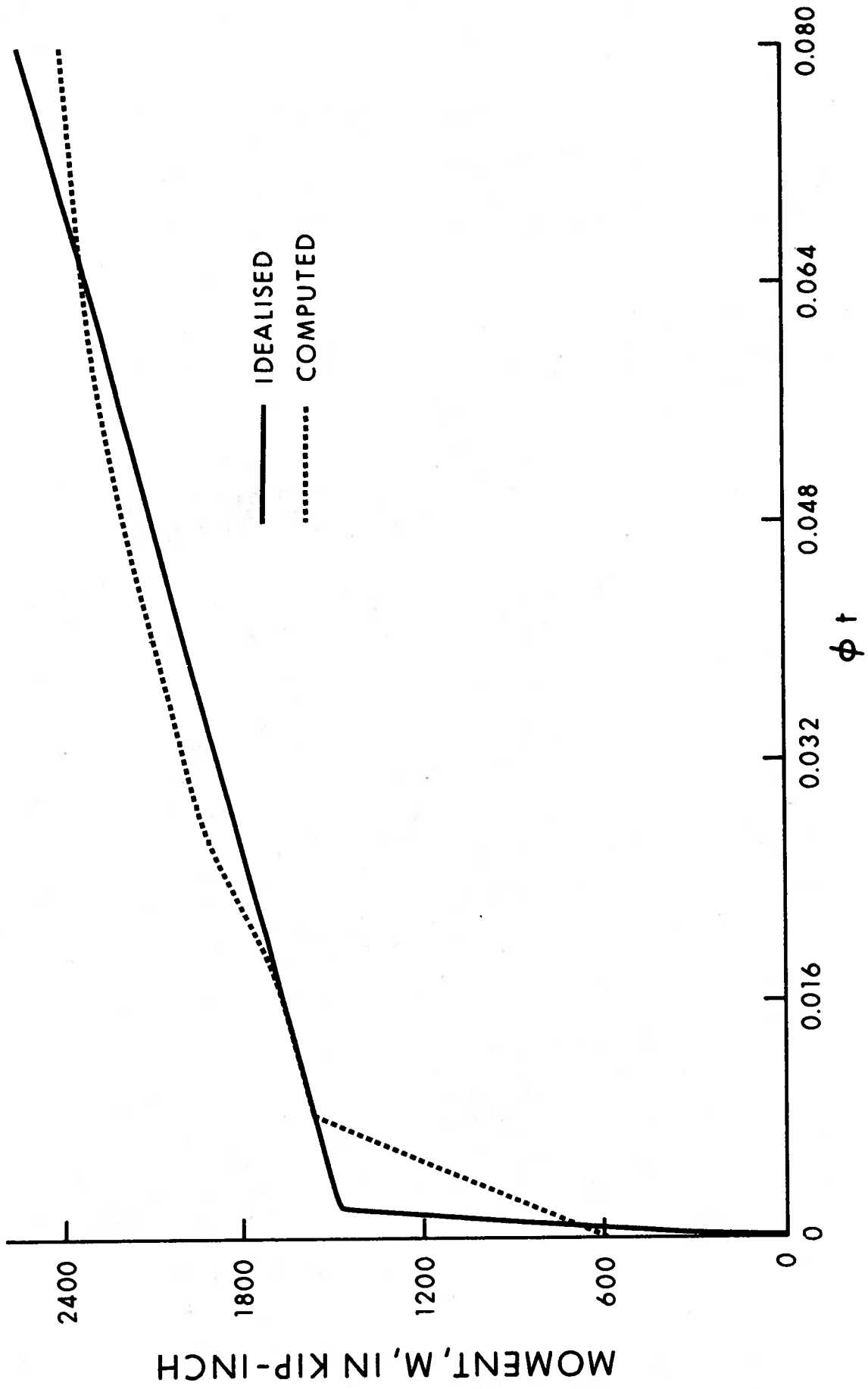
FIGURE 8.6 WALL BASE RESPONSE

MOMENT, M, IN KIP-INCH

ϕ t

IDEALISED
COMPUTED

200

CHAPTER IX

COMPARISON OF PREDICTED
vs.
ACTUAL BEHAVIOUR OF FOUR STORY TEST FRAME

9.1 Introduction

A four story one bay reinforced concrete frame was tested under combined vertical and lateral loads. The test frame was described in CHAPTER VII and the results of the test were presented in CHAPTER VIII and APPENDIX D. In this CHAPTER a comparison is made between the observed behaviour and that predicted by the shear wall-frame analysis presented in CHAPTER III in order to illustrate the validity of the method of analysis. The comparisons have been made with respect to moments, shears and the sequence of hinge formation.

The test results presented in this CHAPTER are those for the second application of load and have been referenced to the beginning of this test. The first loading was stopped because of failure of the electrical equipment. It should be noted that the beams were cracked in the first loading sequence.

9.2 Behaviour of Test Frame

The lateral load deflection diagram for the fourth floor of the test frame is presented in FIGURE 9.1. The data for both load applications are included in this diagram. The deflections have been referenced to the

beginning of the second load application. A positive deflection is one towards the applied loads (to the east). The loads referred to with letters and numbers in this figure are those for the first and second loadings, respectively.

In each test, the first three load increments consisted of vertical loads of 0, 5.8 and 50.2 kips, respectively, applied to the center of the column and wall, at the top of the structure. Under these loadings the column shortened more than the wall and the structure deflected to the west. Lateral loads were then applied to pull the frame to the east. Two increments of lateral load were applied in the first test. During the second lateral load increment, small cracks developed at the ends of the beams in the floors. Flexural cracks also developed in the wall in the bottom story.

The residual lateral deflection at the fourth floor was 0.18 inches to the east after all the loads had been removed. Of this, at least 0.10 inches was creep deflection which occurred during the time measurements were taken at loads D and E. The balance of the residual deflection was probably caused by the change in frame stiffness due to cracking of the beams.

In the second test of the frame, the behaviour essentially paralleled that observed in the first test. More extensive cracking was observed in the beams at load 5 and some flexural cracks were observed in the bottom story of the wall. A diagonal crack was observed in the third and fourth beam to column joints. The cracks in the third floor joints are shown in FIGURE 5.1. Between loads 5 and 6

the pipe sleeve (see FIGURES 7.11 and 8.5) below the floor at the west end of the wall yielded and the west end of the wall gradually lifted off the floor, rotating about a point near the east end of the wall. For the rest of the test, the base of the wall probably behaved according to a moment-rotation relationship similar to the one shown in FIGURE 8.6. At load 6, diagonal cracks were observed in the second beam to column joint.

At load 7, a diagonal crack was observed in the first beam to column joint and some bond distress appeared to be developing at the top beam to column joint. The flexural cracks in the bottom two stories of the wall extended to form inclined cracks which tended to cross pre-existing flexural cracks. The loads were very difficult to maintain and dropped off about 10 percent at this load increment. The measured rotations at the base of the wall indicated that the moment-rotation relationship for the base of the wall had reached its peak and had started to descend. Crushing was noted at the wall end of the second, third and top beams.

As the deflections were increased after load 7, the loads dropped continuously. Horizontal loading was stopped when the maximum horizontal jack stroke had been reached. Between loads 7A and 8, crushing occurred at the bottom of the column and at all other hinges. The top beam-column joint failed in bond.

FIGURE 9.2 shows the cracks in the frame after the test. FIGURE 9.3 traces the progress of hinging observed in the test. Plastic hinges were assumed to exist if very wide cracks developed and if the measured moments reached the computed plastic moments at any point in a

member.

9.3 Analysis of Test Frame

In the approximate analysis program the test frame can be represented by defining the stiffnesses of the left hand beams in the analytical model (FIGURE 3.1) as zero. The wall base response computed in section 8.10 was assumed to represent the behaviour of the first segment of the wall above the base of the wall. The idealized stiffnesses and ultimate moment capacities of various members used in the analysis were computed according to sections 8.4 and 8.10 and are presented in TABLE 9.1. The ultimate moment capacities of the beams presented in TABLE 9.1 differ from those in TABLE 9.2 since the moment capacities of the beams at the wall end were used in the analysis.

The shear wall-frame analysis described in CHAPTER III assumes that the rotation of the wall section occurs about its center line when computing the vertical deflection of points on the face of the wall. Since the base of the wall in the test frame rotated about a point close to the east edge of the wall section, the deflections of points on the west face of the wall were approximately equal to those assumed to occur in a wall of twice the actual width. For this reason the depth of wall section was assumed to be 48 inches for the purpose of this analysis.

The computer program, described in CHAPTER III, assumes constant stiffness and ultimate moment capacities throughout the length of a member. Accordingly, it was necessary to modify the program to allow a

different moment-curvature relationship for the bottom-most segment
of the wall.

The resulting moments from this analysis and observed moment
during the test are presented in TABLE 9.2 and are compared in section
9.4.

9.4   Comparison of Measured and Computed Moments

The moment diagram for all the members are shown in FIGURES 9.4,
9.5, 9.6 and 9.7 for loads number 4, 5, 6 and 7 respectively. The
points and solid lines refer to the moments computed from the curva-
tures measured in the test and the dashed line shows the predicted
moments. In general the analysis underestimated the column moments
in the top story and overestimated them in the bottom three stories
in the initial stages of loading. For load number 7 the column moments
are in fairly good agreement. As for the wall, the agreement in the
measured and computed moments are fair except for the bottom story.
The measured moments are shown for this wall but the points have not
been joined because of the scatter in the points. This difference
is probably due to errors in the readings resulting from the cramped
working space adjacent to the bottom story.

The beam moments at the wall end are overestimated, by the
analysis, during the prehinging stages of loading and are in good
agreement after hinges formed in the beams. The explanation of this
may lie in the fact that the effect of local deformations at the beam
to wall joints was ignored in the analysis. A method of correcting for

this in which the beam is assumed to extend into the shear wall, ½ of the beam depth beyond the face of the wall, has been suggested in reference (M10). The effective change in length of the beams may be increased by cracking of the members and the joint. To take these factors into account the test frame was re-analyzed by the analysis developed in CHAPTER III with the beam length extended by half its cross-sectional depth. However, the reduction in beam moments with respect to previous analysis was found to be less than two percent at the ends of the two beams and 5 percent at the measuring stations which were located about 7½" from the face of the wall or 10½" from the 'end' of the extended beam.

Another reason for the discrepancy in the moment diagrams lies on the fact that stiffnesses and moment capacities of the beams used in the analysis were derived for the sections near the wall end. In fact the stiffnesses and moment capacity of the beam varied along the length because the reinforcement was displaced during casting. The observed moments in the beams at the column to beam joints were found to be higher than the predicted moments since the stiffnesses and moment capacities of the beams were higher at these joints than the wall to beam joints.

It can also be seen from FIGURES 9.4, 9.5, 9.6 and 9.7 that the moment balance is better at the top two joints than at the other joints. This difference may be caused by difference in axial loads on the columns and walls. The beam shear produces a tensile force in the columns and a compressive force on the wall, as a result the columns and walls carries different axial loads than the one measured by the hydraulic jacks. These discrepancies in the axial

loads are greater in the bottom story than at relatively higher stories.

Part of the difference in the moments may be caused by ignoring the relative axial shortening of column and wall in the analysis. The measured axial shortening of the column and wall reveal that it can cause a moment ranging from 1.50 inch-kips at the ends of bottom beam to 1.80 inch-kips at the ends of the top beam. If this were included in the analysis however, the errors in the predicted moments would increase slightly.

The other factor affecting the moments might be due to the way in which hinges are assumed to form in the analysis. The analysis assumes that point hinges form at the intersection of the members at the joints but the test indicated that the hinges in the beams formed away from the joints by about half the beam depth and are spread over a finite length. This can be seen in FIGURES 5.1 and 9.2.

The idealization of moment-curvature diagram can also produce some differences in the observed and predicted moment. As mentioned in CHAPTER IV, the moment-curvature diagram for reinforced concrete cross-section is not exactly bi-linear. The analysis uses a bi-linear moment-curvature diagram which is only an approximation of the exact moment-curvature relationship. In addition the exact moment-curvature diagram for all sections in a beam may be difficult to derive, since the various factors which affect this relationship, discussed in CHAPTER IV, may not be consistent at all cross-sections

along the length of a member. For example the strength of concrete, which depends on the compaction, void ratio, proportion of mix etc. cannot be maintained exactly constant along the full length of the member. These factors may give rise to different properties at different sections along the same member. Therefore, the moments derived from the measured curvature, using moment-curvature relationship for different members, presented in CHAPTER VIII, will give only an estimate of moments, not the exact value of the developed moments.

9.5 Comparison of Shears

The shear diagrams for all the columns and walls are compared in FIGURES 9.8, 9.9, 9.10 and 9.11 for load numbers 4, 5, 6 and 7, respectively. The dotted lines show the predicted shear whereas solid lines give the observed shear. The applied shear is calculated from the loads measured by horizontal jacks. The P-Δ shear has been computed from the measured horizontal deflections of the floor levels and the applied vertical loads measured by the vertical jacks. Total shears are the sum of the applied shear and the P-Δ shear. The frame and wall shears have been computed from the observed moments and are given by the sum of the top and bottom moments observed in a story divided by the story height. Since the observed moments in the bottom story wall are not known, as mentioned in section 9.4, it was not possible to compute the observed wall shear in this story. The P-Δ shears and frame shears are plotted on an enlarged scale.

It can be seen in FIGURES 9.8, 9.9, 9.10 and 9.11 that the sum of the observed frame and wall shears do not agree with the total shears. This is because of the fact that the observed moments in section

9.4 are not in good agreement which resulted in the discrepancy of
the shears. If the P-Δ shears are computed as the sum of frame and
wall shears minus the applied shear the result would be different
from the P-Δ shears computed from the measured vertical loads and
measured deflections. Since the measured deflections are in good
agreement with the predicted deflections by the analysis, at least
for loads 4, 5 and 6, the P-Δ shears plotted in FIGURES 9.8, 9.9 and
9.10 are in good agreement and hence the total shear in the structure.
For load number 7 the P-Δ shears are not in agreement, as can be
seen in FIGURE 9.11, because the difference in the measured and
predicted deflections are large. It should be remembered, however,
that load 7 is close to the peak point of load-deflection curve
(see FIGURE 9.1) and little difference in the load can cause a
greater change in the deflections. Since the shears have been
computed from the moments, the discrepancies in the moment diagrams
are liable to be carried and echoed in shear diagrams.

It can also be seen from FIGURES 9.8, 9.9, 9.10 and 9.11
that the shear wall attracts a greater percentage of the shear in
the bottom story whereas the frame seems to attract the greater
portion of the shear in the top stories. This is partly because the
column is stiffer in the fourth story than in the other three stories.
The major reason, however, is the interaction between the shear wall
and the frame. In tall structures, the wall will frequently have
negative shears at the top of the building and as a result the frame
may have very high shears in top stories (K2, M8).

9.6 Comparison of Deflections

The predicted and observed deflection diagrams for the various floor are given in FIGURES 9.12, 9.13, 9.14 and 9.15. The theoretical analysis seems to overestimate the deflection in the beginning and under-estimates it in the later stage of loading. The explanation of this lies on the idealization of the "elastic" portion of the moment-curvature relationship for the section. As shown in FIGURE 8.2 for example, the idealization of this curve leads to underestimate the stiffness at low loads so that the predicted deflections initially are in excess of the measured values and tends to overestimate the stiffness at later stages of loading resulting in an underestimation of the subsequent deflections. The observed deflections include the shear deformations whereas the analysis consider only the bending deformation. This may cause little discrepancies in the measured and predicted deformations. However, the agreement in general is satisfactory. The falling branch of the load-deflection curve is not possible to find by the analysis since it does not consider the falling branch of moment-curvature relationships for the cross-sections.

9.7 Formation of Hinges

FIGURE 9.3 compares the plastic hinges observed in the test to those predicted by the analysis. No hinges were found in the theoretical analysis, or in the test up to load 5. The observed and predicted hinges for load 6 and 7 are compared in FIGURE 9.3. No hinges were observed at load 6 in the test although the analysis detected hinges at the wall end of all the beams. The observed moments were very

close to the hinging capacities at this load, however. At load 7
all the hinges are comparable. In general the formation of plastic
hinges detected in the analysis were close to that observed in
the test. It is also observed that the hinges form away from the
joints by about half the member's depth and spread over a finite
length (see FIGURE 9.2). The hinges form with severe cracking of
concrete.

9.8 Summary

The predicted and observed behaviour of the test frame
was compared in this CHAPTER. The comparisons of moments, shears,
deflections and formation of plastic hinges were made in sections
9.4, 9.5, 9.6 and 9.7., respectively. In general the analysis seems
to give a good description of the behaviour. It was found that the
various assumptions such as the idealization of moment-curvature
relationship, idealization of material properties, consideration of
point hinges, neglecting shear deformations etc. have very little
effect on the analysis. However, the method of testing does not
focus on the assumptions of lumping and loading made in CHAPTER III.
These assumptions have been discussed in CHAPTER VI and a lumping
procedure has been derived.

TABLE 9.1

STIFFNESS AND MOMENT CAPACITY OF VARIOUS MEMBERS

Member	EI in K-in^2	Ultimate Moment M_u, in K-in.
Beam 1	134,000	86.0
Beam 2	160,200	119.0
Beam 3	141,000	111.0
Beam 4	138,500	109.0
Col. 1	87,000	63.0
Col. 2	84,100	63.0
Col. 3	85,000	61.0
Col. 4	114,000	94.5
Wall 1	20,100,000	3255.0
Wall Base	20,100,000	1470.0
Wall 2	15,500,000	2260.0
Wall 3	10,800,000	1480.0
Wall 4	10,700,000	1480.0

TABLE 9.2

MEASURED AND PREDICTED MOMENTS AT CRITICAL SECTIONS IN FRAME

Member	Section*	Calculated Ultimate Moments K-in.**	Measured Moments in K-in At Loads				Calculated Moments in K-in*** At Loads			
			4	5	6	7	4	5	6	7
Col. 1	Bottom	63.00	9.50	28.00	46.00	63.00	11.49	22.48	54.14	63.00
	Top	63.00	-4.50	-11.00	-21.00	-30.00	-7.95	-15.56	-37.34	-34.34
Col. 2	Bottom	63.00	7.00	22.00	35.00	52.00	14.54	28.44	47.76	51.55
	Top	63.00	-6.00	-23.00	-46.00	-64.00	-14.86	-29.06	-51.36	-58.00
Col. 3	Bottom	61.00	9.20	26.00	44.00	63.00	16.69	32.61	53.83	61.00
	Top	61.00	-11.60	-27.00	-44.00	-55.00	-14.34	-28.02	-45.92	-44.77
Col. 4	Bottom	94.50	21.80	48.00	69.00	90.00	19.84	38.70	63.74	66.23
	Top	94.50	-27.80	-54.00	-85.00	-105.00	-24.52	-47.85	-82.94	-94.50
Beam 1	Col. end	95.00	15.40	48.00	87.00	118.00	22.49	44.00	85.11	86.00
	Wall end	86.00	-17.00	-46.00	-69.00	-85.00	-26.35	-51.56	-86.00	-86.00
Beam 2	Col. end	133.30	28.30	64.00	95.00	159.00	31.55	61.67	105.18	119.00
	Wall end	119.00	-27.00	-62.00	-98.00	-142.00	-39.57	-77.35	-119.00	-119.00

TABLE 9.2 (contd.)

Beam 3	Col. end	133.00	32.00	76.00	123.00	178.00	34.18	66.72	109.66	111.00
	Wall end	111.00	-30.00	-68.00	-112.00	-138.00	-38.89	-75.91	-111.00	-111.00
Beam 4	Col. end	129.30	28.30	54.00	83.00	130.00	24.52	47.85	82.94	94.50
	Wall end	109.00	-28.00	54.00	-84.00	-102.00	-32.74	-63.87	-109.00	-109.00
Wall 1	Bottom	1470.00	-	-	-	-	756.03	1479.86	1810.27	2427.80
	Top	3255.00	-	-	-	-	317.76	620.49	688.72	1085.53
Wall 2	Bottom	2260.00	285.00	710.00	890.00	1250.00	358.07	699.35	823.60	1220.67
	Top	2260.00	20.00	60.00	0.00	200.00	52.48	100.86	31.26	249.93
Wall 3	Bottom	1480.00	80.00	170.00	220.00	270.00	112.37	217.93	214.31	436.93
	Top	1480.00	-55.00	-120.00	-245.00	-160.00	-68.16	-134.63	-252.93	-172.52
Wall 4	Bottom	1480.00	0.00	-20.00	-60.00	-50.00	-8.40	-17.96	-78.88	1.91
	Top	1480.00	-35.00	-90.00	-160.00	-210.00	-49.10	-95.78	-167.04	-167.14

* Column and beam end moments are at the center of joint except that wall end moments are at the face of the wall.

** From analysis section 8.4

*** From analysis CHAPTER III.
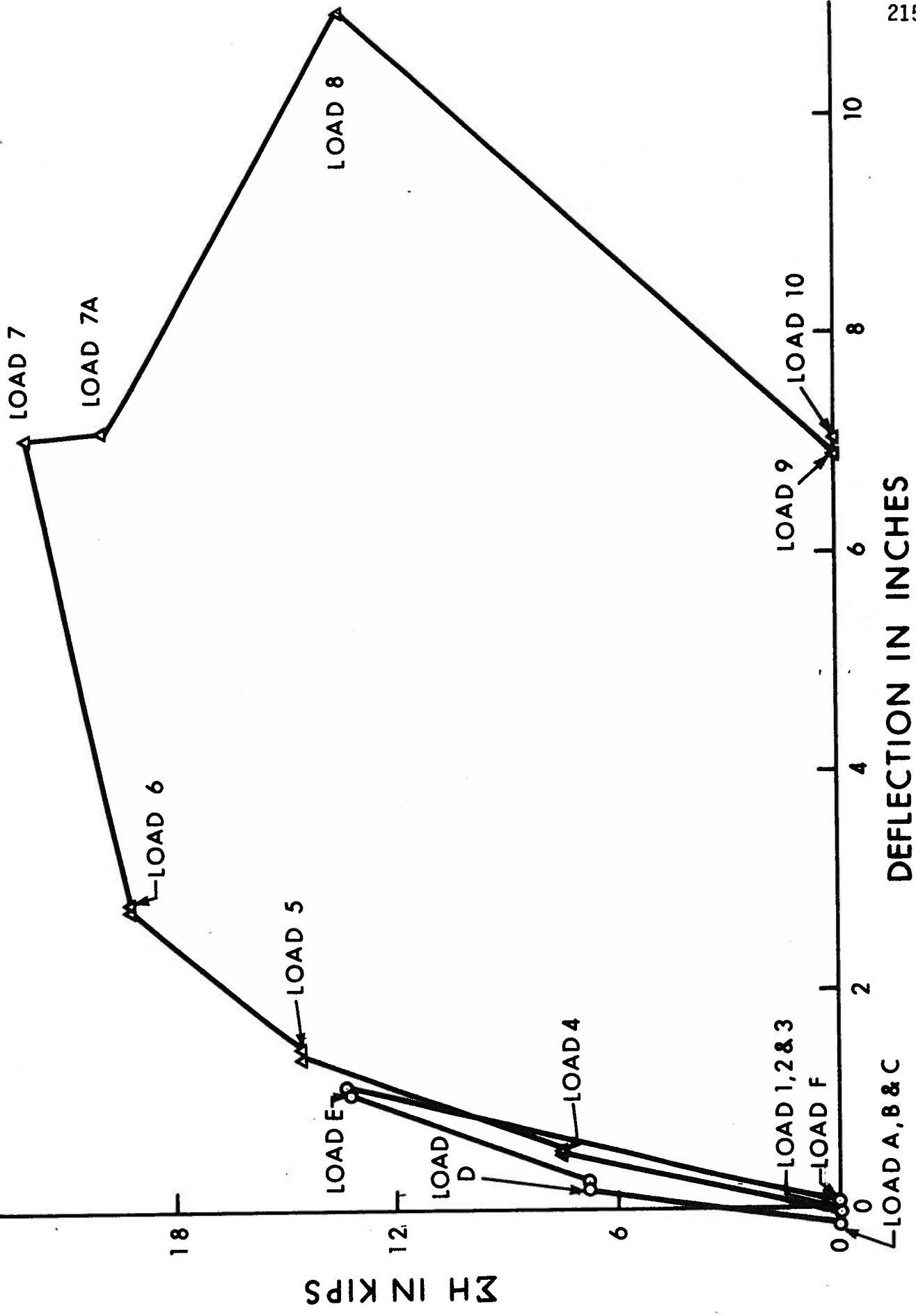
FIGURE 9.1 LOAD - DEFELECTION DIAGRAM FOR TOP FLOOR

215
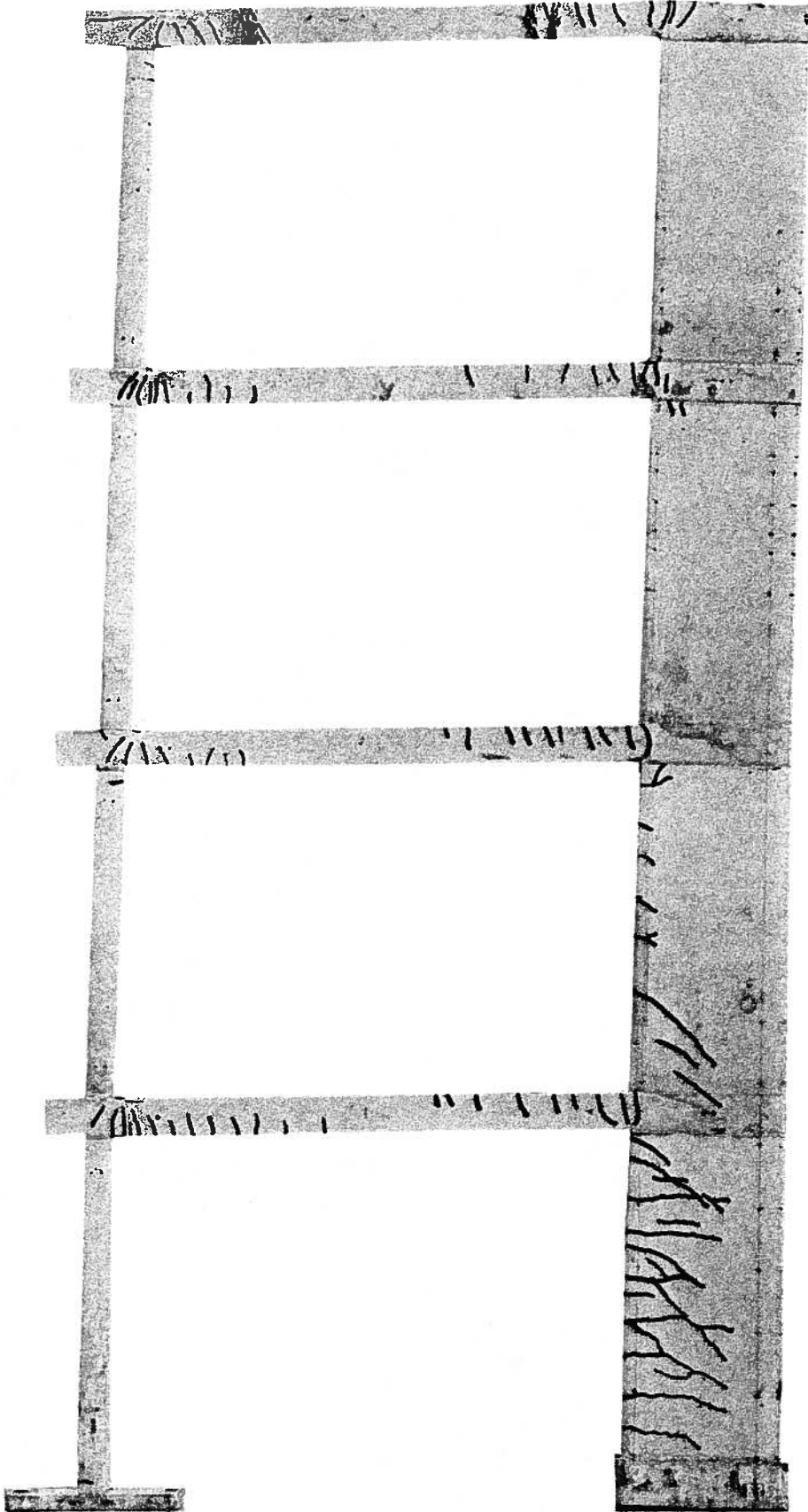
FIGURE 9.2 SPECIMEN AFTER TEST SHOWING CRACKS
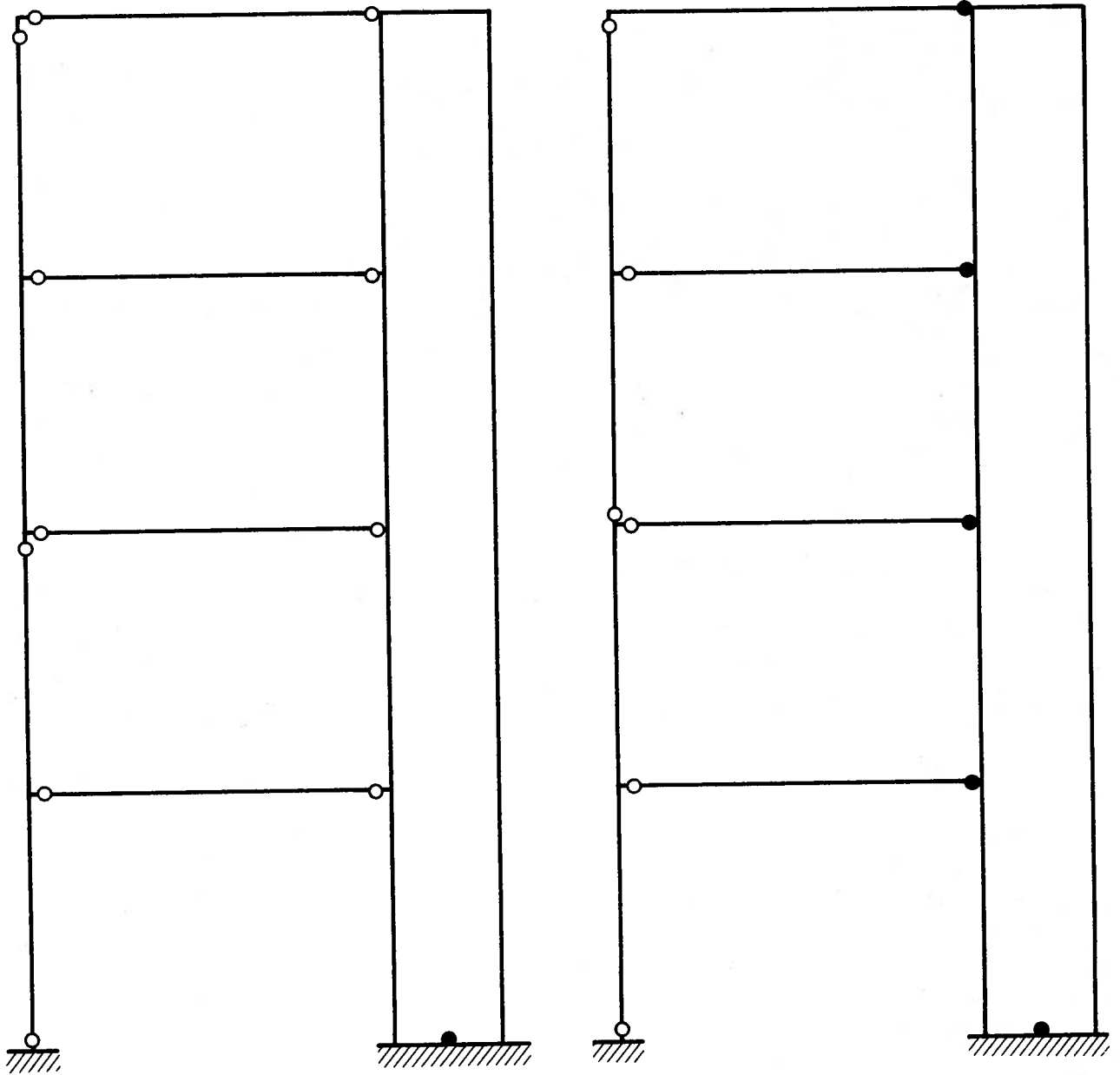
(a) TEST (b) ANALYSIS

LOAD 6 ●
LOAD 7 ○

FIGURE 9.3 HINGE PATTERN IN TEST FRAME
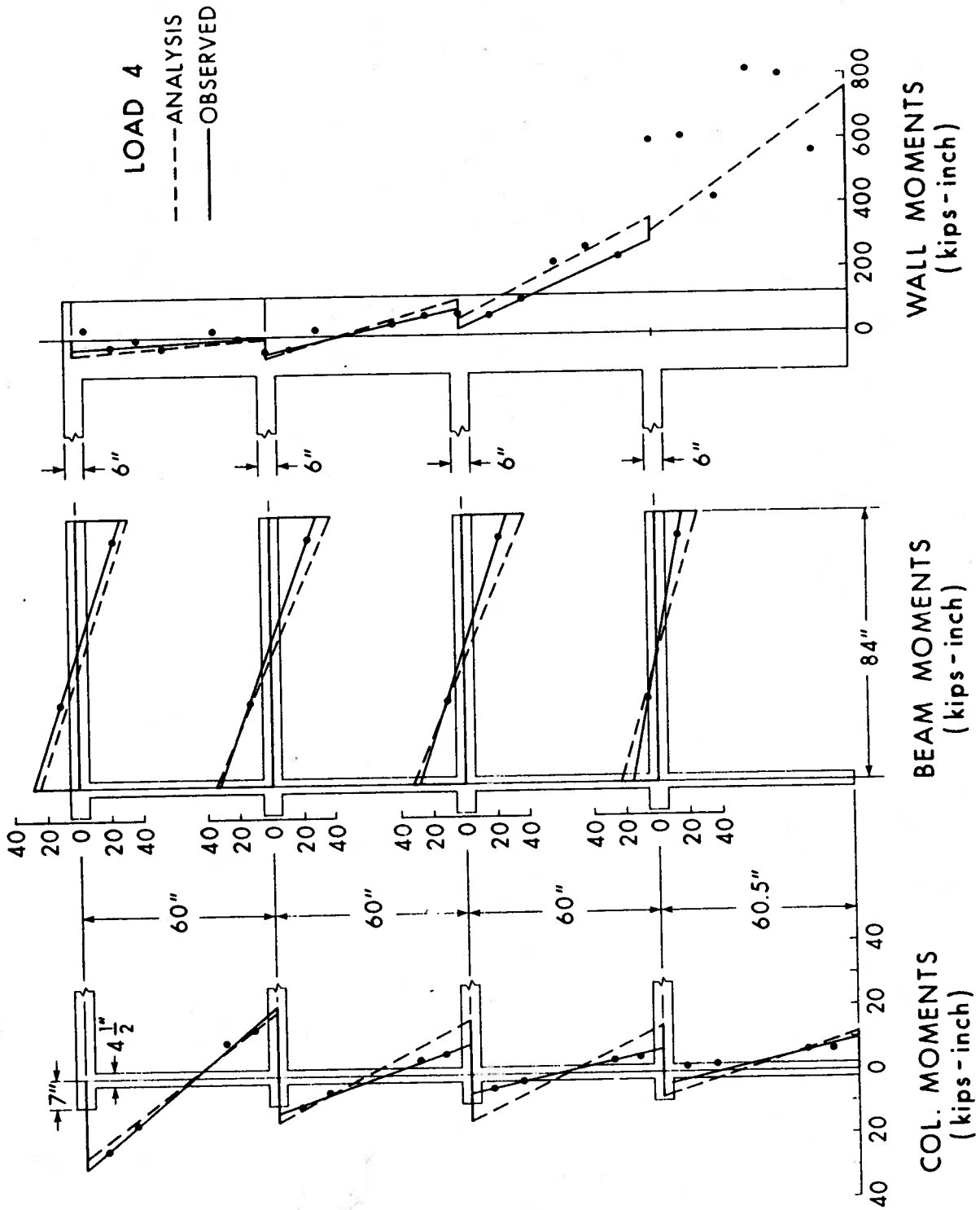
FIGURE 9.4 MOMENT DIAGRAM FOR LOAD 4
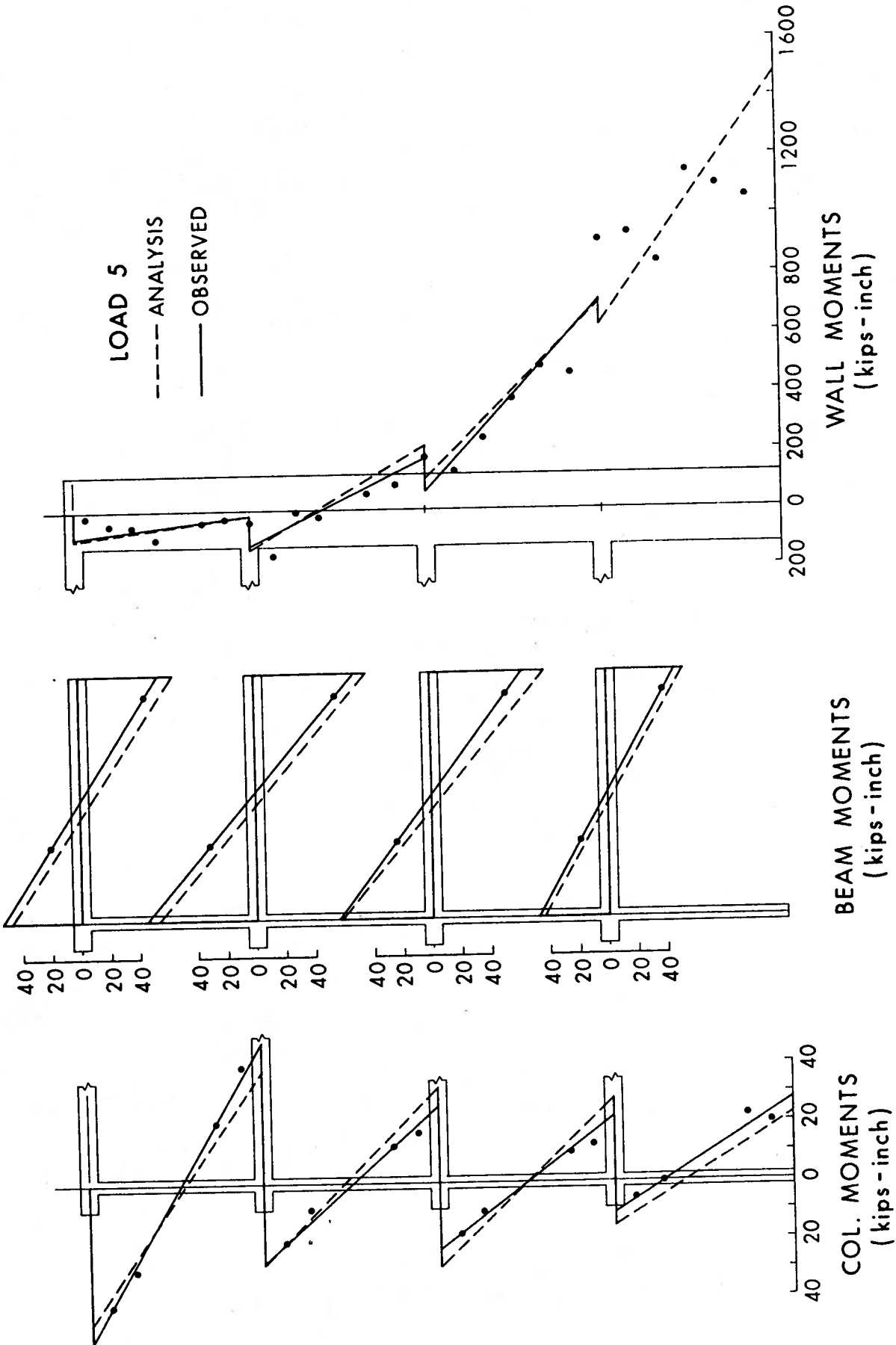
FIGURE 9.5 MOMENT DIAGRAM FOR LOAD 5
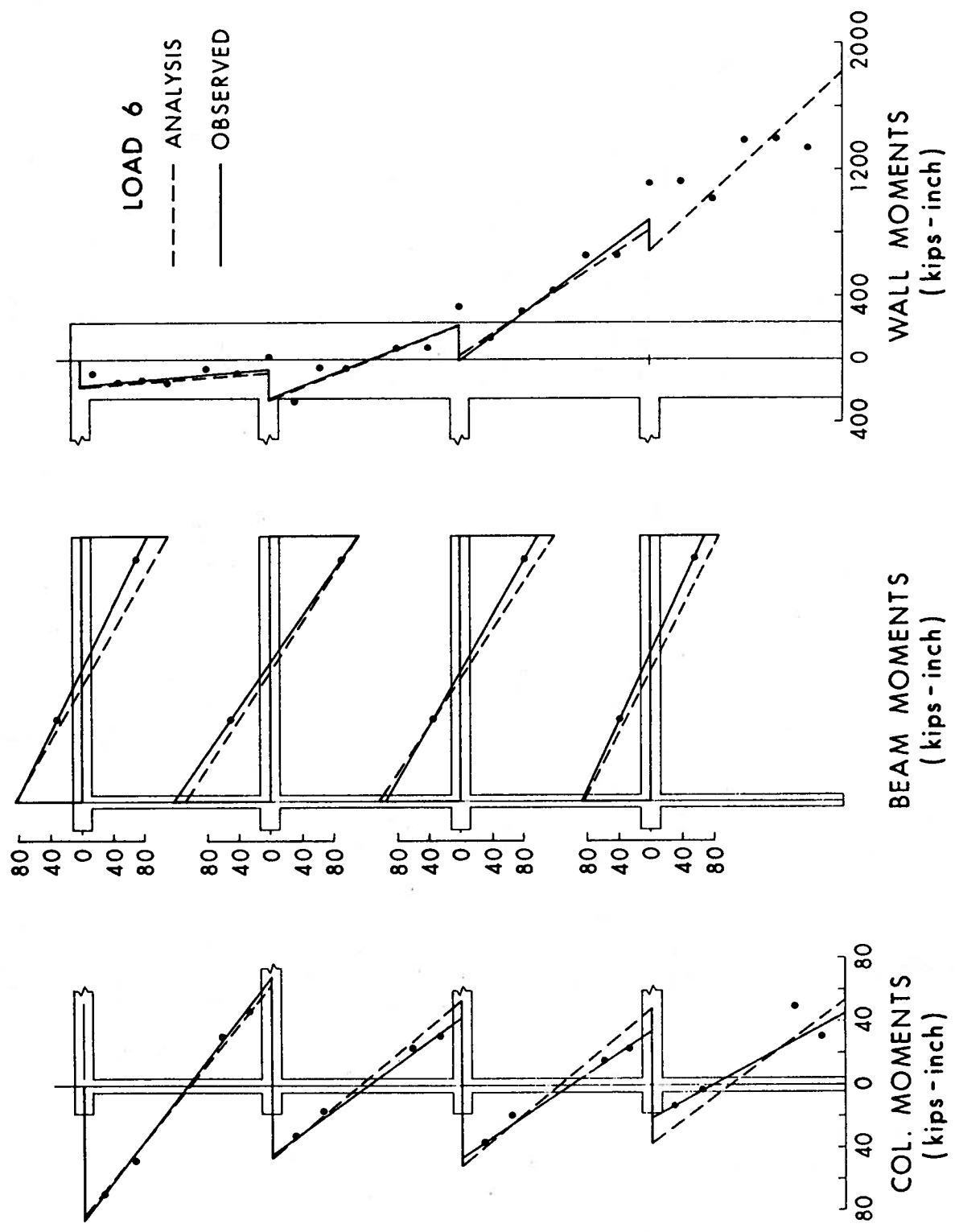
FIGURE 9.6 MOMENT DIAGRAM FOR LOAD 6
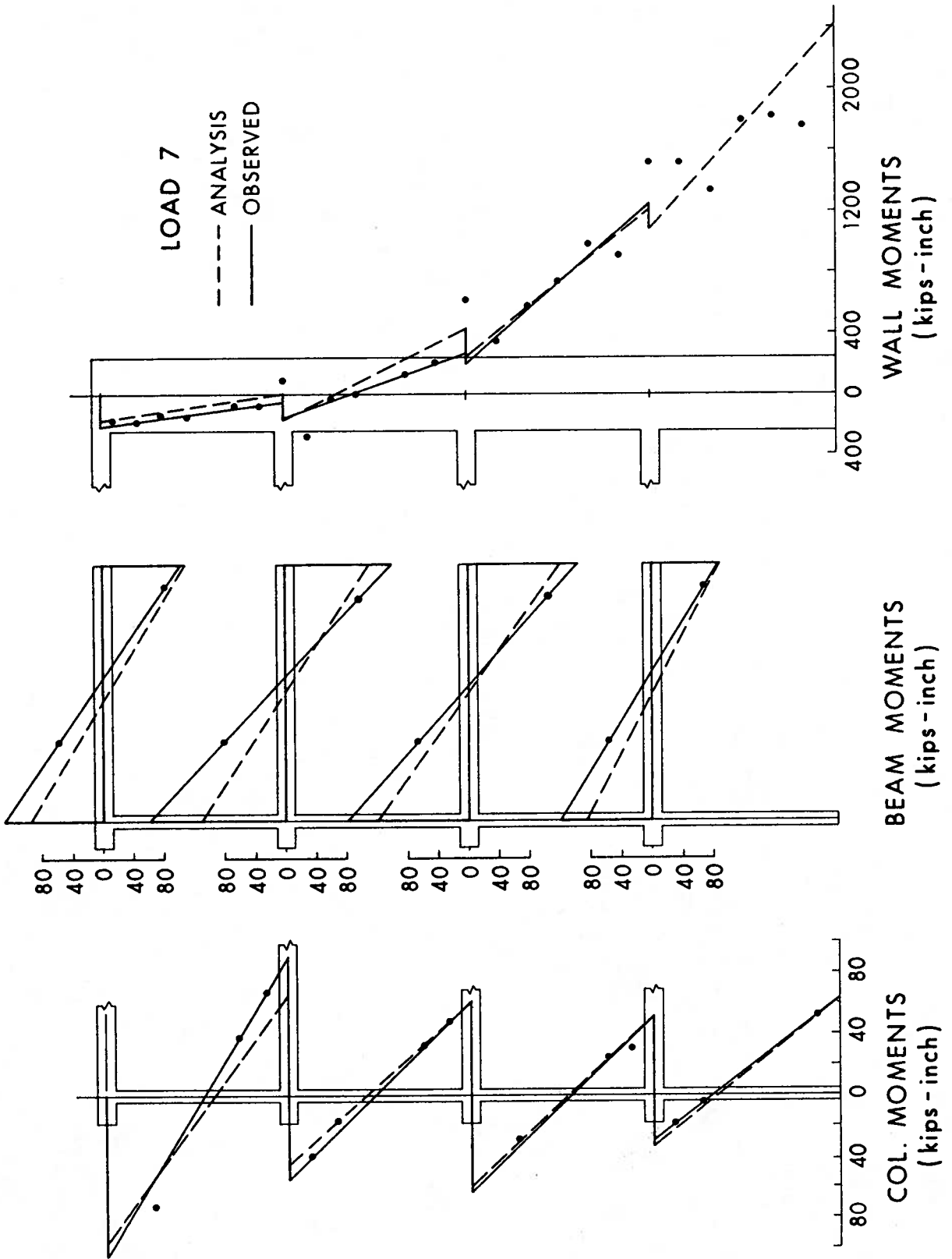
FIGURE 9.7 MOMENT DIAGRAM FOR LOAD 7
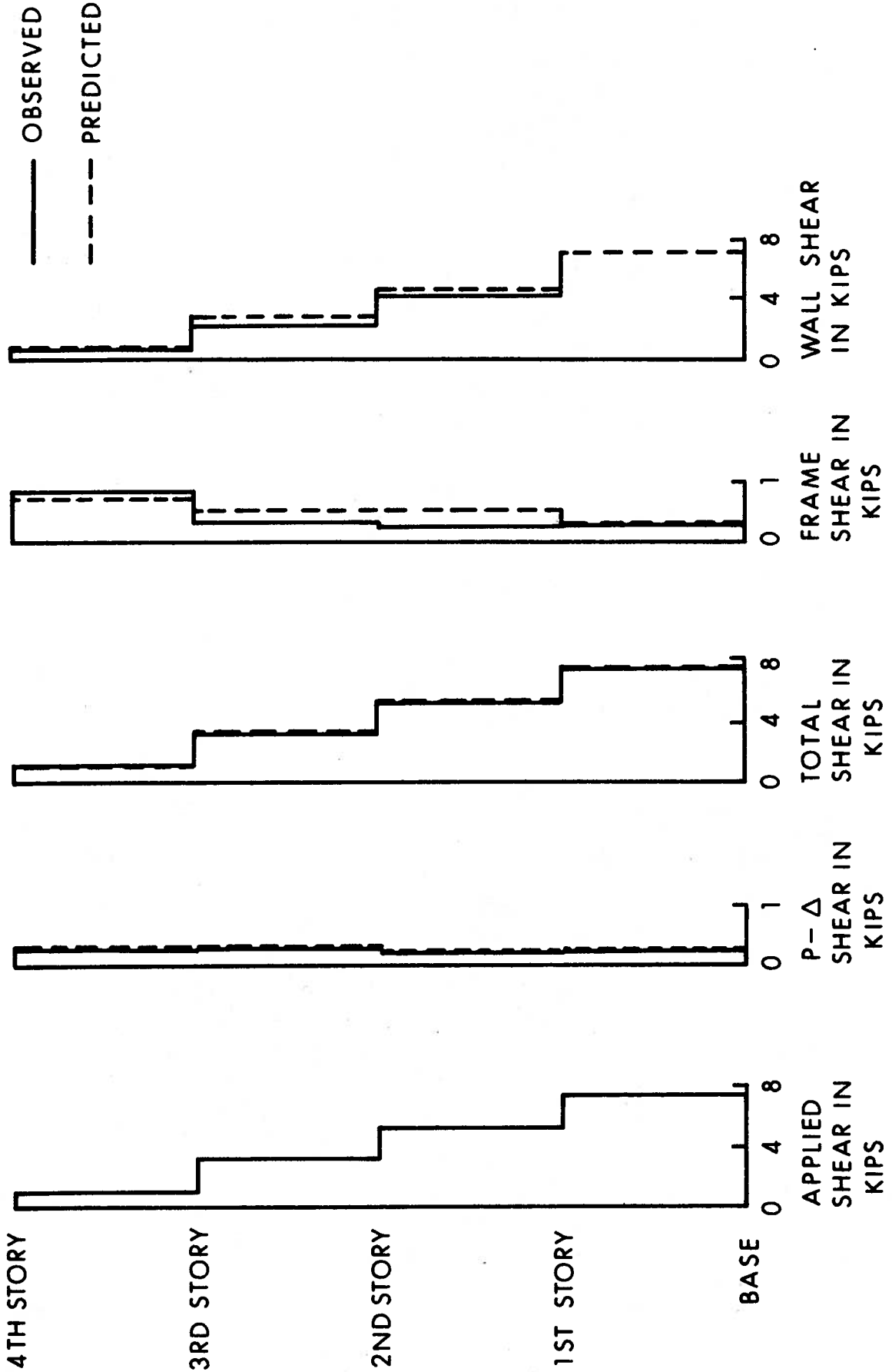
FIGURE 9.8 SHEAR DIAGRAM FOR LOAD 4

223
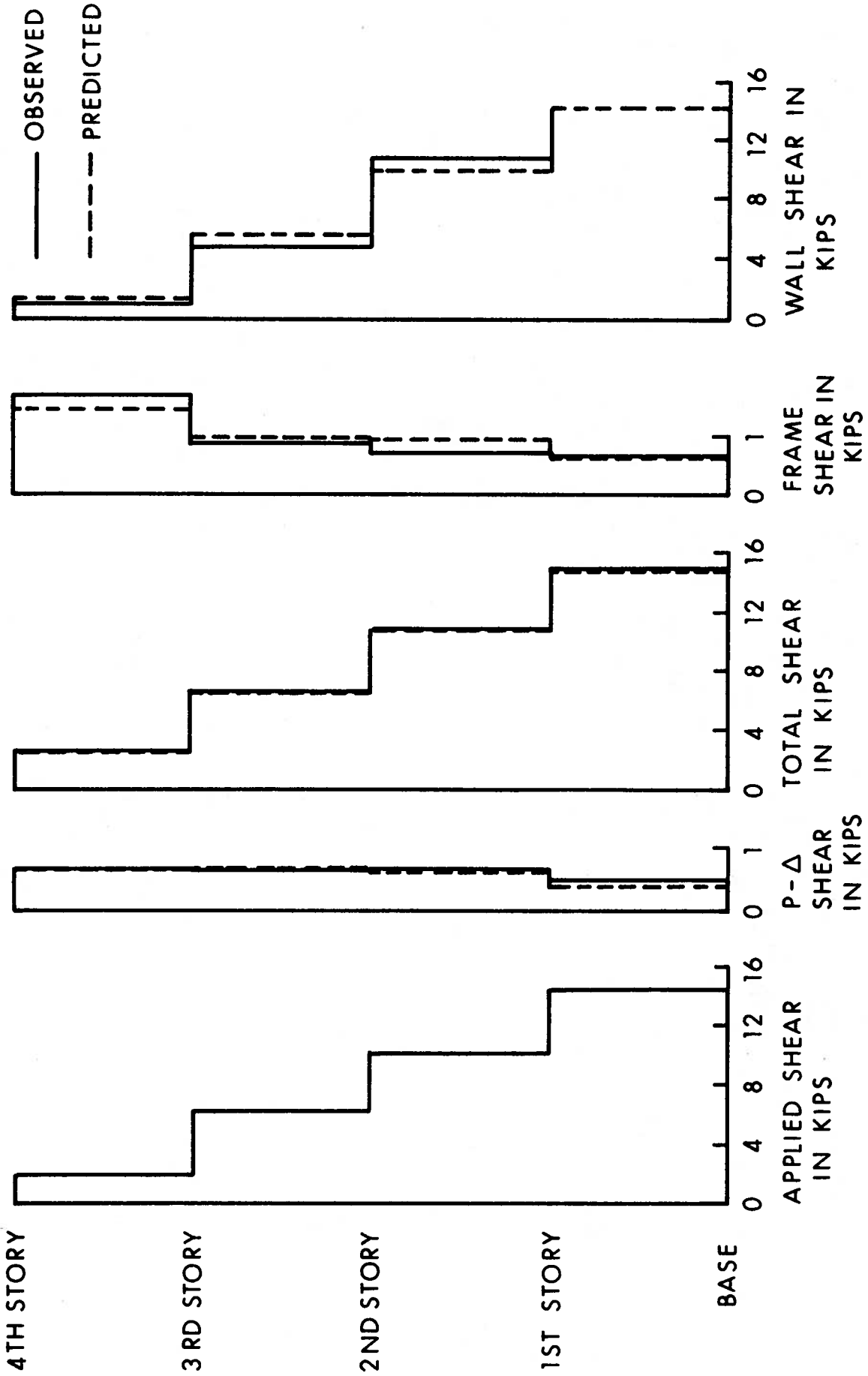
FIGURE 9.9 SHEAR DIAGRAM FOR LOAD 5

224
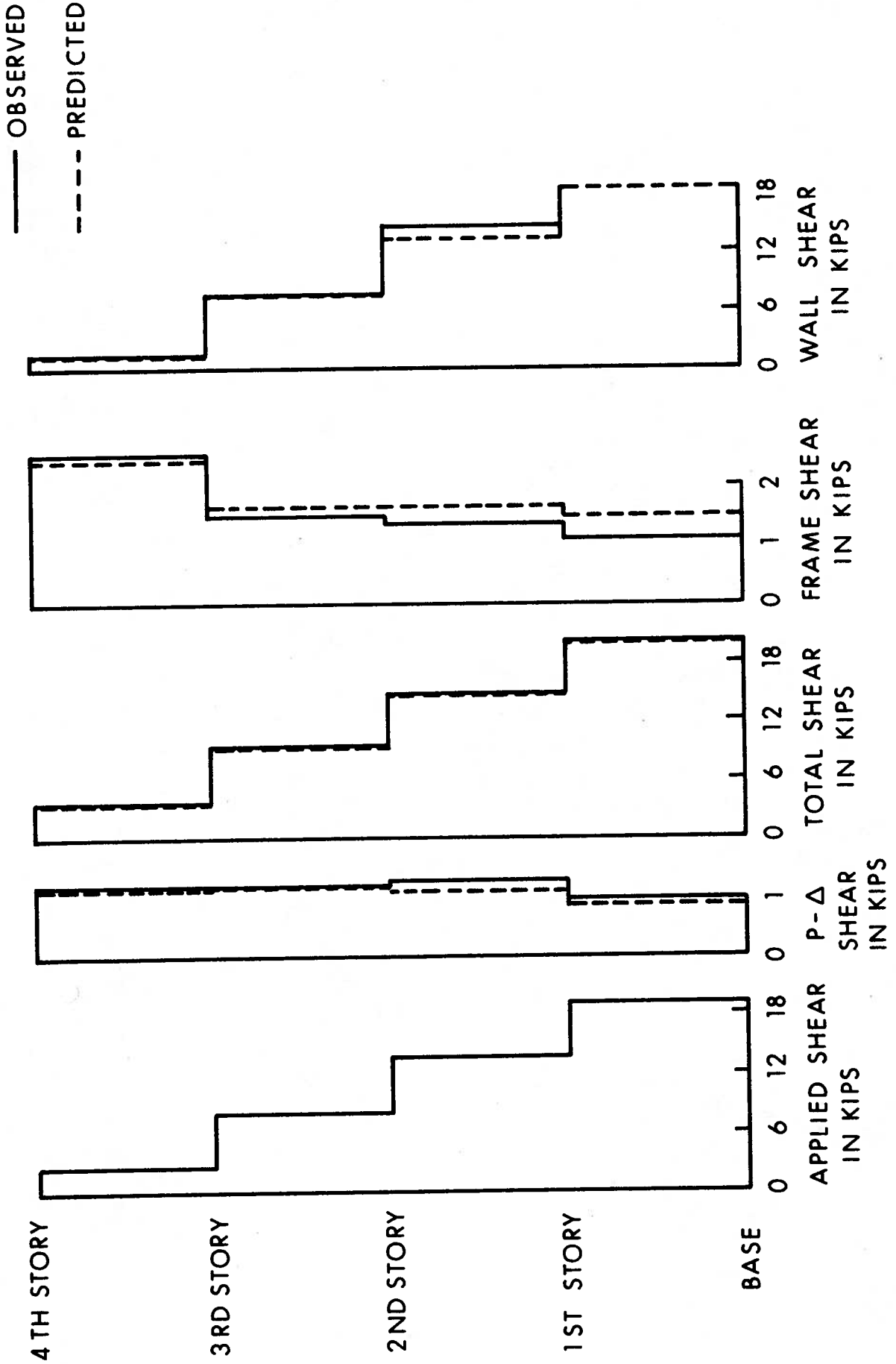
FIGURE 9.10 SHEAR DIAGRAM FOR LOAD 6
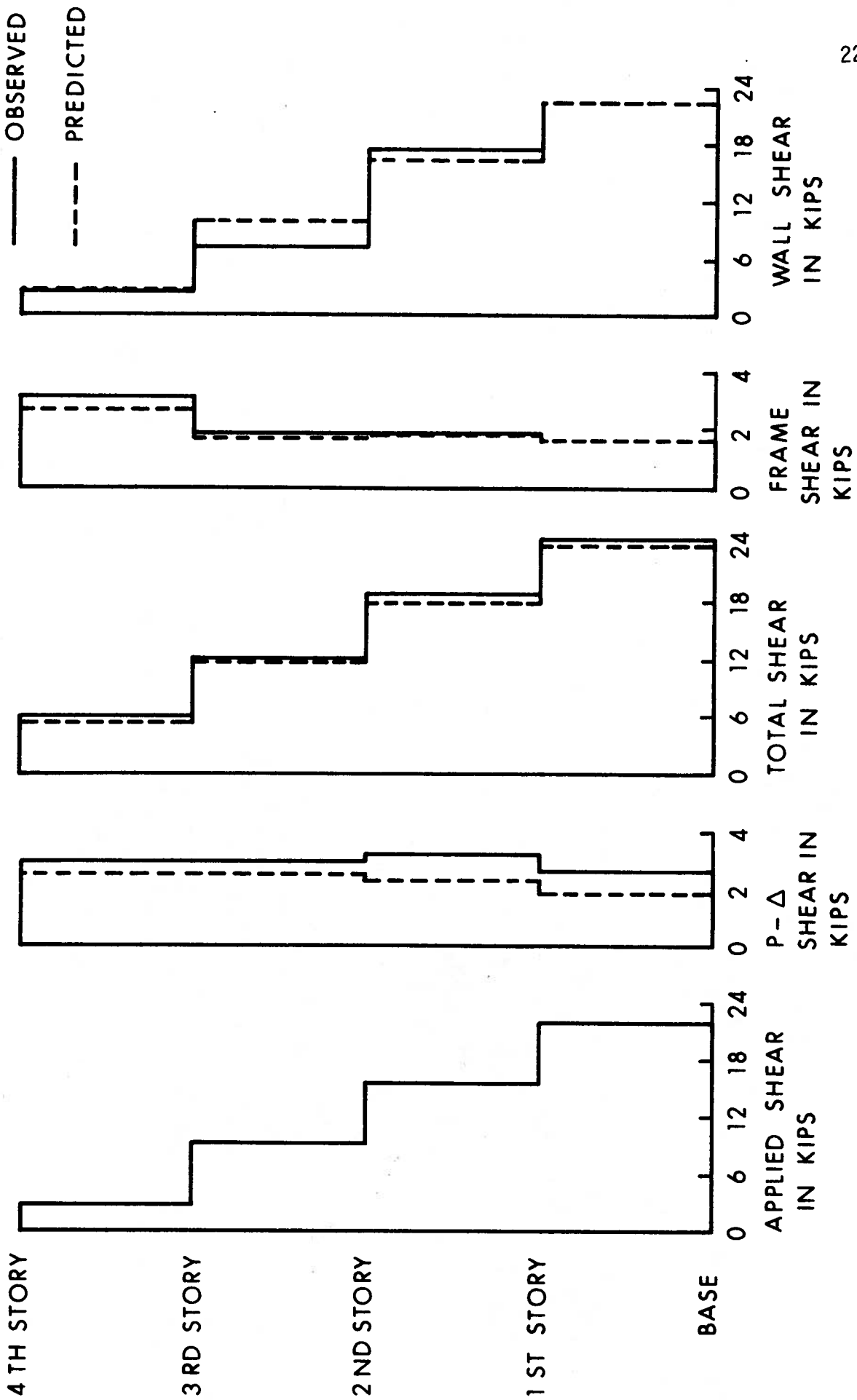
FIGURE 9.11 SHEAR DIAGRAM FOR LOAD 7

225
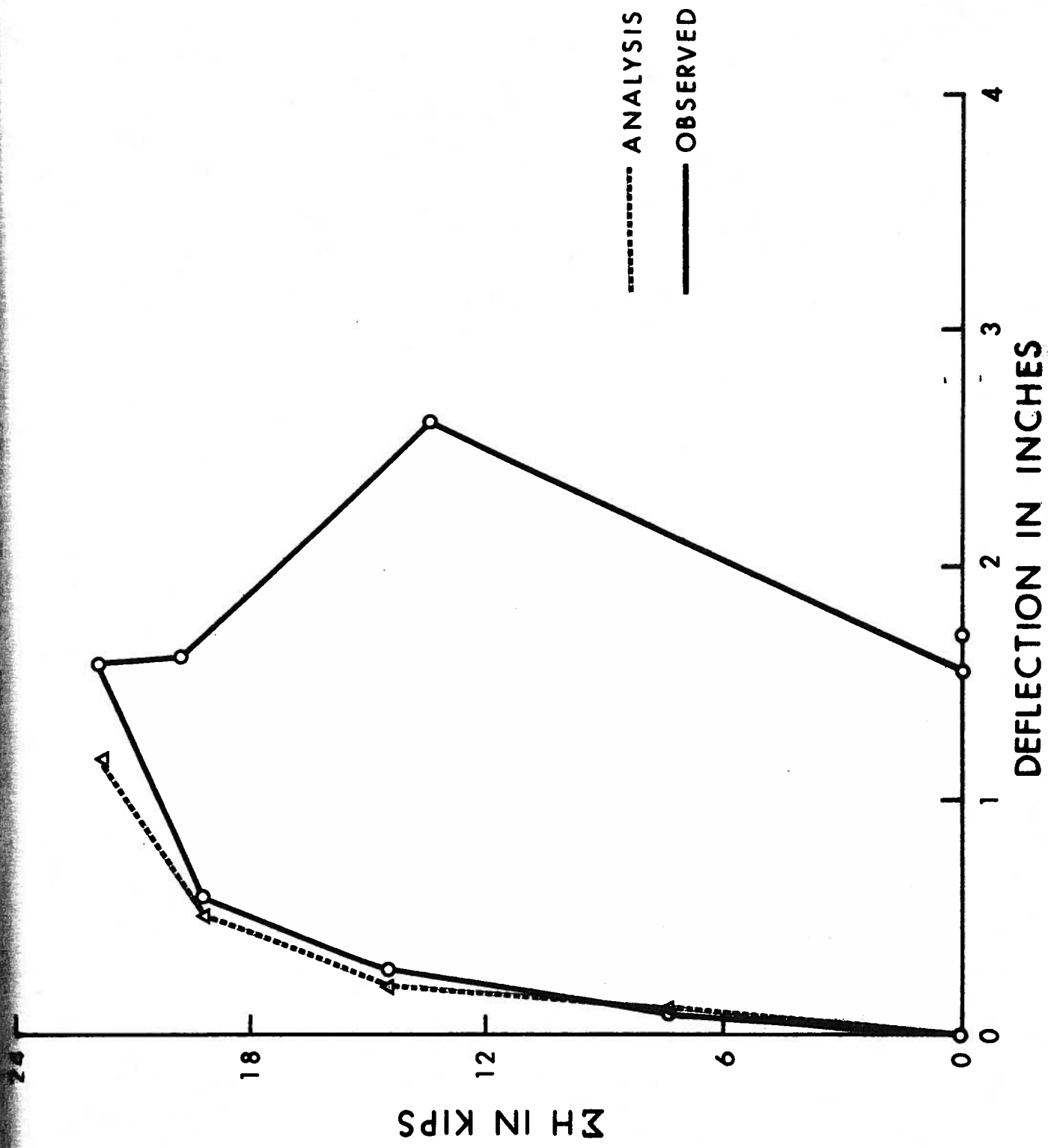
FIGURE 9.12 LOAD - DEFELECTION DIAGRAM FOR FLOOR 1

FIGURE 9.13 LOAD - DEFELECTION DIAGRAM FOR FLOOR 2
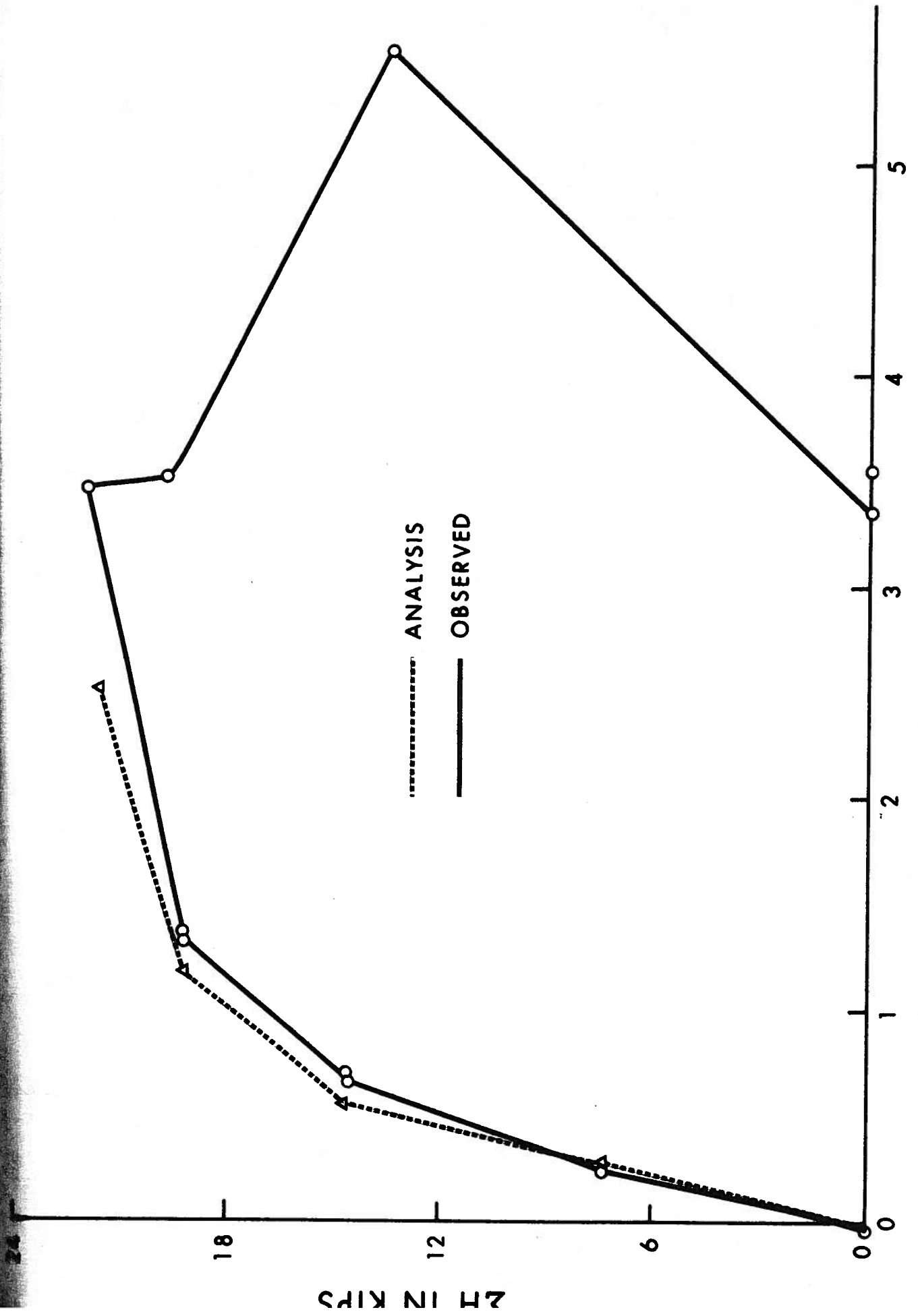
DEFLECTION IN INCHES

ANALYSIS

OBSERVED

ΣH IN KIPS
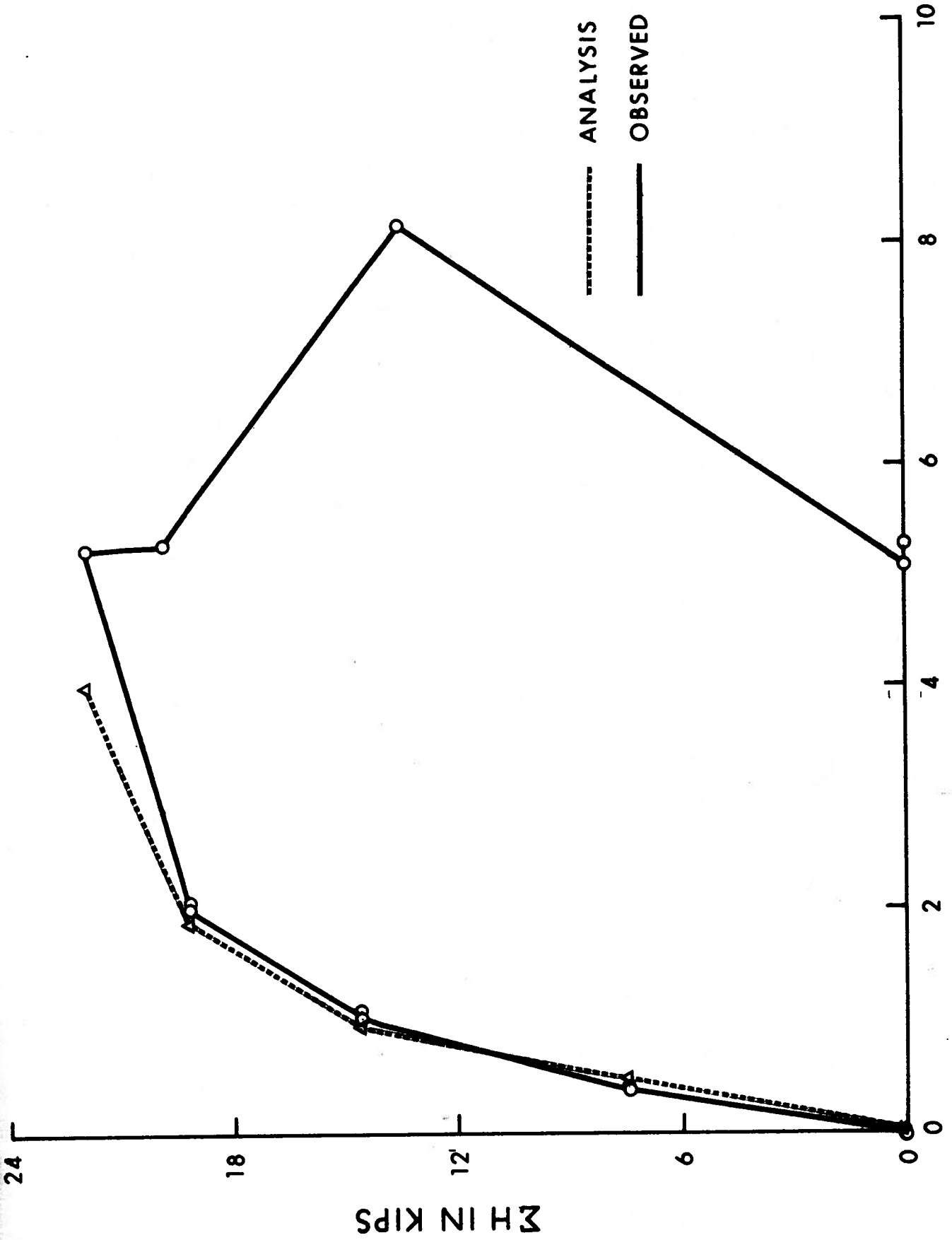
FIGURE 9.14 LOAD - DEFELECTION DIAGRAM FOR FLOOR   3
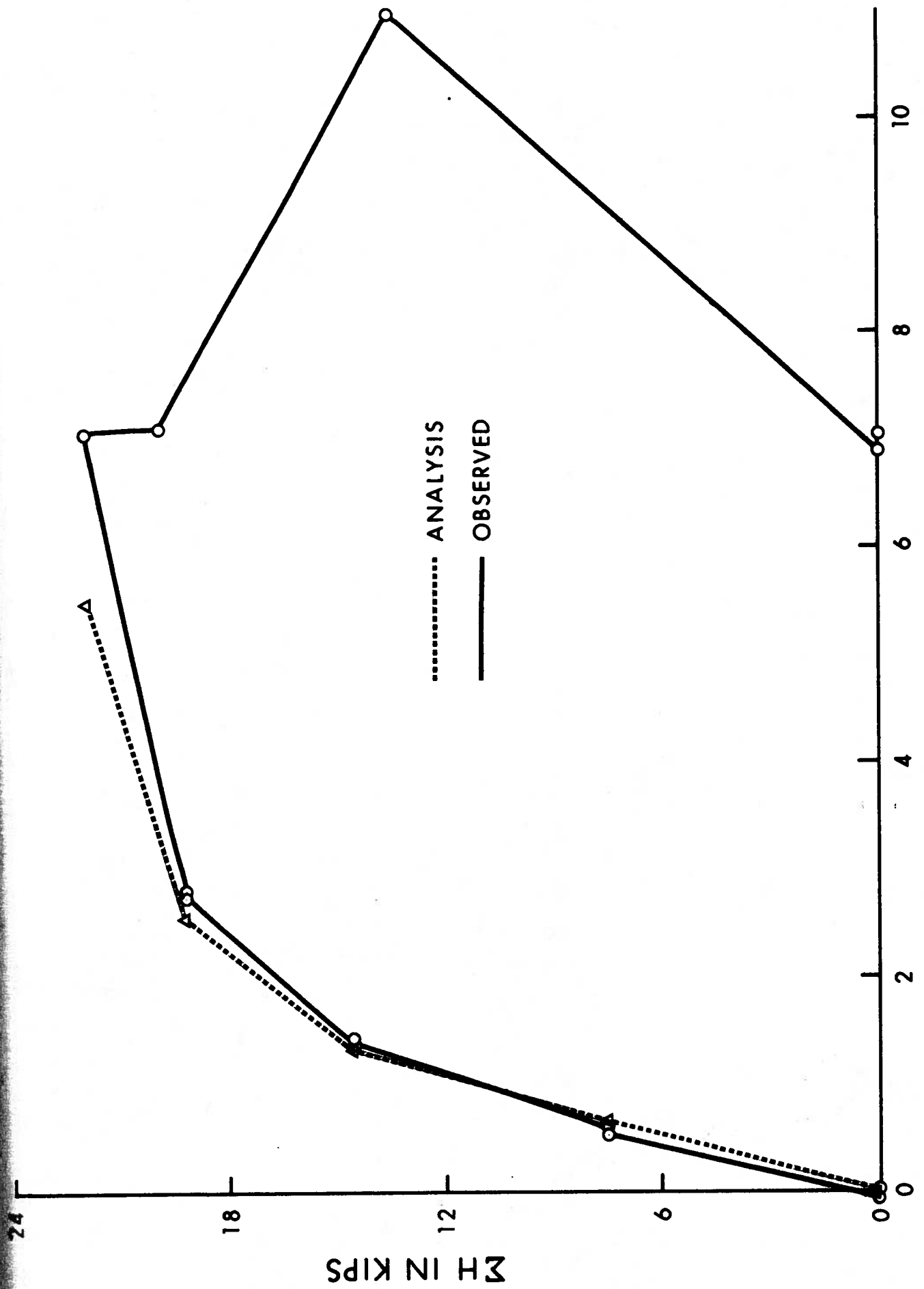
FIGURE 9.15 LOAD – DEFELECTION DIAGRAM FOR FLOOR 4

CHAPTER X

SUMMARY AND CONCLUSIONS

10.1 Summary

A method of analysis which traces the second order elastic-
inelastic behaviour of shear wall frame structures has been presented.
The analysis considers a simplified lumped model derived in CHAPTER VI.
The iteration procedure has been used for the analysis. Equilibrium
was formulated on the deformed structure to consider the effect of the
P-Δ moment. Constant concentrated vertical load on each story were
considered. The horizontal loads were assumed to be concentrated at
the floor levels and were applied in increments. The analysis allows
for the finite width of wall but neglects the axial and shear deform-
ations and flexibility of joints. A computer program in FORTRAN IV
language for IBM system OS/360 was developed to perform the computa-
tions and is presented in CHAPTER III. The assumptions in the analysis
are discussed in CHAPTERS IV, V and VI. A design example has been
presented in APPENDIX A.

Elastic-perfectly plastic and elastic-strain hardening
moment-curvature relationships were assumed for columns and beams,
and for walls respectively. A method was developed to find the load-
moment-curvature relationships for reinforced rectangular cross-sections.
A computer program was written for the purpose and was presented in
CHAPTER IV.

The lumping procedure for the structure has been derived in CHAPTER VI. The total uniformly distributed load on each story was replaced by a concentrated load. In order to take this into account, the plastic moment capacities of the beams were reduced by a reduction factor α. The analytical checks were also presented to see the validity of the approximate analysis.

A full scale test on 20 feet high, 4 story, one bay structure was described in CHAPTER VII. The test was carried under fixed vertical load and incremental lateral load. The machine processing of the test data was described in CHAPTER VIII. Reasonable correlation was obtained between the results of the test and analysis. The comparison was presented in CHAPTER IX.

10.2 Conclusions

The analytical checks in CHAPTER VI and the frame test suggest that the analysis gives a good indication of the behaviour of the shear wall frame structure. The model used is relatively simple to develop. The test and analysis have clearly shown the necessity of considering the interaction between the frame and the shear wall. The shear developed in the top of the frame was found to be much larger than the shear in the wall. The test does not show the development of negative shear in top of the wall for the model tested, but it did show that tendency. The analysis has shown the development of negative shear on the top of the wall in high rise structures, in CHAPTER VI, which suggests that in many structures the frame has a tendency to limit the deflection of the shear wall. Therefore it is

necessary to evaluate the interaction between the frame and the shear wall if true behaviour of the structure has to be established. Neglecting this factor could lead to excessive deformations and possible failure of the affected frame members.

The test indicated some differences in the observed and predicted moment and shear diagram. The beam moments were overestimated by the analysis during the prehinging stage of the loading and are in better agreement after the hinges have formed. The hinges in the test frame were observed to form away from the joint and were spread over a finite length. The analysis tended to overestimate the deflection of the test frame in the beginning and underestimated in the later stage of loading. However, the test has clearly indicated that the assumption of point hinges and rigid joints and ignoring the shear deformations has little effect on the analysis. The analysis slightly overestimated the overall stiffness of the structure.

The analysis does not consider the unloading branch of load-moment-curvature relationship of the cross-section. The load-moment-curvature diagram shows the unloading of the cross-section after reaching its ultimate capacity. The development of load-moment-curvature diagram indicated that maximum compressive strain corresponding to ultimate moment capacities varies and depends on the axial load, percentage and placing of reinforcement. The effect of the tensile stress in the concrete was found to be considerable especially in the case of under-reinforced concrete cross-sections. However, the effect was considerable when the tensile strain of the extreme fibre is close to the cracking strain. The stiffnesses and ultimate moment capacities

were found to be dependent on axial load on the cross-section. At
high axial load, the section did not have sufficient rotation
capacity to permit plastic hinging. However, the load-moment-
curvature relationship developed here was found to be satisfactory
in estimating the stiffnesses and ultimate moment capacities.

The load-deflection characteristics of the structure was
found to resemble well with the lumped model. The lumped model
gives accurate description of behaviour of the buildings when sub-
jected to lateral load only. For the buildings subjected to combined
load the lumped model gives the latter softening but earlier failure
of the structure. In such cases the predicted ultimate loads were
found to be underestimated but the degree of conservatism was not
in considerable error. The predicted ultimate load by the approxi-
mate analysis was in good agreement with the other analyses (C6,P2,
G2). Thus, the procedure developed for lumping the building is found
to be satisfactory.

In the development of the lumping procedure for walls it
has been found that the moments and shears in the individual shear
wall cannot be determined simply by the ratios of their respective
stiffnesses. The moment diagram in individual members of the building
should be found from the deflected shape of the structure.

10.3 Recommendations for Future Research

The method of analysis can be extended to consider the
axial and shear deformations. The analysis can also be extended
to consider the unloading branch of load-moment-curvature relationships

and insufficient rotation capacity of the section.

Much more extensive large scale laboratory testing of shear wall frame structures is required to study the behaviour more completely. Studies of multi-story and multi-bay structures will illustrate the effect of lumping procedure used in this analysis.

Test on cross-sections are required to accurately determine the behaviour of the sections. These should include tests on cross-sections with small percentage of reinforcement to determine accurately the influence of the uncracked concrete between tension cracks on the stiffness of the member. Test on cross-sections composed of high strength concrete and reinforcing steel are also required, since the multi-story construction may require high strength of the materials.

LIST OF REFERENCES

A1   ACI Committee 318, "Building Code Requirements for Reinforced Concrete (ACI 318-63)", June, 1963.

A2   ACI Committee 318, "Commentary on Building Code Requirements for Reinforced Concrete (ACI 318-63)", ACI, Publication SP-10, 1965.

A3   ACI Committee 340, "Ultimate Strength Design Handbook", Vol. 1, ACI, Publication No. 17, April, 1968.

A4   Avram, C., Anastasesen, D., Hirsu, O., and Manateaunu, I., "Recherches concernant le calcul et le comportement des structures de grende hauteur on cadres-refends, realisees on beton arme et seumises aux charges horitals".

A5   Anonymous, "Lateral Load Analysis of Multi-Story Frames with Shear Walls," Portland Cement Association, 1968.

B1   Bleich, F., "Buckling Strength of Metal Structures", McGraw-Hill Book Company Inc., New York, 1952.

B2   Broms, B., and Viest, I.M., "Ultimate Strength Analysis of Long Hinged Reinforced Concrete Columns", Journal of Structural Division, Proc. ASCE, January, 1956.

B3   Benjamin, J.R., and Williams, H.A., "The Behaviour of one-story Reinforced Concrete Shear Walls", Proc. ASCE, Vol. 83, No. ST5, 1957.

B4   Benjamin, J.R., and Williams, H.A., "Behaviour of one-story Wall Containing Openings", Journal ACI, Vol. 30, 1958.

B5   Benjamin, J.R., and Williams, H.A., "The Behaviour of one-story Brick Shear Walls", Proc. ASCE, Vol.84, No. ST4, 1958.

B6   Benjamin, J.R., and Williams, H.A., "Reinforced Concrete Shear Wall Assemblies", Proc. ASCE, Vol. 86, No. ST8, 1960.

B7   Beckwith, T.G. and Buck, N.L., "Mechanical Measurements", Addison-Wesley, Massachusetts, 1961.

B8   Blume, J.A., Newmark, N.M. and Cornig, L.H., "Design of Multi-Story Reinforced Concrete Buildings for Earthquake Motions", PCA, 1961.

B9   Beck, H., "Contribution to the Analysis of Coupled Shear Walls",
          ACI Journal, Vol. 59, August, 1962.

B10   Bandel, H., "Frames Combined with Shear Trusses under Lateral
          Loads", Journal of Structural Division, ASCE, Vol. 88,
          No. ST6, 1962.

B11   Breen, J.E., "The Restrained Long Concrete Column as a part of
          a Rectangular Frame", Ph.D. Thesis, University of Texas,
          June, 1962.

B12   Barnard, P.R., "Researches into the Complete Stress-Strain Curve
          for Concrete", Magazine of Concrete Research, Cement and
          Concrete Association, Vol. 16, No. 49, December, 1964.

B13   Beedle, L.S., "Plastic Design of Steel Frames", John Wiley & Sons,
          November, 1966.

B14   Barnard, P.R., and Schwaighofer, J., "Interaction of Shear Walls
          Connected Solely Through Slabs", Tall Buildings, Pergamon
          Press, London, 1967.

B15   Benjamin, J.R., "Statically Indeterminate Structures", McGraw-Hill,
          New York, 1959.

C1   Cardan, B., "Concrete Shear Walls Combined with Rigid Frames in
          Multi-Story Buildings Subjected to Lateral Loads", ACI
          Journal, Vol. 58, September, 1961

C2   Chang, W.F., "Long Restrained Reinforced Concrete Columns", Ph.D.
          Thesis, University of Texas, 1961.

C3   Clough, R.W., King, I.P. and Wilson, E.L., "Structural Analysis
          of Multi-Story Buildings", Journal of the Structural Division,
          ASCE, Vol. 90, No. ST3, 1964.

C4   Coull, A. and Choudhary, J.R., "Stresses and Deflections in Coupled
          Shear Walls", ACI Journal, February, 1967.

C5   Clark, W.J., MacGregor, J.G. and Adams, P.F., "Inelastic Behaviour
          of Reinforced Concrete Shear Wall Frame", Eighth Congress,
          International Association for Bridge and Structural Engin-
          eering, September, 1968.

C6   Clark, W.J., "Analysis of Reinforced Concrete Shear Wall Frame
          Structures", Ph.D. Thesis, University of Alberta, Edmonton,
          November, 1968.

C7   C.E.B., "Recommendations for an International Code of Practice
          for Reinforced Concrete", ACI and Cement and Concrete Associa-
          tion, 1963.

D1   Desayi, P. and Krishnan, S., "Equations for the Stress-Strain Curve

of Concrete", ACI Proc., Vol. 61, No. 3, March, 1964.

D2   Davies, J.M., "The Stability of Plane Frame Works under Static
        and Repeated Loading", Ph.D. Thesis, Victoria University
        of Manchester, 1965.

D3   Daniels, J.H., and Lu, L.W., "The Subassemblage Method of
        Designing Unbraced Multi-Story Frames", Fritz Engineering
        Laboratory, Report No. 273.37, February, 1966.

E1   Ernst, G.C., Hromadik, J.J. and Riveland, A.R., "Inelastic
        Buckling of Plain and Reinforced Concrete Columns,
        Plates and Shells", Eng. Experiment Station, Bulletin,
        No. 3, University of Nebraska, August, 1953.

F1   Frischmann, W.W., Prahhu, S.S. and Toppler, J.F., "Multi-Story
        Frames and Interconnected Shear Walls Subjected to
        Lateral Loads - I", Concrete and Constructional Engineering,
        June, 1963.

F2   Fowler, T.J., "Reinforced Concrete Columns Governed by Concrete
        Compression", Ph.D. Thesis, University of Texas, January,
        1966.

F3   Ferguson, F.M., "Reinforced Concrete Fundamentals", John Wiley
        & Sons, Inc., New York, March 1966.

G1   Gould, P.L., "Interaction of Shear Wall Frame System in Multi-
        Story Buildings", ACI Journal, Vol. 62, January, 1965.

G2   Goldberg, J.E., "Analysis of Multi-Story Buildings Considering
        Shear Walls and Floor Deformations", Tall Buildings,
        Pergamon Press, London, 1967.

H1   Hogenstad, E., "A Study of Combined Bending and Axial Load in
        Reinforced Concrete Members", Bulletin, No.399, University
        of Illinois, Engineering Experiment Station, November,
        1951.

H2   Heyman, J., "An Approach to the Design of Tall Steel Buildings",
        Proc. ICE, Vol. 17, December, 1960.

H3   Horne, M.R., "Elastic-Plastic Failure Loads of Plane Frames",
        Proc. of Royal Society of Architects, Vol. 274, 1963.

H4   Hanson, N.W. and Conner, H.W., "Seismic Resistance of Reinforced
        Concrete Beam-Column Joints", Proc. ASCE, Vol. 93, No. ST5,
        1967.

J1   Jennings, A., and Majid, K., "An Elastic-Plastic Analysis by
        Computer for Framed Structures Loaded up to Collapse",
        The Structural Engineer, Vol. 43, No. 12, 1965.

J2   Jenkins, W.M. and Harrison, T., "Analysis of Tall Buildings with Shear Walls under Bending and Torsion", Tall Buildings, Pergamon Press, London, 1967.

K1   Kloucek, C.V., "Distribution of Deformation", Translated from Czechoslovakian and German Editions by Waddell-Zalund, A.H., and Zalud, F.H., Orlius Ltd., Czechoslovakia, 1950.

K2   Khan, F.R., and Sbarounis, J.A.,"Interaction of Shear Walls and Frames", Journal of Structural Division, ASCE, Vol. 90, No. ST3, 1964.

K3   Kabaila, A., Saenz, L.P., Tulin, L.G., Grestle, K.H., Desayi, P. and Krishnan, S., Discussion of the paper "Equation for the Stress Strain Curve of Concrete", ACI Proc. Vol. 61, No. 9, September, 1964.

K4   Khan, F.R., "On Some Special problems of Analysis and Design of Shear Wall Structures", Tall Buildings, Pergamon Press, London, 1967.

K5   Korn, A., "The Elastic-Plastic Behaviour of Multi-Story, Unbraced, Planar Frames", Research Report No. 2, School of Engineering and Applied Science, Washington University, St. Louis, 1967.

L1   Lightfoot, E., "Substitute Frames in the Analysis of Rigid Jointed Structure - Part 1 and Part II", Civil Engineering and Public Works Review, December 1957 and January 1958.

L2   Lu, L.W., "Plastic Design of Multi-Story Frames", Fritz Engineering Laboratory, Report No. 273.20, Lehigh University, 1965.

M1   Merchant, W., "The Failure Load of Rigidly Jointed Frameworks as Influenced by Stability", The Structural Engineer, Vol. 32, 1954.

M2   Manuel, R.F., and MacGregor, J.G.,"The Behaviour of Restrained Reinforced Concrete Columns under Sustained Load", Report No. 2, Department of Civil Engineering, University of Alberta, Edmonton, January, 1966.

M3   McCracken, D.D., "A Guide to Fortran IV Language Programming", John Wiley & Sons, Inc., New York, June, 1966.

M4   MacGregor, J.G., and Barter, S.L., "Long Eccentrically Loaded Concrete Columns Bent in Double Curvature", Symposium on Reinforced Concrete Columns, Publication SP-13, ACI, 1966.

M5   MacGregor, J.G., "Stress-Strain Curves for Concrete", Unpublished, August, 1966.

M6   Mauch, "Effect of Creep and Shrinkage on the Capacity of Concrete Columns", Symposium on Reinforced Concrete Columns, ACI, Publication SP-13, 1966.

M7   Majid, K.I., "An Evaluation of the Elastic Critical Load and Rankine Load of Frames", Proc. ICE, Vol 36, 1967.

M8   Majumdar, S.N.G., Nikhed, R.P., MacGregor, J.G., and Adams, P.F., "Approximate Analysis of Frame-Shear Wall Structures" Structural Engineering Report No. 14, Department of Civil Engineering, University of Alberta, Edmonton, May 1968.

M9   MacGregor, J.G., Breen, J.E. and Pfrang, E.O., "Proposal for a Revision to Section 915 and 916 of ACI 318-63", ACI Committee 441.

M10   Michael, D., "The Effect of Local Wall Deformations on the Elastic Interaction of Cross Walls Coupled by Beams", Tall Buildings, Pergamon Press, 1967.

N1   Neville, A.M., "Properties of Concrete", Sir Isaac Pitman & Sons, Ltd., 1963.

O1   Okamura, H., Liu, H.W., Chu, C.S. and Liebowitz, H., "Cracked Column under Compression", Engineering Fracture Mechanics, Vol. 1, No. 3, April, 1969.

P1   Pfrang, E.O., "A Study of the Relationships between Load Moment and Curvature for Reinforced Concrete Cross-sections", Technical Report No. 2, Department of Civil Engineering, University of Delaware, Newark, Delaware, June 1963.

P2   Parikh, B.P., "Elastic-Plastic Analysis and Design of Unbraced Multistory Steel Frames", Fritz Engineering Report No. 273.44, Lehigh University, May 1966.

P3   Parme, A.L., "Design of Combined Frames and Shear Walls", Tall Buildings, Pergamon Press, London 1967.

R1   Richart, E.F., "Reinforced Concrete Column Investigation", Tentative Final Report of Committee 105, Journal ACI, Vol. 29, February, 1933.

R2   Rosenblueth, E., and Holtz, I., "Elastic Analysis of Shear Walls In Tall Buildings", ACI Journal, Vol. 31, June 1960.

R3   Rosman, R., "Approximate Analysis of Shear Walls Subjected to Lateral Loads", ACI Journal, Vol. 61, June 1964.

R4   Rosman, R., "Laterally Loaded Systems Consisting of Walls and Frames", Tall Buildings, Pergamon Press, London 1967.

S1   Selby, S.M., and Girling, B., "Standard Mathematical Tables", 14th Edition, The Chemical Rubber Co., July, 1965.

S2   Soane, A.J.M., "The Analysis of Interconnected Shear Walls by Analogue Computation", Tall Buildings, Pergamon Press, London, 1967.

T1   Tezcan, S.S., "Analysis and Design of Shear Wall Structures", Tall Buildings, Pergamon Press, London 1967.

T2   Traum, E.E., "Multi-Story Pierced Shear Walls of Variable Cross-Section", Tall Buildings, Pergamon Press, London, 1967.

W1   Whitney, C.S., Anderson, B.G., and Cohen, E., "Design of Blast Resistance Construction for Atomic Explosion", Journal ACI, Vol. 51, 1953.

W2   Wood, R.H., "The Stability of Tall Buildings", Proc. ICE, Vol. II, 1958.

W3   Welch, G.B., "Tensile Strains in Unreinforced Concrete Beams", Magazine of Concrete Research, Vol. 18, No. 54, March 1966.

W4   Wang, C.K., "Matrix Methods of Structural Analysis", International Text Book Co., Pennsylvania, 1966.

W5   Webster, J.A., "The Static and Dynamic Analysis of Orthogonal Structures Composed of Shear Walls and Frames", Tall Buildings, Pergamon Press, London 1967.

W6   Wynhoven, J.H., and Adams, P.F., "Elastic Torsional Analysis of Multi-Story Structures", Structural Engineering, Report No. 15, Department of Civil Engineering, University of Alberta, Edmonton, Canada.

W7   Winokur, A., and Gluck, J., "Lateral Loads in Asymmetric Multi-Story Structures", Journal of the Structural Division, ASCE, ST3, Vol. 94, March, 1968.

Y1   Yarmina, E., Yura, J.A., and Lu, L.W., "Techniques for Testing Structures permitted to Sway", Fritz Engineering Report, No. 273, 40, Lehigh University, May 1966.

1.   "Handbook of Steel Construction", First Edition, October, 1967, Canadian Institute of Steel Construction, Ontario, Canada.

2.   "IBM System/360, Fortran IV Language", Sixth Edition, IBM Corp., 1966.

ACKNOWLEDGEMENTS

APPENDIX A

EXAMPLE OF A REINFORCED CONCRETE

BUILDING DESIGN

A.1 Introduction

A preliminary design of 20 story building 160' x 62' in plan, shown in FIGURE 6.28, has been presented here. The objective was to design the building for vertical load and investigate the behaviour of the structure, under combined lateral and vertical load, using the approximate analysis program developed in CHAPTER III. The axial loads were computed from the normal assumptions of tributary areas. The checker board loadings were used for the consideration of live load in the design. The members were proportioned by ultimate strength design procedure[A1].

A.2 Design for Vertical Loads

The building consisted of seven frames and two shear walls in the direction of wind as shown in FIGURE 6.28. Each frame had four column lines interconnected with beams at each floor level. There was no cross girders. The thickness of the slab was assumed to be 4 inches. The assumed vertical loadings were 100 psf live load on the floors and 50 psf live load on the roof. For simplicity it was assumed that slab and beams are not monolithic in construction so that the beams could be designed as a simple rectangular beam rather than as a T-beam.

The chosen strength of concrete and steel were 4 and 60 ksi respectively.

The beam moments were computed using coefficients given in section 904 of ACI Building Code (1963). The gravity load on the beams

were taken as $(1.5D1 + 1.8LL)^{(A1)}$. Clear span length of 19 feet were

used for the computation of moments in negative and positive moment

region. However, to maintain the uniformity and simplicity all the beams

were proportioned, for the maximum moment of $wl'^2/10\phi$, by ultimate

strength design procedure. ϕ is the capacity reduction factor defined

in section 1504 of ACI Building Code (1963) and was taken as 0.9.

While proportioning the beams, equal amount of reinforcement were

assumed in the tension and compression face and the width of beam

was taken approximately half the depth. The percentage of reinforce-

ment in the beams were selected to satisfy[A1]:

$$q = \frac{p_t f_y}{f'_c} = 0.18 \qquad \qquad ....(A.1)$$

where p_t = percent of reinforcement based on gross area

f_y = yield strength of reinforcement

and f'_c = concrete strength

The section of the beams designed are presented in TABLE A.1. The

moment of inertias and plastic moment capacities are also presented

in TABLE A.1. The moment of inertias were computed using equation

(4.4) suggested in CHAPTER IV.

The analysis of column loads were based on the assumed tri-

butary areas. The moments were computed for the full dead load and

the live load placed as a checker board. The columns were designed

for the axial loads and moments as per requirement of section 914 of

ACI Building Code (1963). The columns were chosen as square tied

column and had approximately four percent reinforcement. The
capacity reduction factor,ϕ, defined in section 1504 of ACI
Building Code (1963), was taken as 0.7. Also the strength reduction
factor for the length of compression members, defined in section
916 of ACI Building Code (1963) was used. All the columns were
proportioned by the ultimate strength design procedure[A1].
The sections, thus obtained, are presented in TABLE A.1. The
moment of inertias of the column sections were computed by equation
(4.4) suggested in CHAPTER IV. TABLE A.2 gives the axial loads on
each column.

The walls at the two ends of the building were taken as
6" thick and 62' wide. These were found to be quite adequate for
the axial loads and moments on the wall giving much extra capacity
than required. A nominal reinforcement of one percent were used.

A.3 Design for Combined Loads

The building designed for vertical loads in section A.2
consisted of seven similar frames and two walls in the windward
direction. This building was reanalyzed to test its performance
under the combined vertical and lateral loads. Lateral loads were
assumed to be the wind load of 25 psf and were assumed to be con-
centrated at the floor levels. For the purpose of combined loads
analysis the vertical loads were taken as 1.25(D1 + LL)[A1].

The building was lumped by the procedure developed in
CHAPTER VI. The two walls were lumped together to give the wall
system in lumped model, shown in FIGURE 3.1. Since the wall will

have a lot of openings for windows etc., an equivalent depth of only 45' was considered for the purpose of computing the stiffnesses and moment capacities. The effect of reinforcement were neglected. However, for computing vertical loads, solid wall of 6" x 62' were considered.

The frame system in the lumped model shown in FIGURE 3.1 was obtained by lumping all the seven frames. All the columns and beams were lumped by the procedure developed in CHAPTER VI. The values of the factor α, defined in CHAPTER VI for the case of uniformly distributed load on beams, were taken as 0.66 for roof level beams and 0.61 for all other beams. These factors were computed from FIGURE 6.10.

The frame system and the wall system were connected by the hinged link beams at all floor levels. Thus the building could be represented by the lumped model for the purpose of approximate analysis developed in CHAPTER III. The moment of inertias of the various members of the lumped models are given in TABLE A.3 and the corresponding moment capacities are given in TABLE A.4. The vertical loads acting on each story and the horizontal loads acting at each floor level of the lumped model are also given in TABLE A.3.

The lumped frame thus obtained was analysed by the program developed in CHAPTER III under fixed vertical load of 1.25 (Dl + LL) and incremental horizontal loads. The load-deflection curve, obtained for the top of the building, is presented in FIGURE A.1. A load factor of 1.35 was found for this building. Under the action of combined

loads the ACI Building Code (1963) requires a load factor of 1.25.
The story deflection at working load factor 1.0 and at a load
factor of 1.25 are plotted in FIGURE A.2. The hinges formed at the
ultimate load are shown in FIGURE A.3.

A.4 Discussion and Conclusions

The vertical load design generally indicated that the
section can be chosen in various ways to satisfy the stiffness
and moment capacity requirement. The chosen relationship between the
various parameters of the section seems to serve the purpose when
the building was subjected to combined vertical and lateral load.
Under 1.25 (D1 + LL) + 1.0WL the maximum story to story deflection was
0.25 inches or 1/576 of the story height. This is near the upper
limit of acceptable values. Under the service load condition of
1.0 (D1 + LL + W1) the deflections would be smaller and it may be
desirable to check these in an actual design. However, the building
as designed has sufficient stiffness under the action of combined
loads and any alteration in sizes are not necessary from the stiffness
point of view. The economical aspects have not been investigated.

The behaviour portrayed under the action of combined loads
are typical of a shear wall structure with the upper floors of the
frame restraining the shear wall from additional deflection and the
lower floors of the frame being restrained from additional deflection
by the shear wall.

All hinges formed only in the beams thus giving a strong
column and weak beam design. The first hinge in the structure was

indicated at a load factor of 1.05. The first wall hinge at the base was indicated at a load factor of 1.30. Due to the importance of the wall to the overall stability and strength of the building the load factor at first hinging of the wall should exceed the desired load factor for the structure.

As a result of the above design it can be said that the structural system employed for this building does not require extra stiffness in the frame or shear walls, to aid in the resistance of lateral loads, over and above that required by the gravity loads.

TABLE A.1

SUMMARY OF THE BEAMS AND COLUMNS SECTION

FOR A TYPICAL FRAME

Beam Sections				
	Size Inch	Area of Reinf. Sq. In.	Moment of Inertia, in^4	Plastic Moment Capacity, K-in.
Roof level	12x24	3.60	7970	2070
All other floors	14x27	4.40	12790	2770

Column Section								
	Interior Column				Exterior Column			
Story	Size In.	Area of Reinf. in^2	Moment of Inertia in^4	Plastic Moment Capacity K-in.	Size In.	Area of Reinf. in^2	Moment of Inertia in^4	Plastic Moment Capacity K-in.
1	36x36	52.00	106800	63600	27x27	29.24	40900	26400
2	36x36	52.00	106800	62500	27x27	29.24	40900	26000
3	32x32	40.50	80000	45000	24x24	22.50	25100	18800
4	32x32	40.50	80000	44500	24x24	22.50	25100	18650
5	30x30	36.00	62200	36700	22½x22½	20.00	19550	15400
6	30x30	36.00	62200	36700	22½x22½	20.00	19550	15380
7	28½x28½	32.50	50800	31700	21x21	17.90	15060	12600
8	28½x28½	32.50	50800	31500	21x21	17.90	15060	12500
9	26x26	27.00	35100	24100	19½x19½	15.24	11120	10350
10	26x26	27.00	35100	23900	19½x19½	15.24	11120	10250
11	24x24	22.50	25200	18800	18x18	12.70	7810	7860
12	24x24	22.50	25200	18800	18x18	12.70	7810	7820
13	22x22	19.36	18020	14600	16x16	10.24	5030	5570
14	22x22	19.36	18020	14300	16x16	10.24	5030	5500
15	19x19	14.40	9990	5570	14x14	8.00	3020	3700
16	19x19	14.40	9990	5470	14x14	8.00	3020	3620
17	16x16	10.24	5030	5520	12x12	5.76	1595	2280
18	16x16	10.24	5030	5300	12x12	5.76	1595	2180
19	12x12	5.76	1595	2260	12x12	5.76	1595	2020
20	12x12	5.76	1595	1950	12x12	5.76	1595	1800

TABLE A.2

VERTICAL LOAD ON COLUMNS OF A TYPICAL FRAME

Story	Interior Column		Exterior Column	
	Dead Load in kips	Live Load in kips	Dead Load in kips	Live Load in kips
1	579.84	805.94	291.71	403.06
2	544.38	764.61	273.50	382.39
3	510.36	723.28	256.07	361.72
4	482.70	681.95	242.24	341.05
5	453.30	640.62	227.42	320.38
6	425.64	599.29	213.61	299.71
7	395.13	557.96	197.98	279.04
8	367.47	516.63	184.19	258.37
9	338.17	475.30	169.59	237.70
10	310.51	433.97	155.76	217.03
11	281.65	392.64	141.26	196.36
12	253.99	351.31	127.43	175.69
13	225.22	309.98	112.79	155.02
14	197.56	268.65	98.96	134.35
15	168.43	227.32	84.40	113.68
16	140.77	185.99	70.57	93.01
17	111.86	144.66	56.12	72.34
18	84.20	103.33	42.29	51.67
19	55.23	62.00	28.46	31.00
20	27.53	20.67	14.63	10.33

TABLE A.3

LOADS AND MOMENT OF INERTIA OF VARIOUS MEMBERS
OF LUMPED MODEL

Story	Horizontal Load in Kips	Vertical Load in Kips	Moment of Inertia of Lumped Beam in^4	Moment of Inertia of Lumped Column in^4	Moment of Inertia of Hinged Link Beam in^4	Moment of Inertia of Lumped Wall in^4
1	76.00	43676.00	537180	2067800	0	63×10^6
2	60.00	41288.00	537180	2067800	0	63×10^6
3	56.00	38955.00	537180	1471400	0	63×10^6
4	56.00	36781.00	537180	1471400	0	63×10^6
5	56.00	34564.00	537180	1144500	0	63×10^6
6	52.00	32388.00	537180	1144500	0	63×10^6
7	48.00	30113.00	537180	922040	0	63×10^6
8	48.00	27940.00	537180	922040	0	63×10^6
9	48.00	25733.00	537180	647080	0	63×10^6
10	48.00	23558.00	537180	647080	0	63×10^6
11	48.00	21341.00	537180	462140	0	63×10^6
12	48.00	19167.00	537180	462140	0	63×10^6
13	48.00	16959.00	537180	322700	0	63×10^6
14	48.00	14785.00	537180	322700	0	63×10^6
15	48.00	12572.00	537180	182140	0	63×10^6
16	48.00	10397.00	537180	182140	0	63×10^6
17	48.00	8190.00	537180	92750	0	63×10^6
18	48.00	6016.00	537180	92750	0	63×10^6
19	48.00	3819.00	537180	44660	0	63×10^6
20	24.00	1643.00	334740	44660	0	63×10^6

TABLE A.4

MOMENT CAPACITIES OF VARIOUS MEMBER
OF LUMPED MODEL

Story	Moment Capacity of Lumped Beam K-in.	Moment Capacity of Lumped Column K-in.	Moment Capacity of Lumped Wall K-in.
1	70980	1260000	1×10^6
2	70980	1229000	1×10^6
3	70980	893200	1×10^6
4	70980	886200	1×10^6
5	70980	729400	1×10^6
6	70980	729120	1×10^6
7	70980	620200	1×10^6
8	70980	616000	1×10^6
9	70980	482300	1×10^6
10	70980	478100	1×10^6
11	70980	373240	1×10^6
12	70980	372680	1×10^6
13	70980	282380	1×10^6
14	70980	277200	1×10^6
15	70980	129780	1×10^6
16	70980	127120	1×10^6
17	70980	109200	1×10^6
18	70980	104720	1×10^6
19	70980	59920	1×10^6
20	57330	52500	1×10^6
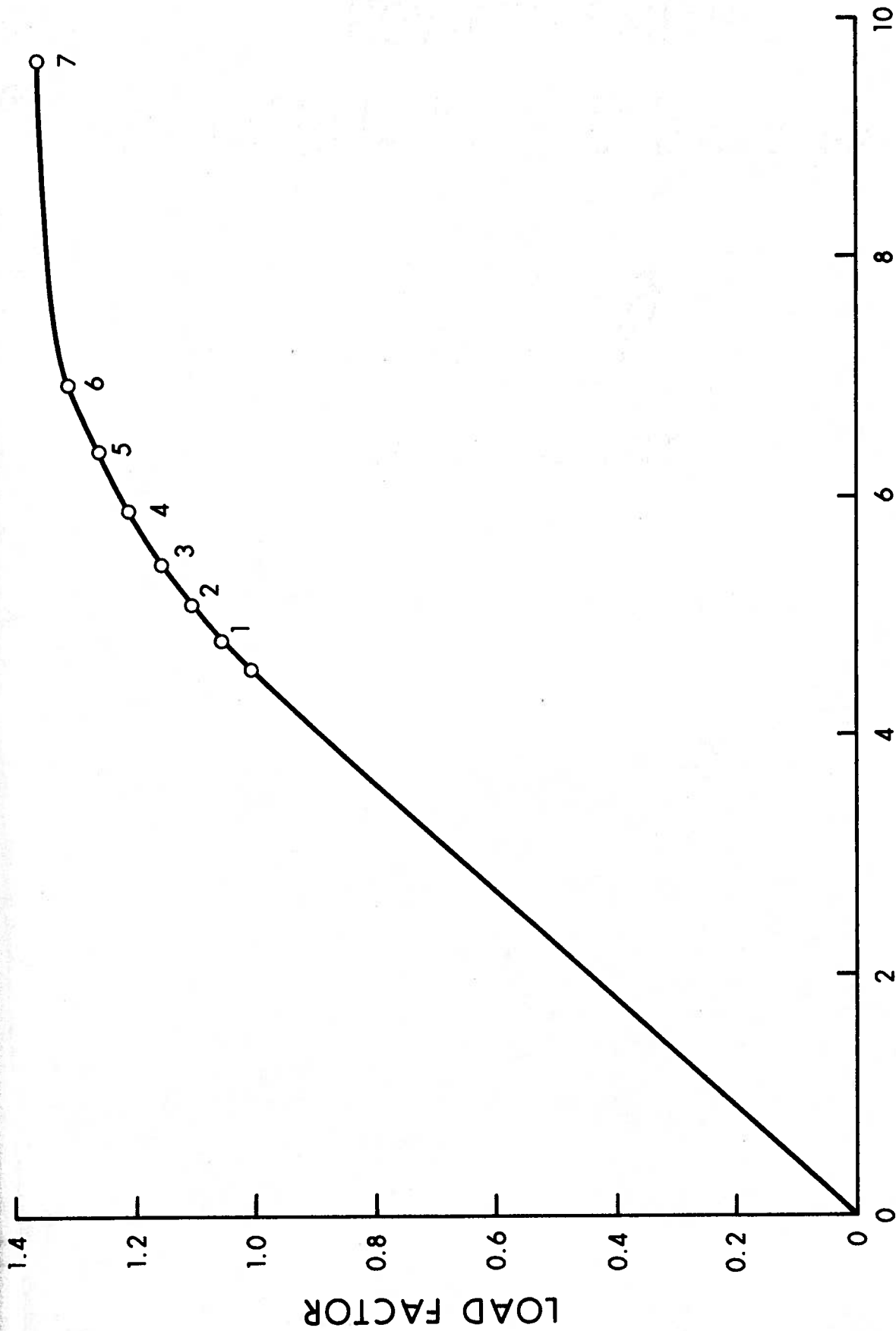
FIGURE A.1 LOAD - DEFELECTION DIAGRAM FOR THE TOP OF THE BUILDING
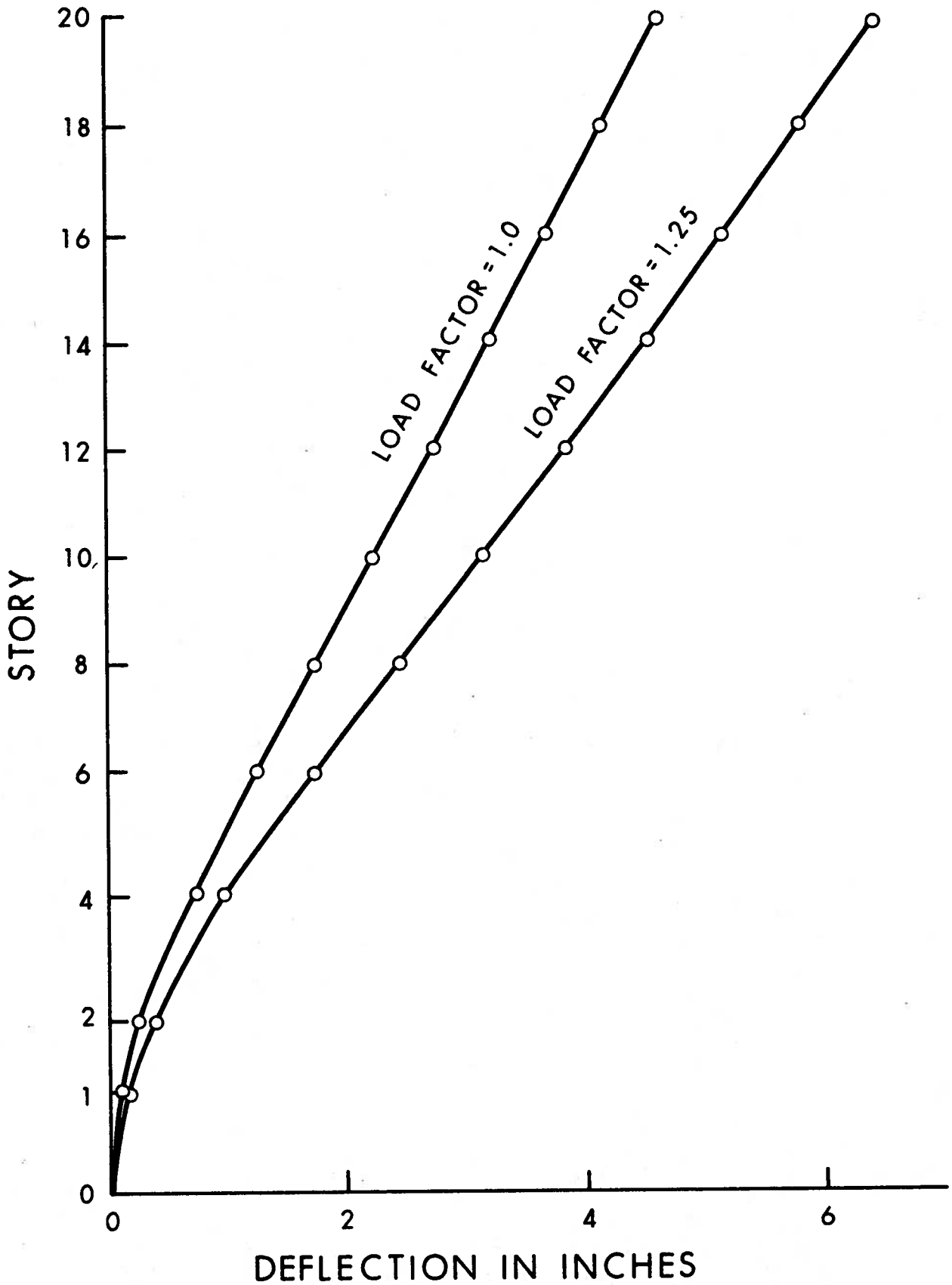
FIGURE A.2 STORY- DEFELECTION DIAGRAM
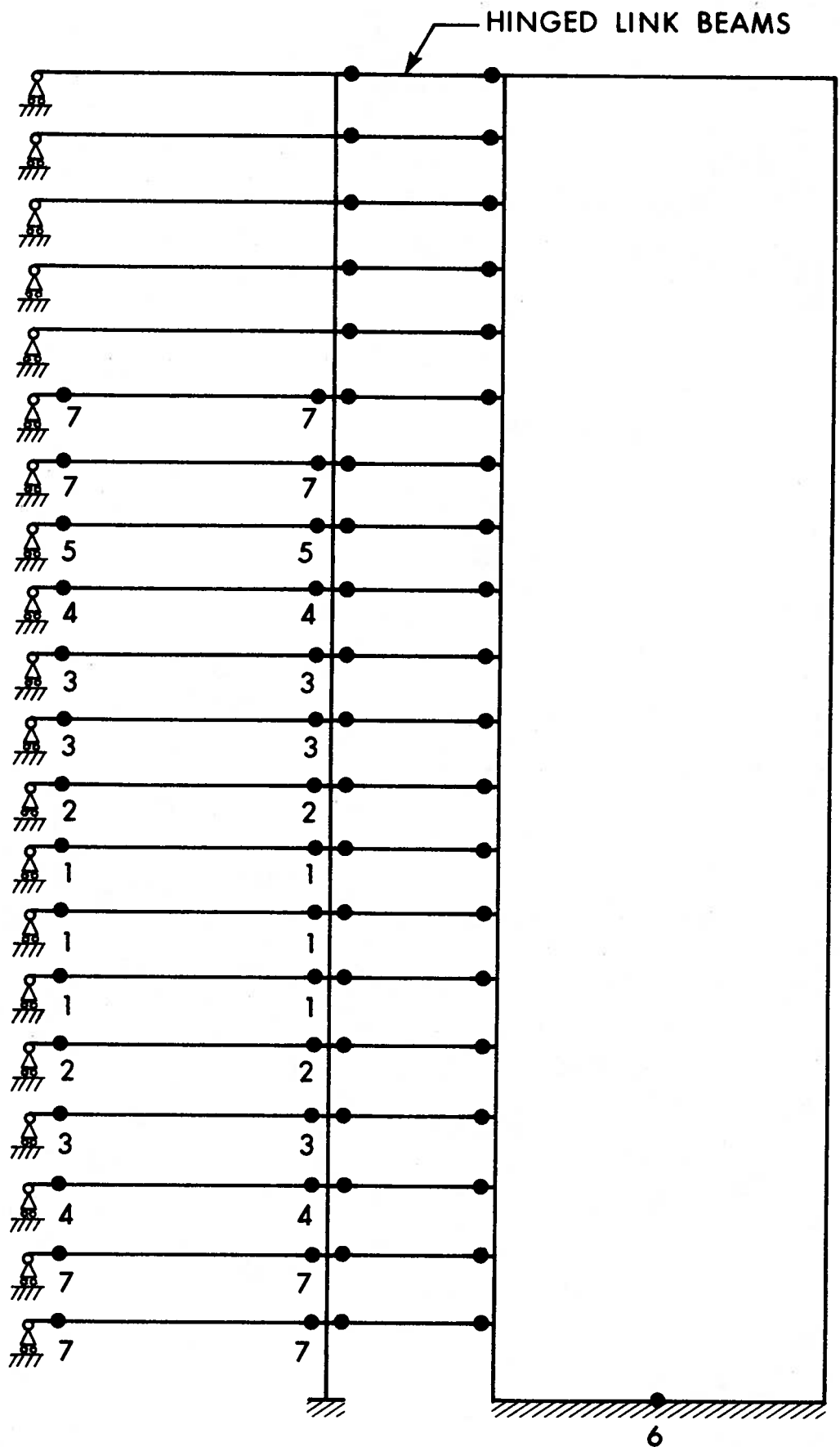
FIGURE A.3 HINGE PATTERN IN THE ANALYTICAL MODEL AT ULTIMATE LOAD

APPENDIX B

DEVELOPMENT OF THE APPROXIMATE

ANALYSIS

B.1 Derviation of Joint Rotation Equation

The frame system has been forced into the deformed shape of the wall shown in FIGURE 3.6. Applying the slope-deflection equations, the moment M_{BWi}, at the end B_i of the right beam is given by:

$$M_{BWi} = S_{BWi}(4\theta_i + 2\theta_{WBi} - 6 R'_i)$$

where $S_{BWi} = EI/L$ is the stiffness of the right beam $(B_i W_i)$ and R'_i is the vertical chord rotation of the right beam connecting the column to the wall. Also in the above equation θ_i is the rotation of the frame joint and θ_{WBi} is the rotation at the wall end of the right beam.

Considering the left beam $B_i F_i$ and applying the slope deflection equation, assuming that the joint rotation at the two ends B_i and F_i are equal, the moment, M_{BFi}, at the end F_i is given by:

$$M_{BFi} = 6 \cdot S_{BFi} \cdot \theta_i$$

where $S_{BFi} = EI/L$ is the stiffness of the left hand beam, $B_i F_i$.

The column $B_i B_{i+1}$ between the ith and the i+1 th story has a stiffness of $S_{c(i+1)}$ and the chord rotation of this column is R_{i+1}. The moment, $M_{c(i+1)}$, at the bottom end B_i of the column $B_i B_{i+1}$ is given by:

$$M_{c(i+1)} = S_{c(i+1)} \; (4\theta_i + 2\theta_{i+1} - 6 R_{i+1})$$

where θ_{i+1} is the rotation of the frame joint at the (i+1) th level.

The moment, M_{ci}, at the top end, B_i, of the column $B_i \; B_{i-1}$ is given by:

$$M_{ci} = S_{ci} \; (4\theta_i + 2\theta_{i-1} - 6R_i)$$

where S_{ci} = EI/L is the stiffness of the column $B_i \; B_{i-1}$ and R_i is the chord rotation of the column. θ_{i-1} is the rotation of the frame joint at the (i-1) th level.

Equating the sum of the joint moments to zero

$$M_{BWi} + M_{BFi} + M_{ci} + M_{c(i+1)} = 0$$

Substituting the values of the end moments from the above equations the joint equilibrium equation becomes:

$$S_{BWi} \; (4\theta_i + 2\theta_{WBi} - 6 R'_i) + 6 S_{BFi} \; \theta_i +$$

$$S_{ci} \; (4\theta_i + 2\theta_{i-1} - 6 R_i) + S_{c(i+1)}$$

$$(4\theta_i + 2\theta_{i+1} - 6 R_{i+1}) = 0$$

after simplification:

$$\theta_i = \{S_{BWi} (6 R'_i - 2\theta_{WBi}) + S_{ci} (6 R_i - 2\theta_{i-1})$$

$$+S_{c(i+1)} (6 R_{i+1} - 2\theta_{i+1}) \} / \{ 4 S_{BWi} + 4 S_{ci} +$$

$$4 S_{c(i+1)} + 6 S_{BFi} \} \qquad\qquad ....(B.1)$$

Equation (B.1) can be written in the following simplified

form:

$$\theta_i = \frac{A + B + C + D}{A' + B' + C' + D'} \qquad\qquad ....(B.2)$$

Where in the numerator,

$$A = S_{BWi} (6 R'_i - 2\theta_{WBi})$$

$$B = S_{ci} (6 R_i - 2\theta_{i-1})$$

$$C = S_{c(i+1)} (6 R_{i+1} - 2\theta_{i+1})$$

and $\qquad D = 0$

And in the demoninator,

$$A' = 4 S_{BWi}$$

$$B' = 4 S_{ci}$$

$$C' = 4 S_{c (i+1)}$$

and $\qquad D' = 6 S_{BFi}$

Equations (B.1) and (B.2) are valid for the elastic analysis only. When a plastic hinge forms at any one of the potential hinge locations, the joint rotation equation must be modified. TABLE B.1 lists the substitutions to be made in Equation (B.2) for the formation of hinges in the various members, so that the joint rotation equation will conform to the particular hinge pattern considered.

In TABLE B.1, MP_{BFi}, MP_{BWi} are the plastic moment capacities of the beams B_iF_i and B_iW_i , and MP_{ci} is the plastic moment capacity (reduced for axial load) of the column.

TABLE B.1

MODIFICATION OF ELASTIC SLOPE-DEFLECTION

EQUATIONS FOR JOINT EQUILIBRIUM

Member	Hinge Location	Substitution to be Made in Equation (B.2)
$B_i W_i$	W_i	$A = 3 S_{BWi} \cdot R'_i - MP_{BWi}/2$ $A' = 3 S_{BWi}$
	B_i or B_i, W_i	$A = - MP_{BWi}$ $A' = 0$
$B_i\ B_{i-1}$	B_{i-1}	$B = 3 S_{ci} \cdot R_i - MP_{ci}/2$ $B' = 3 S_{ci}$
	B_i or $B_i,\ B_{i-1}$	$B = - MP_{ci}$ $B' = 0$

TABLE B.1 (contd.)

Member	Hinge Location	Substitution to be Made in Equation (B.2)
$B_i \ B_{i+1}$	B_{i+1}	$C = 3 \ S_{c(i+1)} \cdot R_{i+1} - MP_{c(i+1)}/2$ $C' = 3 \ S_{c(i+1)}$
	B_i or B_{i+1}	$C = -MP_{c(i+1)}$ $C' = 0$
$B_i \ F_i$	F_i	$D = -MP_{BFi}/2$ $D' = 3 \ S_{BFi}$
	B_i or $B_i, \ F_i$	$D = -MP_{BFi}$ $D' = 0$

B.2 Nomenclature for FORTRAN IV Program

BAKA	A SUBROUTINE SUBRPOGAM
BMOM	BOTTOM MOMENT IN A SEGMENT OF THE SHEAR WALL (KIP-IN)
BMOMF	BOTTOM MOMENT IN THE BOTTOM OF THE LOWEST SEGMENT IN A STORY (KIP-IN)
CON	CONVERGENCE LIMIT FOR THE DEFLECTION AND ROTATION
CDEFF	FLOOR LEVEL DEFLECTION OF SHEAR WALL AFTER APPLYING CONVERGENCE FORMULA
CROTF	FLOOR LEVEL ROTATION OF SHEAR WALL AFTER APPLYING CONVERGENCE FORMULA
DEF	DEFLECTION OF WALL AT A SECTION (IN)
DEFF	DEFLECTION OF THE WALL AT THE FLOOR LEVEL (IN)
DMBF	MOMENT AT THE COLUMN END OF THE LEFT HAND BEAM COMPUTED IN THE PREVIOUS LOADING CONDITION (KIP-IN)
DMBW	MOMENT AT THE COLUMN END OF THE RIGHT HAND BEAM COMPUTED IN THE PREVIOUS LOADING CONDITION (KIP-IN)
DMCB	MOMENT AT THE BOTTOM END OF COLUMN IN A PARTICULAR STORY COMPUTED IN THE PREVIOUS LOADING CONDITION (KIP-IN)
DMCT	MOMENT AT THE TOP END OF A COLUMN IN A PARTICULAR STORY COMPUTED IN THE PREVIOUS LOADING CONDITION (KIP-IN)
DMFB	MOMENT AT THE LEFT END OF THE LEFT HAND BEAM COMPUTED IN THE PREVIOUS LOADING CONDITION (KIP-IN)
DMWB	MOMENT AT THE WALL END OF THE RIGHT HAND BEAM COMPUTED IN THE PREVIOUS LOADING CONDITION (KIP-IN)

DW	WIDTH OF SHEAR WALL (IN)
EF	YOUNGS MODULUS OF ELASTICITY OF THE FRAME (KIP/IN^2)
EW	YOUNGS MODULUS OF ELASTICITY OF THE WALL (KIP/IN^2)
F	APPLIED FORCE ON THE WALL FROM FRAME ANALYSIS (KIP)
FD	HORIZONTAL DESIGN LOAD ACTING AT FLOOR LEVEL (KIP)
FRAME	A SUBROUTINE SUBPROGRAM
FOC	FRAME FORCE AT THE FLOOR LEVEL (KIP)
FW	FINAL FORCE ON WALL AT EACH FLOOR LEVEL (KIP)
HBF	LENGTH OF LEFT HAND BEAM (IN)
HBW	LENGTH OF RIGHT HAND BEAM (IN)
HLI	PERCENTAGE OF ORIGINAL HORIZONTAL LOAD TO BE INCREASED IN THE ELASTIC RANGE
HLIR	PERCENTAGE OF ORIGINAL HORIZONTAL LOAD TO BE INCREASED IN THE INELASTIC RANGE
HS	STORY HEIGHT (IN)
HSF	HEIGHT OF FLOOR LEVEL FROM BASE (IN)
IK, IX	DUMMY CONSTANTS
IVL	DUMMY CONSTANTS FOR STOPPING THE PROGRAM IF THE DEFORMATION EXCEEDS CERTAIN SPECIFIED LIMIT
KB	SPRING CONSTANT AT THE BASE OF THE SHEAR WALL (KIP-IN /RAD)
KC	SPRING CONSTANT AT THE BASE OF THE COLUMNS (KIP-IN/RAD)
L	PRODUCT OF NUMBER OF STORY AND NUMBER OF SEGMENTS IN A STORY
MAX	MAXIMUM NO. OF CYCLE TO BE PERFORMED FOR ANY ITERATION PROCESS
MI	MOMENT OF INERTIA OF SHEAR WALL (IN^4)

MIBF	MOMENT OF INERTIA OF LEFT HAND BEAM (IN^4)
MIBW	MOMENT OF INERTIA OF RIGHT HAND BEAM (IN^4)
MIC	MOMENT OF INERTIA OF COLUMN (IN^4)
MII	MOMENT OF THE SEGMENT OF THE SHEAR WALL (IN^4)
MM	NO. OF PROBLEMS TO BE SOLVED
MMCB	MOMENT AT THE BOTTOM OF A COLUMN IN A STORY (KIP-IN)
MMCT	MOMENT AT THE TOP OF A COLUMN IN A STORY (KIP-IN)
MMMM	COUNTER FOR ITERATION WITH THE EFFECT OF AXIAL LOAD
MOMB	MOMENT AT THE BASE OF THE SHEAR WALL (KIP-IN)
MOMBF	MOMENT AT THE COLUMN END OF THE LEFT HAND BEAM IN THE CYCLE UNDER CONSIDERATION (KIP-IN)
MOMBW	MOMENT AT THE COLUMN END OF THE RIGHT HAND BEAM IN THE CYCLE UNDER CONSIDERATION (KIP-IN)
MOMFB	MOMENT AT THE LEFT END OF THE LEFT HAND BEAM IN THE CYCLE UNDER CONSIDERATION (KIP-IN)
MOMP	MOMENT IN A STORY DUE TO AXIAL LOAD (KIP-IN)
MOMW	TOTAL MOMENT AT FLOOR LEVEL ON THE SHEAR WALL DUE TO END MOMENT AND SHEAR FROM THE RIGHT HAND BEAM (KIP-IN)
MOMWB	MOMENT AT THE RIGHT END OF THE RIGHT HAND BEAM IN THE CYCLE UNDER CONSIDERATION (KIP-IN)
MPC	PLASTIC MOMENT CAPACITY OF COLUMN IN A PARTICULAR STORY (KIP-IN)
MPF	PLASTIC MOMENT CAPACITY OF THE LEFT HAND BEAM (KIP-IN)
MPS	PLASTIC MOMENT CAPACITY OF THE WALL SEGMENT (KIP-IN)
MPSW	PLASTIC MOMENT CAPACITY OF THE SHEAR WALL (KIP-IN)
MPW	PLASTIC MOMENT CAPACITY OF THE RIGHT HAND BEAM (KIP-IN)
ND	NUMBER OF DIVISION IN A STORY

NI	NUMBER OF TIMES HORIZONTAL LOAD TO BE INCREMENTED
NM	LENGTH OF A SEGMENT OF A WALL IN A STORY (IN)
NNMM	SEGMENT HEIGHT FROM BASE OF WALL(IN)
NS	NUMBER OF STORIES
PS	VERTICAL LOAD ON COLUMN (KIPS)
PSW	VERTICAL LOAD ON WALL (KIPS)
PPS	VERTICAL LOAD ON STORY (KIPS)
ROB	SWAY ROTATION OF RIGHT HAND BEAM
ROFA	A SUBROUTINE SUBPROGRAM
ROS	STORY ROTATION OF FRAME
RMWP	RATIO OF MOMENT TO PLASTIC MOMENT CAPACITY OF WALL
RPWP	RATIO OF CURVATURE TO CURVATURE CORRESPONDING TO RMWP
ROT	ROTATION OF WALL IN A SEGMENT (RAD)
ROTF	ROTATION OF WALL AT THE FLOOR LEVEL (RAD)
ROTFF	JOINT ROTATION OF FRAME (RAD)
ROTO	JOINT ROTATION AT THE BASE OF COLUMN (RAD)
SBF	STIFFNESS OF LEFT HAND BEAM (KIP-IN)
SBW	STIFFNESS OF RIGHT HAND BEAM (KIP-IN)
SC	STIFFNESS OF COLUMN (KIP-IN)
SHEARR	SHEAR AT THE ENDS OF LEFT HAND BEAM (KIP)
SHEARW	SHEAR AT THE ENDS OF RIGHT HAND BEAM (KIP)
SHEC	SHEAR IN COLUMN IN A STORY (KIP)
SR	A SUBROUTINE SUBPROGRAM
SR 1	A SUBROUTINE SUBPROGRAM
SR 3	A SUBROUTINE SUBPROGRAM
SSB	SLOPE OF THE SECOND BRANCH OF SHEAR WALL MOMENT-CURVATURE DIAGRAM

TMOMF   TOP MOMENT IN THE TOP OF THE TOPMOST SEGMENT IN
                    A STORY (KIP-IN)

TMOM   TOP MOMENT IN A SEGMENT OF THE SHEAR WALL (KIP-IN)

VDEF   VERTICAL UPLIFT OF THE BEAM CONNECTED WITH THE
                    WALL (IN)

B.3 FLOW DIAGRAM OF THE COMPUTER PROGRAM

B.3.1 MAIN PROGRAM

B.3.2 SUBROUTINE 'SR'

```
                    ╭───────╮
                   (   S R   )
                    ╰───┬───╯
                        │
                        ▼
              ╱─────────────────╲
             │     INPUT          │
             │   STATEMENTS       │
             │   FOR DATA         │
              ╲─────────────────╱
                        │
                        ▼
    ┌─────────────────────────────────────┐
    │              COMPUTE                  │
    │   1.  FLOOR HEIGHT FROM THE BASE      │
    │   2.  STIFFNESS OF MEMBERS            │
    │   3.  TOTAL VERTICAL LOAD             │
    └─────────────────────────────────────┘
                        │
                        ▼
            ╱───────────────────────╲
           │   OUTPUT STATEMENTS      │
           │     FOR DATA OF          │
           │      FRAME AND           │
           │     SHEAR WALL           │
            ╲───────────────────────╱
                        │
                        ▼
                 ╭─────────────╮
                (    RETURN      )
                 ╰─────────────╯
```

B.3.4 SUBROUTINE 'FRAME'

B.3.5 SUBROUTINE 'ROFA'

```
                    ( ROFA )
                        |
                        v
  /                                                    \
 <     OUTPUT STATEMENTS FOR                             >
 <  1.   JOINT ROTATIONS                                 >
 <  2.   MOMENTS AT POTENTIAL HINGE                      >
 <       LOCATIONS IN FRAME MEMBERS                      >
 <  3.   STORY SHEAR AND FORCES                          >
  \                                                    /
                        |
                        v
                  ( RETURN )
```

B.3.6 SUBROUTINE 'SR3'

```
                    ( S R 3 )
                        |
                        v
  /                                      \
 |  OUTPUT STATEMENTS FOR                  |
 |  1.   SLOPE                             |
 |  2.   DEFLECTION                        |
 |  3.   MOMENT AND SHEAR                  |
 |       IN THE SHEAR WALL                 |
  \                                      /
                    |
                    v
               ( RETURN )
```

B.3.7 <u>SUBROUTINE 'SR1'</u>

```
                    ( SR 1 )

      MOMENT AT A
     POTENTIAL HINGE
  LOCATION HAS EXCEEDED THE        NO
  PLASTIC MOMENT CAPACITY     ---------->   ( RETURN )
     OF THE MEMBER?

                  YES

     OUTPUT STATEMENT
   INDICATING LOCATION
   OF PLASTIC HINGE AND
    THE MAGNITUDE OF
        MOMENT

      SET THE MOMENT AT
  HINGE LOCATION .0001 GREATER
  THAN PLASTIC MOMENT CAPACITY

         ( RETURN )
```

```
C
C
      FORTRAN PROGRAM FOR THE ANALYSIS OF SHEAR WALL-FRAME STRUCTURE
C
C
C
C
C

      DIMENSION F(99,30),HSF(30),DW(30),FOC(30),SHEAR(30),ROTF(99,30),
     1ROTFF(99,31),ROTO(99),SHEC(30),FD(30),FW(30),SHEARW(30),PS(30),
     2SHEARR(30),CPHI(300),D(300),D1(300),H(99,30),DELTA(99,30),
     3FA(30),PPS(31),CROTF(99,30),CDEFF(99,31),  PPD(30),ZM(300),
     4 DEFF(99,30),       HBF(30),HBW(30),HS(31),SBF(30),SC(31),SBW(30),
     5F11(30),TMOM(300),BMOM(300),TMOMF(30),BMOMF(30),DMFB(30),
     6DMBF(30),DMBW(30),DMWB(30),CSHEC(30), DMCB(31),DMCT(31)
      REAL  NNM(300),NNMM(300),       MIA(300),MII(300),MMCT(30),MMCB(30),
     1KB,KC,    MOMW(30),   MOMWB(30),MOMBW(30),MOMBF(30),MOMFB(30)
     2,MPF(30),MPW(30),MPC(31),MPS(300)
      COMMON IUNB
   20 FORMAT(1H1)
   21 FORMAT(1HK)
   22 FORMAT(1H )
      READ(5,130) MM
  130 FORMAT(1X,I3)
      DO 400 JJ=1,MM
C
C     INPUT STATEMENTS FOR DATA BY SUBROUTINE SR.
C
      CALL          SR (L,NS,ND,    EW,KC,KB,FD,NI,HS,DW,PS,          MPF,NNM,
     1 MPW,MPC,        SC,SBW,SBF,IVL,PPD,                   HBF,HBW,
     2     RMWP,RPWP,MAX,CON,HLI,HLIR,HSF,F,MII,MPS,NNMM,MIA,PPS,ALPHA)
      NL=JJ-1
      KP=0
      SSB=(RMWP-1.0)/(RPWP-1.0)
      DO 302 NJ=1,NI
C
C     SHEAR WALL ANALYSIS BEGINS.
C
      IK=0
      IX=0
      MMMM=1
      DO 131 K=1,NS
      H(NJ,K)=F(1,K)
  131 CONTINUE
  132 CALL          BAKA (IK,IX,MMMM,L,NS,ND,EW,KC,KB,HS,DW,PS,NNM,MPF,MPW,
     1MPC,SC,SBW,SBF,HBW,MAX,CON,HSF,F,MII,NNMM,TMOM,BMOM,MOMW,ROTB,TMOM
     2F,BMOMF,ROTF,DEFF,ROTFF,ROTO,ITER,NJ,DMCB,DMCT,DMBF,DMFB,DMBW,
     3DMWB,MMCB,MMCT,MOMBW,MOMWE,FOC,SHEC,CSHEC,SHEARW,NCYCLE,SHEAR,CDEF
     4F,CROTF,ZM,MIA)
      IF(IX .EQ. 1)GO TO 245
      IF(IK .EQ. 1) GO TO 272
  233 IF(PPS(1) .LE. 0.0) GO TO 260
      IF(MMMM .EQ. 1 .AND. NJ .EQ. 1)  GO TO 235
      IF(MMMM .EQ. 1) GO TO 256
      DO 234 N=1,NS
      IF(ABS((CDEFF(MMMM,N)-CDEFF(MMMM-1,N))/CDEFF(MMMM,N)) .GE. CON .OR
     1. ABS((CROTF(MMMM,N)-CROTF(MMMM-1,N))/CROTF(MMMM,N)) .GE. CON) GO
     2TO 251
```

```
  234 CONTINUE
      GO TO 260
C
C     OUTPUT STATEMENTS FOR RESULTS OF FRAME ANALYSIS BY SUBROUTINE ROFA
C          (WITHOUT THE EFFECT CF AXIAL LOADS)
C
  235 WRITE(6,240)
  240 FORMAT(/45X,'RESULT WITHOUT THE EFFECT OF AXIAL LOAD'//)
      CALL ROFA (ROTFF,SHEC,FOC,MMCB,MMCT,ROTO,NS,NCYCLE,ITER,MMMM)
      DO 242 N=1,NS
      MOMFB(N)=SBF(N)*6.0*ROTFF(ITER,N)
      MOMBF(N)= MOMFB(N)
      SHEARR(N)=2.0*MOMFB(N)/HBF(N)
      WRITE(6,241) N,MOMBW(N),MOMWB(N),MOMBF(N),MOMFB(N),SHEARW(N),SHEAR
     1R(N)
  241 FORMAT(13X,I3,1X,4F19.2,5X,F10.2,7X,F10.2/)
  242 CONTINUE
      WRITE(6,21)
      DO 244 K=1,NS
      F11(K)=F(1,K)-FOC(K)
      F(1,K)=F11(K)
  244 CONTINUE
      IX=1
      GO TO 132
  245 WRITE(6,22)
C
C     OUTPUT STATEMENTS FOR RESULTS OF SHEAR WALL ANALYSIS BY SUBROUTINE
C      SR3 (WITHOUT THE EFFECT OF AXIAL LOADS)
C
      CALL SR3 (BMOMF,TMOMF,ROTB,NS,F11,FOC,SHEAR,ROTF,DEFF,CROTF,CDEFF,
     1MMMM)
      IX=0
      WRITE(6,21)
C
C     ADDITIONAL HORIZONTAL LOACLTO SIMULATE P-DELTA EFFECT
C
  251 IF(MMMM .EQ. MAX) GO TO 254
  256 PPS(NS+1)=0.0
      HS(NS+1)=5000.0
      CDEFF(MMMM,NS+1)=CDEFF(MMMM,NS)
      F(1,1)=H(NJ,1)+ALPHA*(PPS(1)*CDEFF(MMMM,1)/HS(1)-PPS(2)*(CDEFF(MMM
     1M,2)-CDEFF(MMMM,1))/HS(2))
      IF(NS .EQ. 1) GO TO 253
      DO 252 N=2,NS
      F(1,N)=H(NJ,N)+ALPHA*(PPS(N)*(CDEFF(MMMM,N)-CDEFF(MMMM,N-1))/HS(N)
     1-PPS(N+1)*(CDEFF(MMMM,N+1)-CDEFF(MMMM,N))/HS(N+1))
  252 CONTINUE
  253 MMMM=MMMM+1
      GO TO 132
C
C     OUTPUT STATEMENTS FOR RESULTS OF FRAME ANALYSIS BY SUBROUTINE ROFA
C
  254 WRITE(6,255)
  255 FORMAT(10X,'CONVERGENCE (CALCULATION OF THE EFFECT OF AXIAL LOAD)
     1WAS NOT ENOUGH'//)
  260 CALL ROFA (ROTFF,SHEC,FOC,MMCB,MMCT,ROTO,NS,NCYCLE,ITER,MMMM)
      DO 270 N=1,NS
```

```
      IF(MMMM.EQ.MAX.OR.NCYCLE.EQ.MAX)  GO  TO  960
      IF(NJ .EQ. 1) GO TO 261
      IF(ABS(DMFB(N)) .GE. MPF(N)) GO TO 262
  261 MOMFB(N)=SBF(N)*6.0*ROTFF(ITER,N)
      GO TO 263
  262 MOMFB(N)=DMFB(N)
  263 MOMBF(N)=MOMFB(N)
  264 SHEARR(N)=2.0*MOMFB(N)/HBF(N)
      WRITE(6,241)N, MOMBW(N),MOMWB(N),MOMBF(N),MOMFB(N),SHEARW(N),SHEARR
     1(N)
  270 CONTINUE
      DO 271 K=1,NS
      DELTA(NJ,K)=CDEFF(MMMM,K)
      F11(K)=F(1,K)-FOC(K)
      F(1,K)=F11(K)
  271 CONTINUE
      IK=1
      GO TO 132
  272 WRITE(6,21)
C
C
C     OUTPUT STATEMENTS FOR RESULTS OF SHEAR WALL ANALYSIS BY
C        SUBROUTINE  SR3
C
      CALL SR3 (BMOMF,TMOMF,ROTB,NS,F11,FOC,SHEAR,ROTF,DEFF,CROTF,CDEFF,
     1MMMM)
      WRITE(6,21)
C
C     DETECTION OF HINGES IN SHEAR WALL.
C
      IF(NL .NE. JJ) GO TO 273
      IF(ABS(DELTA(NJ,NS)) .GT. STOPD) GO TO 960
  273 SSB=(RMWP-1.0)/(RPWP-1.0)
      DO 284 J = 1,L
      D(J)=(TMOM(J)+BMOM(J))/(2.0*MPS(J))
      D1(J)=D(J)*MPS(J)
      IF(ABS(D(J)) .LT. 1.0) GO TO 284
      IF(NL .NE. JJ) GO TO 274
      CPHI(J)=(ABS(D(J))-1.0)/SSB+1.0
      MII(J)=(ABS(D(J)))*MIA(J)/CPHI(J)
  274 KP=KP+1
      IF(KP .GE. 2) GO TO 281
  275 WRITE(6,280)
  280 FORMAT(45X,37HDETECTION OF HINGES IN THE SHEAR WALL///)
  281 WRITE(6,282)J,D(J),D1(J)
  282 FORMAT(5X,20HHINGE IN SECTION NO.,I3,2X,51HRATIO OF MOMENT IN WALL
     1 TO PLASTIC MOMENT CAPACITY=,F5.2,2X,15HMOMENT IN WALL=,F14.2/)
      WRITE(6,283) MII(J),MIA(J)
  283 FORMAT (5X,'REDUCED MOMENT OF INERTIA =',F13.2,3X,'INITIAL MOMENT
     1 OF INERTIA =',F13.2//)
  284 CONTINUE
      WRITE(6,21)

      DETECTION OF HINGES ON FRAME BY SUBROUTINE SR1.

      CALL        SR1 (DMFB,DMBF,DMBW,DMWB,DMCT,DMCB,MOMFB,MOMBF,MOMBW,MO
     1MWB,MMCT,MMCB,NS,M3,MPF,MPW,MPC)
      IK=0
```

```
      IF(NL .EQ. JJ) GO TC 285
      IF(KP .GE. 1 .OR. M3 .GE. 1) GO TO 295
C
C     HORIZONTAL LOAD IS INCREMENTEC
C
  285 IF(NJ .EQ. NI) GO TC 960
      WRITE(6,21)
      WRITE(6,291)
  291 FORMAT(50X,'HORIZONTAL LOAD INCREMENTED'//)
      WRITE(6,292)
  292 FORMAT(10X,'FLOOR NC.',5X,'HORIZONTAL LOAD(K)',5X,'VERTICAL  LOAD(
     1K)'//)
      DO 294 K=1,NS
      F(1,K)=H(NJ,K)+HLI*FD(K)
      IF(IVL .LE. 0) GO TC 296
      PPS(K)=PPS(K)+HLI*PPD(K)
  296 WRITE(6,293)K,F(1,K),PPS(K)
  293 FORMAT(13X,I3,11X,F8.2,16X,F8.2/)
  294 CONTINUE
      KP=0
      GO TO 302
C
C     HORIZONTAL LOAD IS DECREMENTED
C
C     COMPUTE SECTION HEIGHT FRCM BASE IN INCH
C
C
  295 IF(NJ .EQ. NI) GO TO 960
      STOPD=90.0*ABS(DELTA(NJ,NS))
      WRITE(6,300)
  300 FORMAT(1HK,15X,'HORIZONTAL LOAD DECREMENTED TO MAKE THE FRAME ELAS
     1TIC SO THAT HORIZONTAL LOAD CAN BE INCREMENTED SLOWLY'///)
      WRITE(6,292)
      DO 301 K=1,NS
      F(1,K)=H(NJ,K)-HLI*FD(K)+HLIR*FD(K)
      IF(IVL .LE. 0) GO TC 303
      PPS(K)=PPS(K)-HLI*PPD(K)+HLIR*PPD(K)
  303 DMFB(K)=0.0
      DMBF(K)=0.0
      DMWB(K)=0.0
      DMBW(K)=0.0
      DMCT(K)=0.0
      DMCB(K)=0.0
      WRITE(6,293) K,F(1,K),PPS(K)
  301 CONTINUE
      HLI=HLIR
      NL=JJ
      KP=0
  302 CONTINUE
C
C     OUTPUT THE ROTATION AND DEFLECTION OF EACH HORIZONTAL LOAD
C
  960 DO 907 N=1,NS
      WRITE(6,915) N
  915 FORMAT(48X,'LOAD-DEFLECTICN DATA FOR FLOOR NO.  ',I3//)
      WRITE(6,905)
  905 FORMAT(10X,'HORIZONTAL LOAD(KIP)',5X,'DEFLECTION(IN)'///)
```

```
      DO   906   K = 1,NJ
      WRITE(6,908) H(K,N),DELTA(K,N)
 908  FORMAT(16X,F8.2,11X,E13.6/)
 906  CONTINUE
 907  CONTINUE
 400  CONTINUE
      STOP
      END
```

```
C
C
C
C
C     SUBROUTINE SR READS IN DATA - COMPUTES CO-ORDINATES OF EACH
C     FLOOR FROM THE BASE AND THE STIFFNESS OF MEMBERS - ALSO ALL
C     THE INPUT QUANTITIES ARE PRINTED OUT
C
C
      SUBROUTINE SR (L,NS,ND,    EW,KC,KB,FD,NI,HS,DW,PS,         MPF,NNM,
     1 MPW,MPC,       SC,SBW,SBF,IVL,PPD,                 HBF,HBW,
     2      RMWP,RPWP,MAX,CON,HLI,HLIR,HSF,F,MII,MPS,NNMM,MIA,PPS,ALPHA)
      DIMENSION FD(30),HS(30),DW(30 ),PS(30),                  SC(30),
     1 SBF(30),SBW(30),                                        HBF(30),
     2HBW(30),HSF(30),F(99,30),PSW(30),PPS(30),PPD(30)
      REAL MI(30),MPF(30),MPW(30),MPC(30),MPSW(30),MIC(30),MIBF(30),
     1 MIBW(30),NM(30),NNM(300),MII(300),MPS(300),NNMM(300),MIA(300),
     2KB,KC
      COMMON IUNB
      READ(5,200)KB,KC,EF,EW,NS,ND,MAX,CON,HLI,NI,HLIR
  200 FORMAT(1X,2E18.5,2F7.0,3I3,2F5.2,I3,F5.2)
      READ(5,470) RMWP,RPWP,ALPHA,IVL,IUNB
  470 FORMAT(1X,2F7.2,F5.2,2I3)
      DO 202 K=1,NS
      READ(5,204)FD(K),HS(K),HBF(K),HBW(K),DW(K),MI(K),MIC(K),
     1MIBF(K),MIBW(K)
  204  FORMAT(1X,F5.2,4F7.2,4F11.2)
  202 CONTINUE
      DO 102 K=1,NS
      READ(5,101)PS(K)   ,PSW(K)
  101 FORMAT(1X,2F8.2)
  102  CONTINUE
      DO  205  K = 1,NS
      READ(5,500)                 MPF(K),MPW(K),MPC(K),MPSW(K)
  500  FORMAT(   17X   ,3F14.2,F21.2)
  205  CONTINUE
C
C     ALL  FORCE  UNITS   ARE  IN  KIPS AND  ALL  LENGTH  UNITS  ARE
C     IN  INCHES  UNLESS  STATEC  OTHERWISE.
C
C
C
      L=NS*ND
      NDN=0
      K=1-ND
      CB=0.0
      DO 22 J=1,NS
      NM(J)=HS(J)/FLOAT(ND)
      HSF(J)=CB+HS(J)
      CB=HSF(J)
      SBW(J)=EF*MIBW(J)/HBW(J)
      SBF(J)=EF*MIBF(J)/HBF(J)
      SC(J)=EF*MIC(J)/HS(J)
      F(1,J)=FD(J)
      PPS(J)=PS(J)+PSW(J)
      PPD(J)=PPS(J)
      K=K+ND
```

```
      NDN=NDN+ND
      DO 23 N=K,NDN
      NNM(N)=NM(J)
      MII(N)=MI(J)
      MIA(N)=MI(J)
      MPS(N) = MPSW(J)
   23 CONTINUE
   22 CONTINUE
C
C     COMPUTE SECTION HEIGHT FRCM BASE IN INCH
C
      BC=0.0
      DO 25 K=1,L
      NNMM(K)=BC+NNM(K)
      BC=NNMM(K)
   25 CONTINUE
      WRITE(6,324)
  324 FORMAT(1H1)
C
C     OUTPUT   STATEMENTS   FOR   DATA   OF   FRAME   AND   SHEAR   WALL.
C
      WRITE(6,51)
   51 FORMAT(50X,29HDATA FOR SHEAR WALL AND FRAME//)
      WRITE(6,351) NS
  351 FORMAT(10X,56HNUMBER OF STORIES                            =
     1    ,I3/)
      WRITE(6,352)ND
  352 FORMAT(10X,56HNUMBER OF DIVISION TO BE MADE IN A STORY =
     1    ,I3/)
      WRITE(6,355) EW
  355 FORMAT(10X,53HMODULUS OF ELASTICITY FOR WALL            =
     1 ,F9.2/)
      WRITE(6,356) EF
  356 FORMAT(10X,53HMODULUS CF ELASTICITY FOR FRAME           =
     1 ,F9.2/)
      WRITE(6,354) KC
  354 FORMAT(10X,43HSPRING CCNSTANT AT BASE OF FRAME          = ,E19.5/)
      WRITE(6,353) KB
  353 FORMAT(10X,43HSPRING CONSTANT AT BASE OF WALL           = ,E19.5/)
      WRITE(6,510) CON
  510 FORMAT(10X,'CONVERGENCE LIMIT',24X,'=',F20.5/)
      WRITE(6,501) ALPHA
  501 FORMAT(10X,'ALPHA',36X,'=',F20.3//)
      WRITE(6,364)
  364 FORMAT(1HK)
      WRITE(6,357)
  357 FORMAT(10X,10HFLOOR NO./,2X,10HFORCE(KIP),3X,17HMOMENT OF INERTIA,
     13X,16HSTORY HEIGHT(IN),3X,14HWALL WIDTH(IN),3X,15HAXIAL LOAD(KIP),
     23X,15HAXIAL LOAD(KIP))
      WRITE(6,358)
  358 FORMAT(10X,9HSTORY NO.,18X,13HOF WALL (IN4),43X,9HON COLUMN,10X,7H
     2ON WALL//)
      DO 10 N=1,NS
      WRITE(6,359)N,FD(N),MI(N),HS(N),DW(N),PS(N),PSW(N)
  359 FORMAT(13X,I3,6X,F8.2,7X,F12.2,9X,F8.2,11X,F7.2,9X,F8.2,9X,F8.2/)
   10 CONTINUE
      WRITE(6,366)
```

```
366    FORMAT(1HK)
       WRITE(6,360)
360    FORMAT(10X,10HFLOOR NO./,2X,14HLENGTH OF BEAM,3X,14HLENGTH CF BEAM
      1,3X,17HMOMENT OF INERTIA,3X,17HMOMENT OF INERTIA,3X,17HMOMENT OF I
      2NERTIA)
       WRITE(6,361)
361    FORMAT(10X,9HSTORY NO.,4X,13HCN ROLLER(IN),3X,14HCONNECTED WITH,4X
      1,14HOF COLUMN(IN4),5X,17HOF BEAM ON ROLLER,3X,17HOF BEAM CONNECTED
      2)
       WRITE(6,362)
362    FORMAT(42X,8HWALL(IN),32X,5H(IN4),10X,14HWITH WALL(IN4)//)
       DO 71 J=1,NS
       WRITE(6,363)J,HBF(J),HBW(J),MIC(J),MIBF(J),MIBW(J)
363    FORMAT(13X,I3,8X,F8.2,9X,F8.2,9X,F11.2,9X,F11.2,9X,F11.2/)
   71  CONTINUE
       WRITE(6,411)
  411  FORMAT(1HK,30X,'PLASTIC MCMENT CAPACITY OF BEAMS, COLUMNS AND WALL'
      1'///)
       WRITE(6,399)
399    FORMAT(10X,10HFLOOR NO./,2X,
      1          15HPLASTIC   MOMENT,2X,15HPLASTIC   MOMENT,2X,15HPLASTIC   MO
      3MENT, 5X,15HPLASTIC   MOMENT)
       WRITE(6,406)
406    FORMAT(10X,9HSTORY NO.,3X,
      1          15HCAPACITY OF THE,2X,15HCAPACITY OF THE,2X,15HCAPACITY OF T
      2HE, 5X,15HCAPACITY OF THE)
       WRITE(6,407)
407    FORMAT(22X,                                          15HBEAM
      2ON ROLLER,2X,15HWALL   SIDE BEAM,2X,15HCOLUMN (KIP-IN), 5X,15HWALL
      3 (KIP-IN).)
       WRITE(6,408)
408    FORMAT(26X,                                          8H(KIP-IN
      1), 7X,8H(KIP-IN)//)
       DO   410 K= 1,NS
       WRITE(6,409) K,               MPF(K),MPW(K),MPC(K),MPSW(K)
409    FORMAT(13X,I3, 6X,                   F14.2,3X,F14.2,3X,F14.2,2X,E18
      1.8/)
410    CONTINUE
       WRITE(6,385)
385    FORMAT(1HK,45X,39HSTIFFNESSES (EI/L) OF BEAMS AND COLUMNS//)
       WRITE(6,365)
365    FORMAT(10X,10HFLOOR NO./,4X,19HSTIFFNESS OF COLUMN,4X,17HSTIFFNESS
      1 OF BEAM,4X,17HSTIFFNESS CF BEAM)
       WRITE(6,367)
367    FORMAT(10X,9HSTORY NO.,10X,8H(KIP-IN),11X,15HCONNECTED   WITH,5X,17
      1HON ROLLER(KIP-IN))
       WRITE(6,368)
368    FORMAT(49X,12HWALL(KIP-IN)//)
       DO 72 J=1,NS
       WRITE(6,369)J,SC(J),SBW(J),SBF(J)
369    FORMAT(13X,I3,9X,F15.2,7X,F15.2,6X,F15.2/)
   72  CONTINUE
       WRITE(6,481)
481    FORMAT(1HK,40X,53HMCMENT   CURVATURE   RELATIONSHIP   OF   THE   SHEAR
      1 WALL///)
       WRITE(6,482)
482    FORMAT(10X,9HPOINT NO.,5X,19HRATIO   OF MOMENT IN,5X,18HRATIO OF CU
```

```
     1RVATURE)
     WRITE(6,483)
483  FORMAT(24X,19HWALL TO THE PLASTIC,5X,18HIN  WALL  TO    THE)
     WRITE(6,484)
484  FORMAT(24X,19HMOMENT   CAPACITY OF,5X,18HCURVATURE  OF    THE)
     WRITE(6,485)
485  FORMAT(29X,9HTHE WALL.,10X,18HWALL AT YIELD  PT.////)
     WRITE(6,488)
 488 FORMAT(13X,'NO.1                  1.00                     1.00'/)
     WRITE(6,487) RMWP,RPWP
 487 FORMAT(13X,'NO.2',15X,F7.2,18X,F7.2/)
     WRITE(6,324)
     RETURN
      END
```

```
C
C
C     SUBROUTINE BAKA COMPUTES THE DISTRIBUTION OF LATERAL LOAD BETWEEN
C     THE FRAME AND SHEAR WALL. MOMENTS AND DEFORMATIONS AT EACH SEGMENT
C     OF THE WALL ARE COMPUTED. THE CONVERGENCE FORMULA IS  APPLIED
C     ( EXCEPT THE FIRST CYCLE ) FOR DEFLECTION AND ROTATION.  THE
C     DEFORMATIONS COMPUTED BY THE CONVERGENCE FORMULA ARE ENFORCED ON
C     THE FRAME SYSTEM. THE JOINT ROTATION CF THE FRAME ARE  COMPUTED IN
C     SUBROUTINE FRAME.
C
C
      SUBROUTINE BAKA (IK,IX,M,MM,L,NS,ND,EW,KC,KB,HS,DW,PS,NNM,MPF,MPW,
     1MPC,SC,SBW,SBF,HBW,MAX,CON,HSF,F,MII,NNMM,TMOM,BMOM,MOMW,RCTB,TMOM
     2F,BMOMF,RCTF,DEFF,ROTFF,RCTO,ITER,NJ,DMCB,DMCT,DMBF,DMFB,DMBW,
     3DMWB,MMCB,MMCT,MOMBW,MOMWB,FOC,SHEC,CSHEC,SHEARW,NCYCLE,SHEAR,CDEF
     4F,CROTF)
      DIMENSION   BMOM(300),BMOMF(30),CSHEC(30),CDEFF(99,30), CROTF(99,30
     1),DEF(300),DEFF(99,30),DMCB(30),DMCT(30),DMBW(30),DMWB(30),DW(30),
     2DMFB(30),DMBF(30),F(99,30),FOC(30),HSF(30),HS(30),HBW(30),PS(30),
     3ROT(300),ROTF(99,30),ROS(30),ROB(30),ROTFF(99,30), ROTO(99),SC(30)
     4,SBW(30),SBF(30),SHEC(30),SHEARW(30),SHEAR(30),TMOM(300),TMOMF(30)
     5,VDEF (30)
      REAL   KB,KC,MOMB,MOMW(30),MII(300),MPC(30),MOMP(30),MPW(30),
     1MPF(30),MMCB(30),MMCT(30),MOMBW(30),MOMWB(30),NNMM(300),NNM(300)
      COMMON IUNB
  132 DO 232 M=1,MAX
C
C     MOMENTS AT VARIOUS SECTIONS (KIP-IN).
C
      MOMB=0.0
      NDN=0
      K=1-ND
      DO 135 N=1,NS
      MOMB=MOMB+F(M,N)*HSF(N)
      K=K+ND
      NDN=NDN+ND
      DO 134 J=K,NDN
      RS=0.0
      DO 133 I=N,NS
  133 RS=RS+F(M,I)*(HSF(I)-NNMM(J))
      TMOM(J)=RS
  134 CONTINUE
  135 CONTINUE
      IF(IK .EQ. 1.OR. IX .EQ. 1) GO TO 140
      IF(M .EQ. 1) GO TO 145
  140 DO 142 N=1,NS
      MOMB=MOMB+MOMW(N)
      RS=0.0
      DO 141 I=N,NS
      RS=RS+MOMW(I)
  141 CONTINUE
      MOMW(N)=RS
  142 CONTINUE
      NDN=0
      K=1-ND
```

```
      DO 144 I=1,NS
      K=K+ND
      NDN=NDN+ND
      DO 143 J=K,NDN
      TMOM(J)=TMOM(J)+MOMW(I)
      BMOM(J)=TMOM(J)+SHEAR(I)*NNM(J)
  143 CONTINUE
  144 CONTINUE
      GO TO 150
  145 BMOM(1)=MOMB
      IF(L .EQ. 1) GO TO 150
      DO 146 J=2,L
  146 BMOM(J)=TMOM(J-1)
C
C     DEFLECTIONS AT VARIOUS SECTIONS (IN)
C
  150 A = (TMOM(1)+MOMB)*NNM(1)/(2.0*EW*MII(1))
      ROTB=MOMB/KB
      ROT(1)=ROTB+A
      DEF(1)=ROTB*NNM(1)+A*NNM(1)/2.0
      IF(L .EQ. 1) GO TO 152
      DO 151 J=2,L
      B=(TMOM(J)+BMOM(J))*NNM(J)/(2.0*EW*MII(J))
      ROT(J) = ROT(J-1) + B
      DEF(J)=DEF(J-1)+ROT(J-1)*NNM(J)+B*NNM(J)/2.0
  151 CONTINUE
C
C     MOMENTS, ROTATIONS AND DEFLECTIONS AT EVERY FLOOR LEVEL
C
  152 DO 153 N=1,NS
      I=N*ND
      K=I+1-ND
      TMOMF(N)=TMOM(I)
      BMOMF(N)=BMOM(K)
      ROTF(M,N)=ROT(I)
      DEFF(M,N)=DEF(I)
  153 CONTINUE
      IF(IX .EQ. 1) RETURN
      IF(IK .EQ. 1) RETURN
      IF(M .EQ. 1) GO TO 155
      DO 154 N=1,NS
      ROTF(M,N)=ROTF(1,N)*ROTF(M-1,N)/(ROTF(M-1,N)-ROTF(M,N))
      DEFF(M,N)=DEFF(1,N)*DEFF(M-1,N)/(DEFF(M-1,N)-DEFF(M,N))
  154 CONTINUE
  155 ROS(1)=DEFF(M,1)/HS(1)
      IF(NS .EQ.  1) GO TO 161
      DO 160 I=2,NS
      ROS(I)=(DEFF(M,I)-DEFF(M,I-1))/HS(I)
  160 CONTINUE
  161 DO 162 N=1,NS
      VDEF(N)=-ROTF(M,N)*DW(N)/2.0
      ROB(N)=VDEF(N)/HBW(N)
  162 CONTINUE
C
C     COMPUTE MOMENT, SHEAR AND FORCE ON FRAME BY SUBROUTINE FRAME
C
      CALL FRAME (MAX,ROTFF,ROTO,SC,ROS,KC,SBW,SBF,ROB,ROTF,NS,ITER,MMMM
```

```
     1 ,    M,   DMCB,DMCT,DMBW,DMWB,DMBF,DMFB,MPC,MPF,MPW,NJ,CON)
     IF(NJ .EQ. 1) GO TO 180
     IF(ABS(DMCB(1)) .GE. MPC(1)) GO TO 181
 180 MMCB(1)=-KC*ROTO(ITER)
     GO TO 182
 181 MMCB(1)=DMCB(1)
 182 IF(NJ .EQ. 1) GO TO 183
     IF(ABS(DMCT(1)) .GE. MPC(1)) GO TO 184
     IF(ABS(DMCB(1)) .GE. MPC(1)) GO TO 185
 183 MMCT(1)=SC(1)*(4.0*ROTFF(ITER,1)+2.0*ROTO(ITER)-6.0*ROS(1))
     GO TO 192
 184 MMCT(1)=DMCT(1)
     GO TO 192
 185 MMCT(1)=SC(1)*(3.0*ROTFF(ITER,1)-3.0*ROS(1))+0.5*DMCB(1)
 192 SHEC(1)=(MMCT(1)+MMCB(1))/HS(1)
 194 IF(NS .EQ. 1) GO TO 210
     DO 205 K=2,NS
     IF (NJ .EQ. 1) GO TO 195
     IF(ABS(DMCB(K)) .GE. MPC(K)) GO TO 196
     IF(ABS(DMCT(K)) .GE. MPC(K)) GO TO 197
 195 MMCB(K)=SC(K)*(4.0*ROTFF(ITER,K-1)+2.0*ROTFF(ITER,K)-6.0*ROS(K))
     GO TO 198
 196 MMCB(K)=DMCB(K)
     GO TO 198
 197 MMCB(K)=SC(K)*(3.0*ROTFF(ITER,K-1)-3.0*ROS(K))+0.5*DMCT(K)
 198 IF(NJ .EQ. 1) GO TO 199
     IF(ABS(DMCT(K)) .GE. MPC(K)) GO TO 200
     IF(ABS(DMCB(K)) .GE. MPC(K)) GO TO 201
 199 MMCT(K)=SC(K)*(4.0*ROTFF(ITER,K)+2.0*ROTFF(ITER,K-1)-6.0*ROS(K))
     GO TO 202
 200 MMCT(K)=DMCT(K)
     GO TO 202
 201 MMCT(K)=SC(K)*(3.0*ROTFF(ITER,K)-3.0*ROS(K))+0.5*DMCB(K)
 202 SHEC(K)=(MMCT(K)+MMCB(K))/HS(K)
 204 FOC(K-1)=SHEC(K)-SHEC(K-1)
 205 CONTINUE
 210 FOC(NS)=-SHEC(NS)
     SHEAR(1)=0.0
     DO 219 K=1,NS
     IF(NJ .EQ. 1) GO TO 211
     IF(ABS(DMBW(K)) .GE. MPW(K)) GO TO 212
     IF(ABS(DMWB(K)) .GE. MPW(K)) GO TO 213
 211 MOMBW(K)=SBW(K)*(4.0*ROTFF(ITER,K)+2.0*ROTF(M,K)-6.0*ROB(K))
     GO TO 214
 212 MOMBW(K)=DMBW(K)
     GO TO 214
 213 MOMBW(K)=SBW(K)*(3.0*ROTFF(ITER,K)-3.0*ROB(K))+0.5*DMWB(K)
 214 IF(NJ .EQ. 1) GO TO 215
     IF(ABS(DMWB(K)) .GE. MPW(K)) GO TO 216
     IF(ABS(DMBW(K)) .GE. MPW(K)) GO TO 217
 215 MOMWB(K)= SBW(K)*(2.0*ROTFF(ITER,K)+4.0*ROTF(M,K)-6.0*ROB(K))
     GO TO 218
 216 MOMWB(K)=DMWB(K)
     GO TO 218
 217 MOMWB(K)=SBW(K)*(3.0*ROTF(M,K)-3.0*ROB(K))+0.5*DMBW(K)
 218 SHEARW(K)=(MOMBW(K)+MOMWB(K))/HBW(K)
     MOMW(K)=-MOMWB(K)-SHEARW(K)*DW(K)/2.0
```

```
      F(M+1,K)=-FOC(K)
      SHEAR(1)=SHEAR(1)+F(M+1,K)
219 CONTINUE
      IF(NS .EQ. 1) GO TO 227
      DO 226 K=2,NS
      SHEAR(K)=SHEAR(K-1)-F(M+1,K-1)
226 CONTINUE
227 IF(M .EQ. 1) GO TO 232
      IF(M .EQ. MAX) GO TO 221
      DO 220 N=1,NS
      IF(ABS((DEFF(M,N)-DEFF(M-1,N))/DEFF(M,N)) .GE. CON .OR. ABS((ROTF(
     1M,N)-ROTF(M-1,N))/RCTF(M,N)) .GE. CON) GO TO 232
220 CONTINUE
      GO TO 223
221 WRITE(6,222) MMMM
222 FORMAT(10X,'CYCLE NO.=',I3,7X,'CONVERGENCE (CALCULATION ON WALL) W
     1AS NOT ENOUGH'/)
223 NCYCLE=M
      SHEAR(1)=0.0
      DO 224 N=1,NS
      CDEFF(MMMM,N)=DEFF(NCYCLE,N)
      CROTF(MMMM,N)=ROTF(NCYCLE,N)
      IF(MMMM .EQ. 1) CSHEC(N)=SHEC(N)
      SHEAR(1)=SHEAR(1)+F(1,N)
224 CONTINUE
      IF(NS .EQ. 1) GO TO 230
      DO 225 K=2,NS
      SHEAR(K)=SHEAR(K-1)-F(1,K-1)
225 CONTINUE
230 DO 231 K=1,NS
      SHEAR(K)=SHEAR(K)+SHEC(K)
231 CONTINUE
      RETURN
232 CONTINUE
      RETURN
      END
```

IN SUBROUTINE FRAME, THE JOINT ROTATIONS OF THE FRAME FOR A
SWAYED POSITION (ENFORCED BY THE WALL) ARE COMPUTED.
THIS IS PERFORMED BY GAUSS-SEIDEL ITERATION METHOD. IF A HINGE
FORMS IN THE STRUCTURE THE JOINT ROTATION EQUATION IS MODIFIED.


```
      SUBROUTINE FRAME (MAX,ROTFF,ROTO,SC,ROS,KC,SBW,SBF,ROB,ROTF,NS,ITE
     1R,MMMM,M,DMCB,DMCT,DMBW,DMWB,CMBF,DMFB,MPC,MPF,MPW,NJ,CON)
      DIMENSION ROTFF(99,31),ROTO(99),SC(31),ROS(31),SBW(30),SBF(30),ROB
     1(30),ROTF(99,30),DMCB(31),DMCT(31),DMBW(30),DMWB(30),DMBF(30),
     2DMFB(30),AA(30),BB(30),CC(30),DD(30),EE(30),FF(30),GG(30),HH(30),B
     3A(30)
      REAL KC,MPC(31) ,MPF(30),MPW(30)
      COMMON IUNB
      DO 174 I=1,MAX
      IF(I .GT. 1) GO TO 164
      DO 163 K=1,NS
      ROTFF(1,K)=0.0
  163 CONTINUE
  164 N=I
      IF(N .EQ. 1) GO TO 165
      N=N-1
  165 SC(NS+1)=0.0
      ROS(NS+1)=ROS(NS)
      ROTFF(N,NS+1)=ROTFF(N,NS)
      MPC(NS+1)=500.0
      DMCB(NS+1)=0.0
      DMCT(NS+1)=0.0
      IF(NJ .EQ. 1) GO TO 10
      IF(ABS(DMCB(1)) .GE. MPC(1)) GO TO 20
      IF(ABS(DMCT(1)) .GE. MPC(1)) GO TO 11
   10 ROTO(I)=(6.0*SC(1)*ROS(1)-2.0*SC(1)*ROTFF(N,1))/(4.0*SC(1)+KC)
      GO TO 20
   11 ROTO(I)=(3.0*SC(1)*ROS(1)-0.5*DMCT(1))/(3.0*SC(1)+KC)
   20 DO 170 J=1,NS
      IF(NJ .EQ. 1) GO TO 21
      IF(ABS(DMBW(J)) .GE. MPW(J)) GO TO 30
      IF(ABS(DMWB(J)) .GE. MPW(J)) GO TO 40
   21 AA(J)=SBW(J)*(6.0*ROB(J)-2.0*ROTF(M,J))
      EE(J)=4.0*SBW(J)
      GO TO 50
   30 AA(J)=-DMBW(J)
      EE(J)=0.0
      GO TO 50
   40 AA(J)=3.0*SBW(J)*ROB(J)-0.5*DMWB(J)
      EE(J)=3.0*SBW(J)
   50 IF(NJ .EQ. 1) GO TO 51
      IF(ABS(DMBF(J)) .GE. MPF(J)) GO TO 60
      IF(ABS(DMFB(J)) .GE. MPF(J)) GO TO 70
   51 BB(J)=0.0
      FF(J)=6.0*SBF(J)
      GO TO 80
   60 BB(J)=-DMBF(J)
```

```
      FF(J)=0.0
      GO TO 80
70    BB(J)=-0.5*DMFB(J)
      FF(J)=3.0*SBF(J)
80    IF(NJ .EQ. 1) GO TO 81
      IF (ABS(DMCT(J)) .GE. MPC(J)) GO TO 90
      IF (ABS(DMCB(J)) .GE. MPC(J)) GO TO 100
81    IF(J .EQ. 1) GO TO 82
      CC(J)=SC(J)*(6.0*ROS(J)-2.0*ROTFF(I,J-1))
      GO TO 83
82    CC(J)=SC(J)*(6.0*ROS(J)-2.0*ROTO(I))
83    GG(J)=4.0*SC(J)
      GO TO 110
90    CC(J)=-DMCT(J)
      GG(J)=0.0
      GO TO 110
100   CC(J)=3.0*SC(J)*ROS(J)-0.5*DMCB(J)
      GG(J)=3.0*SC(J)
110   IF(NJ .EQ. 1) GO TO 111
      IF(ABS(DMCB(J+1)) .GE. MPC(J+1)) GO TO 120
      IF(ABS(DMCT(J+1)) .GE. MPC(J+1)) GO TO 130
111   DD(J)=SC(J+1)*(6.0*ROS(J+1)-2.0*ROTFF(N,J+1))
      HH(J)=4.0*SC(J+1)
      GO TO 140
120   DD(J)=-DMCB(J+1)
      HH(J)=0.0
      GO TO 140
130   DD(J)=3.0*SC(J+1)*ROS(J+1)-0.5*DMCT(J+1)
      HH(J)=3.0*SC(J+1)
140   BA(J)=EE(J)+FF(J)+GG(J)+HH(J)
      IF(ABS(BA(J)) .LT. 0.0001) GO TO 170
      ROTFF(I,J)=(AA(J)+BB(J)+CC(J)+DD(J))/BA(J)
170   CONTINUE
171   ITER=I
      IF(ITER .EQ. 1)GO TO 174
      IF(ABS(DMCB(1)) .GE. MPC(1)) GO TO 176
      IF(IUNB.EQ.1)GO TO 176
      IF(ABS((ROTO(I)-ROTO(I-1))/ROTO(I)) .GT. CON ) GO TO 173
176   DO 172 K=1,NS
      IF(ABS(BA(K)) .LE. C.0001) GO TO 172
      IF(ABS((ROTFF(I,K)-ROTFF(I-1,K))/ROTFF(I,K)) .GT. CON )GO TO 173
172   CONTINUE
      RETURN
173   IF(I .EQ. MAX) GO TO 175
174   CONTINUE
175   WRITE(6,181) M,MMMM
181   FORMAT(10X,'CYCLE NO.=',I3,2X,'TO',I3,7X,'CONVERGENCE (CALCULATION
     1 ON FRAME) WAS NOT ENOUGH'/)
      RETURN
      END
```

```
C
C
C      OUTPUT STATEMENTS FOR FRAME FORCES AND DEFORMATIONS
C
C
       SUBROUTINE ROFA (ROTFF,SHEC,FOC,DMCB,DMCT,ROTO,NS,NCYCLE,ITER,MM
      1)
       DIMENSION ROTFF(99,30),SHEC(30),FOC(30),ROTO(30),DMCB(30),CMCT(3
       COMMON IUNB
       WRITE(6,371)
  371  FORMAT(50X,28HRESULTS   OF   FRAME   ANALYSIS///)
       WRITE(6,372) MMMM,NCYCLE
  372  FORMAT(10X, 'CYCLE NO.   MMMM=',I3,2X,'NCYCLE=',I3///)
       WRITE(6,200)
  200  FORMAT(10X,7HCOLUMNS//)
       WRITE(6,373)
  373  FORMAT(10X,10HFLOOR NO./,3X,19HJOINT ROTATION(RAD),3X,18HBOTTOM
      1MENT(KIN),3X,16HTOP   MOMENT(KIN),3X,10HSHEAR(KIP),3X,10HFORCE(KI
      2)
       WRITE(6,374)
  374  FORMAT(10X,9HSTORY NO.//)
       WRITE(6,375)ROTO(ITER)
  375  FORMAT(12X,4HBASE,10X,E13.6/)
       DO 377 K =1,NS
       WRITE(6,378)K,ROTFF(ITER,K),DMCB(K),DMCT(K),SHEC(K),FOC(K)
  378  FORMAT(13X,I3,10X,E13.6,8X,F14.2,6X,F14.2,4X,F10.2,3X,F10.2/)
  377  CONTINUE
  814  WRITE(6,386)
  386  FORMAT(1HK)
       WRITE(6,201)
  201  FORMAT(//10X,5HBEAMS//)
       WRITE(6,380)
  380  FORMAT(10X,9HFLOOR NO.,3X,16HMOMENT   IN   WALL,3X,16HMOMENT   IN
      1LL,3X,16HMOMENT AT COLUMN,3X,16HMOMENT AT ROLLER,3X,14HSHEAR   AT
      2THE,3X,14HSHEAR   AT   THE)
       WRITE(6,381)
  381  FORMAT(22X,16HSIDE BEAM AT THE,3X,16HSIDE BEAM AT THE,3X,16HEND
      1   THE BEAM,3X,16HEND OF   THE BEAM,3X,14HENDS   OF   WALL,3X,14HEND
      2 OF   BEAM)
       WRITE(6,382)
  382  FORMAT(22X,16HCOLUMN END(K-IN),3X,16HWALL   END (K-IN),3X,16HON
      1LLER(K-IN),3X,16HON   ROLLER(K-IN),3X,14HSIDE BEAM(KIP),3X,14HON
      2LLER(KIP)//)
       RETURN
C
C
C
       END
```

```
C
C
C         OUTPUT STATEMENTS FOR SHEAR WALL FORCES AND DEFORMATIONS
C
C
          SUBROUTINE SR3 (BMOMF,TMOMF,ROTB,NS,F11,FOC,SHEAR,ROTF,DEFF,CROTF,
         1CDEFF,MMMM)
          DIMENSION F11(30),FOC(30),SHEAR(30),ROTF(99,30),DEFF(99,30),
         1CROTF(99,30),CDEFF(99,30),BMOMF(30),TMOMF(30)
          COMMON IUNB
          WRITE(6,55)
   55     FORMAT(39X,52HSHEAR WALL ANALYSIS AND FINAL SLOPES AND DEFLECTIONS
         1///)
          WRITE(6,312)
  312     FORMAT(3X,10HFLOOR NO./,3X,15HWALL FORCE(KIP),3X,16HFRAME FORCE(K
         1IP),3X,15HWALL SHEAR(KIP),9X,17HWALL MOMENT(K-IN),9X,10HSLOPE(RAD)
         23X,14HDEFLECTION(IN))
          WRITE(6,401)
  401     FORMAT(3X,9HSTORY NO.,62X,6HBOTTOM,13X,3HTOP//)
          WRITE(6,20)ROTB
   20     FORMAT(5X,4HBASE,93X,E13.6/)
          DO 400 K=1,NS
          WRITE(6,313) K,F11(K),FOC(K),SHEAR(K),BMOMF(K),TMOMF(K),ROTF(1,K)
         1DEFF(1,K)
  313     FORMAT(6X,I3,7X,F8.2,11X,F8.2,9X,F10.2,5X,F14.2,3X,F14.2,4X,E13.6
         13X,E13.6/)
  400     CONTINUE
          WRITE(6,404)
  404     FORMAT(1HK,50X,31HCHECK ON SLOPES AND DEFLECTIONS//)
          WRITE(6,405)
  405     FORMAT(5X,9HFLOOR NO.,5X,10HSLOPE(RAD),4X,14HDEFLECTION(IN)//)
          DO 402 N=1,NS
          WRITE(6,403) N,CROTF(MMMM,N),CDEFF(MMMM,N)
  403     FORMAT(8X,I3,7X,E13.6,4X,E13.6/)
  402     CONTINUE
          RETURN
          END
```

```
C
C
C       IN SUBROUTINE SR1 FORMATION OF PLASTIC HINGE IN A MEMBER  OF
C       THE FRAME IS DETECTED
C
C
        SUBROUTINE SR1  (DMFB,DMBF,DMBW,DMWB,DMCT,DMCB,MOMFB,MOMBF,MOMBW,MO
     1MWB,MMCT,MMCB, NS, M3, MPF,MPW,MPC)
        DIMENSION DMFB(30),DMBF(30),DMBW(30),DMWB(30),DMCT(30),DMCB(30)
        REAL      MOMFB(30),MOMBF(30),MOMBW(30),MOMWB(30),MMCT(30),
     1MMCB(30),MPF(30),MPW(30),MPC(30)
        COMMON IUNB
        M3=0
        DO 403 K=1,NS
        DMFB(K)=MOMFB(K)
        DMBF(K)=MOMBF(K)
        DMBW(K)=MOMBW(K)
        DMWB(K)=MOMWB(K)
        DMCT(K)=MMCT(K)
        DMCB(K)=MMCB(K)
  403   CONTINUE
C
C
        DO 610 K=1,NS
        WRITE(6,633)
  633   FORMAT(1HK)
        IF((ABS(DMCB(K))).LT.MPC(K))GO TO 616
        M3=M3+1
        WRITE(6,617)K,DMCB(K)
  617   FORMAT(10X,50HHINGE  AT  BOTTOM  POINT  OF  COLUMN  IN  STORY NO.,I
     13,5X,40HMOMENT    AT  BOTTOM  POINT  OF  COLUMN =,F14.2,5H K-IN/)
        IF(DMCB(K) .LT. 0.0) GO TO 10
        DMCB(K)=MPC(K)+0.0001
        GO TO 616
   10   DMCB(K)=-MPC(K)-0.0001
  616   IF((ABS(DMCT(K))).LT.MPC(K))GO TO 602
        M3=M3+1
        WRITE(6,618)K,DMCT(K)
  618   FORMAT(10X,50HHINGE  AT    TOP    POINT  OF  COLUMN  IN  STORY NO.,I
     13,5X,40HMOMENT    AT    TOP    POINT  OF  COLUMN =,F14.2,5H K-IN/)
        IF(DMCT(K) .LT. 0.0) GO TO 20
        DMCT(K)=MPC(K)+0.0001
        GO TO 602
   20   DMCT(K)=-MPC(K)-0.0001
  602   IF((ABS(DMFB(K))).LT.MPF(K))GO TO 604
        M3=M3+1
        WRITE(6,603)K,DMFB(K)
  603   FORMAT(10X,50HHINGE AT ROLLER END OF BEAM ON ROLLER OF FLOOR NO.,I
     13,5X,40HMOMENT AT ROLLER END OF BEAM ON ROLLER =,F14.2,5H K-IN/)
        IF(DMFB(K) .LT. 0.0) GO TO 30
        DMFB(K)=MPF(K)+0.0001
        GO TO 604
   30   DMFB(K)=-MPF(K)-0.0001
  604   IF((ABS(DMBF(K))).LT.MPF(K))GO TO 606
        M3=M3+1
```

```
      WRITE(6,605)K,DMBF(K)
  605 FORMAT(10X,50HHINGE AT COLUMN END OF BEAM ON ROLLER OF FLOOR NO.,I
     13,5X,40HMOMENT AT COLUMN END OF BEAM ON ROLLER =,F14.2,5H K-IN/)
      IF(DMBF(K) .LT. 0.0) GO TO 40
      DMBF(K)=MPF(K)+0.0001
      GO TO 606
   40 DMBF(K)=-MPF(K)-0.0001
  606 IF((ABS(DMBW(K))).LT.MPW(K))GO TO 608
      M3=M3+1
      WRITE(6,607)K,DMBW(K)
  607 FORMAT(10X,50HHINGE AT COLUMN END OF WALL SIDE BEAM OF FLOOR NO.,I
     13,5X,40HMOMENT AT COLUMN END OF WALL SIDE BEAM =,F14.2,5H K-IN/)
      IF(DMBW(K) .LT. 0.0) GO TO 50
      DMBW(K)=MPW(K)+0.0001
      GO TO 608
   50 DMBW(K)=-MPW(K)-0.0001
  608 IF((ABS(DMWB(K))).LT.MPW(K))GO TO 610
      M3=M3+1
      WRITE(6,609)K,DMWB(K)
  609 FORMAT(10X,50HHINGE AT  WALL  END OF WALL SIDE BEAM OF FLOOR NO.,I
     13,5X,40HMOMENT AT  WALL END OF WALL SIDE BEAM  =,F14.2,5H K-IN/)
      IF(DMWB(K) .LT. 0.0) GO TO 60
      DMWB(K)=MPW(K)+0.0001
      GO TO 61C
   60 DMWB(K)=-MPW(K)-0.0001
  610 CONTINUE
      RETURN
      END
```

APPENDIX C

DERIVATION OF MOMENT-THRUST-CURVATURE RELATIONSHIP

FOR REINFORCED CONCRETE CROSS-SECTION

C.1 Cross-Section

The cross-section considered is shown in FIGURE C.1. The nomenclature used to define the cross-section is also shown. The subscript n refers to the total number of layers of steel. The steel layers are numbered starting from the tension face. Only rectangular cross-sections are considered. The stress-strain curves of the concrete and steel are defined in section 4.2.1 and 4.2.2, respectively.

The corresponding areas of steel, A_{sn} and percentages, $P_{tn} = \dfrac{A_{sn}}{bt}$ of steel in each layer are given by A_{s1}, A_{s2}, A_{s3}...., A_{sn} and P_{t1}, P_{t2}, P_{t3}......, P_{tn} respectively. The total area and percentage of steel are given by equations (C.1) and (C.2).

$$A_{st} = A_{s1} + A_{s2} + A_{s3} + \ldots\ldots + A_{sn} \qquad \ldots\ldots(C.1)$$

$$P_t = P_{t1} + P_{t2} + P_{t3} + \ldots\ldots + P_{tn} \qquad \ldots\ldots(C.2)$$

The strain in various layers of steel, starting from tension face are given by $\varepsilon(1)$, $\varepsilon(2)$,......., $\varepsilon(n)$ whereas the strains at the extreme fibre of the section are given by ε_4 and ε_1 at compressive and tensile (or least compressed) face respectively. The positive value of ε_1 shows compression on the tensile face whereas negative value shows tension on the tensile face. FIGURE (C.1) also shows a typical strain configuration. For any strain configuration the following hold true.

The curvature, ϕ, is given by:

$$\phi = \frac{\varepsilon_4 - \varepsilon_1}{t}$$

or $\quad \phi t = \varepsilon_4 - \varepsilon_1$ $\qquad\qquad\qquad$ ....(C.3)

The strain, ε, at any depth, h, from compression face is given by:

$$\varepsilon = \varepsilon_4 - \phi h \qquad\qquad\qquad ....(C.4)$$

The strain in any layer of steel is given by:

$$\varepsilon(n) = \varepsilon_4 - \phi t(1 - \frac{dn}{t}) \qquad\qquad ....(C.5)$$

The stress, f_{sn}, in any layer of steel is given by:

$$f_{sn} = \varepsilon(n) \times E_s \leq f_y \qquad\qquad ....(C.6)$$

Where E_s is the modulus of elasticity of reinforcing steel and f_y is the yield strength.

The total axial force in the reinforcing steel will be given by:

$$P_s = A_{s1} f_{s1} + A_{s2} f_{s2} + \quad ...... + A_{sn} f_{sn}$$

or $\quad A = \dfrac{P_s}{btf_c''} = \dfrac{1}{f_c''} \times (P_{t1}\, f_{s1} + P_{t2} f_{s2} + ... + P_{tn} f_{sn})$

$$\qquad\qquad\qquad\qquad\qquad\qquad ....(C.7)$$

The moment contribution of these steel layers will be given by:

$$M_s = -A_{s1}f_{s1}\left(\frac{t}{2} - d_1\right) - A_{s2}f_{s2}\left(\frac{t}{2} - d_2\right) \ldots - A_{sn}f_{sn}\left(\frac{t}{2} - d_n\right)$$

$$\text{or} \quad B = \frac{M_s}{bt^2f''_c} = -\frac{1}{2f''_c}\left\{P_{t1}f_{s1}\left(1 - \frac{2d_1}{t}\right) + \ldots + P_{tn}f_{sn}\left(1 - \frac{2dn}{t}\right)\right\}$$

$$\ldots (C.8)$$

The derivations of loads and moments relating curvature and fibre strains for different possible strain domains are described below. The reduction in the gross area of concrete due to presence of steel has been neglected.

C.1.1 Sections under Compression Strain Only

This strain configuration is shown in FIGURE (C.1). Considering an element of depth dh, at a depth h from top, where the concrete stress is f_c, the axial load and moment will be given by:

$$\frac{P}{btf''_c} = A + \frac{1}{btf''_c} \int_o^t bf_c dh \qquad \ldots (C.9)$$

$$\text{and} \quad \frac{M}{bt^2f''_c} = B + \frac{1}{bt^2f''_c} \int_o^t bf_c\left(\frac{t}{2} - h\right)dh \quad \ldots (C.10)$$

Substituting the value of f_c from equation (4.1) and integrating we have:

$$\frac{P}{btf''_c} = A + \frac{\varepsilon_4 + \varepsilon_1}{\varepsilon_0} - \frac{0.386}{(\varepsilon_0)^{1.67}{}_{\phi t}} \{(\varepsilon_4)^{2.67} - (\varepsilon_1)^{2.67}\}$$

$$\ldots\text{(C.11)}$$

$$\text{and} \quad \frac{M}{bt^2 f''_c} = B + \frac{\phi t}{6\varepsilon_0} - \frac{0.193}{(\varepsilon_0)^{1.67}{}_{\phi t}} \{(\varepsilon_1)^{2.67} + (\varepsilon_4)^{2.67}\}$$

$$+ \frac{0.105}{(\varepsilon_0)^{1.67}(\phi t)^2} \{(\varepsilon_4)^{3.67} - (\varepsilon_1)^{3.67}\} \quad \ldots\text{(C.12)}$$

C.1.2 Pure Axial Load Capacity

In the case of uniform strain over the cross-section the curvature becomes zero and equations (C.11) and (C.12) do not hold true, since M will be zero in this case. Therefore the value of P in this case can be found by integrating the uniform stress over the section which will be given by:

$$\frac{P}{btf''_c} = A + \frac{2\varepsilon_4}{\varepsilon_0} - 1.03 \left(\frac{\varepsilon_4}{\varepsilon_0}\right)^{1.67} \quad \ldots\text{(C.13)}$$

$$M = 0 \quad \ldots\text{(C.14)}$$

$$\text{and} \quad \phi = 0 \quad \ldots\text{(C.15)}$$

For the stress-strain curve presented in section 4.2.1, this will lead to a maximum value of P when $\varepsilon_4 = 1.252\varepsilon_0$. Thus the pure axial load capacity of, the section allowing for the reduction in gross area of concrete due to presence of steel, will be given by:

$$\frac{P_o}{btf''_c} = A + 1.002 \ (1-p_t) \qquad\qquad \dots.(C.16)$$

These values are essentially similar to those presented in reference (A1).

C.1.3 Sections Partly in Tension but Uncracked

The strain configuration is shown in FIGURE (C.2).

The depth of neutral axis DN, is given by:

$$DN = \varepsilon_4 \ /\phi$$

The axial load and moment for this strain configuration will be given by:

$$\frac{P}{btf''_c} = A + \frac{1}{btf''_c} \ \{ \int_o^{DN} bf_c dh + \int_{DN}^t bf_t dh\} \ \dots.(C.17)$$

$$\text{and } \frac{M}{bt^2f''_c} = B + \frac{1}{bt^2f''_c} \ \{ \int_o^{DN} bf_c(\frac{t}{2} - h)dh + \int_{DN}^t bf_t(\frac{t}{2}-h)dh\}$$

$$\dots.(C.18)$$

Substituting the values of f_c and f_t from equations (4.1) and (4.2) and integrating, we have

$$\frac{P}{btf''_c} = A + \frac{(\varepsilon_4)^2}{\varepsilon_o \phi t} - \frac{0.386(\varepsilon_4)^{2.67}}{(\varepsilon_o)^{1.67} \phi t}$$

$$+ \{ \frac{(\varepsilon_1)^2}{\varepsilon_{ult}\phi t} - \frac{(\varepsilon_1)^4}{4(\varepsilon_{ult})^3} \}_{\phi t} \frac{f'_t}{f''_c} \qquad \dots.(C.19)$$

$$\text{and}\quad \frac{M}{bt^2 f_c''} = B + \frac{(\varepsilon_4)^2}{2\varepsilon_0 \phi t} - \frac{(\varepsilon_4)^3}{3\varepsilon_0 (\phi t)^2}$$

$$- \frac{0.193(\varepsilon_4)^{2.67}}{(\varepsilon_0)^{1.67}\phi t} + \frac{0.105(\varepsilon_4)^{3.67}}{(\varepsilon_0)^{1.67}(\phi t)^2}$$

$$- \frac{f_t'}{f_c''}\left\{\frac{(\varepsilon_1)^2}{2\varepsilon_{ult}\phi t} + \frac{(\varepsilon_1)^3}{3\varepsilon_{ult}(\phi t)^2} - \frac{(\varepsilon_1)^4}{8(\varepsilon_{ult})^3}\phi t\right.$$

$$\left. - \frac{(\varepsilon_1)^5}{20(\varepsilon_{ult})^3 (\phi t)^2}\right. \qquad \ldots\text{(C.20)}$$

C.1.4 Section Partly In Tension and Cracked

The strain configuration is shown in FIGURE (C.3).

The depth of neutral axis, DN, and the depth below which the section is cracked, dcr, are given by:

$$DN = \varepsilon_4/\phi$$

$$\text{and}\quad dcr = \frac{\varepsilon_4 - \varepsilon_{ult}}{\phi}$$

The axial load and moment for this strain configuration will be given by:

$$\frac{P}{btf_c''} = A + \frac{1}{btf_c''}\left\{\int_0^{DN} bf_c\,dh + \int_{DN}^{dcr} bf_t\,dh\right\} \quad\ldots\text{(C.21)}$$

and

$$\frac{M}{bt^2 f_c''} = B + \frac{1}{bt^2 f_c''}\left\{\int_0^{DN} bf_c\left(\frac{t}{2} - h\right)dh\right.$$

$$\left. + \int_{DN}^{dcr} bf_t\left(\frac{t}{2} - h\right)dh\right\} \qquad \ldots\text{(C.22)}$$

Substituting the values of f_c and f_t from equations (4.1) and (4.2) we have

$$\frac{P}{btf''_c} = A + \frac{(\varepsilon_4)^2}{\dot{\varepsilon}_0 \, \phi t} - \frac{0.386(\varepsilon_4)^{2.67}}{(\dot{\varepsilon}_0)^{1.67} \, \phi t} + \frac{f'_t}{f''_c} \cdot \frac{3\varepsilon_{ult}}{4 \, \phi t}$$

$$\ldots\ldots (C.23)$$

$$\frac{M}{bt^2 f''_c} = B + \frac{(\varepsilon_4)^2}{2\varepsilon_0 \phi t} - \frac{(\varepsilon_4)^3}{3\varepsilon_0 (\phi t)^2} - \frac{0.193(\varepsilon_4)^{2.67}}{(\dot{\varepsilon}_0)^{1.67} \, \phi t}$$

$$+ \frac{0.105(\varepsilon_4)^{3.67}}{(\dot{\varepsilon}_0)^{1.67} \, (\phi t)^2} + \frac{f'_t}{f''_c} \left\{ \frac{3\varepsilon_{ult}}{4 \, \phi t} \left(\frac{1}{2} - \frac{\varepsilon_4}{\phi t} \right. \right.$$

$$+ \left. \frac{\varepsilon_{ult}}{\phi t} \right) - \frac{17}{60} \frac{(\varepsilon_{ult})^2}{(\phi t)^2} \qquad \ldots\ldots (C.24)$$
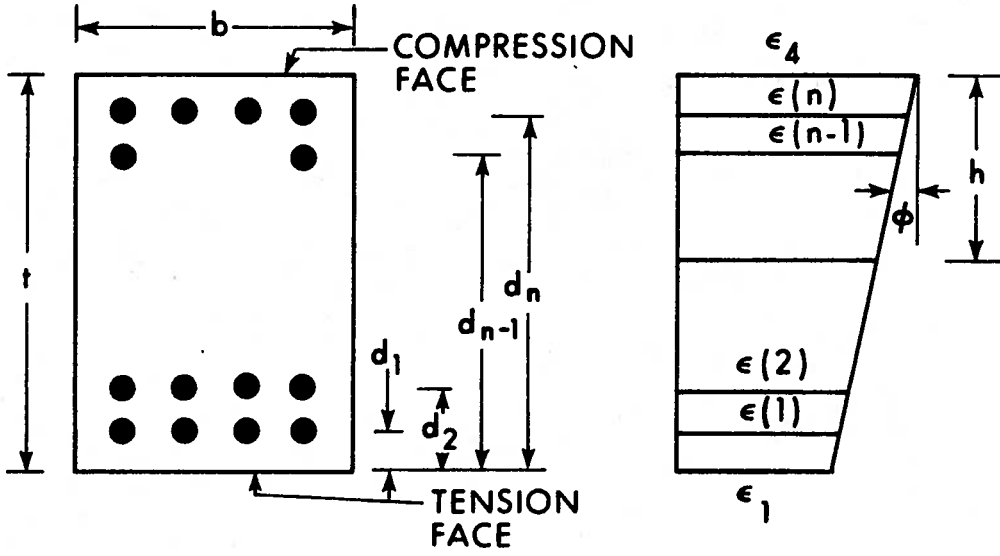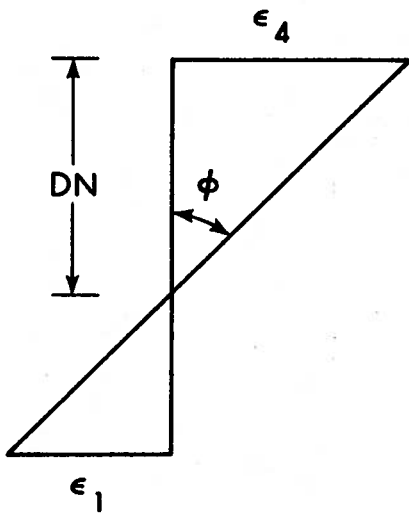
FIGURE C.1

FIGURE C.2
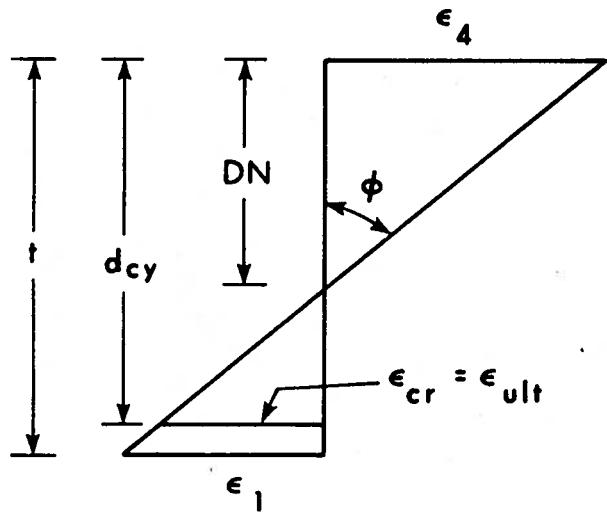
FIGURE C.3

C.2 Program Nomenclature

A
AXIAL LOAD CONTRIBUTION DUE TO REINFORCEMENT IN THE FORM OF P/bt IN lbs. AND INCH UNIT

AL
GIVEN AXIAL LOAD ON SECTION IN lbs.

AS(N)
AREA OF REINFORCEMENT IN Nth LAYER IN IN^2

B
WIDTH OF SECTION (IN MAIN PROGRAM) IN INCHES

B
MOMENT CONTRIBUTION DUE TO REINFORCEMENT IN THE FORM OF $(-^{2M}/bt^2)$, IN SUBROUTINE PM.

C(N)
DISTANCE OF CENTROID OF STEEL REINFORCEMENT IN Nth LAYER FROM BOTTOM FACE IN INCHES.

DT(N)
THE RATIO C(N)/T

EAV
STRAIN AT MID-DEPTH OF SECTION

EC
MODULUS OF ELASTICITY OF CONCRETE IN lbs/IN^2

ECC
ECCENTRICITY OF AXIAL LOAD IN INCHES

EO
ε_o (AS DEFINED IN EQUATION 4.1)

ES
MODULUS OF ELASTICITY OF STEEL IN lbs/IN^2

EU
LIMIT ON COMPRESSIVE FIBRE STRAIN, ε_4

EUL
CRACKING STRAIN, ε_{ult}

E1
STRAIN AT BOTTOM FACE OF SECTION

E4
STRAIN AT TOP FACE OF SECTION

FC1
CONCRETE STRENGTH IN DIRECT COMPRESSION, f'_c, in psi

FC2
CONCRETE STRENGTH IN FLEXURE, $0.85f'_c$, in psi

FS(N)
STRESS IN Nth LAYER OF STEEL IN PSI

FY
YIELD STRENGTH OF REINFORCEMENT IN PSI

FT2
CONCRETE STRENGTH IN TENSION IN PSI

M	MOMENT IN THE FORM OF $M/bt^2 f_c''$
NL	NUMBER OF REINFORCING LAYERS
NP	NUMBER OF PROBLEMS TO BE ANALYZED
P	AXIAL LOAD IN THE FORM OF $P/bt f_c''$
PG	GIVEN AXIAL LOAD IN THE FORM OF $P/bt f_c''$
PHIT	CURVATURE TIMES THE DEPTH OF SECTION
PO	ULTIMATE AXIAL LOAD IN THE FORM OF $P/bt f_c''$
PTL	TOTAL PERCENTAGE OF STEEL IN THE FORM OF A_{st}/bt
PT(N)	PERCENTAGE OF STEEL IN Nth LAYER OF REINFORCEMENT IN THE FORM OF A_{sn}/bt
T	TOTAL DEPTH OF SECTION IN INCHES

C.3 FLOW DIAGRAM OF THE COMPUTER PROGRAM

C.3.1 MAIN PROGRAM

```
       ┌─────────────────────┐
        READ NO. OF PROBLEMS
          TO BE SOLVED
       └─────────────────────┘
                 │
                 ▼
  ┌──┐    ┌─────────────────────┐
  │ 1│───▶│ SET INDEX FOR THE   │
  └──┘    │ PROBLEM             │
   ▲      └─────────────────────┘
   │                │
                    ▼
       ┌─────────────────────┐
        READ AND WRITE DATA
        FOR THE PROBLEM IN
             PROCESS
       └─────────────────────┘
                 │
                 ▼
       ┌─────────────────────┐
       │ COMPUTE ULTIMATE    │
       │ AXIAL LOAD, P_0     │
       └─────────────────────┘
                 │
                 ▼
             ◇ IS
          GIVEN AXIAL LOAD
              ≥                ── YES ──┐
          ULTIMATE AXIAL LOAD           │
                 │ NO                   ▼
                 ▼                    (20)
       ┌─────────────────────┐
       │       SET           │
       │  ε_4 =0    φt=0     │
       └─────────────────────┘
                 │
                 ▼
  ┌──┐   ┌─────────────────────┐
  │37│──▶│ COMPUTE ε_1 AND     │
  └──┘   │ CALL SUBROUTINE 'PM'│
   ▲     └─────────────────────┘
   │                │
                    ▼
```

IS GIVEN AXIAL LOAD, PG, > 0.05

YES

NO

IS ABS(PG-P) ≤ 1%

YES

NO

(36)

(47)

IS ABS(PG-P)≤0.001

YES

NO

(36)

IS ϵ_4>0.004

YES

NO

(39)

INCREASE ϵ_4 BY 0.000001

(37)

(36)

WRITE OUT ALL THE PERTINENT INFORMATION

IS ϵ_4 > 0.004

YES

NO

(20)

INCREASE φt BY 0.0003

NO

IS φt ≥ 0.003

YES

INCREASE φt BY 0.001

(39)

(20)

(39)

END

YES

IS ALL PROBLEM DONE ?

NO

(1)

C.3.2 <u>SUBROUTINE 'PM'</u>

```
┌─────────────────────────┐
│          SET            │
│   A=0.0      B=0.0      │
└─────────────────────────┘
             │
             ▼
┌──────────────────────────────────┐
│ COMPUTE STRESS AND STRAIN IN ALL  │
│ STEEL LAYERS. SET THIS STRESS     │
│ EQUAL TO f_y IN THE LAYER OF STEEL│
│ WHICH HAS YIELDED                 │
└──────────────────────────────────┘
             │
             ▼
┌──────────────────────┐
│  COMPUTE  A  AND  B   │
└──────────────────────┘
             │
             ▼
         ◇ IS φt = 0.0 ◇ ──── YES
             │ NO
             ▼
         ◇ IS ε_1 < 0.0 ◇  ── YES
             │ NO
```

YES — IS $\varepsilon_1 < \varepsilon_{ult}$

IS φt = 0.0 — YES

IS $\varepsilon_1 < 0.0$ — YES

| COMPUTE P AND M FOR UNCRACKED TENSILE FAILURE |
| COMPUTE P AND M FOR COMPRESSION FAILURE |
| COMPUTE P AND M FOR CRACKED TENSILE FAILURE |
| COMPUTE P FOR M AND φ EQUAL TO ZERO |
| COMPUTE ECCENTRICITY |

RETURN

```
      DIMENSION DT(10),PT(10),FS(10),E(10),AS(10),C(10)
      REAL M
      READ(5,105)NP
  105 FORMAT(1X,I3)
      DO 20 JJ=1,NP
      WRITE(6,510)JJ
  510 FORMAT(1HK/54X,'PROBLEM NO.',I2///)
      READ(5,100)ES,FC1,FY,NL,B,T,AL,EUL
  100 FORMAT(1X,E9.1,F7.1,F8.1,I2,2F6.2,F9.1,F9.6)
      READ(5,101)(AS(K),K=1,NL)
  101 FORMAT((1X,10F7.4))
      READ(5,102)(C(L),L=1,NL)
  102 FORMAT((1X,10F7.3))
      DO 15 I=1,NL
      PT(I)=(AS(I)/(B*T))
      DT(I)=(C(I)/T)
   15 CONTINUE
      FC2=0.85*FC1
      EC=57400.0*(FC1**0.5)
      EO=((2.0*FC2)/EC)
      EY=FY/ES
      FT2=7.0*(FC1**0.5)
      EU=0.0040
      WRITE(6,516)
  516 FORMAT(50X,'DATA FOR THE ANALYSIS'////)
      WRITE(6,517)
  517 FORMAT(5X,'E FOR STEEL',3X,'CONC. STRENGTH',3X,'STEEL STRENGTH',3X
     1,'NO. OF STEEL LAYERS',3X,'GIVEN AXIAL LOAD',3X,'CRACKING STRAIN'/
     2)
      WRITE(6,518)ES,FC1,FY,NL,AL,EUL
  518 FORMAT(6X,E9.3,7X,F7.1,9X,F8.1,15X,I2,15X,F9.1,10X,F9.6///)
      PTL=0.0
      WRITE(6,103)
  103 FORMAT(5X,'% OF STEEL',3X,'COVER RATIO'/)
      DO 51 J = 1,NL
      WRITE(6,104)PT(J),DT(J)
  104 FORMAT(7X,F7.4,7X,F6.3/)
      PTL=PTL+PT(J)
   51 CONTINUE
C     FIND ULTIMATE AXIAL LOAD
      PO=(1.002*(1.0-PTL))+((PTL*FY)/FC2)
C     CALCULATIONS OF MOMENTS FOR GIVEN AXIAL LOAD AND CURVATURE
      WRITE(6,514)
  514 FORMAT(34X,'RESULTS FOR THE MOMENT CURVATURE RELATIONSHIP FOR GIVE
     1N AXIAL LOAD'//)
      WRITE(6,513)
  513 FORMAT(5X,'TOP STRAIN',3X,'BOTTOM STRAIN',3X,'AVERAGE STRAIN',5X,'
     1CURVATURE',8X,'ECC.',10X,'AXIAL LOAD',8X,'MOMENT',3X,'GIVEN AXIAL
     2LOAD'/)
      PG=(AL/(B*T*FC2))
      IF(PG.GE.PO)GO TO 20
      E4=0.000
      PHIT=0.0
   37 E1=E4-PHIT
      CALL PM(E4,E1,PHIT,P,M,EO,EUL,FC2,FS,PT,ES,FY,DT,E,FT2,ECC,NL)
      IF(PG.GT.0.05)GO TO 48
      IF((ABS(PG-P)).LE.0.001)GO TO 36
```

```
         GO TO 47
  48     Z=ABS(PG-P)/PG
         IF(Z.LE.0.010)GO TO 36
  47     IF(E4.GT.0.0039995)GO TO 36
  39     E4=E4+0.0000010
         GO TO 37
  36     EAV=(E4+E1)/2.0
         WRITE(6,520)E4,E1,EAV,PHIT,ECC,P,M,PG
 520     FORMAT(6X,F8.6,6X,F8.6,9X,F8.6,8X,F8.4,7X,F8.4,8X,F9.4,6X,F9.4,7X,
        1F9.4/)
         IF(E4.GT.0.0039995)GO TO 20
         IF(PHIT.GT.0.00295)GO TO 45
         PHIT=PHIT+0.0003
         GO TO 39
  45     PHIT=PHIT+0.001
         GO TO 39
  20     CONTINUE
         STOP
         END
```

'PM'

```
      SUBROUTINF PM(E4,E1,PHIT,P,M,EO,EUL,FC2,FS,PT,ES,FY,DT,E,FT2,ECC,N
     1L)
      DIMENSICN FS(10),DT(10),PT(10),E(10)
      REAL M
      A=0.0
      B=0.0
      DO 53 J=1,NL
      E(J)=E4-(PHIT*(1.0-CT(J)))
      FS(J)=E(J)*ES
      IF(E(J).LT.0.0)GO TO 54
      IF(FS(J).GT.FY)FS(J)=FY
      GO TO 55
   54 IF((ABS(FS(J))).GT.FY)FS(J)=-FY
   55 A=A+(PT(J)*FS(J))
      B=B-(PT(J)*(1.0-(2.0*DT(J)))*FS(J))
   53 CONTINUE
      IF(PHIT.EQ.0.0)GO TO 25
      IF(E1.LT.0.0)GO TO 20
C     COMPRESSION FAILURE
      P=(A/(1.0*FC2))+((E4+E1)/EO)-((0.386*((E4**2.67)-(E1**2.67)))/((EO
     1**1.67)*PHIT))
      M=(B/(2.0*FC2))+(PHIT/(6.C*EO))
     1-((0.193*((E4**2.67)+(E1**2.67)))/((EO**1.67)*PHIT))+((0.105*((E4*
     2*3.67)-(E1**3.67)))/((EO**1.67)*(PHIT**2.0)))
      GO TO 21
   20 IF(E1.LT.EUL)GO TO 26
      P=(A/(1.0*FC2))+((E4**2.0)/(EO*PHIT))-((0.386*(E4**2.
     167))/((EO**1.67)*PHIT))+((FT2/FC2)*(((E1**2)/(EUL*PHIT))-(E1**4
     2)/(4.0*(EUL**3)*PHIT)))
      M=(B/(2.0*FC2))+((E4**2.0)/(2.0*EO*PH
     1IT))-((E4**3.0)/(3.0*EO*(PHIT**2.0)))-((0.193*(E4**2.67))/((EO**1.
     267)*PHIT))+((0.105*(E4**3.67))/((EO**1.67)*(PHIT**2.0)))-((FT2/FC2
     3)*(((E1**2)/(2.0*PHIT*EUL))+((E1**3)/(3.0*(PHIT**2.0)*EUL))-((
     4E1**4)/(8.0*PHIT*(EUL**3)))-((E1**5)/(20.0*(PHIT**2.0)*(EUL*
     5*3)))))
      GO TO 21
C     CRACKED TENSILE FAILURE
   26 P=(A/(1.0*FC2))+((E4**2.0)/(EO*PHIT))-((0.386*(E4**2.
     167))/((EO**1.67)*PHIT))+((FT2*0.75*EUL)/(FC2*PHIT))
      M=(B/(2.0*FC2))+((E4**2.0)/(2.0*EO*PH
     1IT))-((E4**3.0)/(3.0*EO*(PHIT**2.0)))-((0.193*(F4**2.67))/((EO**1.
     267)*PHIT))+((0.105*(E4**3.67))/((EO**1.67)*(PHIT**2.0)))+((FT2/FC2
     3)*((((3.0*EUL)/(4.0*PHIT))*(0.5-(E4/PHIT)+(EUL/PHIT)))-(17.0*(EUL*
     4*2)/(60.0*(PHIT**2.0)))))
      GO TO 21
   25 P=(A/FC2)+(2.0*E4/EO)-(1.03*((E4/EO)**1.67))
      M=0.0
      ECC=0.0
   21 IF(P.EQ.0.0)GO TO 22
      ECC=M/P
   22 RETURN
      END
```

APPENDIX D

REDUCTION OF TEST DATA

D.1 <u>Curvature and Fibre Strains from Dial Gauge Readings for Columns and Beams</u>

FIGURE D.1 shows two curvature meter arms mounted on a section of depth (h+g). The dial gauges are located at distances b and c from the centre line of the section as shown. Let ε_4 and ε_1 are the extreme fibre strains as shown. M and (M+1) are the dial gauge number on the station number, N which is numbered (M+1)/2 where M is an odd number. DR(M+1,K) and DR(M,K) indicates the dial readings in Mth and (M+1)th gauge for load increment number K. The dotted line shows the bent position of the section. Therefore, if the strain profile over the cross-section is extended then the average strain over the length, a, at a distance b and c, as shown, from the centre line will be given by:

$$G_4/a \quad = \quad \{DR(M+1,K) - DR(M+1,1) \} \quad /a \qquad ....(D.1)$$

$$G_1/a \quad = \quad \{DR(M,K) - DR(M,1)\} \quad /a \qquad ....(D.2)$$

Therefore the curvature will be given by:

$$\phi \quad = \quad \frac{(G_4 - G_1)}{a(b+c)} \qquad\qquad ....(D.3)$$

and from similar triangles the fibre strains will be given by:

$$\varepsilon_4 \quad = \quad \phi(b+g) + G_1/a \qquad ....(D.4)$$

$$\varepsilon_1 \quad = \quad \phi(b-h) + G_1/a \qquad ....(D.5)$$

The above derived equations hold true for all possible strain configuration.

D.2 Curvature and Fibre Strains for Wall

FIGURE D.2 shows the placing of Whittemore or Demec points at a particular section. The reading on the gauges will give an average strain over the length, a, if divided by the gauge length. Let Y_1, Y_2 and Y_3 represent the strains at a distance X_1, X_2 and X_3 from the inner face of the wall. The strains Y_1, Y_2 and Y_3 are given by the difference in reading at some load increment K and the initial readings divided by the gauge length for the corresponding gauge line. At each load increment a best fit straight line was fitted to the strain readings using least squares. This was done assuming that a straight line distribution of strains existed at every section and the equation of straight line is given by:

$$Y = a_0 + a_1 X \qquad \ldots (D.6)$$

The inner face was taken as the origin. The constant a_0 and a_1 in the above equation can be derived [S1] as follows:

$$\Sigma X = X_1 + X_2 + X_3 \qquad \ldots (D.7)$$

$$\Sigma Y = Y_1 + Y_2 + Y_3 = a_0 n + a_1 \Sigma X \qquad \ldots (D.8)$$

$$\Sigma X^2 = X_1^2 + X_2^2 + X_3^2 \qquad \ldots (D.9)$$

$$\Sigma XY = X_1 Y_1 + X_2 Y_2 + X_3 Y_3 = a_0 \Sigma X + a_1 \Sigma X^2 \qquad \ldots (D.10)$$

where n is the number of known points, in this case, three. Solving equations (D.8) and (D.10) gives:

$$a_1 = \frac{\Sigma Y . \Sigma X - n \Sigma XY}{(\Sigma X)^2 - n \Sigma X^2} \qquad \ldots (D.11)$$

and $\qquad a_0 = \dfrac{\Sigma Y - a_1 \Sigma X}{n}$ $\qquad\qquad$ ....(D.12)

The corrected fibre strains can be computed using equation (D.6) by substituting the value of a_1 and a_0 and proper value of X. To find ε_1 the value of X will be zero whereas ε_4 will be given by substituting t for X.
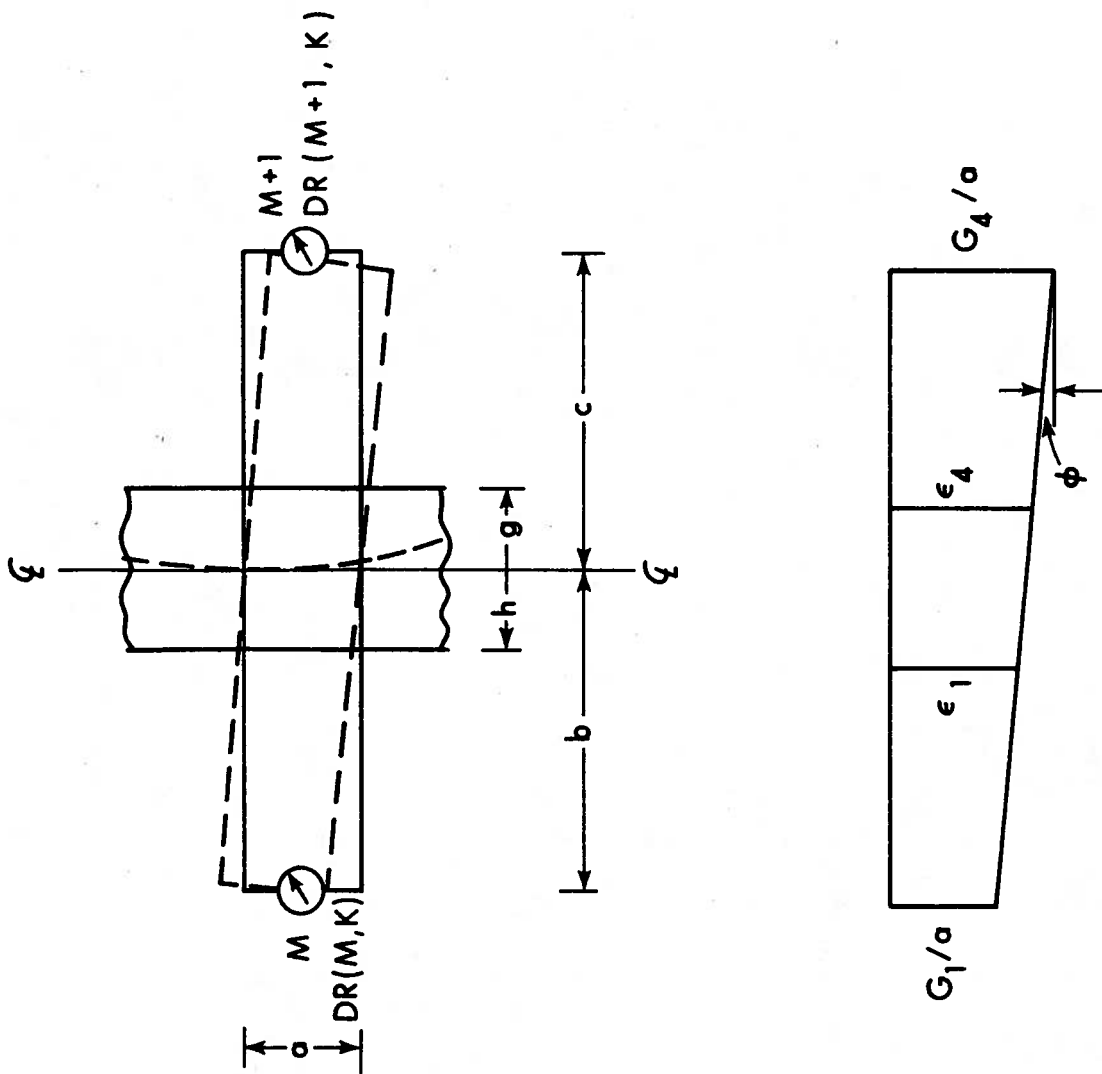
FIGURE D.2
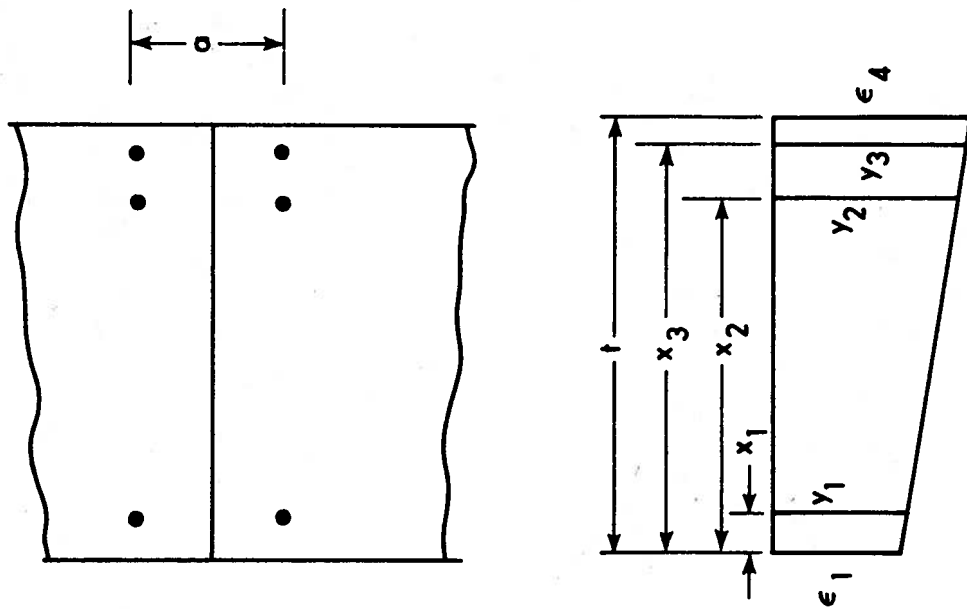
FIGURE D.1

D.3 Program Nomenclature

A(J)	GAUGE LENGTH OF Jth STATION, OVER WHICH THE MEASUREMENT HAS BEEN TAKEN, IN INCHES.
AA	A TEMPORARY LOCATION USED IN SUBROUTINE 'BMKP'.
AS(N,L)	AREA OF REINFORCING STEEL IN THE SECTION AT Nth STATION AND Lth LAYER
AO	A CONSTANT IN THE LEAST SQUARE LINE EQUATION
A1	A CONSTANT IN THE LEAST SQUARE LINE EQUATION
B(J)	DISTANCE OF DIAL GAUGE, IN CURVATURE METER, FROM THE CENTRE LINE OF THE SECTION, AT Jth STATION, TOWARDS OUTER FACE OF COLUMNS OR BOTTOM FACE OF BEAMS, IN INCHES.
BB	A TEMPORARY LOCATION USED IN SUBROUTINE 'BMKP'
BM(N,K)	MOMENT IN KIP-INCH AT Nth STATION FOR Kth LOAD
BMG(I,N)	MOMENT, IN THE GIVEN M-ϕ RELATIONSHIP, CORRESPONDING TO Nth POINT IN Ith CURVE, IN THE FORM OF M/bt^2f_c'' .
C(J)	DISTANCE OF DIAL GAUGE, IN CURVATURE METER, FROM THE CENTRE LINE OF THE SECTION, AT Jth STATION, TOWARDS INNER FACE OF COLUMNS OR TOP FACE OF BEAMS, IN INCHES
CA	TEMPORARY LOCATION USED IN SUBROUTINE 'FSAC'
CB	TEMPORARY LOCATION USED IN SUBROUTINE 'FSAC'
CC	TEMPORARY LOCATION USED IN SUBROUTINE 'BMKP'
CCA	TEMPORARY LOCATION USED IN SUBROUTINE 'FSAC'
CCB	TEMPORARY LOCATION USED IN SUBROUTINE 'FSAC'
CO(N,L)	DISTANCE OF CENTROID OF STEEL IN THE SECTION, In Lth LAYER AND Nth STATION, FROM THE TENSION FACE, IN INCHES

CURV(I,N) CURVATURE, IN GIVEN M-ϕ RELATIONSHIP, CORRESPONDING TO Nth POINT IN Ith CURVE, IN THE FORM OF ϕt.

C1 TEMPORARY LOCATION USED IN MAIN PROGRAM

C2 TEMPORARY LOCATION USED IN MAIN PROGRAM

C3 TEMPORARY LOCATION USED IN MAIN PROGRAM

DR(I,J) READING OF Ith DIAL GAUGE FOR Jth LOAD

DS(J) DISTANCE OF Jth STATION FROM THE BOTTOM OR LEFT END OF THE MEMBER, ON WHICH THE Jth STATION LIES, IN INCHES

ES(J) MODULUS OF ELASTICITY OF STEEL IN Jth MEMBER IN PSI

E1(N,K) STRAIN AT THE OUTER FACE OF COLUMN OR BOTTOM FACE OF BEAM OR INNER FACE OF WALL, AT Nth STATION FOR Kth LOAD

E4(N,K) STRAIN AT THE INNER FACE OF COLUMN OR TOP FACE OF BEAM OR OUTER FACE OF WALL AT Nth STATION FOR Kth LOAD

FC1(J) CONCRETE STRENGTH OF Jth MEMBER IN PSI

FY(J) YIELD STRENGTH OF STEEL IN Jth MEMBER IN PSI

G(J) DISTANCE OF COMPRESSION FACE OF THE SECTION, AT Jth STATION, FROM CENTRE LINE IN INCHES

G4 DIFFERENCE IN DIAL GAUGE READING AT ANY LOAD, FROM THE INITIAL READING ON THE INNER FACE OF COLUMN, OR TOP FACE OF BEAMS OR OUTER FACE OF WALL

G1 DIFFERENCE IN DIAL GAUGE READING AT ANY LOAD, FROM THE INITIAL READING ON THE OUTER FACE OF COLUMN OR BOTTOM FACE OF BEAMS OR INNER FACE OF WALL

H(J) DISTANCE OF TENSION FACE OF THE SECTION, AT Jth STATION, FROM CENTRE LINE IN INCHES

LS(N) NUMBER OF LAYER OF STEEL IN THE SECTION AT Nth STATION

NC TOTAL NUMBER OF CURVATURE METER

ND	TOTAL NUMBER OF DIAL GAUGES IN CURVATURE METERS
NGC	TOTAL NUMBER OF SUPPLIED MOMENT-CURVATURE CURVE
NL	TOTAL NUMBER OF LOAD INCREMENT
NM	TOTAL NUMBER OF MEMBERS IN THE TEST FRAME
NPC(N)	TOTAL NUMBER OF GIVEN POINTS TO DEFINE Nth MOMENT-CURVATURE CURVE
NS	TOTAL NUMBER OF MEASURING STATIONS
NSM(J)	TOTAL NUMBER OF MEASURING STATIONS IN Jth MEMBER
NWD	TOTAL NUMBER OF WHITTEMORE AND DEMEC GAUGES
NWL	NUMBER OF WHITTEMORE OR DEMEC LINES ON WALL
PHI	CURVATURE AT ANY STATION
PHIT(N,K)	CURVATURE TIMES DEPTH OF SECTION AT Nth STATION FOR Kth LOAD
SCX	TEMPORARY LOCATION USED IN SUBROUTINE 'FSAC'
SCX2	TEMPORARY LOCATION USED IN SUBROUTINE 'FSAC'
SX	TEMPORARY LOCATION USED IN SUBROUTINE 'FSAC'
SX2	TEMPORARY LOCATION USED IN SUBROUTINE 'FSAC'
SXY	TEMPORARY LOCATION USED IN SUBROUTINE 'FSAC'
SY	TEMPORARY LOCATION USED IN SUBROUTINE 'FSAC'
W	WIDTH OF TEST FRAME IN INCHES
X(J)	DISTANCE OF Jth LINE FOR WHITTEMORE OR DEMEC GAUGE FROM INNER FACE OF WALL
Y	TEMPORARY LOCATION USED IN SUBROUTINE 'FSAC'

D.4 FLOW DIAGRAM OF THE COMPUTER PROGRAM

D.4.1 MAIN PROGRAM

```
 _____
\  READ ALL THE DATA REQUIRED            \
 \ FOR THE ANALYSIS                       \
  _____/
                    |
                    v
  _____
 \  WRITE OUT ALL THE DATA                \
  \           SUPPLIED                     \
   _____/
                    |
                    v
  _____
 |  CORRECT ALL THE INITIAL               |
 |  GAUGE READINGS AND WRITE              |
 |              OUT                       |
 |_____|
                    |
                    v
              < CALL 'FSAC' >
                    |
                    v
              < CALL 'BMKP' >
                    |
                    v
              (    END    )
```

D.4.2 <u>SUBROUTINE 'FSAC'</u>

```
┌─────────────────────────────────┐
│  COMPUTE FIBRE STRAINS AND      │
│  CURVATURE IN BEAM AND COLUMN   │
│  SECTIONS FOR ALL LOADS         │
└─────────────────────────────────┘
                │
                ▼
┌─────────────────────────────────┐
│  COMPUTE FIBRE STRAINS AND      │
│  CURVATURES IN WALL SECTIONS    │
│  FOR ALL LOADS                  │
└─────────────────────────────────┘
                │
                ▼
  ╱──────────────────────────────────╲
 ╱   WRITE OUT FIBRE STRAINS AND      ╲
╱    CURVATURES AT ALL SECTIONS        ╲
╲    FOR ALL LOADS                     ╱
 ╲────────────────────────────────────╱
                │
                ▼
          ╭─────────────╮
          │   RETURN    │
          ╰─────────────╯
```
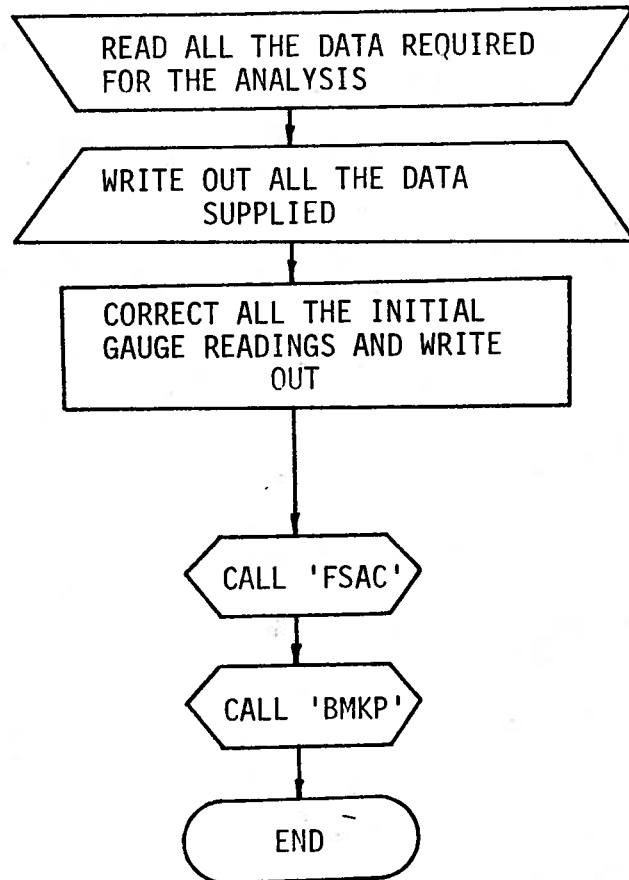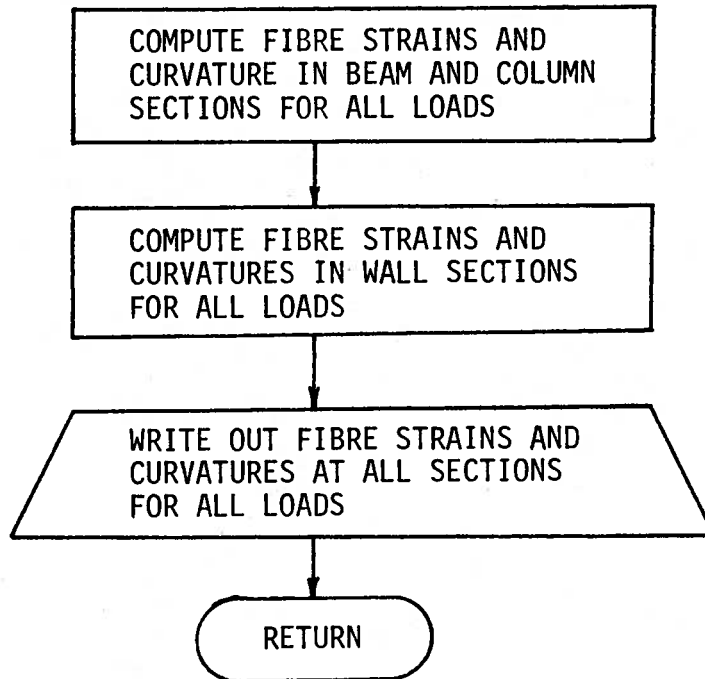
D.4.3 <u>SUBROUTINE 'BMKP'</u>
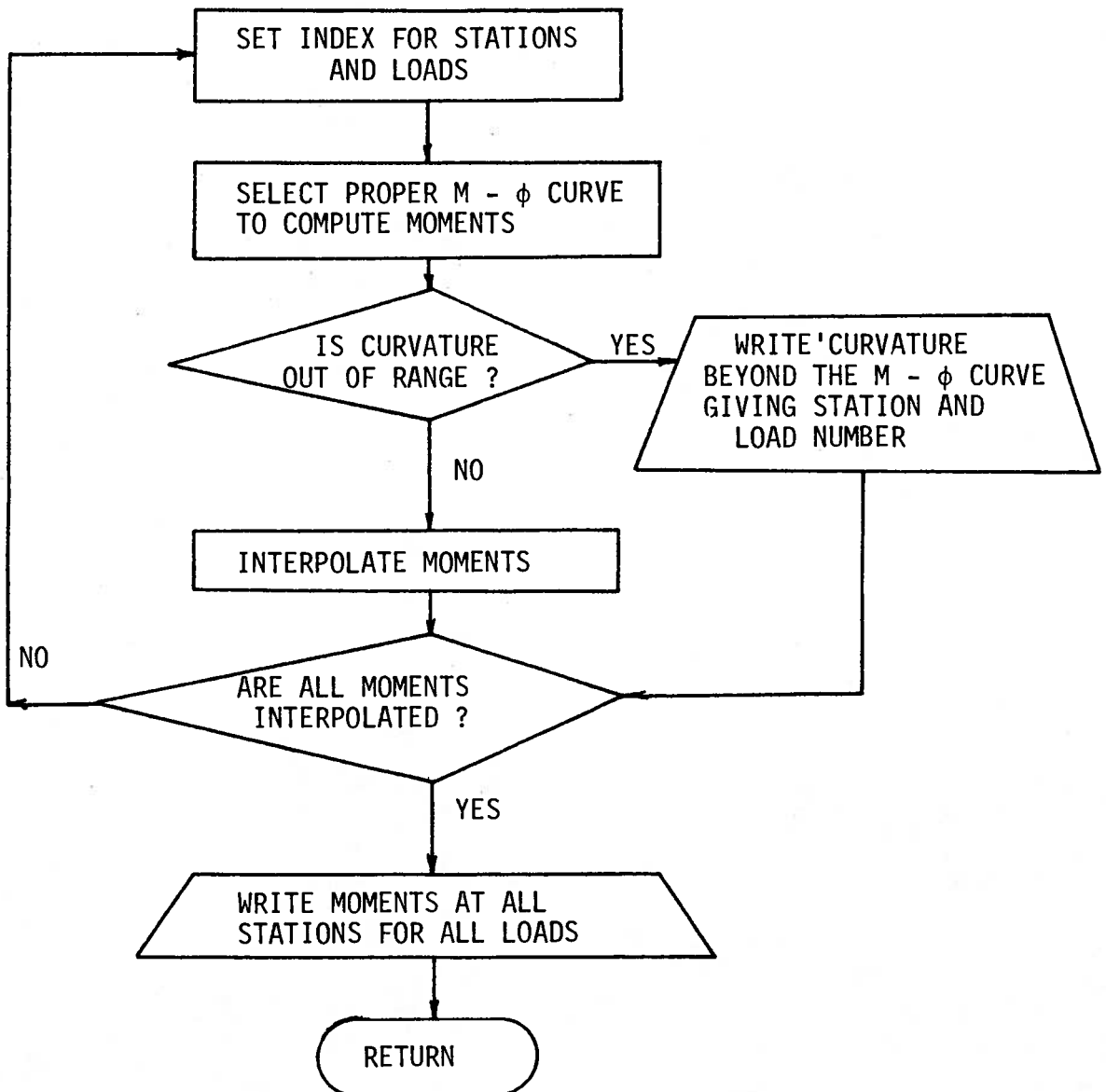
MAIN

```
 READ AND WRITE ALL POSSIBLE DATAS OF THE TEST FRAME
 DOUBLE PRECISION DR,WR,E4,E1,PHIT,C1,C2,C3
 DIMENSION A(50),B(25),C(25),G(50),H(50),DR(50,15),E4(50,15),T(50),
1E1(50,15),PHIT(50,15),AS(50,10),CO(50,10),LS(50),WR(75,15),X(10),N
2PC(35),CURV(35,70),NSM(15),SM(15),DS(50),BML(15,15),BMR(15,15),BMG
3(35,70),BM(50,15),FC1(15),FY(15),ES(15)
 READ(5,101)ND,NWD,NWL,NL,NM,NGC,W
101 FORMAT(1X,6I4,F6.2)
 NC=ND/2
 NS=NC+NWD/NWL
 READ(5,503)(NSM(J),J=1,NM)
503 FORMAT((1X,26I3))
 READ(5,799)(SM(J),J=1,NM)
799 FORMAT((1X,13F6.2))
 READ(5,850)(FC1(J),J=1,NM)
850 FORMAT((1X,11F7.1))
 READ(5,851)(FY(J),J=1,NM)
851 FORMAT((1X,9F8.1))
 READ(5,300)(ES(J),J=1,NM)
300 FORMAT((1X,8E9.1))
 READ(5,503)(LS(J),J=1,NS)
 DO 30 N=1,NS
 I=LS(N)
 READ(5,102)((AS(N,L),CO(N,L)),L=1,I)
30 CONTINUE
 READ(5,102)(A(J),J=1,NS)
 READ(5,102)(B(J),J=1,NC)
 READ(5,102)(C(J),J=1,NC)
 READ(5,102)(G(J),J=1,NS)
 READ(5,102)(H(J),J=1,NS)
 READ(5,102)(DS(J),J=1,NS)
 READ(5,102)(X(J),J=1,NWL)
102 FORMAT((1X,9F8.4))
 READ(5,107)((DR(I,J),J=1,NL),I=1,ND)
 READ(5,107)((WR(I,J),J=1,NL),I=1,NWD)
107 FORMAT((1X,9F8.5))
 READ(5,503)(NPC(N),N=1,NGC)
 DO 600 I=1,NGC
 JJ=NPC(I)
 READ(5,502)(CURV(I,N),N=1,JJ)
 READ(5,502)(BMG(I,N),N=1,JJ)
502 FORMAT((1X,11F7.4))
600 CONTINUE
 WRITE(6,350)
350 FORMAT(50X,'VALUES OF CONSTANTS'//)
 WRITE(6,700)NM,NL,ND,NWD,NC,NS,NWL,NGC,W
700 FORMAT(1H0,5X,'NO. OF MEMBERS IN THE FRAME =',I3/6X,'NO. OF LOAD I
1NCREMENT =',I3/6X,'NO. OF DIAL GUAGES =',I3/6X,'NO. OF WHITTEMORE
2DIAL GUAGES =',I3/6X,'NO. OF CURVATURE METERS =',I3/6X,'NO. OF POS
3ITIONS =',I3/6X,'NO. OF WHITTEMORE LINES =',I3/6X,'NO. OF GIVEN M-
4PHI-P CURVES =',I3/6X,'WIDTH OF FRAME =',F6.2///)
 WRITE(6,852)
852 FORMAT(1H0,10X,'MEMBER NO.',3X,'CONC. STRENGTH(PSI)',3X,'STEEL STR
1ENGTH(PSI)',3X,'SPAN(IN)',3X,'NO.OF STATIONS',3X,'E FOR STEEL'//)
 DO 853 M=1,NM
 WRITE(6,854)M,FC1(M),FY(M),SM(M),NSM(M),ES(M)
854 FORMAT(14X,I3,13X,F7.1,14X,F8.1,10X,F6.2,9X,I3,9X,F11.1)
```

```
  853 CONTINUE
      WRITE(6,353)
  353 FORMAT(1H0,45X,'REINFORCEMENT AREAS AND COVER'//)
      WRITE(6,354)
  354 FORMAT(1X,'POSITION NO.')
      DO 31 N = 1,NS
      I=LS(N)
      WRITE(6,355)N,(L,L=1,I)
  355 FORMAT(8X,I3,4X,'STEEL LAYER NO.',4X,I3,9I10/(34X,I3,9I10))
      WRITE(6,356)(AS(N,L),L=1,I)
  356 FORMAT(15X,'STEEL AREAS',4X,10F10.4/(30X,10F10.4))
      WRITE(6,357)(CO(N,L),L=1,I)
  357 FORMAT(15X,'COVER',10X,10F10.4/(30X,10F10.4))
   31 CONTINUE
      WRITE(6,704)
  704 FORMAT(1H0,30X,'VALUES OF CONSTANTS FOR MEASURING STATIONS')
      WRITE(6,150)
  150 FORMAT(1H0,10X,'POSITION NO.',7X,'G',10X,'H',9X,'DS',10X,'A',10X,'
     1B',10X,'C'//)
      DO 50 J=1,NC
      WRITE(6,151)J,G(J),H(J),DS(J),A(J),B(J),C(J)
  151 FORMAT(13X,I3,6X,6F11.4)
   50 CONTINUE
      MM=NC+1
      DO 52 J=MM,NS
      WRITE(6,145)J,G(J),H(J),DS(J),A(J)
  145 FORMAT(13X,I3,6X,4F11.4)
   52 CONTINUE
      JM=NWL-1
      WRITE(6,116)(X(N),N=1,JM)
  116 FORMAT(1H0,10X,'WHITTEMORE LINES ARE AT A DISTANCE OF',(10(F6.2,',
     1')/))
      WRITE(6,117)X(NWL)
  117 FORMAT(11X,'AND',F6.2,' INCH FROM THE OUTER FACE OF WALL')
      WRITE(6,152)
  152 FORMAT(1H0,50X,'DIAL GAUGE READINGS'//)
      WRITE(6,153)(K,K=1,NL)
  153 FORMAT(6X,'DIAL NO./LOAD NO.',3X,I3,9I10/(26X,I3,9I10))
      DO 51 N =1,ND
      WRITE(6,154)N,(DR(N,K),K=1,NL)
  154 FORMAT(9X,I3,10X,10F10.5/(22X,10F10.5))
   51 CONTINUE
      WRITE(6,115)
  115 FORMAT(1H0,50X,'WHITTEMORE GAUGE READINGS'//)
      WRITE(6,153)(K,K=1,NL)
      DO 53 N =1,NWD
      WRITE(6,154)N,(WR(N,K),K=1,NL)
   53 CONTINUE
      DO 601 I=1,NGC
      WRITE(6,701)I
  701 FORMAT(1H0,20X,'M-PHI CURVE NO.',I3/)
      WRITE(6,702)
  702 FORMAT(10X,'POINT NO.',3X,'CURVATURE X T',3X,'MOMENT/BTTFC2'/)
      JJ=NPC(I)
      DO 602 N=1,JJ
      WRITE(6,703)N,CURV(I,N),BMG(I,N)
  703 FORMAT(14X,I3,8X,F7.4,8X,F7.4)
```

```
602 CONTINUE
601 CONTINUE
    DO 75 N=1,ND
    C3=DR(N,3)-DR(N,2)
    IF(DABS(C3).EQ.0.0)GO TO 90
    C2=44.44/C3
    C1=5.77-C2*DR(N,2)
    DR(N,1)=(-C1/C2)
    GO TO 75
 90 DR(N,1)=DR(N,2)
 75 CONTINUE
    DO 76 N=1,NWD
    C3=WR(N,3)-WR(N,2)
    IF(DABS(C3).EQ.0.0)GO TO 91
    C2=44.44/C3
    C1=5.77-C2*WR(N,2)
    WR(N,1)=(-C1/C2)
    GO TO 76
 91 WR(N,1)=WR(N,2)
 76 CONTINUE
    WRITE(6,400)
400 FORMAT(1H0,10X,'CORRECTED DIALS AND WHITTEMORE INITIAL READINGS'//
   1)
    DO 77 N=1,ND
    WRITE(6,401)N,DR(N,1),WR(N,1)
401 FORMAT(10X,I3,2F10.5)
 77 CONTINUE
    II=ND+1
    DO 78 N=II,NWD
    WRITE(6,402)N,WR(N,1)
402 FORMAT(10X,I3,10X,F10.5)
 78 CONTINUE
    CALL FSAC(NC,ND,NWD,NWL,NL,NS,A,B,C,G,H,E4,E1,PHIT,DR,WR,X)
    CALL BMKP(PHIT,NS,NL,FC1,W,T,NGC,NM,NPC,CURV,BMG,NSM,BM)
    STOP
    END
```

```
      SUBROUTINE FSAC(NC,ND,NWD,NWL,NL,NS,A,B,C,G,H,E4,E1,PHIT,DR,WR,X)
C     PROGRAMME FOR CONVERSION OF DIALS AND WHITTEMORE READINGS TO
C     STRAINS AND  CURVATURE
      DOUBLE PRECISION DR,WR,E4,E1,PHIT,G4,G1,PHI,Y,SY,SXY,A1,A0
      DIMENSION A(50),B(25),C(25),G(50),H(50),E4(50,15),E1(50,15),PHIT(5
     10,15),DR(50,15),WR(75,15),X(10),Y(10)
      DO 22 M=1,ND,2
      N=(M+1)/2
      DO 23 K=2,NL
      G4=DR(M+1,K)-DR(M+1,1)
      G1=DR(M,K)-DR(M,1)
      PHI=(G4-G1)/(A(N)*(B(N)+C(N)))
      E4(N,K)=PHI*(B(N)+G(N))+G1/A(N)
      E1(N,K)=PHI*(B(N)-H(N))+G1/A(N)
      PHIT(N,K)=E4(N,K)-E1(N,K)
   23 CONTINUE
   22 CONTINUE
      SX=0.0
      SX2=0.0
      DO 58 N=1,NWL
      SX=SX+X(N)
      SX2=SX2+(X(N)**2)
   58 CONTINUE
      KK=NWD/NWL
      CA=FLOAT(NWL)
      CB=(SX**2)-(CA*SX2)
      DO 59 J=1,KK
      N=NC+J
      DO 60 K=2,NL
      SY=0.0
      SXY=0.0
      IJ=0
      SCX=SX
      SCX2=SX2
      DO 61 I =1,NWL
      M=J+((I-1)*KK)
      IF(WR(M,K).EQ.0.0)GO TO 80
      Y(I)=(WR(M,K)-WR(M,1))/A(N)
      GO TO 81
   80 Y(I)=0.0
      IJ=IJ+1
      SCX=SCX-X(I)
      SCX2=SCX2-(X(I)**2)
   81 SY=SY+Y(I)
      SXY=SXY+X(I)*Y(I)
   61 CONTINUE
      IF(IJ.GT.0)GO TO 82
      A1=(SY*SX-CA*SXY)/CB
      A0=(SY-A1*SX)/CA
      GO TO 83
   82 CCA=FLOAT(NWL-IJ )
      CCB=(SCX**2)-(CCA*SCX2)
      A1=(SY*SCX-CCA*SXY)/CCB
      A0=(SY-A1*SCX)/CCA
   83 E4(N,K)=A0
```

```
      E1(N,K)=A0+A1*(G(N)+H(N))
      PHIT(N,K)=E4(N,K)-E1(N,K)
   60 CONTINUE
   59 CONTINUE
      WRITE(6,200)
  200 FORMAT(1H0,25X,'INNER FACE STRAIN IN COL. OR TOP STRAIN IN BEAMS O
     1R OUTER FACE STRAIN IN WALL'//)
      WRITE(6,201)(K,K=2,NL)
  201 FORMAT(2X,'POSITION NO./LOAD NO.',3X,I3,9I10/(26X,I3,9I10))
      DO 25 N=1,NS
      WRITE(6,202)N,(E4(N,K),K=2,NL)
  202 FORMAT(9X,I3,10X,10F10.6/(22X,10F10.6))
   25 CONTINUE
      WRITE(6,203)
  203 FORMAT(1H0,25X,'OUTER FACE STRAIN IN COL. OR BOTTOM STRAIN IN BEAM
     1S OR INNER FACE STRAIN IN WALL'//)
      WRITE(6,201)(K,K=2,NL)
      DO 26 N=1,NS
      WRITE(6,202)N,(E1(N,K),K=2,NL)
   26 CONTINUE
      WRITE(6,206)
  206 FORMAT(1H0,50X,'CURVATURES AT VARIOUS POSITIONS'//)
      WRITE(6,201)(K,K=2,NL)
      DO 27 N=1,NS
      WRITE(6,202)N,(PHIT(N,K),K=2,NL)
   27 CONTINUE
      RETURN
      END
```

```
      SUBROUTINE BMKP(PHIT,NS,NL,FC1,W,T,NGC,NM,NPC,CURV,BMG,NSM,BM)
C     PROGRAMME FOR FINDING MOMENTS FROM KNOWN M-PHI CURVES
      DOUBLE PRECISION PHIT
      DIMENSION NPC(35),CURV(35,70),BMG(35,70),PHIT(50,15),BM(50,15),NSM
     1(15),T(50),FC1(15)
      DO 605 M =1,NM
      IA=NSM(M)
      IF(M.EQ.1)GO TO 626
      KK=NSM(M-1)+1
      GO TO 627
  626 KK=1
  627 DO 603 N =KK,IA
      DO 604 K=2,NL
      IF(DABS(PHIT(N,K)).LT.1D-9)GO TO 625
      IF(M.LE.4.OR.M.GE.9)GO TO 621
      I=M
      IF(N.EQ.17)I=1
      IF(N.EQ.19)I=2
      IF(N.EQ.21)I=3
      IF(N.EQ.23)I=4
      GO TO 610
  621 IF(K.EQ.2)GO TO 608
      IF(K.EQ.NL)GO TO 609
      IF(M.LE.4)I=M+8
      IF(M.GE.9)I=M+12
      GO TO 610
  608 IF(M.LE.4)I=M+12
      IF(M.GE.9)I=M+16
      GO TO 610
  609 IF(M.LE.4)I=M+16
      IF(M.GE.9)I=M+20
  610 JJ=NPC(I)
      DO 611 J =2,JJ
      A=(DABS(PHIT(N,K)))-CURV(I,J)
      IF(A.GT.0.0)GO TO 612
      IF(A.EQ.0.0)GO TO 613
      IF(A.LT.0.0)GO TO 614
  612 IF(J.EQ.JJ)GO TO 615
      GO TO 611
  613 BM(N,K)=BMG(I,J)
      GO TO 616
  614 AA=(DABS(PHIT(N,K)))-CURV(I,J-1)
      BB=BMG(I,J)-BMG(I,J-1)
      CC=CURV(I,J)-CURV(I,J-1)
      BM(N,K)=BMG(I,J-1)+AA*BB/CC
      GO TO 616
  611 CONTINUE
  615 WRITE(6,706)N,K,I
  706 FORMAT(1H0,5X,'CURVATURE AT POSITION NO.',I3,' AND LOAD NO.',I3,'
     1IS BEYOND THE GIVEN CURVE NO.',I3)
      GO TO 604
  616 BM(N,K)=(0.85*FC1(M)*W*(T(N)**2)*BM(N,K))/1000.0
      IF(PHIT(N,K).LT.0.0)GO TO 630
      GO TO 604
  625 BM(N,K)=0.0
```

```
      GO TO 604
630   BM(N,K)=(-BM(N,K))
604   CONTINUE
603   CONTINUE
605   CONTINUE
      WRITE(6,707)
707   FORMAT(1H0,50X,'MOMENTS FOR KNOWN P IN KIP INCH'//)
      WRITE(6,708)(K,K=2,NL)
708   FORMAT(2X,'POSITION NO./LOAD NO.',3X,I3,9I10/(26X,I3,9I10))
      DO 617 N=1,NS
      WRITE(6,709)N,(BM(N,K),K=2,NL)
709   FORMAT(9X,I3,10X,10F10.2/(22X,10F10.2))
617   CONTINUE
      RETURN
      END
```

TABLE D.1

OBSERVED CURVATURE X DEPTH OF SECTION

Member	Load No. / St. No.	2	3	4	5	6	7	8	9	10
Col. 1	1	-0.000011	-0.000099	0.000239	0.000289	0.001286	0.002480	0.003850	0.002452	0.002961
	2	0.000013	0.000117	0.000240	0.000945	0.002307	0.006789	0.004776	0.001458	0.001739
	3	-0.000008	-0.000066	0.000088	0.000001	-0.000122	-0.000189	-0.000221	0.000655	0.000296
	4	0.000018	0.000153	0.000062	-0.000229	-0.000517	-0.000761	-0.000767	0.000530	0.000014
Col. 2	5	-0.000004	-0.000034	0.000191	0.000524	0.000965	0.001294	0.001211	-0.000114	-0.000023
	6	0.000001	0.000013	0.000161	0.000423	0.000686	0.001015	0.000768	-0.000128	-0.000062
	7	0.000008	0.000068	-0.000099	-0.000431	-0.000783	-0.001258	-0.001205	-0.000176	-0.000213
	8	0.000012	0.000105	-0.000196	-0.000743	-0.001575	-0.002881	-0.002830	0.000154	-0.000795
Col. 3	9	-0.000004	-0.000038	0.000260	0.000733	0.001300	0.002241	0.002210	0.000373	0.000363
	10	-0.000002	-0.000020	0.000183	0.000548	0.000967	0.001375	0.001443	0.000266	0.000206
	11	-0.000003	-0.000023	-0.000238	-0.000380	-0.000667	-0.000694	-0.000784	0.000029	0.000115
	12	-0.000014	-0.000121	-0.000404	-0.000839	-0.001366	-0.001775	-0.001918	-0.000332	-0.000060
Col. 4	13	0.000019	0.000169	0.000444	0.001228	0.001460	0.002454	0.002421	0.000808	0.000538
	14	0.000018	0.000159	0.000326	0.000629	0.000938	0.001166	0.001193	0.000350	0.000131
	15	-0.000019	-0.000162	-0.000446	-0.000903	-0.001499	-0.002907	-0.002099	-0.000603	-0.000486
	16	-0.000025	-0.000221	-0.000691	-0.001283	-0.002606	-	-	-	-

TABLE D.1 (contd.)

Beam 1	17	-0.000001	-0.000008	0.000181	0.000715	0.001440	0.002104	0.001949	0.000058	0.000168
	18	-0.000001	-0.000007	-0.000635	-0.001672	-0.002464	-0.003010	-0.010182	-0.006824	-0.007462
Beam 2	19	0.000006	0.000052	0.000303	0.000729	0.000995	0.001980	0.001873	0.000471	0.000436
	20	-0.000014	0.000119	-0.000816	-0.001864	-0.003062	-0.004935	-	-	-
Beam 3	21	0.000003	0.000026	0.000348	0.000906	0.001471	0.002342	0.002029	0.000363	0.000357
	22	-0.000015	-0.000130	-0.000999	-0.002300	-0.003893	-0.006431	-	-	-
Beam 4	23	0.000011	0.000092	0.000309	0.000613	0.000924	0.001748	0.001275	0.000547	0.000387
	24	-0.000030	-0.000257	-0.000983	-0.001950	-0.003118	-0.003747	-0.007090	-0.002946	-0.002738
Wall 1	25	-0.000013	-0.000111	0.000400	0.001032	0.001453	0.002047	0.001330	0.000657	0.000150
	26	0.000001	0.000008	0.000585	0.001096	0.001541	0.002143	0.001502	0.000899	0.000194
	27	-0.000002	-0.000020	0.000628	0.001169	0.001525	0.002103	0.001431	0.000954	0.000186
	28	-0.000006	-0.000051	0.000294	0.000643	0.000956	0.001441	0.000961	0.000678	0.000243
	29	-0.000002	-0.000021	0.000451	0.000821	0.001146	0.001706	0.001186	0.000936	0.000199
	30	-0.000001	-0.000006	0.000433	0.000794	0.001136	0.001732	0.001290	0.000997	0.000328
Wall 2	31	-0.000000	-0.000003	0.000197	0.000384	0.000564	0.001078	0.000735	0.000635	0.000234
	32	-0.000002	-0.000018	0.000223	0.000407	0.000557	0.001255	0.000916	0.000864	0.000378
	33	0.000003	0.000023	0.000186	0.000307	0.000367	0.000692	0.000557	0.000724	0.000107

TABLE D.1 (contd.)

34		-0.000005	-0.000045	0.000089	0.000200	0.000256	0.000490	-0.000322	-0.000185	-0.000013
35		-0.000009	-0.000075	0.000048	0.000106	0.000115	0.000283	0.000142	0.000443	0.000082
36		-0.000004	-0.000036	0.000053	0.000147	0.000297	0.000525	0.000445	0.000515	0.000215
37	Wall 3	-0.000001	-0.000012	0.000058	0.000079	0.000073	0.000200	0.000137	0.000285	0.000052
38		-0.000001	-0.000009	0.000033	0.000052	0.000067	0.000119	0.000113	0.000259	0.000050
39		-0.000002	-0.000013	0.000004	-0.000022	-0.000047	-0.000001	-0.000027	0.000259	0.000034
40		0.000004	0.000031	0.000039	-0.000007	-0.000044	-0.000027	-0.000003	0.000346	0.000128
41		-0.000001	-0.000006	-0.000045	-0.000145	-0.000245	-0.000259	-0.000235	0.000201	-0.000024
42		-0.000002	-0.000020	-0.000045	-0.000035	0.000020	0.000090	0.000262	0.000438	0.000202
43	Wall 4	0.000003	0.000022	-0.000001	-0.000023	-0.000078	-0.000072	-0.000052	0.000124	0.000043
44		0.000004	0.000038	0.000019	-0.000038	-0.000045	-0.000065	-0.000026	0.000131	0.000021
45		-0.000003	-0.000027	-0.000034	-0.000086	-0.000134	-0.000135	-0.000101	0.000105	0.000023
46		0.000001	0.000012	-0.000005	-0.000046	-0.000110	-0.000120	-0.000096	0.000018	0.000015
47		0.000002	0.000017	-0.000025	-0.000042	-0.000129	-0.000171	-0.000149	-0.000031	-0.000016
48		0.000005	0.000045	0.000029	-0.000016	-0.000079	-0.000156	-0.000144	0.000078	-0.000004

TABLE D.2

OBSERVED BENDING MOMENTS IN KIP-INCH

Member	Load No. / St. No.	2	3	4	5	6	7	8	9	10
Col. 1	1	-0.41	-2.40	5.78	20.22	31.07	52.23	61.85	51.94	32.62
	2	0.49	2.83	5.81	22.99	50.32	-	60.20	35.07	19.96
	3	-0.27	-1.59	2.13	0.01	-2.96	-4.57	-5.35	16.00	10.75
	4	0.64	3.70	1.51	-5.55	-12.63	-18.57	-18.72	12.95	0.52
Col. 2	5	-0.14	-0.81	4.49	12.40	22.79	30.32	28.45	-2.68	-0.81
	6	0.05	0.31	3.78	10.00	16.24	23.95	18.17	-3.02	-2.23
	7	0.28	1.61	-2.32	-10.19	-18.53	-29.52	-28.33	-4.13	-7.62
	8	0.43	2.46	-4.62	-17.58	-36.60	-54.88	-54.43	3.63	-12.36
Col. 3	9	-0.15	-0.89	6.11	17.37	30.50	47.79	47.46	8.80	10.93
	10	-0.08	-0.48	4.30	12.99	22.85	32.20	33.75	6.26	7.30
	11	-0.10	-0.55	-5.60	-8.97	-15.81	-16.45	-18.58	0.69	4.09
	12	-0.49	-2.83	-9.55	-19.86	-31.99	-40.92	-43.35	-7.83	-2.13
Col. 4	13	0.83	5.44	14.39	39.71	46.95	66.75	66.24	26.22	15.84
	14	0.78	5.12	10.51	20.42	30.41	37.72	38.61	11.31	5.57
	15	-0.80	-5.23	-14.44	-29.26	-48.19	-73.68	-60.95	-19.55	-15.17
	16	-1.09	-7.14	-22.41	-41.43	-69.14	-	-	-	-

TABLE D.2 (contd.)

Beam 1	17	-0.02	-0.21	5.07	19.73	39.22	56.63	52.58	1.61	4.69
	18	-0.02	-0.17	-14.85	-38.28	-55.60	-67.14	-87.07	-86.57	-86.70
Beam 2	19	0.21	1.84	10.74	25.67	34.84	67.85	64.32	16.67	15.44
	20	-0.38	-3.33	-22.72	-50.75	-81.40	-115.99	-	-	-
Beam 3	21	0.11	0.94	12.42	31.88	51.11	79.89	69.63	12.94	12.71
	22	-0.37	-3.25	-24.54	-54.87	-89.65	-110.06	-	-	-
Beam 4	23	0.36	3.11	10.48	20.62	30.83	57.15	42.14	18.44	13.10
	24	-0.71	-6.19	-23.31	-45.23	-70.41	-83.40	-108.66	-66.82	-62.42
Wall 1	25	-18.55	-159.54	558.77	1062.08	1339.51	1758.24	1254.74	849.15	215.48
	26	1.37	11.75	798.32	1101.89	1400.33	1826.07	1372.80	980.21	279.71
	27	-3.39	-29.16	833.20	1146.86	1388.94	1797.94	1324.39	1014.00	267.80
	28	-8.45	-72.69	421.17	841.56	1015.40	1331.37	1018.14	860.42	350.44
	29	-3.54	-30.47	625.66	937.61	1132.82	1516.81	1157.44	1003.03	286.26
	30	-1.05	-8.99	595.58	913.57	1114.67	1519.46	1214.94	1029.72	445.92
Wall 2	31	-0.37	-3.13	240.69	460.09	663.40	907.29	761.88	718.88	290.52
	32	-2.55	-21.67	272.06	486.65	655.30	985.03	839.38	817.09	405.68
	33	3.37	28.65	227.12	374.20	442.02	743.35	654.93	757.26	133.28

TABLE D.2 (contd.)

	34	-6.39	-54.36	108.01	244.39	312.50	579.49	-390.73	-225.46	-16.59
	35	-10.75	-91.44	58.92	129.79	140.36	345.82	173.52	527.28	101.49
	36	-5.16	-43.91	64.34	178.77	362.28	619.89	529.57	607.90	267.05
Wall 3	37	-1.52	-12.79	61.79	83.86	77.07	212.50	145.56	302.91	56.93
	38	-1.12	-9.43	34.72	55.24	71.23	125.99	119.90	275.14	54.28
	39	-1.66	-13.99	4.05	-23.54	-50.07	-0.73	-29.20	275.22	37.32
	40	3.97	33.38	40.98	-7.48	-46.58	-28.54	-2.70	363.58	139.51
	41	-0.78	-6.60	-47.46	-153.94	-260.42	-275.64	-249.11	213.97	-26.15
	42	-2.54	-21.38	-48.09	-36.78	21.24	95.35	278.08	454.41	219.70
Wall 4	43	2.85	24.10	-1.21	-25.43	-84.72	-77.85	-56.52	134.90	47.54
	44	4.92	41.66	20.33	-40.95	-48.72	-70.05	-28.29	141.80	23.74
	45	-3.50	-29.61	-36.48	-93.78	-145.30	-146.20	-109.33	114.28	25.34
	46	1.54	13.07	-5.37	-50.02	-119.07	-130.63	-104.42	19.56	16.50
	47	2.22	18.80	-26.94	-45.38	-139.74	-185.47	-162.16	-33.29	-17.75
	48	5.79	49.00	31.46	-17.17	-86.22	-168.83	-156.17	-84.78	-4.42